2009

# Fine- to basin-scale distributions of Calanus finmarchicus and its predators in three deep basins of the Gulf of Maine during December 1998 and 1999 from Video Plankton Recorder (VPR) data

Christian Briseño-Avena
*Louisiana State University and Agricultural and Mechanical College*

# FINE- TO BASIN-SCALE DISTRIBUTIONS OF *CALANUS FINMARCHICUS* AND ITS PREDATORS IN THREE DEEP BASINS OF THE GULF OF MAINE DURING DECEMBER 1998 AND 1999 FROM VIDEO PLANKTON RECORDER (VPR) DATA

**A Thesis**
**Submitted to the Graduate Faculty of the**
**Louisiana State University and**
**Agricultural and Mechanical College**
**in partial fulfillment of the**
**requirements for the degree of**
**Master of Science**

**in**

**The Department of Oceanography and Coastal Sciences**

**by**
**Christian Briseño-Avena**
**B.S., Universidad de Guadalajara, 2004**
**August 2009**

## ACKNOWLEDGEMENTS

I wish to thank my advisor and mentor Dr. Mark Benfield for his wise guidance, but most of all for the great support he showed to me during the course of my work at Louisiana State University. I am also grateful for his invaluable friendship. I also would like to thank my committee, Robert S. Carney, Michael Hellberg and Malinda Sutor, for their helpful comments on the final preparation of this manuscript.

I am indebted to the numerous workers of the U. S. GLOBEC Northwest Atlantic/Georges Bank Study program. Their hard work made it possible the collection of data on which I relied to write this thesis.

Last, but definitely not least, thanks to the friends I found at LSU and in Baton Rouge. James Fisher, Amber Gates, Emily McAlister, Imtiaz Hussein, Rohan Duhrandhar. You were my family away from home. You made my stay in Baton Rouge much more amenable and enjoyable.

I am always thankful to my family and friends at home who never stopped supporting and believing on me. I love you all.

This work of course wouldn't have been possible without the financial assistance of the Department of Oceanography and Coastal Sciences at Louisiana State University. A grant to help subsidize my expenses was awarded to me by the Universidad de Guadalajara, Mexico.

## TABLE OF CONTENTS

## ABSTRACT

The calanoid copepod *Calanus finmarchicus* is broadly distributed in the North Atlantic, where it dominates the spring zooplankton biomass of shelf ecosystems. *Calanus finmarchicus* diapauses in the deep basins of the Gulf of Maine (GOM) during late-summer through early-winter. During diapause, predators that co-occur in regions of high copepod abundance may reduce survivorship through predation. Consequently it is important to measure the distribution patterns of *C. finmarchicus* and its predators. Two cruises were carried out during December of 1998 and 1999 in the GOM. Video Plankton Recorder (VPR) data collected in Wilkinson, Jordan and Georges Basins were used to describe the fine- to basin-scale distributions of *C. finmarchicus* and its predators. The locations of individual zooplanktors were mapped by towyoing a Video Plankton Recorder (VPR), mounted on the towed-body BIOMAPER-II, across the basins. Volumetric distribution patterns were estimated by interpolated abundance data using 3D Kriging. The abundance of *C. finmarchicus* was lower in December 1998 than in December 1999. This difference is discussed in terms of the spatial distributions and abundances of cnidarian, ctenophore, and crustacean predators. Gelatinous plankton were more abundant during December 1998 than in December 1999. Gelatinous plankton (siphonophores, ctenophores and medusae) were identified as the most aggressive taxa preying on *C. finmarchicus*. An inverse spatial pattern between *C. finmarchicus* and predators was observed in all three deep basins during December 1998, suggesting depletion of *C. finmarchicus* through predation. Water temperatures were generally cooler and fresher during December 1998 and warmer and saltier during December 1999. This hydrological regime changes caused by the shift between the Labrador Subarctic Slope Water and the Slope Water, respectively, seemed to affect both, *C. finmarchicus* and its invertebrate predators. During December 1998, *C. finmarchicus* was broadly distributed (0-200 m) in the water column probably due to broader distribution of cooler temperatures. During December 1999 *C. finmarchicus* was found below 150 m, where cooler temperatures dominated. The low *C.*

*finmarchicus* abundances observed during December 1998 were possibly caused by the combined action of predation and advection losses since diapausing populations above sill depth (~200 m) are likely advected out of the system.

# CHAPTER I

## GENERAL INTRODUCTION

*Calanus finmarchicus* has been considered a key ecological species in the shelf ecosystems of the North Atlantic. Fluctuations in its abundance have been observed over the last decades and it is thought that other species that feed on this copepod are affected by these changes that can be of seasonal, inter annual, and decadal scales. The major working hypothesis relates fluctuations of *C. finmarchicus* abundances to atmospheric-driven phenomena. But some authors have pointed out the importance of predation as a mechanism shaping the spatial and temporal variations of *C. finmarchicus* in the Gulf of Maine. In the present work, spatial and temporal distributions of selected invertebrate predators with respect to *C. finmarchicus* are studied in order to explore their potential predation pressure over diapausing *C. finmarchicus* populations in the Gulf of Maine.

*Calanus finmarchicus* is a calanoid copepod with a broad distribution in the North Atlantic. In the western North Atlantic, *C. finmarchicus* occurs from the Arctic south to the Chesapeake Bay during winter (Davis 1987). Within the Gulf of Maine (GOM), *C. finmarchicus* dominates the mesozooplankton biomass during the spring and early summer (Fish, 1936; Clarke, 1940; Durbin and Casas, 2006). At any given time *C. finmarchicus* and other five species of copepods make up over 80% of the zooplankton total abundance in the GOM (Davis, 1987).

The GOM is a semi-enclosed body of water located in the Northeast coast of the United States (Fig. 1.1). The GOM is limited to the west by the U.S. coast and to the east by Georges Bank and the Atlantic Ocean. Three major basins are readily identified inside the GOM: Wilkinson Basin (7,075.6 $km^2$, ~290 m depth) to the west; Jordan Basin (6,695 $km^2$, ~300 m depth) to the northeast; and Georges Basin (4,103.7 $km^2$, 366 m depth) to the east. The deep basins are separated from each other below the 200 m isobaths (Xue et al., 2000). The GOM is

connected to the Atlantic Ocean at the northeast through the Northeast Channel, and to the southeast through the Great South Channel (Fig. 1.1).

A portion of the *Calanus finmarchicus* population overwinters in the GOM deep basins in a resting phase known as diapause. Diapause is a period of arrested development that occurs commonly in the genus *Calanus* during a specific period of their life cycle (Conover, 1988). In *C. finmarchicus*, diapause occurs primarily during the fifth copepodite stage (CV). Diapause is thought to be an adaptation for surviving food-limiting conditions during winter periods (Saumweber and Durbin, 2006). At the onset of diapause during mid- to late-summer, CV stage *C. finmarchicus* migrate out of the epipelagic zone into deeper waters where they remain through the winter (Fig. 1.2). During diapause *C. finmarchicus* reduces its metabolism and survives using the wax esters stored in a large oil sac. The role that this oil sac plays on determining the depth and duration of diapause in *Calanus* and other diapausing calanoid genera is an ongoing topic of research (Irigoien, 2004; Campbell and Dower, 2008; Johnson et al., 2008). In oceanic waters off the western North Atlantic, *C. finmarchicus* is reported to diapause at depths from 500 to 1000 m or deeper (Hirche, 1996; Saumweber and Durbin, 2006). However, in the GOM, *C. finmarchicus* overwinters only in the deep basins at depths from 50 to 300 m (Meise and O'Reilly, 1996). Overwintering at deeper waters is thought to reduce the risk of predation (Kaartvedt, 1996; Gislason et al., 2007) and to increase the retention of overwintering populations in the deep waters of the GOM (Johnson et al., 2006). The degree to which diapausing stocks are retained in each basin varies among basins and years, however, Wilkinson Basin is considered to have the highest retention rate of *C. finmarchicus* diapausing populations (Johnson et al., 2006).

*Calanus finmarchicus* is commonly considered an oceanic species that dominate the spring time zooplankton biomass in the shelf ecosystems of the Gulf of Maine (Greene et al. 2003). Overwintering *C. finmarchicus* in the GOM are considered endogenous populations (that may be partially self-replenishing in Wilkinson Basin and to a lesser extent in Jordan Basin and

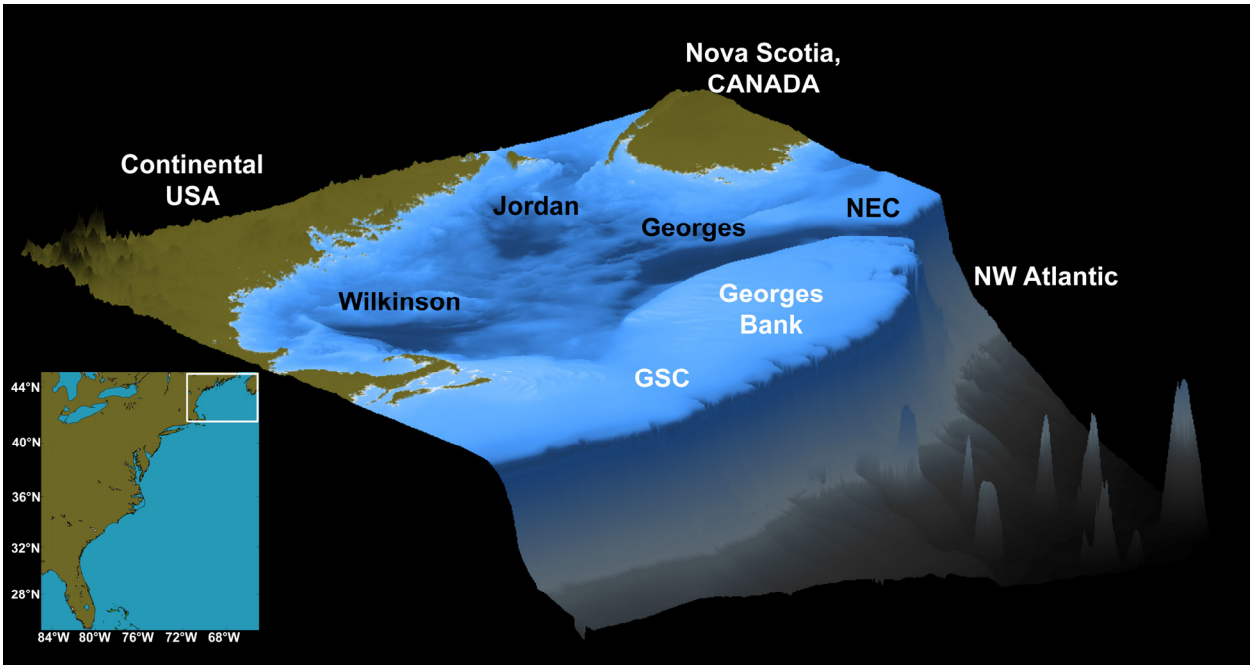


**Figure 1.1** Bathymetric (blue) features of the Gulf of Maine. The darker blue areas represent the deep basins of the gulf: Wilkinson Basin, Jordan Basin and Georges Basin. NEC=Northeast Channel; GSC=Great South Channel.

Georges Basin), which rely on sources outside of the GOM to maintain their stocks (Miller et al., 1998). The replenishment of *C. finmarchicus* is known to occur via the Northeast Channel when Slope and Scotian Shelf water masses flow into the GOM (Johnson et al., 2006). Slope Water (SLW) flows through the Northeast Channel into Georges Basin, and then the SLW moves to Jordan and Wilkinson Basin following the current patterns of the GOM (Warn-Varnas et al., 2005). Moreover, molecular studies have suggested that *C. finmarchicus* from the GOM, Georges Bank, Gulf of St. Lawrence, Labrador Current and Scotian Shelf, constitute a single interbreeding population (Bucklin and Kocher, 1996).

*Calanus finmarchicus* abundance usually peaks during spring and early summer, when diapausing copepods mature and migrate to the surface right after the spring bloom to feed and reproduce (Sherman et al., 1987). This constitutes an initial generation ($G_0$) for the productive season, which typically starts in early spring and ends in early summer (Fig. 1.2). Three subsequent generations ($G_1$, $G_2$, $G_3$) are common for *C. finmarchicus* in the GOM during the productive season (Fish, 1936; Miller, 2004). However, $G_3$ may or may not have sufficient

survivorship to reach diapause (Miller, 2004). By the end of the summer and early fall, $G_2$ and $G_3$ (provided the latter generation survives) start migrating down into the deep basins of the GOM to enter diapause when they reach the CV stage (Fig. 1.2). Predictions estimate that diapause has duration of 3.5 and 5.5 months (Saumweber and Durbin, 2006). The survival of this diapausing stock contributes to the next year's secondary production in the GOM. A portion of this population will be advected from the GOM to seed Georges Bank during spring, and some will be exchanged between the basins or transported to the Atlantic Ocean via the deep currents of the GOM (Johnson et al., 2006; Li et al., 2006). These exchanges may contribute to the overall abundance fluctuations inside the GOM, however mortality may also have an impact on variability in abundance (Johnson et al., 2006).

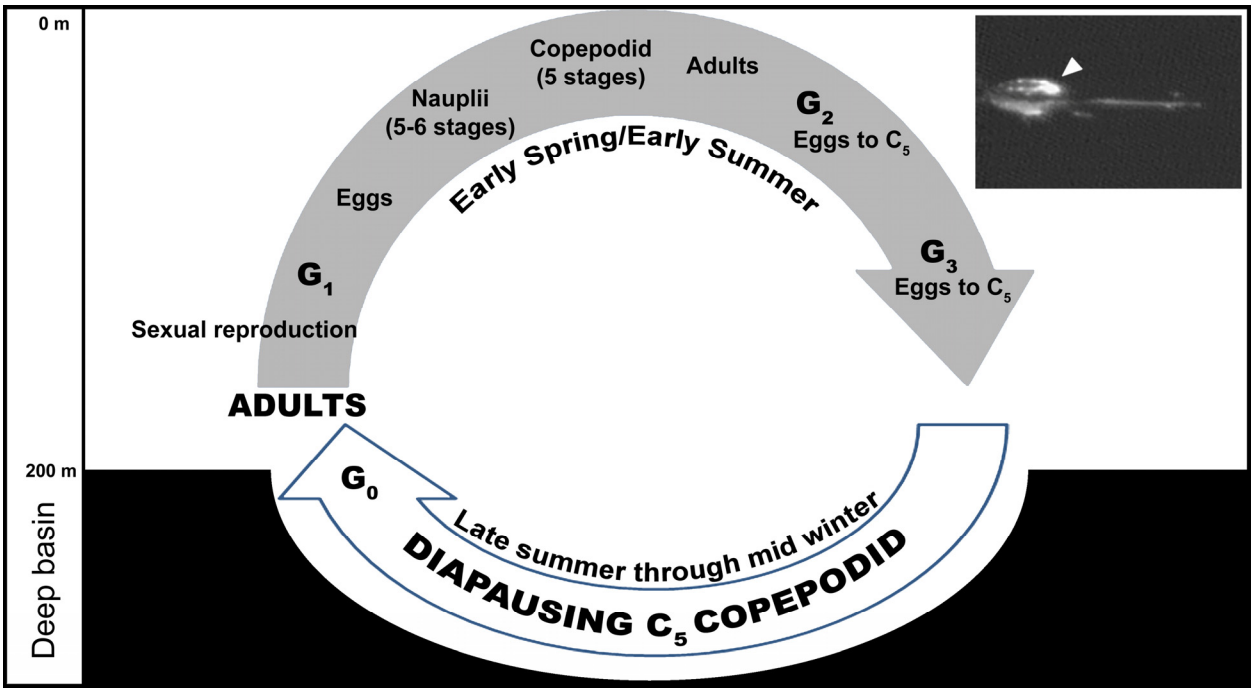


**Figure 1.2.** Generalized *Calanus finmarchicus* life cycle in the Gulf of Maine. $C_5$ represents copepodid stage 5. G1, G2 and G3 represent generation one, two and three, respectively. G3 may or not may survive to go into diapause. Depression in figure represents the deep basins of the Gulf of Maine whose sill depth is ~200 m. Diapausing usually occurs from 50 to 300 m. Inset: example of *C. finmarchicus* imaged by the VPR. Its characteristic oil sac is indicated by the arrowhead.

The GOM is considered a major source of *C. finmarchicus* nauplii stages for Georges Bank (Li et al., 2006), whose *C. finmarchicus* population is not considered self-sustaining (Bucklin and Kocher, 1996; Durbin and Casas, 2006). Georges Bank has historically supported a very large commercial fishery based in New England that exploits a variety of groundfish species including cod (*Gadus morhua*) and haddock (*Melanogrammus aeglefinus*). Early life stages of these and other commercially-important fishes on Georges Bank depend on *C. finmarchicus* to survive (Avent et al., 2001; Li et al., 2006; Wiebe et al., 2006). Indeed, a strong correlation has been reported between fish larval growth rates and copepod prey concentrations (*Pseudocalanus* spp. and *C. finmarchicus*) by Buckley and Durbin (2006). Moreover, *C. finmarchicus* is considered an important food source for large planktivorous vertebrates. The GOM is considered a major feeding ground for cetaceans (*Eubalaena glacialis*) and basking sharks (*Cetorhinus maximus*) where they congregate to feed on *C. finmarchicus* (Durbin et al., 1995; Kenney et al., 1995; Wishner et al., 1995; Beardsley et al., 1996). Because of the major role of the GOM in seeding Georges Bank and neighboring areas with *C. finmarchicus*, it is important to quantify and study its spatial and temporal abundances in the region. In order to study the *C. finmarchicus* population standing stock, synoptic (simultaneous observations over large areas) or quasi-synoptic (observations close enough in time to be considered simultaneous) information on its distribution and abundance over a large area of the GOM is needed.

Planktonic populations vary substantially in space and time over a wide range of scales (Haury et. al., 1978). Several studies have observed fluctuations in the abundance of *C. finmarchicus* in the North Atlantic and have identified seasonal, interannual and decadal fluctuations (Conversi et al., 2001). Spatial variations have been studied as well, and driving factors include winds, surface and deep currents (Dale et al., 2001). Fewer biological factors affecting the abundance of *C. finmarchicus* have been implicated (Davis, 1984; Li et al., 2006). Water masses in the deep basins of the deep GOM are replaced every 12 months (Xue et al.,

2000). Differences in retention (as summarized earlier) affected by this water exchange may be one of the many factors contributing to inter-annual differences in *C. finmarchicus* abundances in the deep basins of the GOM. Spatial heterogeneities may also be a result of asynchronous emergence from diapause at different latitudes in the North Atlantic (Johnson et al., 2008). Earlier observations suggest asynchronous emergence may even occur between the southwest and northeast regions of the GOM (Fish, 1936; Meise and O'Reilly, 1996).

Temporal fluctuations in the abundance of *C. finmarchicus* have traditionally been linked to atmospherically-driven phenomena and by shifts in ocean circulation. For instance, variations in *C. finmarchicus* abundance have been correlated with fluctuations of the North Atlantic Oscillation Index (NAO) in the decadal and inter-annual time scales (Conversi et al., 2001; Piontkovski et al., 2006), in the so called “advection-based hypothesis” (Greene and Pershing, 2000). According to this hypothesis *C. finmarchicus* abundances are closely related to physical oceanographic responses to the NAO (Greene and Pershing, 2000; Greene et al., 2003). For example, a single dramatic drop in *C. finmarchicus* abundance in the GOM during 1998 was believed to be the result of the replacement of the warmer more-saline SLW at the bottom of the deep basins with the cooler fresher Labrador Subarctic Slope Water (LSSW). Such an event was interpreted as a response by ocean circulation to the NAO that started in 1996 — two years earlier. According to the authors, this event was episodic and conditions returned to normal on 1999.

Although atmospherically-driven phenomena may explain much of the variability in *C. finmarchicus* abundance fluctuations in the western North Atlantic, the biological processes shaping *C. finmarchicus* populations over time remain poorly understood. Using a simulation approach, Davis (1984) proposed that *C. finmarchicus* seasonal variations may be controlled by predators (he used chaetognaths and ctenophores only) in Georges Bank. His experimental run outputs fitted the observed patterns obtained from field data. In addition, it has been suggested that region-specific biological interactions can substantially modify the effects of physical climate

variability and render simple linear relationships between climate and zooplankton abundance unlikely (Ohman et al., 2004). While an entirely physical model cannot explain *C. finmarchicus* abundance fluctuations, a mere biological model may not be capable of explaining these changes completely either. Coupled comprehensive physical-biological approaches have pointed out the importance of mortality (biological control, predation) on the interannual abundance fluctuations of *C. finmarchicus* (Lynch et al., 1998; Johnson et al., 2006; Li et al., 2006).

Theoretical and observational works have demonstrated the importance of patchiness at different scales in inter-species relationships, such as predator-prey interactions. Plankton patchiness has very important consequences for the survivorship of zooplanktivorous fish larvae (Winemiller and Rose, 1993; Lough and Mountain, 1996). *Calanus finmarchicus*, for example is known to be an important food resource for fish larvae of haddock and Atlantic cod during critical stages (Kane, 1984; Lynch et al., 2001; Heath and Lough, 2007). At the same time, physical factors affect the formation of plankton patches and the interaction of fish larvae within these patches (Lough and Mountain, 1996). In addition to vertebrate predators (ichthyoplankton, cetaceans and basking sharks), there are also zooplanktivorous invertebrate predators. Invertebrate predators, such as siphonophores, medusae, ctenophores, chaetognaths, euphausiids, and larger copepods are all potentially capable of feeding on *C. finmarchicus* in the Gulf of Maine (Rogers et al., 1978; Sullivan and Meise, 1996; Dalsgaard et al., 2003; Rossi et al., 2008).

A common problem in studying plankton populations is their characteristic patchy distribution at different time and spatial scales. One disadvantage shared by most traditional sampling gear is their inability to resolve plankton distributions in time and spatial scales of ecological significance (Benfield et al., 1999). Traditional plankton samplers (nets, pumps, oceanographic bottles) have the ability to resolve large-scale (tens of kilometers to basin-scales) patchiness, but they are limited in resolving small-scale (centimeters to kilometers)

patchiness. In addition, data obtained from traditional techniques come from discrete, usually pooled or averaged counts of plankton sub-samples. Such samples are collected over hundreds of meters or kilometers in distance at discrete depth intervals (e.g. using multiple opening-closing nets) or from the entire water column (e.g. bongo nets). Another disadvantage of traditional techniques is the time-consuming process and high level of effort required to identify and count individuals under a microscope, plus the need for personnel who are trained in taxonomy to accurately identify the species in samples. New technological developments in optical and acoustical fields have contributed to the development of sampling techniques that allow zooplankton population dynamics to be studied at scales ranging from a few centimeters to hundreds of kilometers (Wiebe and Benfield, 2003; Benfield et al., 2007).

Each type of sampling gear has inherent advantages and disadvantages. Nets, pumps, and oceanographic bottles (i.e. Niskin) have the advantage of collecting the organism, which is of great importance for species identification and for molecular studies. While most image-forming devices cannot resolve identities to the species level, they can provide information at large group or taxonomic level, i.e. copepods, medusae, chaetognaths, amphipods, and so on. However, image-forming devices become very powerful when used along with more traditional samplers since they can be “ground-truthed” with the information collected with the traditional gear (Benfield et al., 1996; Broughton and Lough, 2006).

In areas of low species richness where the zooplankton assemblage is dominated by a few taxa, imaging devices have been proven useful. The North Atlantic and the GOM represent such areas. Surveys utilizing imaging devices like the Video Plankton Recorder (VPR) have been successful in studying plankton distributions at micro- and basin-scales (Davis et al., 1992; Benfield et al., 1996). Imaging and acoustic devices can survey plankton in a continuous non-invasive way, a particular advantage when studying fragile gelatinous taxa (Benfield et al., 1996), which are usually destroyed by pumps and nets, or poorly represented in oceanographic bottles. With the VPR it is also possible to resolve patches of several species at different spatial

scales. When combined with the right sampling program, these patches can be resolved in a three-dimensional fashion (Benfield et al., 1999). In this way, researchers gain the ability to answer more specific questions, such as how a particular species is distributed with respect to another on fine- to coarse spatial scales. The latter would help studying inter species dynamics like predator-prey interactions. One disadvantage of imaging devices however, is their relatively small sampling volume and the inherent undersampling of rare and low abundance plankters (Benfield et al., 1996). This problem is usually addressed by supplementing imaging systems with conventional sampling gear (Benfield et al., 1996; Broughton and Lough, 2006).

The VPR is the best-known example of an imaging system designed to study zooplankton. The VPR is an underwater video system capable of imaging particles in the size range of 10 microns to several centimeters and to quantify abundance from micro- to basin scales (Davis et al., 1992; Davis et al., 1996). The VPR is capable of identifying plankton to major groups (i.e. copepods, ctenophores, euphausiids). However, in areas of low species richness where the plankton biomass is dominated by few taxa, it is possible to identify the organisms in images down to genus, and in some cases to species. This is the case of the Gulf of Maine where *C. finmarchicus* dominates the mesozooplankton along with other five other species of copepods. For instance, its large size along with its characteristic shiny oil sac and prominent antennae enabled the identification of *C. finmarchicus* on VPR images with respect to smaller copepods.

Plankton patchiness is a dynamic phenomenon that results from the interaction of biological and physical processes. Since the VPR can be deployed along with auxiliary sensors (CTD, fluorometer, transmissometer, acoustics), mechanisms underlying the process of patch formation can be addressed (Gallager et al., 1996). The capabilities of the VPR also allow the three-dimensional distribution of plankton to be investigated with respect to physical and biological features.

Traditional methods do not permit the study of the relative positions of individual zooplankters. Using the VPR along with environmental sensors, allows the identification of individual targets and enables the user to associate them with location data (depth, latitude, longitude) and environmental information (temperature, salinity). This allows the user to map the three dimensional distributions of each taxon in relation to hydrological conditions. Consequently, the locations of prey patches can be mapped in relation to predator patches, which is a substantial advantage for the study of predator-prey interactions. Although this has been attempted by means of direct observations by professional divers and manned submersibles (Rogers et al., 1978; Mills, 1995), these techniques have many limitations and disadvantages.

The data used in this study were collected during December 1998 and December 1999 under the Global Ocean Ecosystem Dynamics (GLOBEC) NW Atlantic/Georges Bank Study program. The data were collected during cruises designed to quantify the distributions and abundances of diapausing *C. finmarchicus* in Wilkinson, Jordan, and Georges Basins. A single-camera VPR mounted on the BIOMAPER II towed vehicle provided a quasi-synoptic picture of the distribution of *C. finmarchicus* and its potential predators in three deep basins of the Gulf of Maine. The concurrent measurement of physical properties of the waters where *C. finmarchicus* occurred allowed an investigation of how these properties affected the distribution of this copepod.

In the present study, dense patches of *C. finmarchicus* were studied in relation to water properties for each of the three deep basins of the Gulf of Maine and for each studied period. Distributions of potential invertebrate predators of *C. finmarchicus* were also examined. The invertebrate predators capable of preying upon diapausing *C. finmarchicus* are: chaetognaths, euphausiids (primarily *Meganyctiphanes norvegica*), the large copepod *Euchaeta norvegica*, siphonophores (*Nanomia cara*, and *Agalma* sp.), ctenophores (*Mertensia* and other cydippid and lobate taxa), and medusae.

Using VPR data collected during two cruises to the GOM in December 1998 and 1999, fine- to –basin scales distributions of *C. finmarchicus* were mapped with reference to potential predators. Temporal and spatial differences observed in the distribution of *C. finmarchicus* and invertebrate predators between December 1998 and 1999 are discussed in the present work. Because environmental data (i.e. temperature, salinity) can be simultaneously collected along with the VPR, it was possible to study *C. finmarchicus* and potential predators' distributions in relation to environmental parameters and to water masses present in the Gulf of Maine.

**1.1 References**


Avent, S. R., S. M. Bollens, M. Butler, E. Horgan, and R. Rountree. 2001. Planktonic hydroids on Georges Bank: ingestion and selection by predatory fishes. Deep Sea Research Part II: Topical Studies in Oceanography **48**: 673-684.

Beardsley, R. C., A. W. Epstein, C. Chen, K. F. Wishner, M. C. Macaulay, and R. D. Kenney. 1996. Spatial variability in zooplankton abundance near feeding right whales in the Great South Channel. Deep Sea Research Part II: Topical Studies in Oceanography **43**: 1601-1625.

Benfield, M. C., C. S. Davis, P. H. Wiebe, S. M. Gallager, R. G. Lough, and N. J. Copley. 1996. Video Plankton Recorder estimates of copepod, pteropod and larvacean distributions from a stratified region of Georges Bank with comparative measurements from a MOCNESS sampler. Deep-Sea Research II: Topical Studies in Oceanography **43**: 1925-1945.

Benfield, M. C., C. S. Davis, P. H. Wiebe, S. M. Gallager, C. H. Greene, F. Werner, D. McGuillicuddy, and T. K. Stanton. 1999. Real time image analysis: instrument to model. ICES C.M.: 1999/M:06.

Benfield, M. C., P. Grosjean, P. F. Culverhouse, X. Irigoien, M. E. Sieracki, A. Lopez-Urrutia, H. G. Dam, Q. Hu, C. S. Davis, A. Hansen, C. H. Pilskaln, E. M. Riseman, H. Schultz, P. E. Utgoff, and G. Gorsky. 2007. RAPID: Research on Automated Plankton Identification. Oceanography **20**: 172-187.

Broughton, E. A. and R. G. Lough. 2006. A direct comparison of MOCNESS and Video Plankton Recorder zooplankton abundance estimates: Possible applications for augmenting net sampling with video systems. Deep Sea Research Part II: Topical Studies in Oceanography **53**: 2789-2807.

Buckley, L. J. and E. G. Durbin. 2006. Seasonal and inter-annual trends in the zooplankton prey and growth rate of Atlantic cod (*Gadus morhua*) and haddock (*Melanogrammus aeglefinus*) larvae on Georges Bank. Deep Sea Research Part II: Topical Studies in Oceanography **53**: 2758-2770.

Bucklin, A. and T. D. Kocher. 1996. Source regions for recruitment of *Calanus finmarchicus* to Georges Bank: evidence from molecular population genetic analysis of mtDNA. Deep Sea Research Part II: Topical Studies in Oceanography **43**: 1665-1681.

Campbell, R. W. and J. F. Dower. 2008. Depth distribution during the life history of *Neocalanus plumchrus* in the Strait of Georgia. Journal of Plankton Research **30**: 7-20.

Clarke, G. L. 1940. Comparative richness of zooplankton in coastal and offshore areas of the atlantic. Biological Bulletin **78**: 226-255.

Conover, R. J. 1988. Comparative life histories in the genera *Calanus* and *Neocalanus* in high latitudes of the northern hemisphere. Hydrobiologia **167/168**: 127-142.

Conversi, A., S. Piontkovski, and S. Hameed. 2001. Seasonal and interannual dynamics of *Calanus finmarchicus* in the Gulf of Maine (Northeastern US shelf) with reference to the North Atlantic Oscillation. Deep Sea Research Part II: Topical Studies in Oceanography **48**: 519-530.

Dale, T., S. Kaartvedt, B. Ellertsen, and R. Amundsen. 2001. Large-scale oceanic distribution and population structure of Calanus finmarchicus, in relation to physical environment, food and predators. Marine Biology **139**: 561.

Dalsgaard, J., M. St. John, G. Kattner, D. Müller–Navarra and W. Hagen. 2003. Fatty acid trophic markers in the pelagic marine environment: a review. Advances in Marine Biology **46**: 225-340.

Davis, C. S. 1984. Predatory control of copepod seasonal cycles on Georges Bank. Marine Biology **82**: 31-40.

Davis, C. S. 1987. Zooplankton life cycles. *In* Backus R. H. and D. W. Bourne (eds). 1987. Georges Bank. Cambridge, Ma, MIT Press**:** 256-267.

Davis, C. S., S. M. Gallager, M. S. Berman, L. R. Haury, and J. R. Strickler. 1992. The video plankton recorder (VPR): Design and initial results. Archiv für Hydrobiologie Beiheft Ergebnisse der Limnologie **36**: 67-81.

Davis, C. S., S. M. Gallager, M. Marra, S. W. Kenneth. 1996. Rapid visualization of plankton abundance and taxonomic composition using the Video Plankton Recorder. Deep Sea Research Part II: Topical Studies in Oceanography **43**: 1947-1970.

Durbin, E. G. and M. C. Casas. 2006. Abundance and spatial distribution of copepods on Georges Bank during the winter/spring period. Deep Sea Research Part II: Topical Studies in Oceanography **53**: 2537-2569.

Durbin, E. G., S. L. Gilman, R. G. Campbell, and Ann G. Durbin. 1995. Abundance, biomass, vertical migration and estimated development rate of the copepod *Calanus finmarchicus* in the southern Gulf of Maine during late spring. Continental Shelf Research **15**: 571-591.

Fish, C. J. 1936. The biology of *Calanus finmarchicus* in the Gulf of Maine and Bay of Fundy. Biological Bulletin **70**: 118-141.

Gallager, S. M., C. S. Davis, A. W. Epstein, A. Solow, and R. C. Beardsle. 1996. High-resolution observations of plankton spatial distributions correlated with hydrography in the Great South Channel, Georges Bank. Deep Sea Research Part II: Topical Studies in Oceanography **43**: 1627-1663.

Gislason, A., K. Eiane, and P. Reynisson. 2007. Vertical distribution and mortality of *Calanus finmarchicus* during overwintering in oceanic waters southwest of Iceland. Marine Biology **150**: 1253-1263.

Greene, C. H. and A. J. Pershing. 2000. The response of *Calanus finmarchicus* populations to climate variability in the Northeast Atlantic: basin-scale forcing associated with the North Atlantic Oscillation. ICES Journal of Marine Science **57**: 1536-1544.

Greene, C. H., A. J. Pershing, A. Conversi, B. Planque, C. Hannah, D. Sameoto, E. Head, P. C. Smith, P.C. Reid, J. Jossi, D. Mountain, M. C. Benfield, P. H. Wiebe, and E. Durbin. 2003. Trans-Atlantic responses of *Calanus finmarchicus* populations to basin-scale forcing associated with the North Atlantic Oscillation. Progress in Oceanography **58**: 301-312.

Haury, L. R., J. A. McGowan, and P. H. Wiebe. 1978. Patterns and processes in the time-space scales of plankton distributions. Spatial pattern in plankton communities. J. H. Steele (*ed*). New York, Plenum Press. **3:** 277-327.

Heath, M. R. and R. G. Lough. 2007. A synthesis of large-scale patterns in the planktonic prey of larval and juvenile cod (*Gadus morhua*). Fisheries Oceanography **16**: 169-185.

Hirche, H. J. 1996. Diapause in the marine copepod, *Calanus finmarchicus* -a review. Ophelia **44**: 129-143.

Irigoien, X. 2004. Some ideas about the role of lipids in the life cycle of *Calanus finmarchicus*. Journal of Plankton Research **26**: 259-263.

Johnson, C. L., A. W. Leising, J. A. Runge, E. J. H. Head, P. Pepin, S. Plourde, and E. G. Durbin. 2008. Characteristics of *Calanus finmarchicus* dormancy patterns in the Northwest Atlantic. ICES Journal of Marine Science **65**: 339-350.

Johnson, C., J. Pringle, and C. Chen. 2006. Transport and retention of dormant copepods in the Gulf of Maine. Deep Sea Research Part II: Topical Studies in Oceanography **53**: 2520-2536.

Kaartvedt, S. 1996. Habitat preference during overwintering and timing of seasonal vertical migration of *Calanus finmarchicus*. Ophelia **44**: 145-156.

Kane, J. 1984. The feeding habits of co-occurring cod and haddock larvae from Georges Bank. Marine Ecology Progress Series **16**: 9-20.

Kenney, R. D., H. E. Winn, and M. C. Macaulay. 1995. Cetaceans in the Great South Channel, 1979-1989: right whale (*Eubalaena glacialis*). Continental Shelf Research **15**: 385-414.

Li, X., J. D. J. McGillicuddy, E. G. Durbin, and P. H. Wiebe. 2006. Biological control of the vernal population increase of *Calanus finmarchicus* on Georges Bank. Deep Sea Research Part II: Topical Studies in Oceanography **53**: 2632-2655.

Lough, R. G. and D. G. Mountain. 1996. Effect of small-scale turbulence on feeding rates of larval cod and haddock in stratified water on Georges Bank. Deep Sea Research Part II: Topical Studies in Oceanography **43**: 1745-1772.

Lynch, D. R., W. C. Gentleman, D. J. McGillicuddy Jr., and C. S. Davis. 1998. Biological/physical simulations of *Calanus finmarchicus* population dynamics in the Gulf of Maine. Marine Ecology Progress Series **169**: 189-210.

Lynch, D. R., C. V. W. Lewis, and F. E. Werner. 2001. Can Georges Bank larval cod survive on a calanoid diet? Deep Sea Research Part II: Topical Studies in Oceanography **48**: 609-630.

Meise, C. J. and J. E. O'Reilly. 1996. Spatial and seasonal patterns in abundance and age-composition of *Calanus finmarchicus* in the Gulf of Maine and on Georges Bank. Deep-Sea Research II: Topical Studies in Oceanography **43**: 1473-1501.

Miller, C. B. 2004. Biological Oceanography. Malden, MA, Blackwell Publishing. 402 p.

Miller, C. B., D. R. Lynch, F. Carlotti, W. Gentleman, and C. V. W. Lewis. 1998. Coupling of an individual-based population dynamic model of *Calanus finmarchicus* to a circulation model for the Georges Bank region. Fisheries Oceanography **7**: 219-234.

Mills, C. E. 1995. Medusae, siphonophores, and ctenophores as planktivorous predators in changing global ecosystems. ICES Journal of Marine Sciences **52**: 575-581.

Ohman, M. D., K. Eiane, E. G. Durbin, J. A. Runge, and H. J. Hirche. 2004. A comparative study of *Calanus finmarchicus* mortality patterns at five localities in the North Atlantic. ICES Journal of Marine Science **61**: 687-697.

Piontkovski, S. A., T. D. O'Brien, S. F. Umani, E. G. Krupa, T. S. Stuge, K. S. Balymbetov, O. V. Grishaeva, and A. G. Kasymov. 2006. Zooplankton and the North Atlantic Oscillation: a basin-scale analysis. Journal of Plankton Research **28**: 1039-1046.

Rogers, C. A., D.C. Biggs, and R.A. Cooper. 1978. Aggregation of the siphonophores *Nanomia cara* in the Gulf of Maine: observations from a submersible. Fisheries Bulletin **76**: 281-284.

Rossi, S., M. J. Youngbluth, C. A. Jacoby, F. Pagès, and X. Garrofè. 2008. Fatty acid trophic markers and trophic links among seston, crustacean zooplankton and the siphonophores *Nanomia cara* in Georges Basin and Oceanographer Canyon (NW Atlantic). Scientia Marina **72**: 403-416.

Saumweber, W. J. and E. G. Durbin. 2006. Estimating potential diapause duration in *Calanus finmarchicus*. Deep Sea Research Part II: Topical Studies in Oceanography **53**: 2597-2617.

Sherman, K., W. G. Smith, J. R. Green, E. B. Cohen, M. S. Berman, K. A. Marti, and J. R. Goulet. 1987. Zooplankton Production and the Fisheries of the Northeastern Shelf. *In* Backus R. H. and D. W. Bourne (eds). Georges Bank. Cambridge, Ma, MIT Press**:** 269-282.

Sullivan, B. K. and C. J. Meise. 1996. Invertebrate predators of zooplankton on Georges Bank, 1977-1987. Deep Sea Research Part II: Topical Studies in Oceanography **43**: 1503-1519.

Warn-Varnas, A., A. Gangopadhyay, J. A Hawkins, and A. R. Robinson. 2005. Wilkinson Basin area water masses: a revisit with EOFs. Continental Shelf Research **25**: 277-296.

Wiebe, P. H. and M. C. Benfield. 2003. From the Hensen net toward four-dimensional biological oceanography. Progress in Oceanography **56**: 7-136.

Wiebe, P. H., R. C. Beardsley, D. G. Mountain, and L. R. Gregory. 2006. Dynamics of plankton and larval fish populations on Georges Bank, the North Atlantic US GLOBEC study site. Deep Sea Research Part II: Topical Studies in Oceanography **53**: 2455-2456.

Winemiller, K. O. and K. A. Rose. 1993. Why do most fish produce so many tiny offspring? The American Naturalist **142**: 585-603.

Wishner, K. F., J. R. Schoenherr, R. Beardsley, and C. Chen. 1995. Abundance, distribution and population structure of the copepod *Calanus finmarchicus* in a springtime right whale feeding area in the southwestern Gulf of Maine. Continental Shelf Research **15**: 475-507.

Xue, H., F. Chai, and N. R. Pettigrew. 2000. A model study of the seasonal circulation in the Gulf of Maine. Journal of Physical Oceanography **30**: 1111-1135

# CHAPTER II

# GENERAL METHODS

## 2.1 Data Sources

Five cruises were conducted between 1997 and 1999 as part of the U. S. GLOBEC North West Atlantic/Georges Bank study (Table 2.1). Data from two cruises (OC334 and EN331) were utilized in the present study to examine the spatial distribution of *Calanus finmarchicus* in the three deep basins of the Gulf of Maine: Wilkinson Basin, Jordan Basin and Georges Basin. The cruise tracks for the cruises included in this work are depicted in Fig. 2.1.

**Table 2.1.**Cruise summary for cruises carried out in the Gulf of Maine as part of the U.S. GLOBEC NW Atlantic/Georges Bank Study, and utilized in the present analyses. Cruises were coded using the first two letters of the vessels, OC= R/V OCEANUS, EN= R/V ENDEAVOR, and cruise number. Distance of covered in the three deep basins is reported. WB= Wilkinson Basin; JB= Jordan Basin; GB= Georges Basin; Northeast Channel. Total hours of video recorded by the VPR, imaged volume, and total in-focus targets counted for all basins are also shown. Cruise data from Greene et al., 1997, 1998a, 1998b, 1999a and 1999b.

| Cruise | Dates | Distance of Track line (km) | Deep Basins covered | Hours of video | VPR total imaged volume ($m^3$) | Total in-focus targets counted |
|---|---|---|---|---|---|---|
| **EN307** | October 7-17, 1997 | 549.2 | WB, JB, GB | 61 | 8.89 | ------- |
| **OC332** | October 21-26, 1998 | 558.6 | WB, JB, GB | 82 | 69.55 | ------- |
| **OC334** | December 4-12, 1998 | 929.6 | WB, JB, GB | 37 | 61.07 | 10,593 |
| **EN330** | October 16-24, 1999 | 1085.6 | WB, JB, GB | 126 | 139.6 | ------- |
| **EN331** | December 4-12, 1999 | 876.3 | WB, JB, GB/NEC | 45 | 99.72 | 12,874 |

The BIOMAPER-II (BIo-Optical Multi-frequency Acoustical and Physical Environmental Recorder) vehicle was used to record environmental parameters. BIOMAPER-II (Fig. 2.2) is a towed, multisensory platform capable of conducting quantitative plankton/nekton distribution surveys (Wiebe et al., 2002). BIOMAPER-II incorporates acoustical and optical sensors and an environmental sensor system (ESS) consisting of a CTD and additional bio-optical sensors. A

single-camera VPR was mounted on the front of BIOMAPER-II to record plankton particles in a continuous fashion. During most deployments, BIOMAPER-II was towed in a saw-tooth vertical trajectory (tow-yo) behind the ship ( i.e. brought to depth and back to the surface repeatedly in a saw-tooth pattern), while it recorded environmental data along its track and acoustic data from five pairs of up- and down-looking echosounders operating at 43, 120, 200, 420, and 1000 kHz. Video data from the VPR were transmitted directly to the ship via an electro-optical cable, where they were stamped with a time code, and stored in 2-h S-VHS tapes for post-processing in the laboratory. Time was synchronized with the BIOMAPER-II sensors and the ship's GPS.

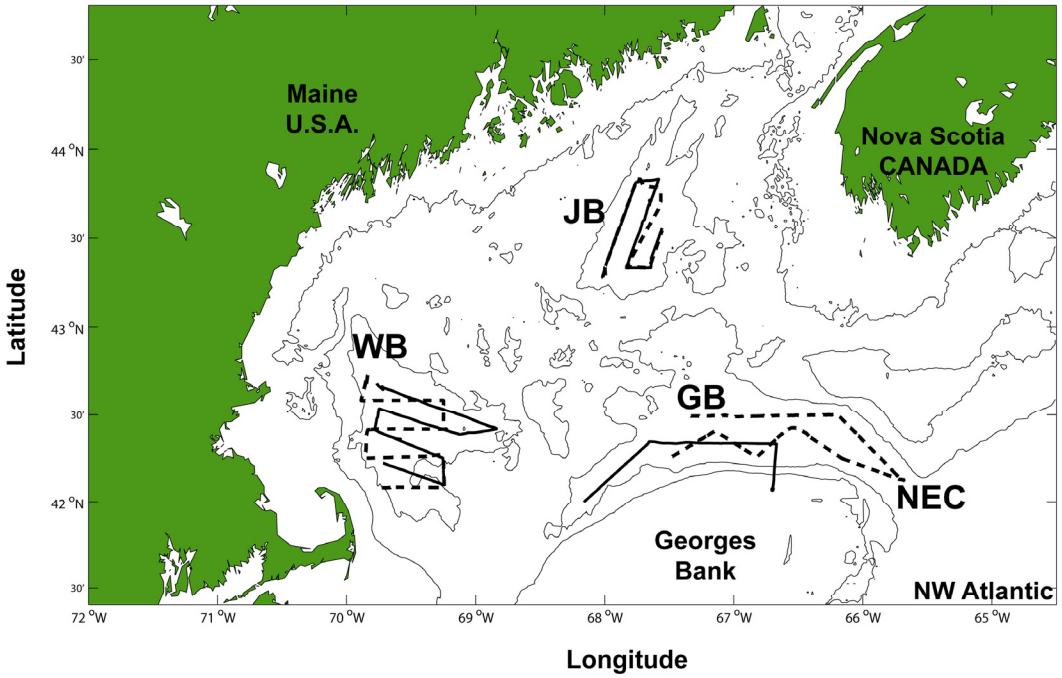


**Figure 2.1.** Gulf of Maine and its major physioregions. Cruise tracks for cruises OC334 (December 1998, solid line) and EN331 (December 1999, dash line) are depicted. WB=Wilkinson Basin; JB=Jordan Basin; GB=Georges Basin; NEC=Northeast Channel.

### 2.2 Environmental Sensor System (ESS) Data

ESS data were obtained from the official U. S. GLOBEC Georges Bank web site (http://globec.whoi.edu/globec_program.html) for cruises OC334 and EN331 (Table 2.1, Fig. 2.1). For each cruise, all ESS sections were merged into a single cruise file. ESS data were smoothed with respect to depth (pressure) information by running a 4 point running mean filter

in Matlab (see Appendix A). Latitude and longitude outliers were manually removed from the ESS file by screening the raw data in Matlab. Salinity data outliers were manually removed in a similar manner. Finally, data from each cruise's ESS file were separated for Wilkinson Basin, Jordan Basin and Georges Basin based on official start and end times of activities in each basin published in the official GLOBEC cruise reports. In this study, ESS data consisted of arrays containing 9 parameters (columns), in the order they are listed: year-day (local time), depth (meters), temperature (°C), salinity (PSU), potential density ($\sigma_0$), fluorescence (volts), light transmittance (volts), latitude (decimal degrees) and longitude (decimal degrees).

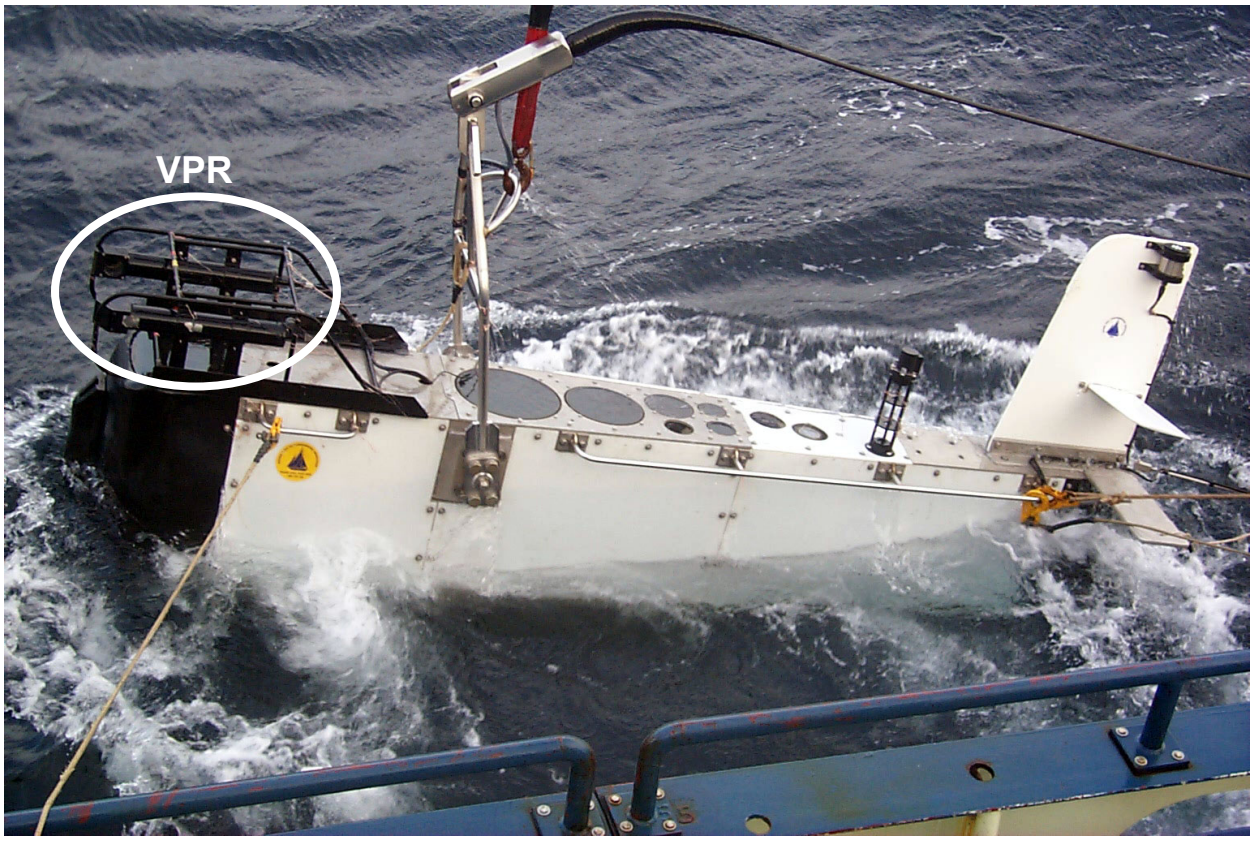


**Figure 2.2.** BIOMAPER-II being recovered after a survey in December 1998. The Video Plankton Recorder (VPR) is shown attached to the upper front part of the platform.

### 2.3 VPR Data Processing

VPR data archived on S-VHS tapes were processed for regions of interest (ROI) using custom image processing hardware and segmentation software from Imaging Technologies Inc. called Real-Time Video Plankton Recorder (RTVPR). Automatic processing of tapes is essential because the VPR collects data at 30 Hz and each image is separated into two non-overlapping fields. Of the 60 images recorded each second, the majority do not contain images of copepods or other zooplankton. Consequently, an automated technique for scanning the tapes and isolating images of valid zooplankton is essential. RTVPR is a program that allows the user to control four parameters that determined whether a valid target (zooplankton or other particle) was selected as a ROI (Greene et al., 1998a): in-focus threshold (degree of sharpness or focus that each target must have to be selected), growth scale (size of the box around a segmented target), minimum blob size (minimum size cut-off level, below which targets are not considered ROIs), and extraction threshold (how distinct a ROI must be relative to the background). For cruise OC334 the RTVPR software settings were: in-focus threshold = 15, growth scale = 150%, minimum blob-size = 175. For cruise EN331 ROI selection parameters were: in-focus threshold = 15, growth scale = 125%, minimum blob-size = 120. Each S-VHS tape was processed three times using three different thresholds in order to ensure that all valid targets were located and extracted. Due to variations in illumination, thresholds differed among cruises, and sometimes among S-VHS tapes within a cruise, but three extraction thresholds were usually within the ranges: 42-48, 60-70 and 82-110.

Once a target was selected as a ROI, it was written to disk as a Tagged Image File Format (TIFF) file and the time-stamp embedded in the video was incorporated into its file name. The time-stamp was the time of day that the ROI was imaged, expressed as the elapsed time (milliseconds) since midnight. Thus, the file name was of critical importance when merging VPR image times with the ESS data. By converting the ROI time to year-day (local EST time) each observation from the VPR could be associated with the appropriate ESS measurements

and GPS data. At the end of this process each ROI was assigned a latitude, longitude, depth and suite of ESS measurements. This array was utilized in the remaining calculations and constituted the basis to estimate the abundance of each taxon at a particular depth and location.

After ROIs were extracted from each tape, the ROIs from each of the three processing runs were combined in a single directory. Varying the threshold settings during each of these three runs meant that in many cases, the same objects were extracted three times. Subtle variations in estimation of the image times meant that, in almost all cases, duplicate ROIs had image times that were within a few milliseconds of each other. All duplicated ROIs were manually removed prior to sorting them in to their respective taxa/category. Sorting was manually done using thumbnail browsing software (ThumbsPlus Version 7, Cerious Software). Next the images were pre-processed manually to remove the most abundant images that were not of interest for this analysis — usually diatom rods and marine snow. The remaining images were manually sorted out into pre-established taxonomic categories. Out-of-focus (OOF) images were eliminated by sorting them into taxonomically-discrete out-of-focus categories. Out-of-focus images were not used in the abundance estimations, as they were not located within the in-focus field of view of the VPR. For more information on the in-focus field of view read the Abundance Estimation section below.

Typically, ROIs were classified into as many as 42 categories (including OOF and unidentified (UID) objects. The number of categories in each tape depended upon the composition of the zooplankton assemblage in the sample area. Of the 19 in-focus categories (Fig. 2.3), only those corresponding to *Calanus finmarchicus*, *Euchaeta norvegica*, chaetognaths, euphausiids, siphonophores, ctenophores, and medusae were included in the present analysis. These taxa were chosen for their potential as predators of diapausing *C. finmarchicus* in the Gulf of Maine. It is worth noting that my categories included both *C. finmarchicus* and copepods. In some cases, images of *C. finmarchicus* may have been assigned to the category “copepods” when there were insufficient recognition characteristics to

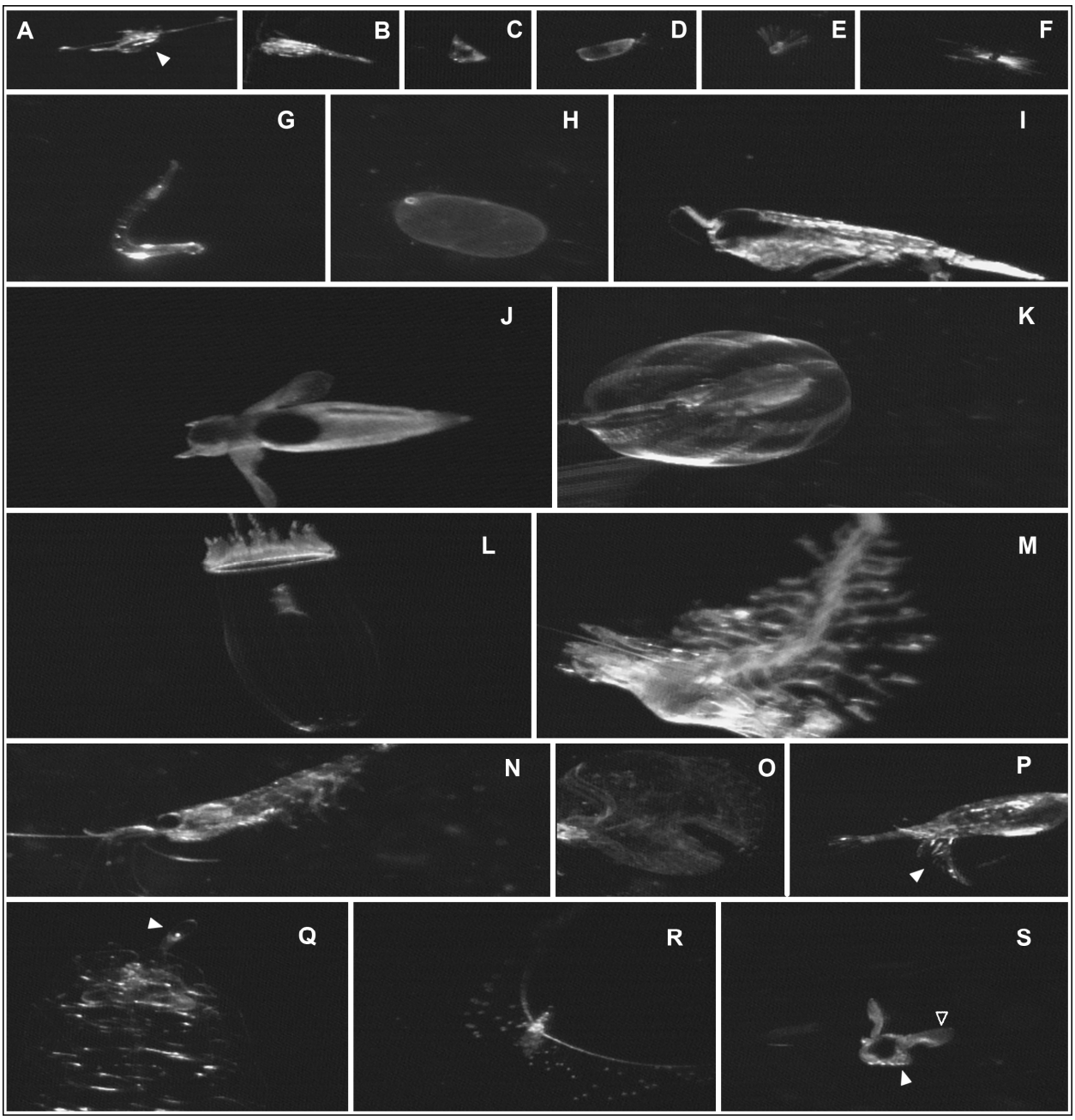


**Figure 2.3**. Examples of in-focus categories used to classify ROIs. (A) *Calanus finmarchicus*, showing its characteristic oil sac (arrowhead); (B) copepod; (C) *Evadne*-type cladoceran;(D) *Conchoecia*-type ostracod; (E) Echinoderm larvae; (F) *Trichodesmium* colony; (G) chaetognath; (H) phaeocystis; (I) hyperiid amphipod; (J) naked pteropod *Clione*; (K) ctenophore; (L) medusa; (M) polychaete; (N) euphausiid *Meganytiphanes norvegica*; (O) larvacean inside its house, probably *Oikopleura dioica*; (P) *Euchaeta norvegica*, showing its distinctive fan-like legs (arrowhead); (Q) portion of a siphonophore colony, with visible pneumatophore (arrowhead); (R) siphonula, an early stage of a siphonophore colony; (S) and the pteropod *Limacina retroversa*, with its parapodia extended (open arrowhead) and its coiled shell (white arrowhead). Aspect rations were not corrected for vertical compression on this set of images.

assign them to the ”*C. finmarchicus*” category. In some cases, the orientation of the copepod made it difficult to differentiate between *C. finmarchicus* and other copepod species. In an attempt to be very conservative in identifying and quantifying *C finmarchicus* some *Calanus*-like copepods were left in the “copepods” category.

**2.4 Abundance Estimation**

The volume imaged by the VPR per 60-s interval was the VPR image volume multiplied by 60 images per second and 60 s per interval during cruises OC332 and OC334, the VPR imaged an effective volume of 3.927 ml per frame (17 mm wide x 11.0 mm tall x 21 mm deep) or 14.1372 L $min^{-1}$. During cruises EN330 and EN331, the VPR imaged a volume of 5.1185 ml per frame (17.5 mm wide x 11.7 mm tall x 25 mm deep) which corresponds to an imaged volume of 18.466 L $min^{-1}$.

Abundances of each taxon were estimated in Matlab using 60-s bins. This routine produced an estimate of the abundance of each taxon at 60-s intervals that was centered at the depth, latitude, and longitude of the temporal midpoint of each interval. Abundances were estimated by summing the number of targets in each 60-s interval, and dividing it by the total volume sampled (imaged) during that interval. For organisms that were small relative to the total image field of view, (*C. finmarchicus*, chaetognaths, ctenophores, and *Euchaeta norvegica*), abundance estimates were a simple sum of all observations because each observation was usually the complete organism. Larger taxa were more problematic because only a fraction of the entire organism was present in an image. For these taxa a different approach was required for abundance estimation because counting part of an animal as a whole animal would lead to an overestimation of their abundance.

Image overlapping was not an issue during these cruises. BIOMAPER-II is a high-speed towing system (6-10 knots during ‘tow-yo’ mode). Mark C. Benfield (personal communication) estimates that overlapping is unlikely to occur at towing speeds equal or greater than 2 knots. The only times when this could have happen is during MOCNESS tows, which were carried out

at 1.5-2.0 knots. During MOCNESS tows BIOMAPER-II was brought to 10-30 meters below the surface and was towed horizontally while capturing data. BIOMAPER-II surveys were resumed after net tows and other CTD operations were finished. Besides the towing speed, the instrument can climb or fall at up to 10 m per minute. This would further make overlapping unlikely while BIOMAPER-II is in operational or 'tow-yo' mode.

In the cases of euphausiids and medusae, each ROI was individually examined and the portion of the organism present in each image was estimated. For example, if only the abdomen or cephalothorax of a euphausiid was completely visible that observation was given a value of 0.5. Completely visible animals were assigned a value of one. A similar approach was used for medusae, with the difference that it was more difficult to use structures as fractional landmarks. Subsequent abundance estimations were performed by summing all fractions visible in each 60-s interval and then dividing by the imaged volume. This method resulted in a more conservative estimation of euphausiid and medusae abundances.

Siphonophores were the largest and most problematic taxa imaged because only a small part of the colony was imaged by the VPR. For these organisms it was not possible to estimate the fraction of the colony present in the image because colonies lack a reliable allometric relationship between colony length and width, and in many cases, the width of the colony exceeded the field of view. In some cases, the pneumatophore — a gas inclusion located at the apex of the colony, was visible. There is only one pneumatophore per colony. Siphonophores abundance from nets is usually calculated by counting pneumatophores. I could have used a similar approach and counted only pneumatophores, however, this method would have resulted in an underestimate of siphonophore abundance because there were some tapes where siphonophores were imaged without the presence of pneumatophores. As a solution, I determined the relationship between the abundance of siphonophore pneumatophores ROIs and the abundance of all siphonophore observation ROIs for each cruise in each period and then fitted a linear regression to the data (Fig. 2.4, Table 2.2). For example, a significant linear

relationship was observed between the two categories in Wilkinson Basin during December 1998 ($R^2$=0.463, $P_{\alpha=0.05}$=0.0026) and December 1999 ($r^2$=0.2915, $P_{\alpha=0.05}$=0.0207). Using this information I calculated the abundances of siphonophores based on all instances found in each 60-s interval and then multiplied the abundance by the appropriate slope of the fitted line as a correction factor. In Wilkinson Basin, the correction factor for December 1998 was 0.09138 and for December 1999 it was 0.07393. This method resulted in a more conservative estimation of siphonophores abundance without suffering from complete loss of abundance data in regions when pneumatophores were not imaged.

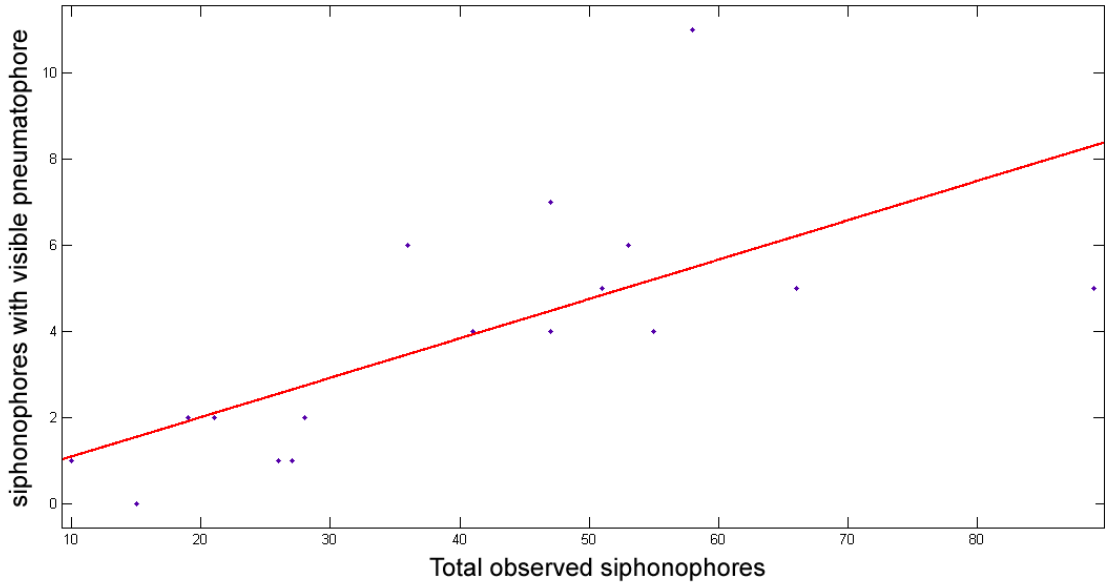


**Figure 2.4**. Scatter plot showing the linear relationship (red line) between siphonophores with visible pneumatophores versus total siphonophores observed from data recorded in Wilkinson Basin on December 1998. The slope of the fitted line (red) was used as the correction factor to estimate siphonophores abundance. Fitting statistics are reported in Table 2.2. See text for details.

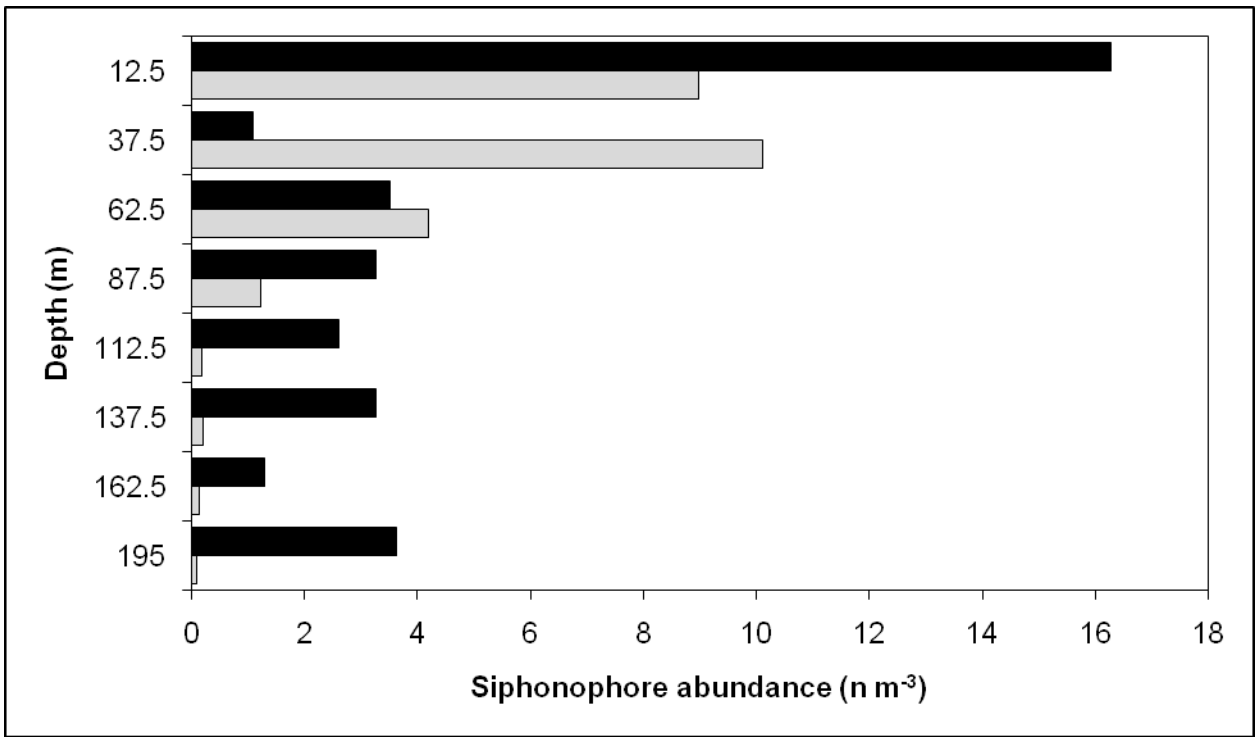


**Figure 2.5.** Comparison of siphonophore abundance estimations obtained from VPR data (black bars) and MOCNESS samples (grey bars) during December 1998 in Wilkinson Basin. VPR data in this figure correspond to the first downcast of BIOMAPPER-II, which is the closest to the end of the MOCNESS tow. MOCNESS data was provided by Nancy Copley from WHOI (pers. comm.).

**Table 2.2.** Correction factors used to estimate siphonophores abundances for Wilkinson, Jordan Basin and Georges Basins for cruises OC334 (December 1998) and EN331 (December 1999). Fitting line statistics are given between parentheses. Regressions marked with * were significant at the 0.05 level.

| | Deep Basin | | |
|---|---|---|---|
| **Cruise ID** | **Wilkinson Basin** | **Jordan Basin** | **Georges Basin** |
| **OC334** | 0.09138 ($r^2$=0.463, $P_{\alpha=0.05}$=0.0026)* | 0.3270 ($r^2$=0.4611, $P_{\alpha=0.05}$=0.0308)* | 0.1523 ($r^2$=0.8997, $P_{\alpha=0.05}$=0.0000) * |
| **EN331** | 0.07393 ($r^2$=0.2915, $P_{\alpha=0.05}$=0.0207)* | 0.01887 ($r^2$=0.009024, $P_{\alpha=0.05}$=0.7811) | 0.1189 ($r^2$=0.3079, $P_{\alpha=0.05}$=0.0111)* |

When siphonophore abundances from the first downcast of cruise OC334 calculated using the correction factor method were compared with data from the first MOCNESS samples taken at the beginning of that cruise, the abundances estimated from the VPR were generally consistent with those of the nets (Fig. 2.5). It should be emphasized that the net casts were conducted at different times from the BIOMAPPER II tows and some spatial variability is expected. The level of variability between the MOCNESS and VPR data is well within the degree of variability among replicate net tows. Variability among replicate net tows for different taxa has been estimated to be between 50 and 200% (Wiebe and Holland, 1968). However, a correspondence between VPR and MOCNESS has been reported to vary between 1:0.5 and 1:2.31 (Benfield et al., 1996). Similar methods were used to estimate abundances for Jordan Basin and Georges Basin, and the resultant correction factors are given in Table 2.2.

To summarize, abundances for *Calanus finmarchicus*, chaetognaths, ctenophores, and *Euchaeta norvegica*, expressed as numbers per meter cube (n $m^{-3}$), were calculated using:

$$A_i = N_{obs_i} / V_i \qquad (1)$$

Where *A* is the abundance in each interval, from interval i=1 to the total number of intervals in the dataset; and $N_{obs}$ is the number of occurrences of a particular taxon during the corresponding interval. In this expression each ROI was considered a single occurrence.

Abundances for euphausiids and medusae were calculated using:

$$A_i = \sum_i f_{j=1}^{n} / V_i \qquad (2)$$

Where *A* is the abundance in each interval, from interval one to the total number of intervals in the dataset; *f* is the fraction visible of the organism. In this case the fractions of all observed organisms in the interval (n) are added up for each interval instead of counting each ROI as a single occurrence.

Abundances for siphonophores were calculated using the following expression:

$$A_i = (N_{obs_i} / V_i) \cdot cf \qquad (3)$$

Where $A$ and $N_{obs}$ are the same as in equation (1). The correction factor *cf* was obtained as explained above and are summarized in Table II.

Customized Matlab routines were written for each of these calculations and are given in Appendix A.

**2.5 Spatial Mapping of Abundances**

For each taxon or category, abundance information was stored in ASCII files containing longitude, latitude, depth, and abundance. These ASCII files were used to perform a 3-D interpolation (Matlab EasyKrig V3.0 toolbox; Chu, 2004) of the data so that volumetric visualizations of the distributional patterns could be estimated. Different model parameters were used for each taxon or category in order to achieve an acceptable fit of the data to the model variogram/correlogram. Variogram model parameters used for Kriging abundances of each taxon are reported in Tables III and IV for Wilkinson Basin, Tables V and VI for Jordan Basin, for both cruises OC334 and EN331, respectively. The validity of each Kriged estimation was evaluated using statistics provided by EasyKrig V3.0 (Q1, Q2 and leaving-one-out). In most cases an acceptable fit of the predicted abundances to the measured abundances was obtained, although in some cases, the kriged data underpredicted the input data.

Wilkinson Basin data were interpolated on to a volume bounded by: latitude 42.08 – 42.68°N, 69.9 – 68.80°W and 0-250 m for OC334 and 0-240 m for EN331. Jordan Basin data were interpolated on to a volume bounded by: 43.2656 - 43.8339 °N, -68.0144 -67.5561 °W and 0-240 m for both, OC334 and EN331. Georges Basin/Northeast Channel for EN331 data were interpolated on to a volume bounded by: 42.1244 – 42.5004 °N, -67.4881 – -65.6831°W and 0-290 m. The resolution used in the latitude and longitude grid for all cruises and basins was 0.01 degrees (0.6 minutes; ~1.1 km for latitude and ~0.82 km for longitude at 43°N). Distance between long parallel cruises legs (Fig. 2.6) for cruise OC334 were approximately 14.72 km in Wilkinson Basin, and 13.62 km in Jordan Basin. In cruise EN331, distances between parallel legs were 18.75 km in Wilkinson Basin, and 15.21-20.0 km in Jordan Basin. Neither of the

cruises in Georges Basin had parallel legs, however distances oscillated between 9.9 and 27.3-47.82 km. Depth resolution was 5 m for all cruises, independently of the maximum depth imaged. Maximum depth was rounded to the closest integer number. Due to the transect design for cruise OC334 in Georges Basin, no three-dimensional kriging was performed for this transect. Instead, two-dimensional kriging was performed and the corresponding variogram/correlogram parameters used are given in Appendix B. The time resolution used for two-dimensional kriging was 0.001 days (86.4 s).

During December of 1998 and 1999, surveys in the three deep basins spanned at least one night and one day period. This provided an opportunity to examine diel vertical migration patterns of *Calanus finmarchicus* and invertebrate predators. Note that surveys were continuously covering new water and that ship was not in the same locations over day and night. Consequently differences in day and night vertical distributions are confounded with different geographical locations. To explore the possibility of vertical migration of *C. finmarchicus* and its potential invertebrate predators, calculated abundances were plotted using depth against time to observe possible diel patterns. To better visualize the possible diel patterns, datasets were split in similar sized subsections, each composed of at least one day or night period (Fig. 2.6) and each subsection was plotted individually.

The Georges Basin data collected during December 1998 were treated differently than those from other data. No 3-D Kriging could be performed for this dataset since cruise OC334 in Georges Basin consisted of only one linear transect. Therefore, 2D Kriging was performed and the variogram/correlogram model parameters used in the preparation of data for Kriging abundances for each taxon for Georges Basin in December 1998 are reported in Appendix B. This set up also allowed the investigation of diel patterns directly from the abundance distribution plots, since 2-D kriged data was plotted using depth against time.

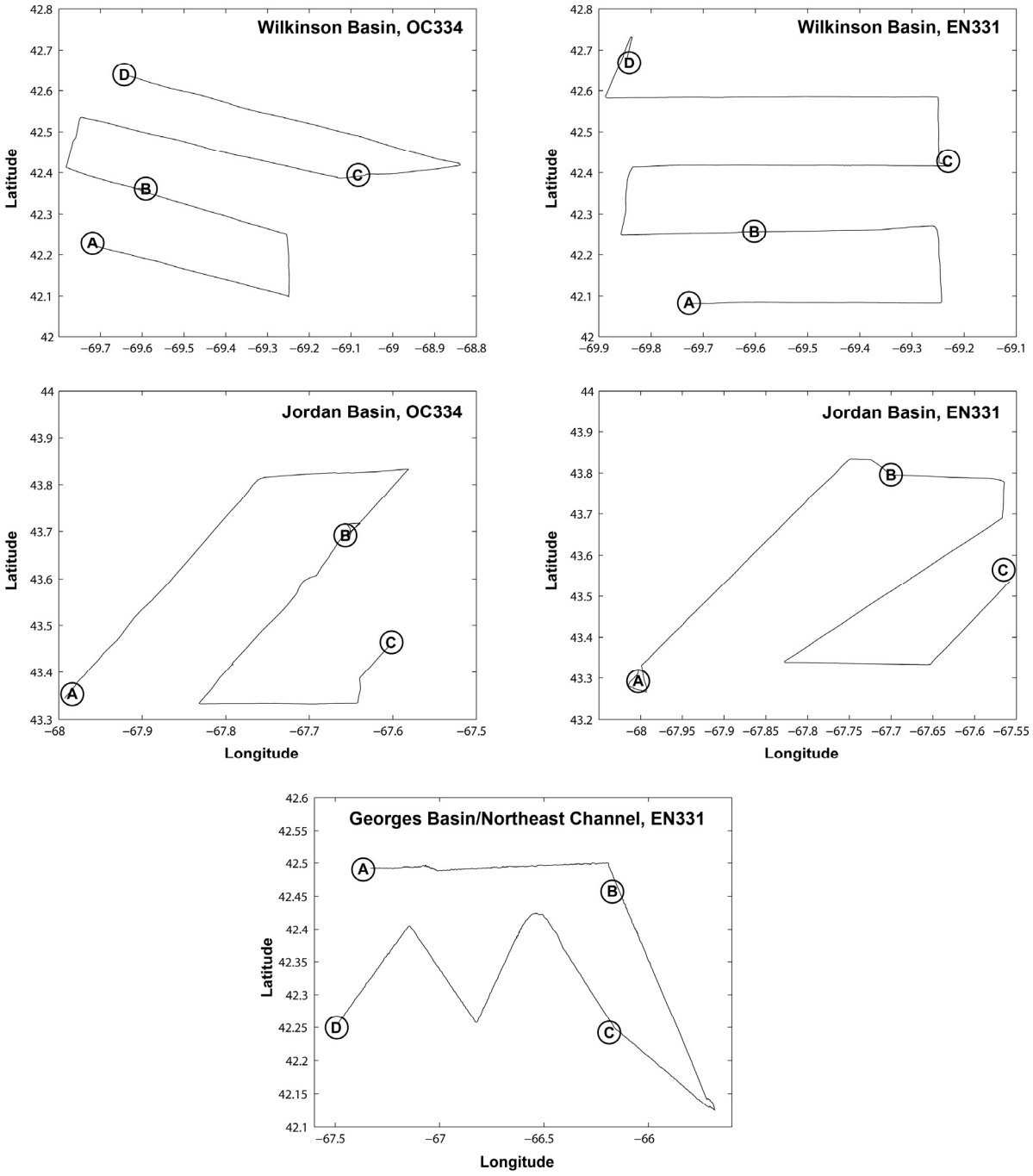


**Figure 2.6.** Sections utilized to investigate diurnal vertical migration on invertebrate predators. Capital letters correspond to letters in day-night vertical distribution figures in Chapters (IV and V). Only one linear transect was used for Georges Basin during December 1998, therefore the dataset was not split into subsections.

## 2.6 Cluster Analysis and Temperature-Salinity-Plankton Plots

Cluster analyses were performed using temperature, salinity, and depth parameters from the ESS data for each cruise and each basin to identify water masses. The centroids of the resulting water masses (clusters) were superimposed in the Temperature-Salinity-Plankton plots to study the potential relationship between plankton abundance distribution and specific water masses. More details about the cluster analysis utilized in this work are given in Chapter III (Hydrological Conditions).

## 2.7 References


Benfield, M. C., C. S. Davis, P. H. Wiebe, S. M. Gallager, R. G. Lough, and N. J. Copley. 1996. Video Plankton Recorder estimates of copepod, pteropod and larvacean distributions from a stratified region of Georges Bank with comparative measurements from a MOCNESS sampler. Deep-Sea Research II: Topical Studies in Oceanography **43**: 1925-1945.

Chu, D. 2004. EasyKrig 3.0. http://globec.whoi.edu/software/kriging/easy_krig/easy_krig.html.

Greene, C., P. Wiebe, H. Sosik, M. C. Benfield, and A. Bucklin. 1997. R/V Endeavor Cruise 307 cruise report. U. S. GLOBEC, NW Atlantic/Georges Bank Study. 47 p. http://globec.whoi.edu/globec-dir/reports/en307/greenrpt.html

Greene, C., M. C. Benfield, H. Sosik, P. Wiebe, L. McGarry, and K. Fisher. 1998a. R/V Oceanus Cruise 332 cruise report. U. S. GLOBEC, NW Atlantic/Georges Bank Study. 63 p. http://globec.whoi.edu/globec-dir/reports/oc332/oc332rpt.html

Greene, C., M. C. Benfield, H. Sosik, P. Wiebe, A. Bucklin, L. McGarry, and K. Fisher. 1998b. R/V Oceanus Cruise 334 cruise report. U. S. GLOBEC, NW Atlantic/Georges Bank Study. 58 p. http://globec.whoi.edu/globec-dir/reports/oc334/cruise-report.html

Greene, C., M. C. Benfield, P. Wiebe, and H. Sosik 1999a. R/V Endeavor Cruise 330 cruise report. U. S. GLOBEC, NW Atlantic/Georges Bank Study. 72 p. http://globec.whoi.edu/globec-dir/reports/en330/en330new.htm

Greene, C., M. C. Benfield, P. Wiebe, and H. Sosik. 1999b. R/V Endeavor Cruise 331 cruise report. U. S. GLOBEC, NW Atlantic/Georges Bank Study. 62 p. http://globec.whoi.edu/globec-dir/reports/en331/en331rpt.6sept2000.html

Wiebe, P. H. and W. R. Holland. 1968. Plankton Patchiness: Effects on Repeated Net Tows. Limnology and Oceanography **13**: 315-321.

Wiebe, P. H., T. K. Stanton, C. H. Greene, M. C. Benfield, H. M. Sosik, T. C. Austin, J. D. Warren, and T. Hammar. 2002. BIOMAPPER-II: An integrated instrument platform for coupled biological and physical measurements in coastal and oceanic regimes. IEEE Journal of Oceanic Engineering **27**: 700-716.

# CHAPTER III

# HYDROLOGICAL CONDITIONS IN THREE DEEP BASINS OF THE GULF OF MAINE DURING DECEMBER 1998 AND 1999

## 3.1 Introduction

The physical oceanography of the GOM has been intensely studied and is summarized elsewhere (i.e. Bumpus, 1973; Pringle et al., 2006). Although the circulation patterns in the GOM are known to vary seasonally and inter-annually, the mean circulation has a counterclockwise (cyclonic) motion (Brooks, 1985; Warn-Varnas et al., 2005). Some authors believe this pattern slows down and may even partially reverse during winter (Brown and Irish, 1993). Although the currents in the GOM have different components (tidal, winds), they are thought to be baroclinic (buoyancy-driven) (Brooks, 1985; Lynch et al., 1997). The variation in the water masses present in the deep basins has a strong influence in this baroclinic component, namely the shifts between the warm, salty Slope Water (SLW) and the cooler, fresher Labrador Subarctic Slope Water (LSSW). Fresh water inputs through other sources, such as river discharge, also influence the current patterns in the eastern GOM (Brown and Irish, 1993).

Local circulation in each deep basin follows a counterclockwise circulation. These recirculation gyres may be closed (Jordan Basin and Wilkinson Basin), or open (Georges Basin) (Brooks, 1985, Xue et al., 2000) and influenced to some degree by the rough topography of the GOM (Brooks, 1985). Some degree of variation in the local circulation would also be expected in the deep basins on seasonal and inter-annual scales (Brooks, 1985; Xue et al., 2000).

Normally, Maine Surface Water (MSW), Maine Intermediate Water (MIW), and the Maine Bottom Water (MBW) are present in the GOM (Hopkins and Garfield, 1979). Their distribution in the GOM varies seasonally, inter-annually (Brown and Irish, 1993), and spatially. Water masses are transported following the general current circulation and mixed in the deep basins by the local circulation patterns. In Wilkinson Basin, a fourth water mass is present during warm conditions and is known as Hot Surface Water (Warn-Varnas et al., 2005). Two other water

masses: the SLW and LSSW, are found intermittently, and their exchanges are known to vary from inter-annual to decadal scales. These water masses are of particular importance due to the biological effects they are believed to trigger in the deep basins of the GOM (MERCINA, 2001). The warm and salty SLW, which originates from the Gulf Stream, has been associated to high nutrients (Ramp et al., 1985; Townsend, 1998) favoring phytoplankton growth and consequently providing good growth conditions for *C. finmarchicus* in the GOM. The cooler, fresher LSSW, which is a mix of Labrador and Subarctic waters, is thought to be poor in nutrients and has been related to poorer growth conditions for *C. finmarchicus*. It is not clear how these water shifts affect other planktonic organisms.

Water masses have a clear influence in the hydrology of the GOM. Both, the SLW and the LSSW are associated with a hydrological regime that is influenced by an atmospheric-driven phenomenon known as the North Atlantic Oscillation (NAO) (MERCINA, 2001). While both water masses are extraneous to the GOM, their presence has a great effect in the interior of the GOM. In the GOM, positive phases of the NAO are related to the influx of the Slope Water into the GOM, while during negative phases the nutrient-rich SLW retracts and gives way to the nutrient-depleted LSSW.

Understanding the dynamic in the currents in the GOM is important because the circulation patterns are thought to have a key role in the spatial and temporal patterns in the abundances of *C. finmarchicus* (Durbin et al., 2000). Temperature and salinity data from ESS from BIOMAPER-II are utilized to identify the principal water masses present in the GOM during December of 1998 and 1999. This information will be useful when interpreting variations observed in the abundance and distribution of *C. finmarchicus* and possible interactions with its potential predators in the GOM during the late-fall/early-winter of 1998 and 1999.

**3.2 Methods**

Water masses are identified by their unique temperature–salinity signatures and by the depths they usually reside at. This is traditionally done by analyzing the shape of the temperature-

salinity profiles from CTD surveys (Warn-Varnas et al., 2005). However, cluster analysis has proven useful for identifying water masses (Kim et al., 1991) and has been used successfully to describe the water masses in the GOM (Warn-Varnas et al., 2005). Using temperature, salinity, and depth parameters from the Environmental Sensor System (ESS) data from BIOMAPER-II, cluster analysis was used to determine if water masses could be identified in each deep basin. The cluster analyses were performed in Matlab using *kmeans*, a technique that works well for large datasets. The default Euclidean distance method was used to determine the centroids of the water masses.

Up to five clusters were indicated in the cluster analysis. Five clusters were used because this corresponds to the maximum number of water masses previously described as being present in the GOM during winter time. Water masses were further identified following parameters previously reported by Warn-Varnas et al. (2005) by comparing the water characteristics from the resulting clusters and those characteristics previously reported.

### 3.3 Results

#### 3.3.1 Wilkinson Basin

Water temperatures in Wilkinson Basin during December 1999 were considerably warmer than those on December 1998. Water temperatures during December 1998 ranged from 6.18 – 8.56°C (mean±standard deviation 7.40 ± 0.73), while during December 1999, water temperatures ranged from 5.01 – 9.97°C (mean±standard deviation 8.18 ± 0.96).

Salinities were not very different between December 1998 and 1999. Salinity increased monotonically with depth during December of both years. The major differences in salinity features were actually observed in the upper 50 m and below 200 m. Fresher water (~32 to ~32.5 psu) dominated in upper 50 m in December 1998, while during 1999 the surface water was slightly saltier (33 to 33.5 psu). Below 200 m depth water masses were slightly saltier (below 34 psu) during December 1999 than during December 1998 (above 34 psu).

Following the parameters previously reported by Warn-Varnas et al. (2005), Wilkinson Basin water masses during December 1998, were identified as: Maine Surface Water (MSW), Maine Intermediate Water (MIW), Maine Bottom Water (MBW), Labrador Subarctic Slope Water (LSSW) and Slope Water (SLW) (Fig. 3.1). Similar water masses were identified in December 1999 in Wilkinson Basin (Fig. 3.2).

However, instead of the LSSW found in Wilkinson Basin during December 1998, the fifth cluster identified during December 1999 corresponded to the Maine Hot Water (MHW), a subdivision of the Maine Surface Water, and thought to be an independent water mass (Warn-Varnas et al. 2005). Water mass properties are summarized in Tables 3.1 and 3.2. The measured water characteristics were within the ranges previously reported by Warn-Varnas (2005).

**Table 3.1.** Water masses present in Wilkinson Basin during December 4-5, 1998 (cruise OC334)

| Water Mass | Number of Data Points | Depth (m) | Mean Depth | Temperature (°C) | Mean Temperature | Salinity (psu) | Mean Salinity |
|---|---|---|---|---|---|---|---|
| **MSW** | 12 201 | 0 – 38 | 13.73 | 7.78 – 8.56 | 8.15 | 31.93 – 32.68 | 32.22 |
| **MIW** | 5 799 | 38 – 87 | 63.69 | 6.38 – 8.49 | 7.65 | 31.94 – 33.08 | 32.50 |
| **MBW** | 5 693 | 87 – 132 | 109.73 | 6.18 – 8.05 | 6.79 | 32.48 – 33.70 | 33.05 |
| **LSSW** | 6 147 | 132 – 177 | 154.33 | 6.23 – 7.39 | 6.61 | 33.04 – 34.10 | 33.55 |
| **SLW** | 3 641 | 177 – 263 | 199.78 | 6.28 – 7.12 | 6.77 | 33.62 – 34.22 | 33.98 |

**Table 3.2.** Water masses present in Wilkinson Basin during December 4-5, 1999 (cruise EN331)

| Water Mass | Number of Data Points | Depth (m) | Mean Depth | Temperature (°C) | Mean Temperature | Salinity (psu) | Mean Salinity |
|---|---|---|---|---|---|---|---|
| **MHW** | 8 476 | 0-31 | 10.48 | 8.38-9.33 | 8.88 | 32.28-33.14 | 32.69 |
| **MSW** | 4 748 | 30-76 | 52.56 | 7.08-9.77 | 8.89 | 32.56-33.53 | 32.93 |
| **MIW** | 5 007 | 75-122 | 98.50 | 5.04-9.95 | 8.09 | 32.56-33.64 | 33.03 |
| **MBW** | 5 139 | 121-168 | 144.66 | 5.01-9.97 | 7.08 | 32.87-34.00 | 33.55 |
| **SLW** | 5 127 | 167-244 | 193.76 | 6.50-8.44 | 7.53 | 33.59-34.52 | 34.06 |

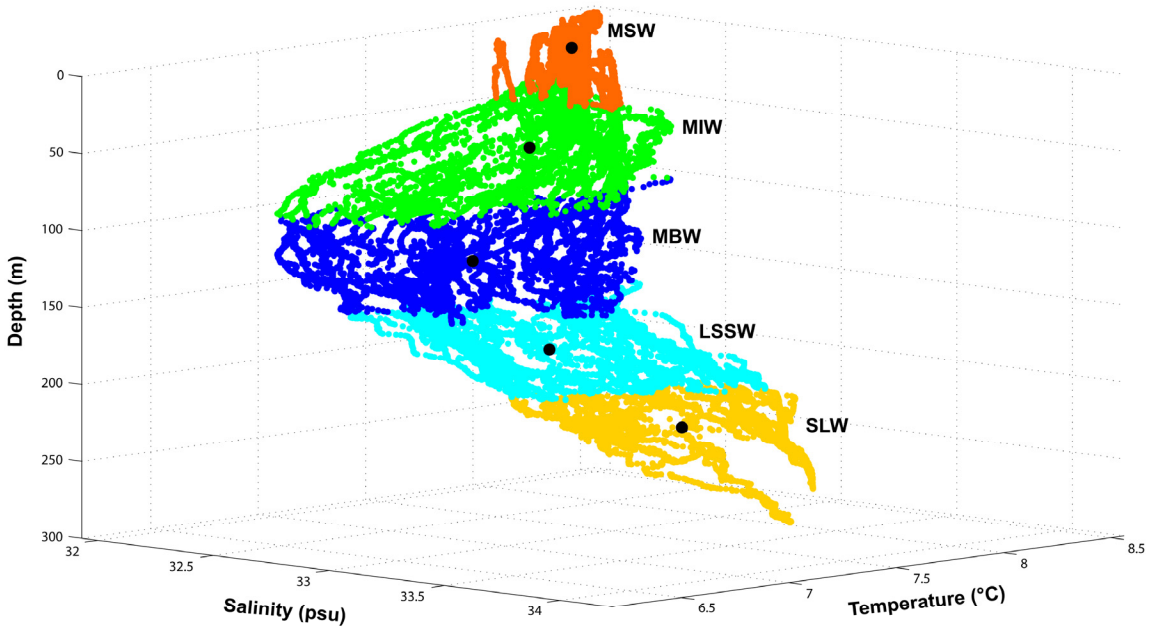


**Figure 3.1.** Water masses in Wilkinson Basin identified by the cluster analysis during December 1998. MSW=Maine Surface Water; MIW=Maine Intermediate Water; MBW=Maine Bottom Water; LSSW=Labrador Subarctic Water; SLW=Slope Water. Each point represents a discrete measurement from BIOMAPER-II.

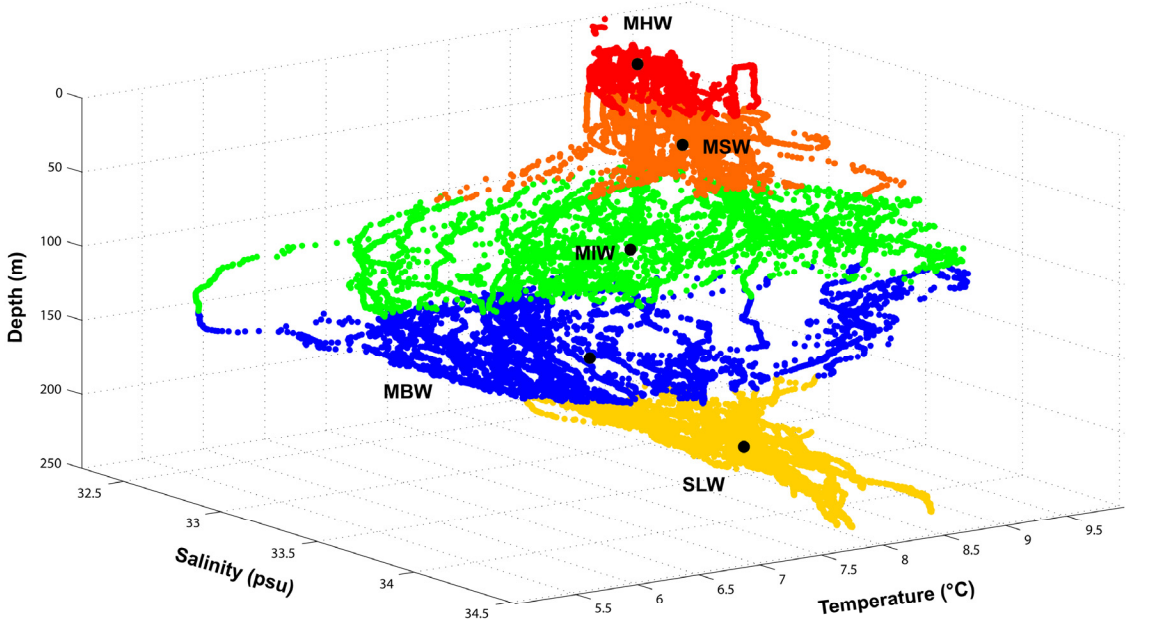


**Figure 3.2.** Water masses in Wilkinson Basin identified by the cluster analysis during December 1999. MHW=Maine Hot Water; MSW=Maine Surface Water; MIW=Maine Intermediate Water; MBW=Maine Bottom Water; SLW=Slope Water. Each point represents a discrete measurement from BIOMAPER-II.

During December 1998, Wilkinson Basin was dominated by water of ~8 – 9°C in the central to western basin, while in the mid- to eastern basin, temperatures were ~7 – 8°C down to a depth of 75 m (Fig. 3.3). These were the characteristics of the MSW and the MIW, respectively. At ~76 m, the MBW started appearing in the southeastern corner of Wilkinson Basin, which extended down to ~148 m depth. Although the cluster analysis positioned the LSSW from 132 m to 177, in the temperature distribution map, it is clear that the LSSW started appearing at about 100 m and was found in the edges of Wilkinson Basin down to approximately 200 m depth. The SLW was found mainly in the western side of the basin from ~173 m and dominated most of the Wilkinson Basin from 200 and below. The salinity distribution map helped clarify the identities and distributions of the water masses (Fig. 3.5).

During December 1999, Wilkinson Basin showed warm water (8 – ~10°C) down to 75 m (Fig. 3.4). Those were the characteristic temperatures of the MHW and the MSW. Colder water (5 – ~7.5°C), identified as MBW, started appearing at approximately 100 m at the edges of the basin during December 1999, and was ubiquitous in the northern Wilkinson Basin from ~127-148 m depth (Fig. 3.4). The same depth interval was shared by the MIW and the SLW at different regions of Wilkinson Basin. However, the MBW was identified in the depth range 121-168 m by the cluster analysis. The warmest temperatures dominated the center of Wilkinson Basin during this period, and were found in a quite well distinguishable warm “tongue” at the south of the central basin from ~100 m down to ~150 m depth. This water mass had the characteristics of the warm, salty SLW, which was confirmed by salinity distribution map (Fig. 3.6). The SLW water dominated the deepest waters of WB during December 1999.

### 3.3.2 Jordan Basin

Water temperatures recorded in Jordan Basin during December 1999 were considerably warmer than in December 1998. Water temperatures during December 1998 ranged from 6.00 – 7.70°C (mean±standard error 6.92 ± 0.36), while during December 1999 water temperature ranged from 8.10 – 10.60°C (mean±standard error 9.40 ± 0.43).

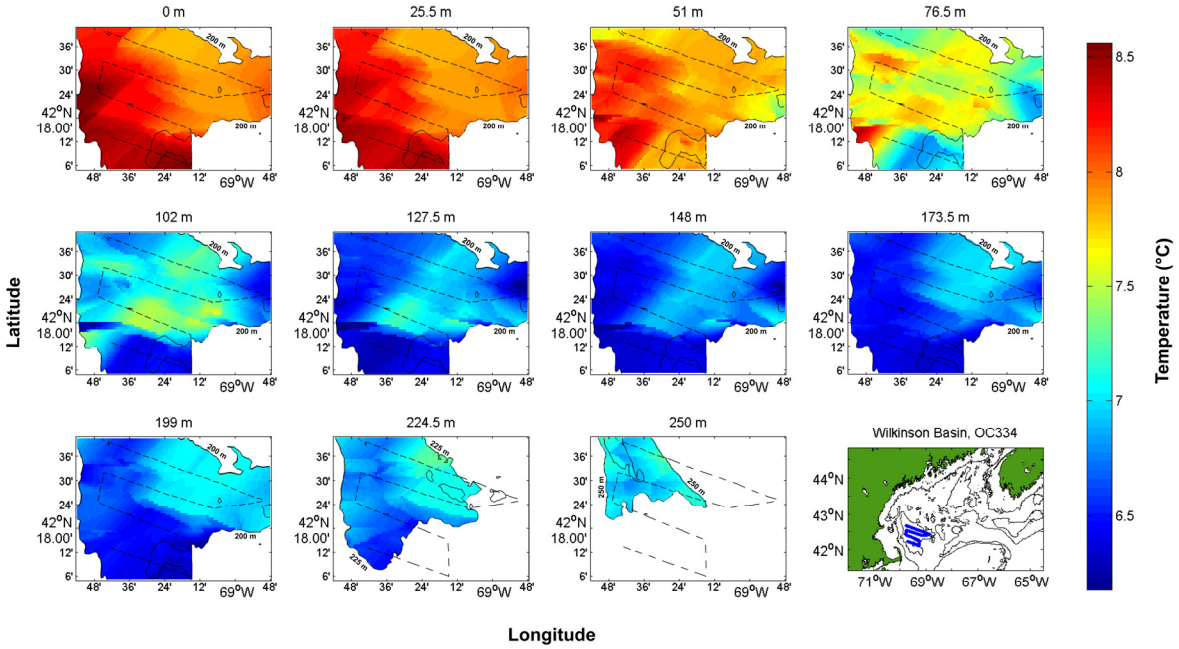


**Figure 3.3.** Temperature (°C) conditions in Wilkinson Basin during December 1998 sampled at ~25 m depth intervals. An objective interpolation method (Kriging) was used to generate the spatial fields. The maximum sampled depth was 250 m. Isobaths (solid line) and cruise track (dashed line) were superimposed for reference.

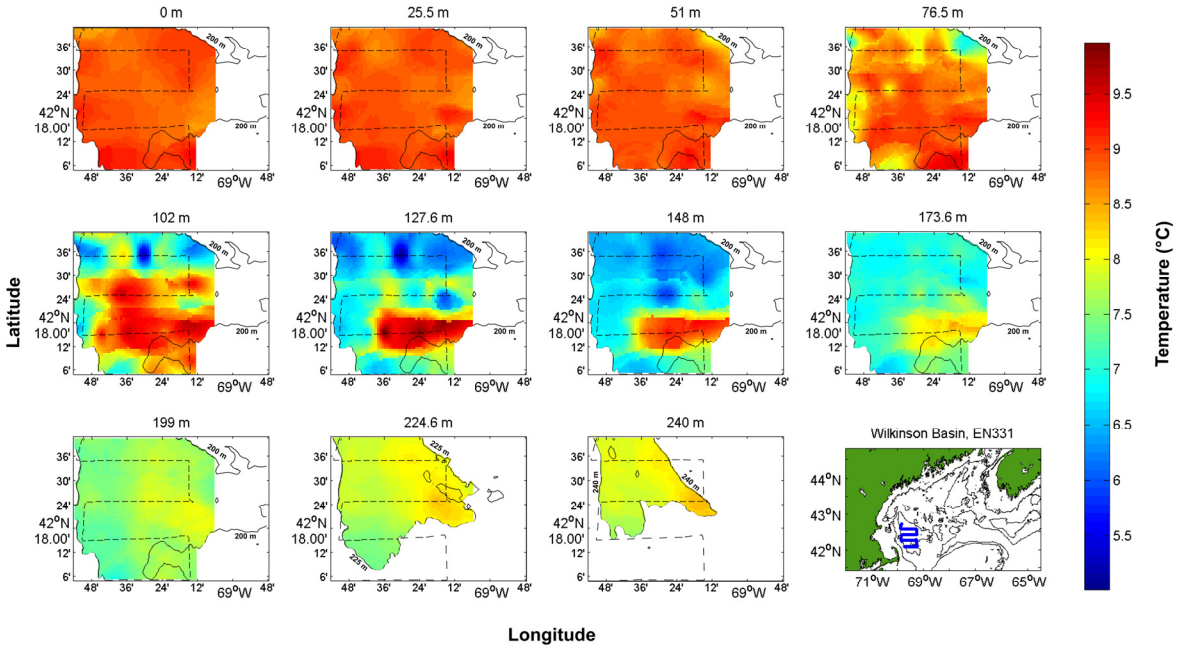


**Figure 3.4.** Temperature (°C) conditions in Wilkinson Basin during December 1999 sampled at every ~25 m intervals. An objective interpolation method (Kriging) was used to generate the spatial fields. The maximum sampled depth was 240 m. Isobaths (solid line) and cruise track (dashed line) were superimposed for reference.

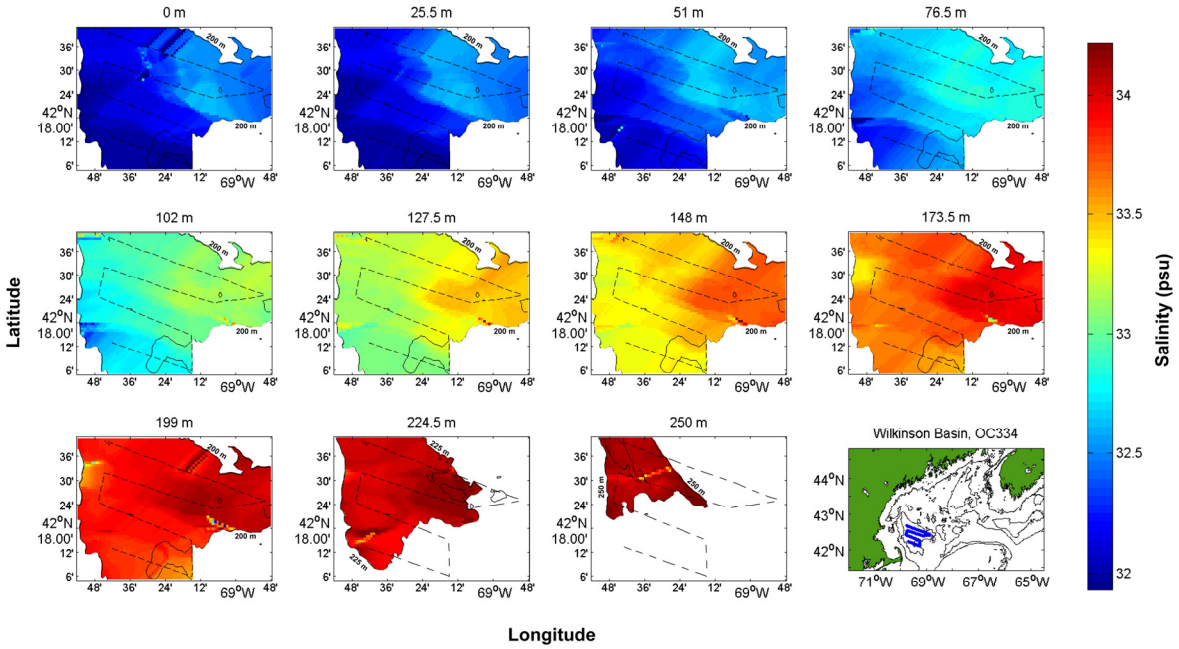


**Figure 3.5.** Salinity (psu) conditions in Wilkinson Basin during December 1998 sampled at every ~25 m depth. The maximum sampled depth was 250 m. An objective interpolation method (Kriging) was used to generate the spatial fields. Isobaths (solid line) and cruise track (dashed line) were superimposed for reference.

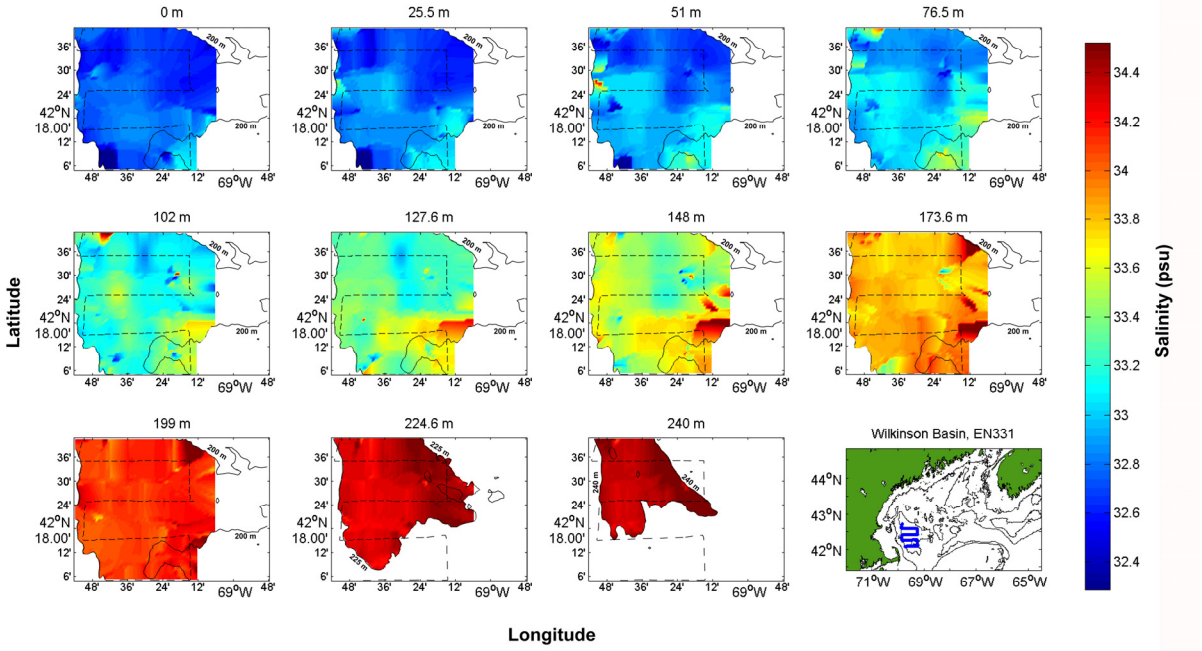


**Figure 3.6.** Salinity (PSU) conditions in Wilkinson Basin during December 1999 sampled at every ~25 m depth. The maximum sampled depth was 240 m. An objective interpolation method (Kriging) was used to generate the spatial fields. Isobaths (solid line) and cruise track (dashed line) were superimposed for reference.

Salinity differences between December 1998 and December 1999 were more subtle compared to those observed for temperature. However, fresher conditions (mean of 32.92 ± 0.79 psu) prevailed during December 1998 while saltier conditions (mean of 34.02 ± 0.37 psu) predominated during December 1999.

Five water masses were identified using cluster analysis in Jordan Basin during December 1998 and 1999 (Figs. 3.7 and 3.8). Four water masses were common during December of both years. In addition, a water mass with the characteristics of the LSSW was identified during December 1998. This water mass was absent in December 1999, however, a water mass corresponding to the MHW, was present. A summary of the identified water masses and their characteristics is given in Tables 3.3 and 3.4.

During December 1998 warmer, saltier water characteristic of MSW dominated the western half of Jordan Basin from 0 to ~25 m while cooler fresher water dominated the eastern half of the basin (Figs. 3.9 and 3.11). The MIW was located from below 25 m and down to 76 m. The 76 – 130 m depth interval was occupied by MBW. The cooler, fresher LSSW was located at 130 – 150 m depth. The LSSW was rapidly replaced by SLW, which dominated the deep waters of Jordan Basin from ~150 to 240 m during December 1998.

During December 1999 the MHW and MSW shared most of Jordan Basin from 0 to 76.5 m deep (Figs. 3.10 and 3.12). The MIW started appearing around 76.5 m and clearly disappeared at around 127.5 m. At this depth, the MBW dominated most of Jordan Basin and by 175 m it was being replaced by the SLW which dominated the basin down to 240 m deep.

### 3.3.3 Georges Basin/ Northeast Channel

Similar to the other deep basins in the Gulf of Maine, water conditions in Georges Basin during December 1998 were cooler than those observed during December 1999. During December 1998, water temperature in Georges Basin ranged from 6.36 – 9.21 °C (mean±standard error 7.41 ±0.72). During December 1999 water temperature ranged between 6.97 – 12.01 °C (mean of 9.61 ±0.56).

**Table 3.3.** Water masses present in Jordan Basin during December 9-10 1998 (cruise OC334)

| Water mass | Number of Data Points | Depth (m) | Mean Depth | Temperature (°C) | Mean Temperature | Salinity (psu) | Mean Salinity |
|---|---|---|---|---|---|---|---|
| **MSW** | 7 704 | 0-38 | 13.53 | 6.82-7.70 | 7.11 | 31.64-32.68 | 32.12 |
| **MIW** | 2 790 | 38-87 | 63.17 | 6.15-7.65 | 7.27 | 32.10-33.80 | 32.64 |
| **MBW** | 3 201 | 87-133 | 110.61 | 6.00-7.50 | 6.72 | 32.59-33.80 | 33.30 |
| **LSSW** | 3 988 | 133-177 | 154.58 | 6.29-6.89 | 6.59 | 33.27-34.03 | 33.69 |
| **SLW** | 2 596 | 177-248 | 200.02 | 6.36-6.89 | 6.73 | 33.64-34.10 | 33.95 |

**Table 3.4.** Water masses present in Jordan Basin during December 8-9 1999 (cruise EN331)

| Water mass | Number of Data Points | Depth (m) | Mean Depth | Temperature (°C) | Mean Temperature | Salinity (psu) | Mean Salinity |
|---|---|---|---|---|---|---|---|
| **MHW** | 5 910 | 0-35 | 11.79 | 9.36-10.02 | 9.65 | 33.50-33.89 | 33.68 |
| **MSW** | 3 088 | 35-82 | 58.82 | 9.36-10.13 | 9.71 | 33.59-34.04 | 33.77 |
| **MIW** | 3 080 | 82-128 | 105.00 | 8.11-10.62 | 9.49 | 33.68-34.49 | 34.01 |
| **MBW** | 3 484 | 128-173 | 150.73 | 8.12-10.63 | 8.82 | 33.98-34.63 | 34.31 |
| **SLW** | 3 179 | 173-242 | 195.00 | 8.43-9.89 | 9.18 | 34.27-34.77 | 34.61 |

Salinity was generally lower during December 1998 than during December 1999 in Georges Basin. Salinities during December 1998 ranged between 31.68 – 34.82 PSU (mean±standard deviation 33.20 ± 1.07), while during December 1999 salinities were 32.63 – 35.18 PSU (mean±standard deviation 33.99 ±0.87).

The cluster analysis clearly identified five water masses in Georges Basin during December 1998 (Figs. 3.13). A summary of the characteristics of these water masses is given in Table 3.5. The first 45 m of the water column were dominated by the warm waters of the MSW, especially to the western portion of the transect (Fig. 3.15). The next layer was shown as a narrow band, which is evident in the salinity plot (Fig. 3.16), and corresponded to the MIW. The MBW was located immediately below this layer, which was found between 100 – 157 m. From 157 m and down, Georges Basin was dominated by two water masses: SLW and the transient LSSW. During December 1998, the LSSW was located above the SLW, especially in the easternmost portion of Georges Basin. The SLW started disappearing towards the western

portion of the basin, limited perhaps by the rising bottom topography and the front created by the LSSW, which was still present in the western portion of Georges Basin.

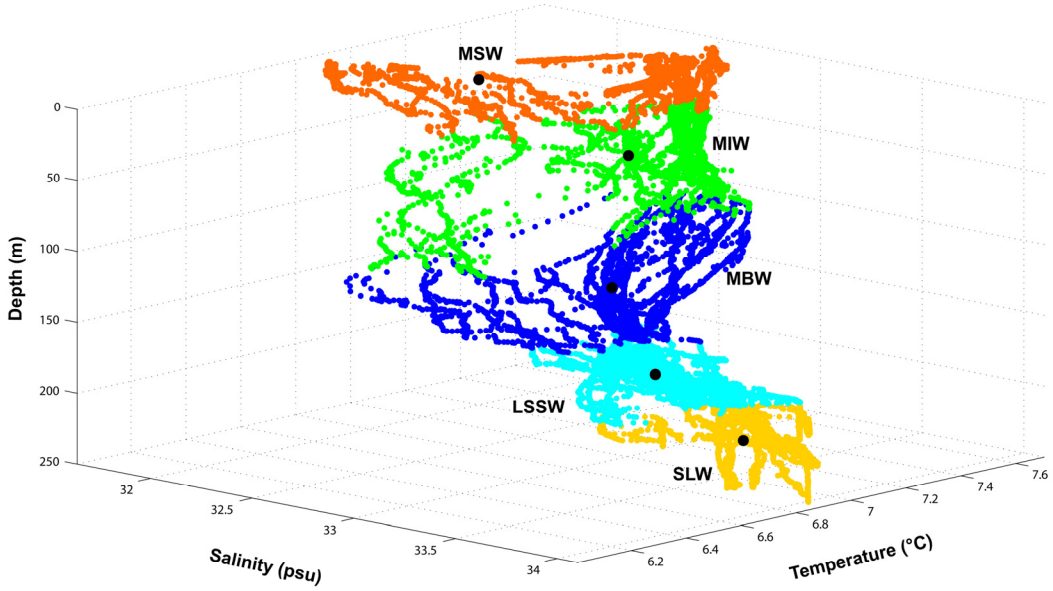


**Figure 3.7.** Water masses in Jordan Basin during December 1998. MSW=Maine Surface Water; MIW=Maine Intermediate Water; MBW=Maine Bottom Water; LSSW=Labrador Subarctic Water; SLW=Slope Water.

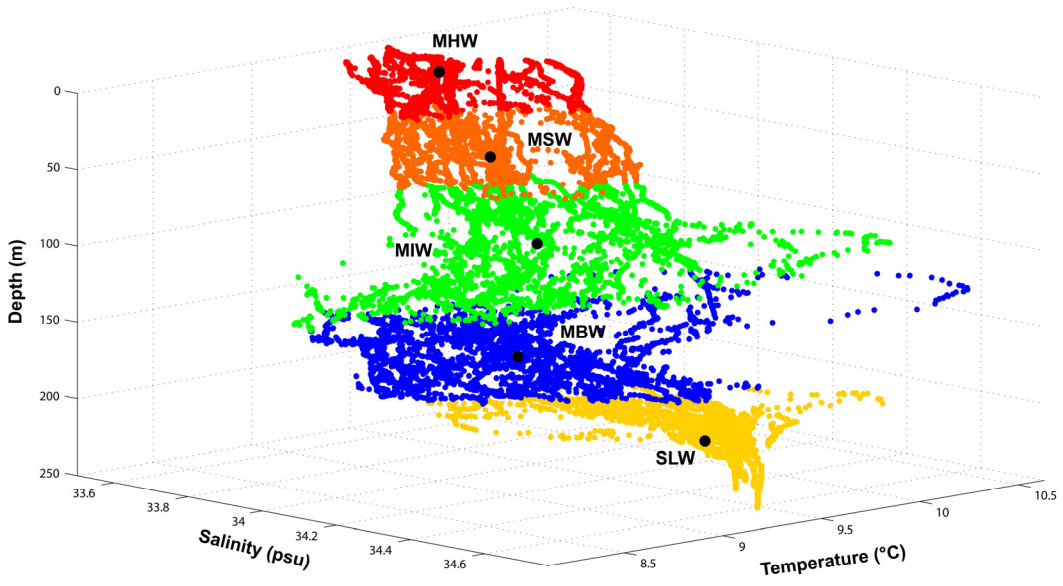


**Figure 3.8.** Water masses in Jordan Basin during December 1999. MHW=Maine Hot Water; MSW=Maine Surface Water; MIW=Maine Intermediate Water; MBW=Maine Bottom Water; SLW=Slope Water.

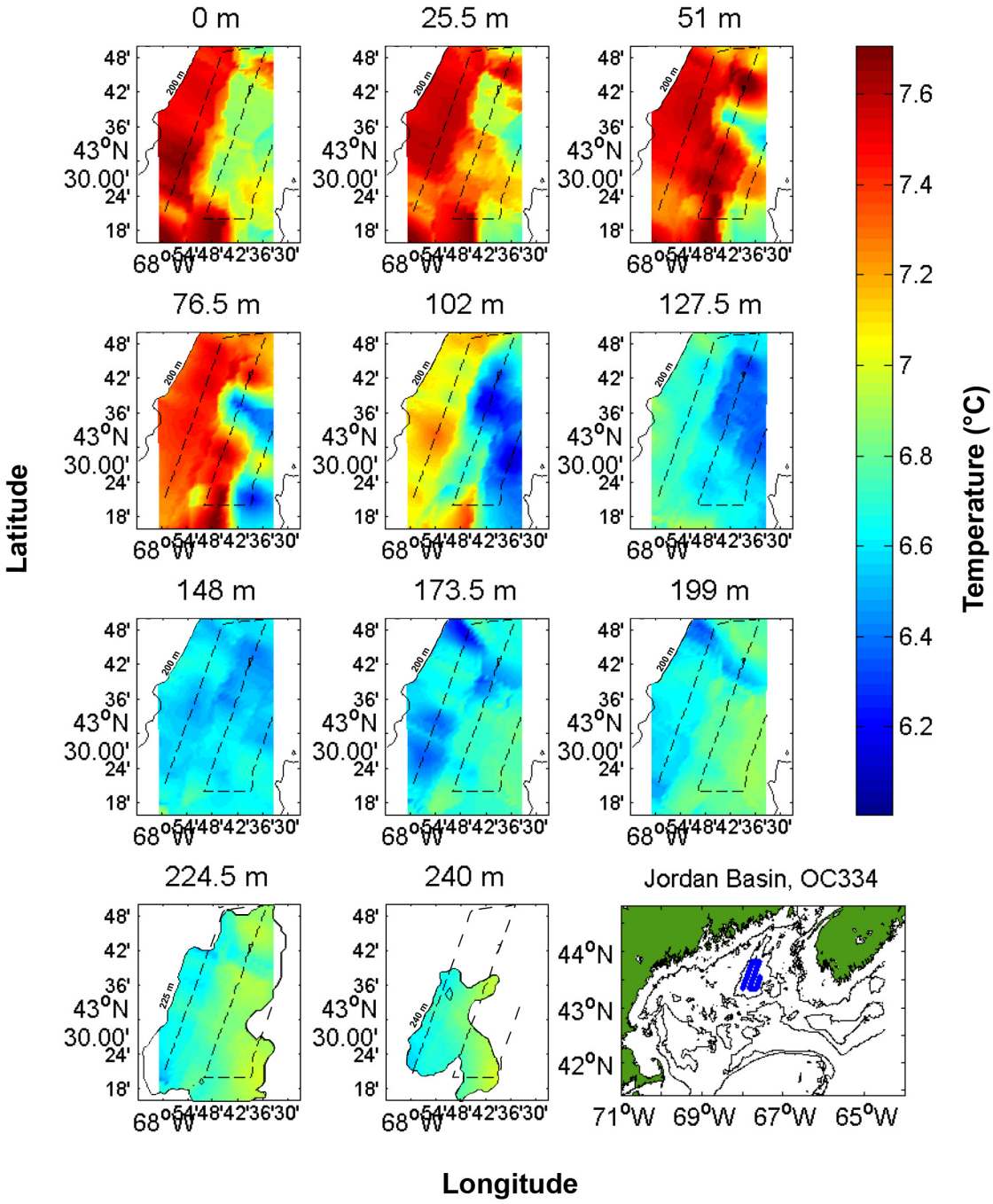


**Figure 3.9.** Temperature (°C) conditions in Jordan Basin during December 1998 sampled at every ~25 m depth. Maximum depth was 240 m. Isobaths (solid line) and cruise track (dashed line) were superimposed for reference.

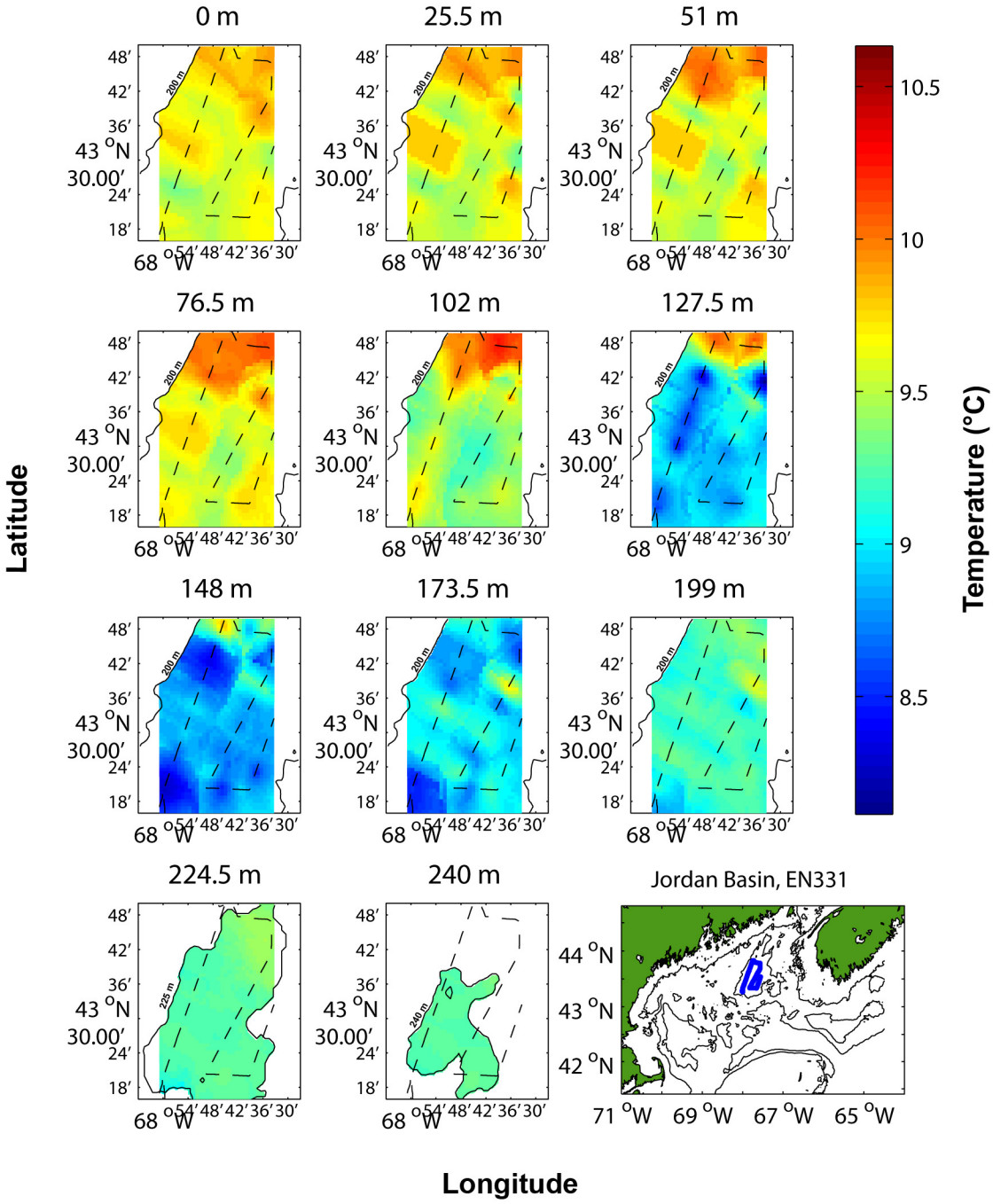


**Figure 3.10.** Temperature (°C) conditions in Jordan Basin during December 1999 sampled at every ~25 m depth. Maximum depth was 240 m. Isobaths (solid line) and cruise track (dashed line) were superimposed for reference.

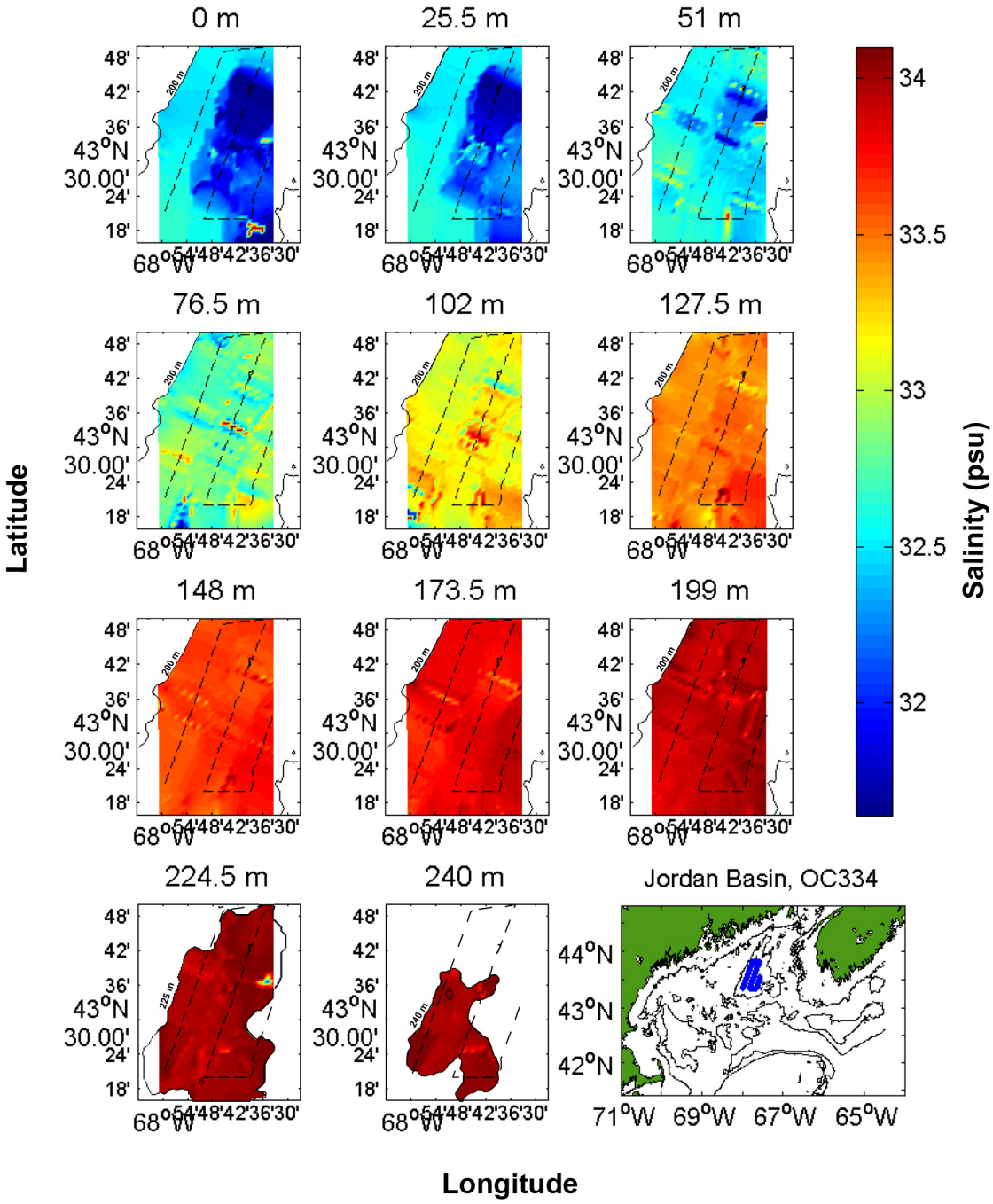


**Figure 3.11.** Salinity (PSU) conditions in Jordan Basin during December 1998 sampled at every ~25 m depth. Maximum depth was 240 m. Isobaths (solid line) and cruise track (dashed line) were superimposed for reference.

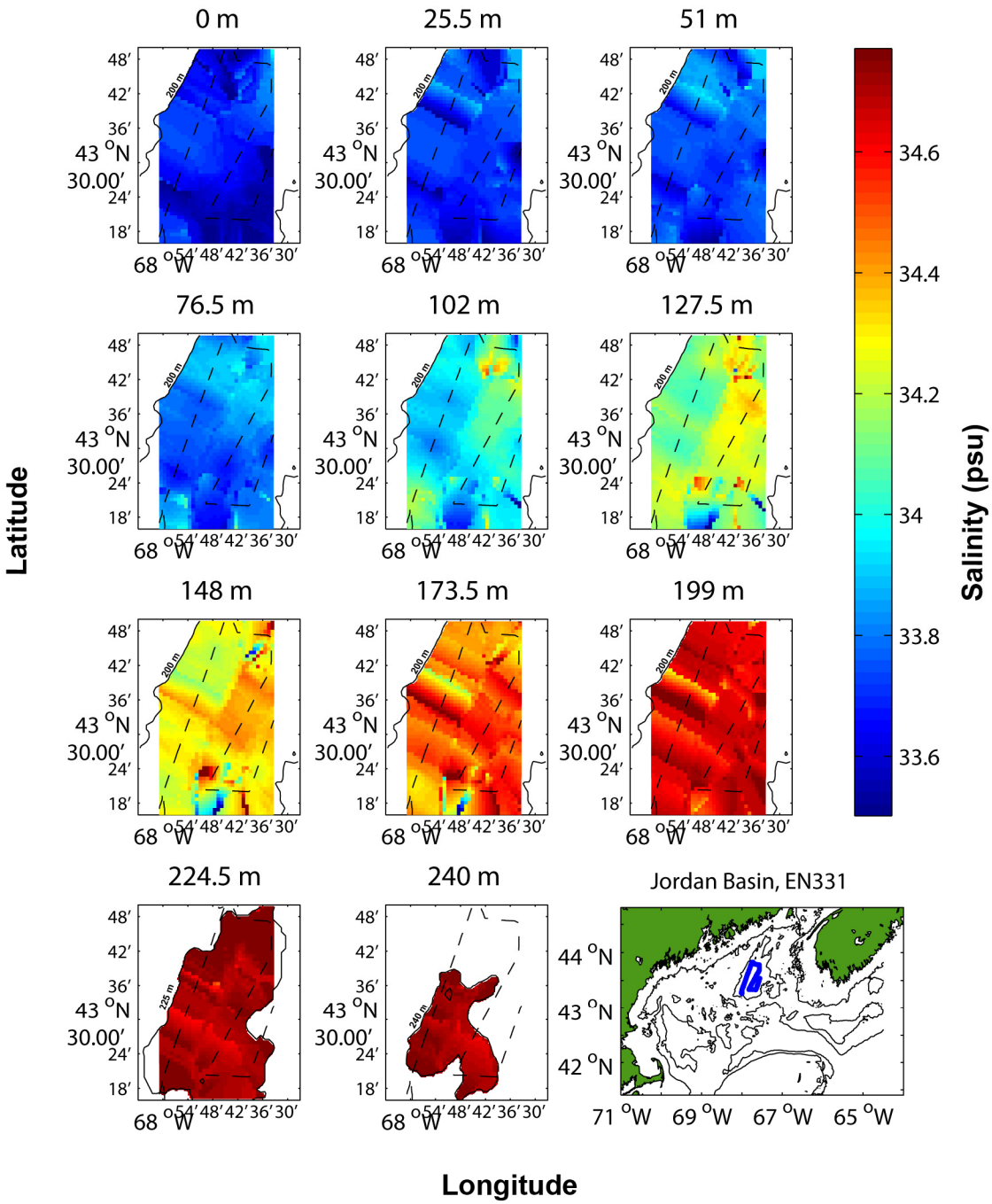


**Figure 3.12.** Salinity (PSU) conditions in Jordan Basin during December 1999 sampled at every ~25 m depth. Maximum depth was 240 m. Isobaths (solid line) and cruise track (dashed line) were superimposed for reference.

The water in Georges Basin was not clearly stratified during December 1999, probably due to the stormy conditions experienced during the survey period (Greene et al., 1999b). The complicated patterns of temperature distribution made it difficult to observe the water masses present in the region. Salinity features in December 1999 revealed a more stratified water column than temperatures did. Salinity increased with depth both in the Georges Basin and in the Northeast Channel regions. However, the cluster analysis yielded five well differentiated water masses: MSW, MIW, MBW, SLW and LSSW (Fig. 3.14, Table 3.6).

In contrast to the conditions in December 1998, during December 1999 the SLW laid on top of the LSSW (Fig. 3.17). Warm waters dominated over all in the Georges Basin/Northeast Channel area. However, the warmest waters were present at mid-depths, both in Georges Basin and in the Northeast Channel. The warmest temperatures, likely of SLW origin, extended from the Northeast Channel into the Georges Basin. Despite the saltier nature of the bottom water, this cool water mass most likely corresponded to the remnants of the LSSW. The cooler, fresher waters in the western Georges Basin were of Maine Surface Water origin (Figs. 3.17 and 3.18).

**3.4 Discussion**

The hydrographic conditions in the three basins of the GOM during December of 1998 and December 1999 were very different. The Gulf was generally colder and fresher during December 1998 while during December 1999 the Gulf was warmer and saltier. These differences were reflected in the general composition of the water masses in the Gulf. Two water masses, the Labrador Subarctic Slope Water (LSSW) and the Slope Water (SLW), were probably responsible for most of these contrasting differences. During December 1998, the LSSW was found in all three deep basins of the Gulf of Maine, however, only the remnants of the LSSW was found in the Northeast Channel during December 1999. My results are in close agreement with the observations of LSSW in the deep basins reported by the MERCINA group (2001) for the same periods.

**Table 3.5.** Water masses present in Georges Basin during December 9-10 1998 (cruise OC334)

| Water mass | Number of Data Points | Depth (m) | Mean Depth | Temperature (°C) | Mean Temperature | Salinity (psu) | Mean Salinity |
|---|---|---|---|---|---|---|---|
| **MSW** | 6 480 | 0-45 | 16.08 | 6.99-9.21 | 8.15 | 31.67-32.43 | 32.13 |
| **MIW** | 3 292 | 45-102 | 73.98 | 6.37-8.63 | 7.29 | 32.09-33.72 | 32.61 |
| **MBW** | 3 049 | 102-158 | 130.65 | 6.35-7.43 | 6.71 | 32.66-34.80 | 33.60 |
| **SSLW** | 3 276 | 158-217 | 185.17 | 6.73-7.52 | 7.05 | 33.58-34.81 | 34.46 |
| **SLW** | 2 152 | 217-298 | 248.40 | 6.79-7.27 | 6.94 | 34.66-34.82 | 34.80 |

**Table 3.6.** Water masses present in Georges Basin-NE Channel during December 8-9 1999 (cruise EN331)

| Water mass | Number of Data Points | Depth (m) | Mean Depth | Temperature (°C) | Mean Temperature | Salinity (psu) | Mean Salinity |
|---|---|---|---|---|---|---|---|
| **MSW** | 10 817 | 0-42 | 15.20 | 8.29-10.10 | 9.60 | 32.62-33.69 | 33.10 |
| **MIW** | 5 737 | 42-95 | 69.53 | 7.24-11.72 | 9.62 | 32.83-34.65 | 33.43 |
| **MBW** | 6 139 | 95-146 | 120.98 | 7.03-12.01 | 10.03 | 33.21-35.11 | 34.40 |
| **SLW** | 6 223 | 146-197 | 171.88 | 7.29-11.40 | 9.58 | 34.22-35.18 | 34.95 |
| **SSLW** | 3 854 | 197-290 | 222.42 | 6.97-10.33 | 9.09 | 34.79-35.17 | 35.07 |

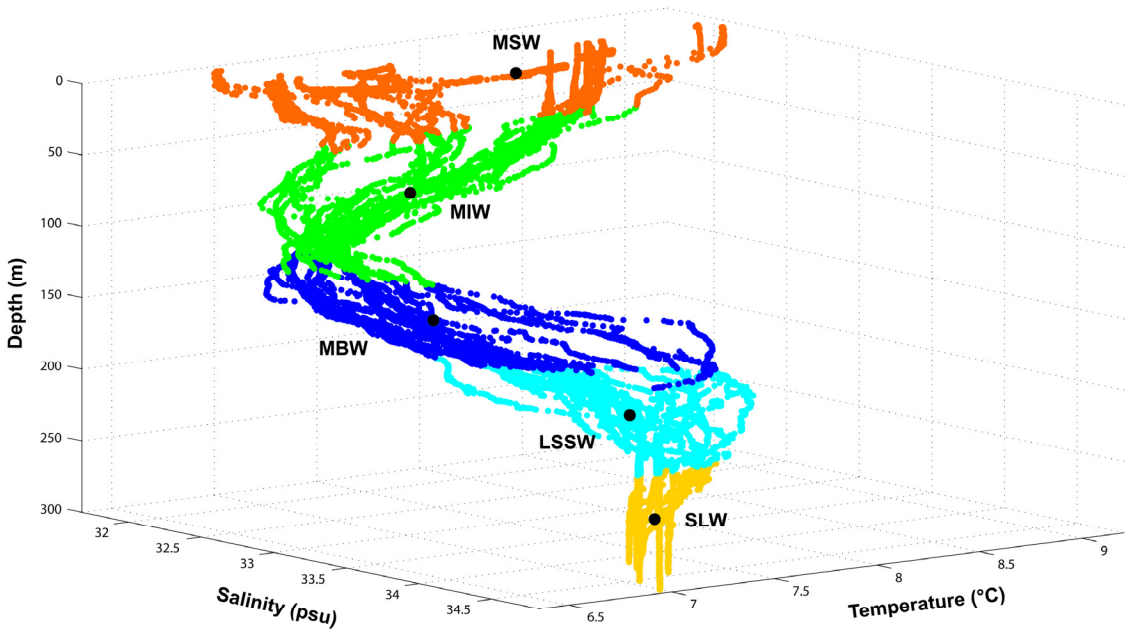


**Figure 3.13.** Water masses in Georges Basin during December 1998. MSW=Maine Surface Water; MIW=Maine Intermediate Water; MBW=Maine Bottom Water; LSSW=Labrador Subarctic Water; SLW=Slope Water.

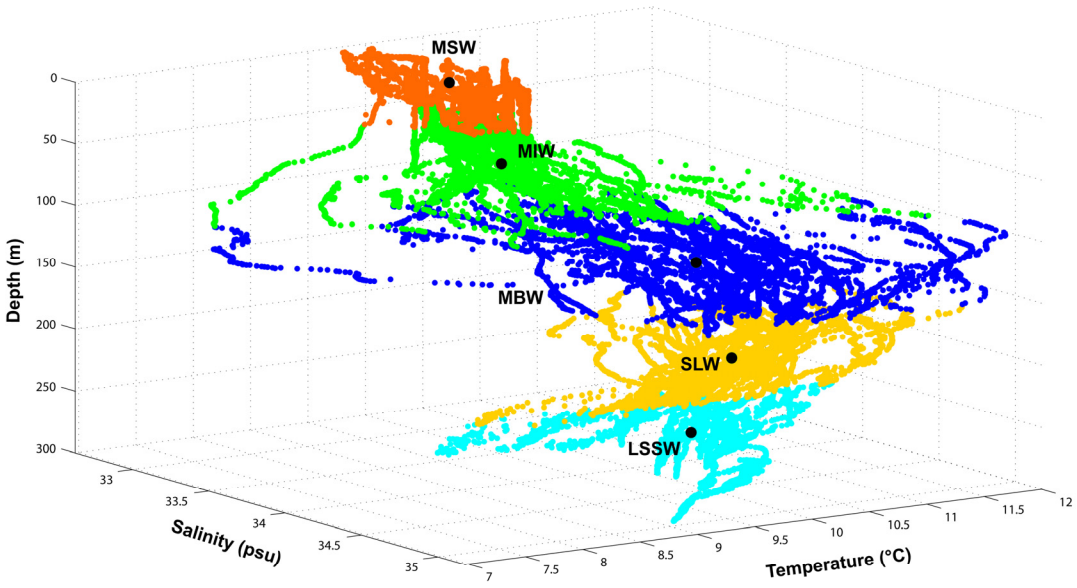


**Figure 3.14.** Water masses in Georges Basin during December 1999. MSW=Maine Surface Water; MIW=Maine Intermediate Water; MBW=Maine Bottom Water; LSSW=Labrador Subarctic Water; SLW=Slope Water.

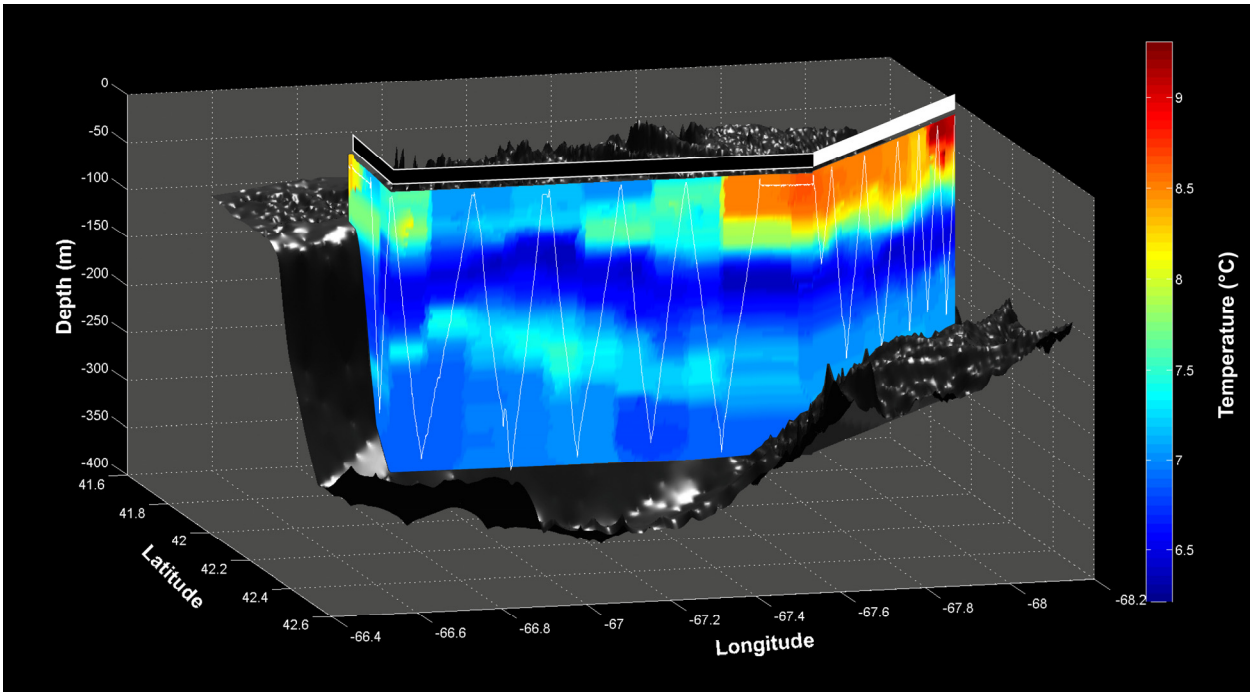


**Figure 3.15.** Temperature (°C) conditions in Georges Basin during December 1998 estimated using Kriging of measured values. The trajectory of BIOMAPPER-II is shown in white. The top bar represents the day (white) and night (black) portions of the transect. The dark grey surface represents the bathymetry of the basin. Georges Bank is behind the "curtain" so that the east is to the left of the graph (X-ordinate) and south is towards the back of the graph (Y-ordinate).

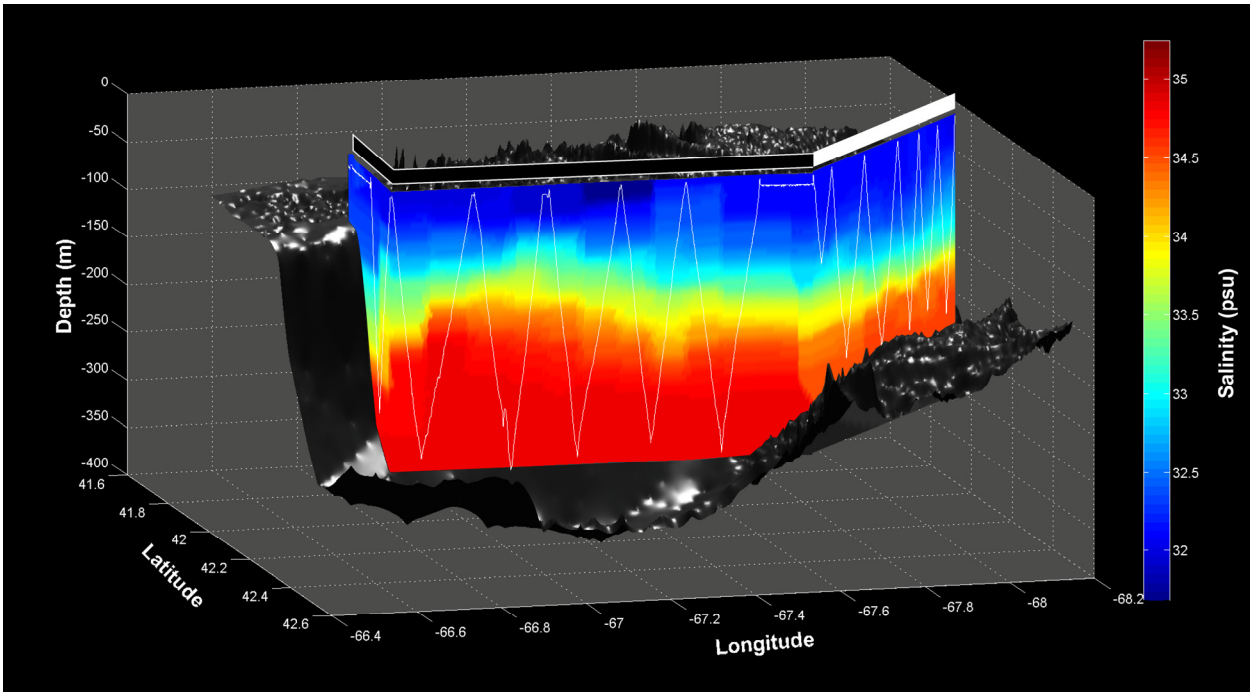


**Figure 3.16.** Salinity (psu) conditions in Georges Basin during December 1998 estimated using Kriging of measured values. The trajectory of BIOMAPPER-II is shown in white. The top bar represents the day (white) and night (black) portions of the transect. The dark grey surface represents the bathymetry of the basin. Georges Bank is behind the "curtain" so that the east is to the left of the graph (X-ordinate) and south is towards the back of the graph (Y-ordinate).

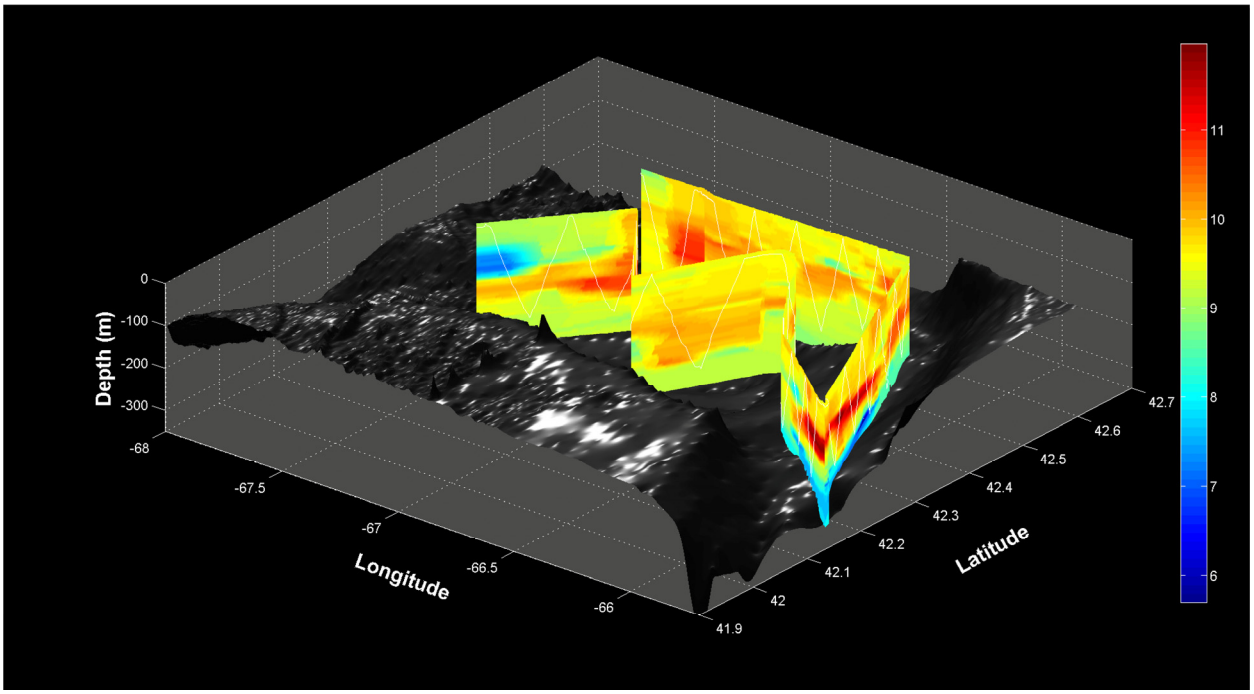


**Figure 3.17.** Temperature (°C) features in Georges Basin/Northeast Channel during December 1999. The dark grey surface represents the bathymetry of the basin.

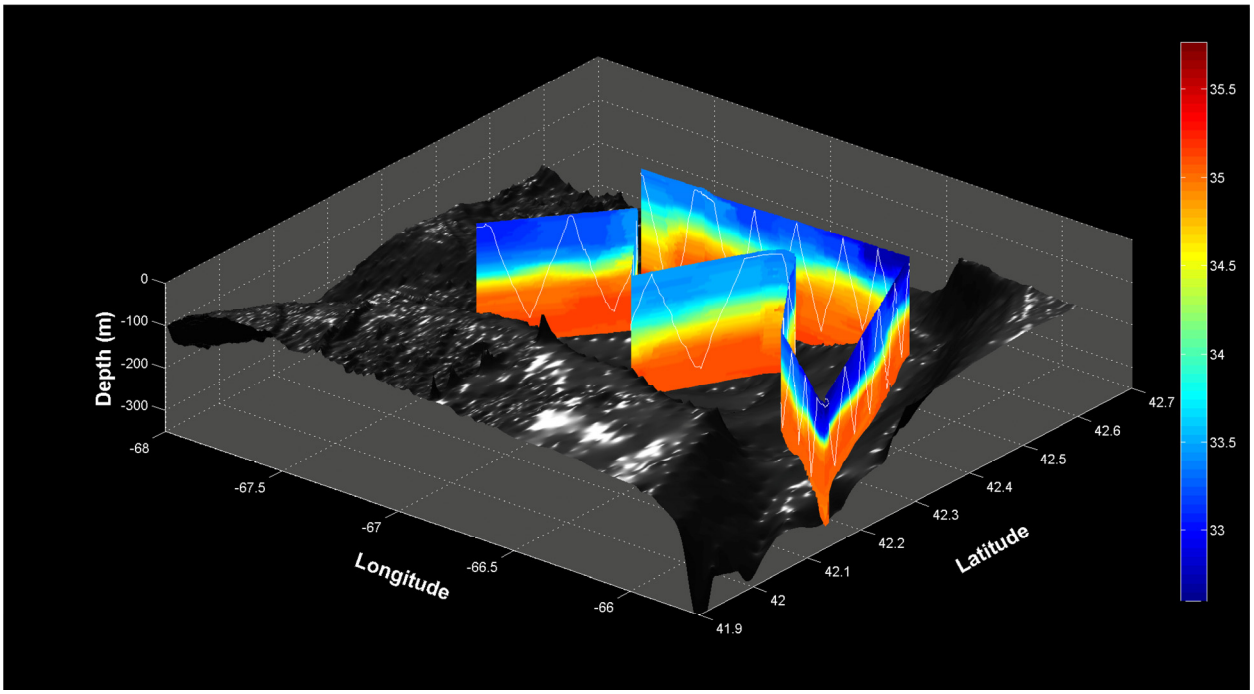


**Figure 3.18.** Salinity (psu) features in Georges Basin/Northeast Channel during December 1999. The dark grey surface represents the bathymetry of the basin.

Although the SLW was identified in all three deep basins during December 1998, this water mass was confined to the very deep waters of the basins. During December 1998, the SLW was always found lying below the LSSW. This arrangement changed during December 1999 in the Northeast Channel, where the LSSW water was found below the SLW.

Inter-annual and decadal fluctuations in hydrological conditions have been observed in the GOM area, and have been related to a lesser or greater extent to the North Atlantic Oscillation index (NAO) (Greene and Pershing, 2000, MERCINA, 2001; Conversi et al., 2001; Greene et al., 2003). The shift in hydrological regimes observed between December 1998 and December 1999 seemed to be related to the NAO index. As discussed elsewhere, during positive NAO years the shelf system of the Gulf of Maine is generally dominated by the deep warm, salty Slope Water (SLW), while during negative NAO years, the deep GOM is dominated by the cold, fresh Labrador Subarctic Slope Water (LSSW). This shift in water masses is thought to be responsible for the variability in *C. finmarchicus* abundance fluctuations in the GOM, and hence the importance of identifying these water masses. During positive NAO conditions, the warm SLW advected in to the GOM system through the Northeast Channel is thought to be rich in *C. finmarchicus*, as well as in many of the copepod's prey items (Ramp et al., 1985; Christensen et al., 1996). During negative NAO years, the warm deep SLW in the GOM is displaced by the cold LSSW, which is thought to be poor in *C. finmarchicus* and its food.

1998 was characterized by a predominantly negative NAO index (Climate Prediction Center, National Weather Center, NOAA). By November 1998, the deep basins of the Gulf of Maine were occupied by the nutrient-poor, cold LSSW (MERCINA, 2001). During December 1998, this water mass was positively identified in Wilkinson Basin, Jordan Basin and Georges Basin/Northeast Channel. On the other hand, during 1999 the NAO index was predominantly positive, and by October 1999 the LSSW was only present in Georges Basin/Northeast Channel (MERCINA, 2001). During December 1999, the LSSW was only positively identified in the

Northeast Channel. The replacement of the LSSW within a year is consistent with the residence time of water masses in the Gulf of Maine, which is about 10 – 12 months (Christensen et al., 1996; Xue et al., 2000).

Exchange of water masses in the Gulf of Maine occurs mainly through the Northeast Channel. From there they accumulate in Georges Basin and eventually dispersed into the interior of the Gulf of Maine following the mean circulation of the area (Brown and Irish, 1993; Warn-Varnas et al., 2005). The only indications of Slope Water entrainment were found in December 1999 in Wilkinson and Georges Basin/Northeast Channel. On the other hand, a deep circulation also influences the transference of Slope Water directly from Georges Basin into Wilkinson Basin (Brooks, 1985). The jet of warm, salty water observed in Wilkinson Basin during December 1999 could have followed this later pathway as the water jet seemed to be originated in the southeastern portion of Wilkinson Basin and extended westward (Fig. 3.4).

The contrasting hydrological conditions observed between the two studied periods were clearly reflected by the shifts between the LSSW and SLW in the deep basins of the GOM. The cooler, fresher waters observed during December 1998 may have been the result of the LSSW, which during this period dominated the deep waters of all three deep basins. However, by December 1999, the GOM was returning to its normal conditions (MERCINA, 2001), and the LSSW was replaced by the warmer, saltier SLW, which dominated all the deep basins. Indeed, the only area where the LSSW was found during December 1999 was found in the deep waters of the NEC and these cool waters were probably the remnants of LSSW.

**3.5 References**

Brooks, D. A. 1985. Vernal Circulation in the Gulf of Maine. Journal of Geophysical Research **90**(C3): 4687-4705.

Brown, W. S. and J. D. Irish. 1993. The annual variation of water mass structure in the Gulf of Maine: 1986-1987. Journal of Marine Research **51**:53-107.

Bumpus, D. F. 1973. A description on the circulation on the continental shelf of the east coast of the United States. Progress in Oceanography **6**: 111-157.

Christensen, J. P., D. W. Townsend, and J. P. Montoya. 1996. Water column nutrients and sedimentary denitrification in the Gulf of Maine. Continental Shelf Research **16**: 489-515.

Climate Prediction Center, National Weather Service, NOAA.

http://www.cpc.ncep.noaa.gov/products/precip/CWlink/pna/nao.shtml

Conversi, A., S. Piontkovski, and S. Hameed. 2001. Seasonal and interannual dynamics of *Calanus finmarchicus* in the Gulf of Maine (Northeastern US shelf) with reference to the North Atlantic Oscillation. Deep Sea Research Part II: Topical Studies in Oceanography **48**: 519-530.

Durbin, E. G., P. R. Garrahan, and M. C. Casas. 2000. Abundance and distribution of *Calanus finmarchicus* on the Georges Bank during 1995 and 1996. ICES Journal of Marine Science **57**: 1664-1685.

Greene, C., M. C. Benfield, P. Wiebe, and H. Sosik. 1999b. R/V Endeavor Cruise 331 cruise report. U. S. GLOBEC, NW Atlantic/Georges Bank Study. 62 p. http://globec.whoi.edu/globec-dir/reports/en331/en331rpt.6sept2000.html

Greene, C. H. and A. J. Pershing 2000. The response of *Calanus finmarchicus* populations to climate variability in the Northeast Atlantic: basin-scale forcing associated with the North Atlantic Oscillation. ICES Journal of Marine Science **57**: 1536-1544.

Greene, C. H., A. J. Pershing, A. Conversi, B. Planque, C. Hannah, D. Sameoto, E. Head, P. C. Smith, P. C. Reid, J. Jossi, D. Mountain, M. C. Benfield, P. H. Wiebe, E. Durbin. 2003. Trans-Atlantic responses of *Calanus finmarchicus* populations to basin-scale forcing associated with the North Atlantic Oscillation. Progress in Oceanography **58**: 301-312.

Hopkins, T. S. and N. Garfield. 1979. Gulf of Maine intermediate water. Journal of Marine Research **37**: 103-139.

Kim, K., K. R. Kim, T. S. Rhee, and H. K. Rho. 1991. Identification of water masses in the YS and East China Sea by cluster analysis. Oceanography of Asian Marginal Seas. K. Takano. Amsterdam, Elsevier**. pp.** 253-267.

Lynch, D. R., M. J. Holboke, and C. E. Naimie. 1997. The Maine coastal current: spring climatological circulation. Continental Shelf Research **17**: 605-634.

MERCINA. 2001. Oceanographic responses to climate in the Northwest Atlantic. Oceanography **14**: 76-82.

Pringle, J. M. 2006. Sources of variability in Gulf of Maine circulation, and the observations needed to model it." Deep Sea Research Part II: Topical Studies in Oceanography **53**: 2457-2476.

Ramp, S. R., R. J. Schlitz, and W. W. Redwood. 1985. The deep flow through the Northeast Channel, Gulf of Maine. Journal of Physical Oceanography **15**: 1790-1808.

Townsend, D. W. 1998. Sources and cycling of nitrogen in the Gulf of Maine. Journal of Marine Systems **16**: 283-295.

Warn-Varnas, A., A. Gangopadhyay, J. A. Hawkins, and A. R. Robinson. 2005. Wilkinson Basin area water masses: a revisit with EOFs. Continental Shelf Research **25**: 277-296.

Xue, H., F. Chai, and N. R. Pettigrew. 2000. A model study of the seasonal circulation in the Gulf of Maine. Journal of Physical Oceanography **30**: 1111-1135.

# CHAPTER IV

# FINE- TO BASIN-SCALE DISTRIBUTIONS OF *CALANUS FINMARCHICUS* IN THREE DEEP BASINS OF THE GULF OF MAINE DURING DECEMBER 1998 AND 1999

## 4.1 Introduction

Due to its important role in the shelf ecosystems of the North Atlantic, *Calanus finmarchicus* has been subjected to intense research for almost a century (Bigelow, 1924; Fish, 1936; Meise and O'Reilly, 1996; Johnson et al., 2008). Basic knowledge on the distribution and abundance of *C. finmarchicus* in the GOM has been highlighted since it is considered as a seeding source for Georges Bank (Lynch et al., 1998). Georges Bank is a historically important fishing ground for Atlantic Cod (*Gadus morhua*) and Haddock (*Melanogrammus aeglefinus*). The early life stages of these commercially important fishes feed on *C. finmarchicus* (Avent et al., 2001; Li et al., 2006;) and other copepods, hence the importance of studying the abundance and general distribution patterns of *C. finmarchicus* in the GOM. Temporal and spatial variations of *C. finmarchicus* and other copepods should have an important affect on the population dynamics of cod, haddock and other commercially important fishes of the GOM (Pershing et al., 2005).

Larger vertebrates also depend on *Calanus finmarchicus* as a main energy source. Whale sharks (*Cetorhinus maximus*) and right whales (*Eubalaena glacialis*) have been observed feeding on high abundance patches of *Calanus finmarchicus* (Durbin et al., 1995; Kenney et al., 1995; Wishner et al., 1995; Beardsley et al., 1996). Right whale calf production in the GOM has been directly related to production of *Calanus finmarchicus* (Greene and Pershing, 2004). Low calf production by right whales has been observed during years when *Calanus finmarchicus* abundance was low while an increase in births has been observed in years when *Calanus finmarchicus* is abundant.

Spatial variations of *C. finmarchicus* in the different regions of the Gulf have been related to the general circulation patterns of the Gulf and to the influence of local gyres found in the

deep basins (Johnson et al., 2006) however, mortality due to predation and starvation may also play a role (Ohman et al., 2004; Saumweber and Durbin, 2006). Temporal patterns in *C. finmarchicus* abundances, from interannual to decadal scales, are complex and local and ocean-scale phenomena are confounded. Regime shifts in the hydrological conditions in the interior of the GOM are thought to be related to atmospherically-driven phenomena, such as the NAO.

**4.2 Methods**

*Calanus finmarchicus* datasets from the VPR and the BIOMAPPER II ESS from cruises OC334 and EN331 were processed as indicated in the GENERAL METHODS section. Abundances were estimated in 60 s time bins and Kriged using Easykrig 3.0 Toolbox for Matlab (Chu, 2004). Appendix A contains the m-files used to calculate abundances. The best variogram-correlogram parameters used during Kriging are reported in Appendix B.

Distribution maps were inspected visually for distribution of *C. finmarchicus* abundance patterns. Non-parametric ANOVAs were performed using Kruskal-Wallis tests to determine whether abundances differed between study periods for all targeted taxa in all three deep basins. Regional abundance differences were also tested using Kruskal-Wallis tests. Non-parametric tests were used because data didn't meet normal distribution criteria even when transformed using a variety of methods (i.e. square root, log10). When significant differences were found, post-hoc pair-wise comparison tests were performed (using $\alpha$=0.05) to investigate which groups were significantly different from others.

Temperature-salinity-plankton plots (TSP) were built using Environmental Sensor System (ESS) data for each of the three deep basins to identify the possible relationship of *C. finmarchicus* and hydrological features. Water masses identified by the cluster analysis were delineated by ovals in the TSP plots to better observe the possible relationships between water masses and abundance features.

### 4.3 Results

The abundances of *Calanus finmarchicus* were significantly different for each of the three deep basins when compared across years (Wilkinson Basin: $p<0.001$; Jordan Basin: $p<0.001$; Georges Basin: $p<0.001$). The pair-wise tests consistently identified December 1999 as having higher *C. finmarchicus* abundances compared to December 1998 (Table 4.1). Regional differences between *C. finmarchicus* abundances were also significant during both studied periods. Georges Basin consistently had the lowest *C. finmarchicus* abundances relative to other basins during both years (Table 4.1). Abundances in Wilkinson Basin were either significantly greater than those in Jordan Basin (1998: $p<0.001$) or statistically non-different (1999: $p\geq0.05$).

**Table 4.1.** Mean (1STD) abundance (n $m^{-3}$) of *Calanus finmarchicus* in the three deep basins of the Gulf of Maine during cruises OC334 (December 1998) and EN331 (December 1999). Pair-wise tests marked with an asterisk were significant at the 95 confidence level.

| Deep Basin | December 1998 | December 1999 | Pair-wise test |
|---|---|---|---|
| Wilkinson Basin | 39.2 (66.5) | 118.5 (192.7) | Dec. 1998 < Dec. 1999* |
| Jordan Basin | 30.6 (59.0) | 144.2 (244.9) | Dec. 1998 < Dec. 1999* |
| Georges Basin/NEC | 10.4 (29.8) | 29.3 (87.3) | Dec. 1998 < Dec. 1999* |
| **Pair-wise test** | WB>JB>GB* | WB=JB>GB* | |

NEC=Northeast Channel; WB=Wilkinson Basin; JB=Jordan Basin; GB=Georges Basin

#### 4.3.1 Wilkinson Basin

*Calanus finmarchicus* was more abundant during December 1999 than in December 1998 ($p < 0.001$) in Wilkinson Basin. Distribution patterns also differed between both years. During December 1998, the distribution of *C. finmarchicus* in Wilkinson Basin (WB) was more dispersed, and it was present at all depths in small numbers (Fig. 4.1). During December 1998 *C. finmarchicus* abundances ranged between 71 and 427 n $m^{-3}$ (mean±standard deviation 39.2 ± 66.5 n $m^{-3}$) across the basin. The maximum abundance at the center of *C. finmarchicus* patches according to kriged data peaked at 270 n $m^{-3}$. While a patch was observed at 25m in

the easternmost portion of Wilkinson Basin, *C. finmarchicus* was more abundant from depths 100-200 m with the densest patches found in the southwest half of Wilkinson Basin (Fig. 4.1).

During December 1999, densities varied between 54 and 1,198 n $m^{-3}$ (mean±standard deviation 118.5 ± 192.7 n $m^{-3}$). The most abundant patches were found at depths below 150 m, where large patches of ~400 n $m^{-3}$ appeared (Fig. 4.2). From 170 m and down, the deep basin was occupied by several dense patches of at least 400 n $m^{-3}$. Maximum abundance at the core of one patch reached 1,198 n $m^{-3}$. The largest patch was centered at ~173 m and started declining at ~200 m. The second largest patch was centered at 200 m. Smaller secondary patches were located to the east of patch 1, and to the west and southeast of patch 2 (Fig. 4.2).

*Calanus finmarchicus* higher abundances were associated to hydrographic features during December of both 1998 and 1999. The temperature-salinity-plankton (TSP) plots for *C. finmarchicus* revealed that highest abundances (200-427 n $m^{-3}$) during December 1998 were associated to water properties characteristic to the Slope Water (SLW) and Maine Bottom Water (MBW) (Fig. 4.3). Nevertheless, few observations with comparable abundances were made in the MSW and MIW. During December 1999, the TSP plot showed that most of the high abundance (400-1,198 n m-3) observations of *C. finmarchicus* were located within the SLW and MBW (Fig. 4.4). However, high abundances in the MBW were observed close to the boundary with the SLW mass. Several observations of at least 55 n $m^{-3}$ but no higher than 400 n $m^{-3}$ were made in surface waters, dominated by the Hot Surface Water (HSW) and Maine Surface Water (MSW). The lowest abundances on December 1999 were observed in association with the Maine Intermediate Water (MIW).

Diel vertical activity was examined for *C. finmarchicus* for December 1998 and 1999. No diel vertical activity was apparent in either case. Similar distributions between day and night were observed during December 1998 (Figs. 4.5 and 4.7) and December 1999 (Figs. 4.6, and 4.8).

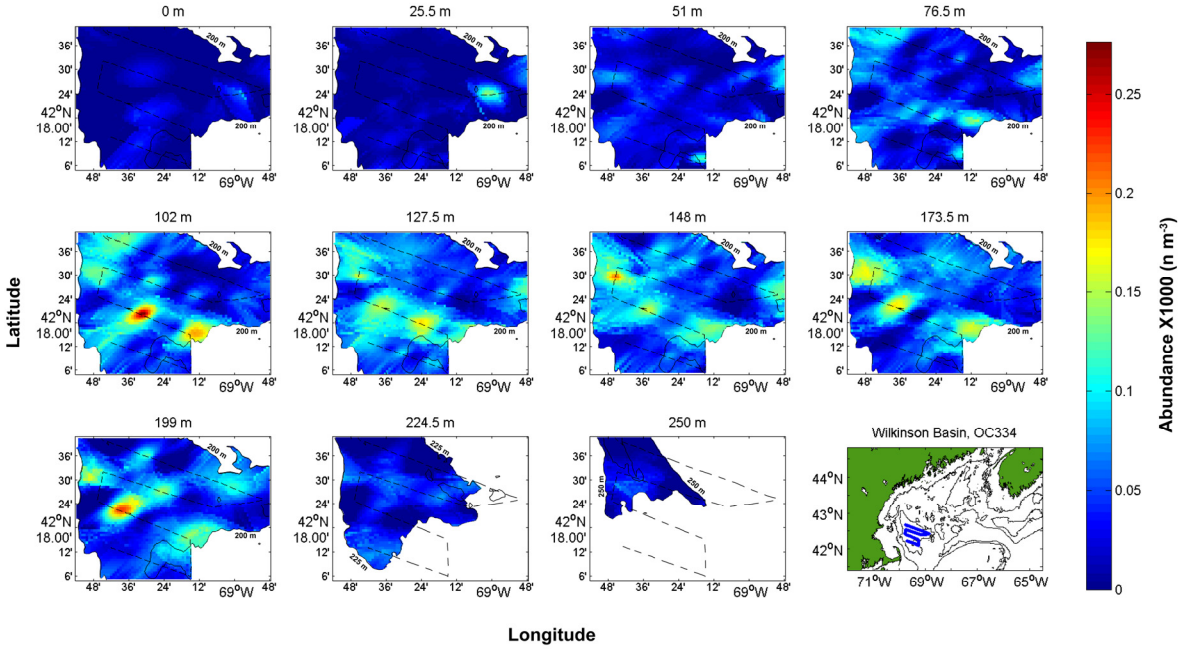


**Fig. 4.1.** *Calanus finmarchicus* abundance in Wilkinson Basin during December 1998 plotted at 25 m intervals. Isobaths (solid line) and cruise track (dashed line) were superimposed for reference.

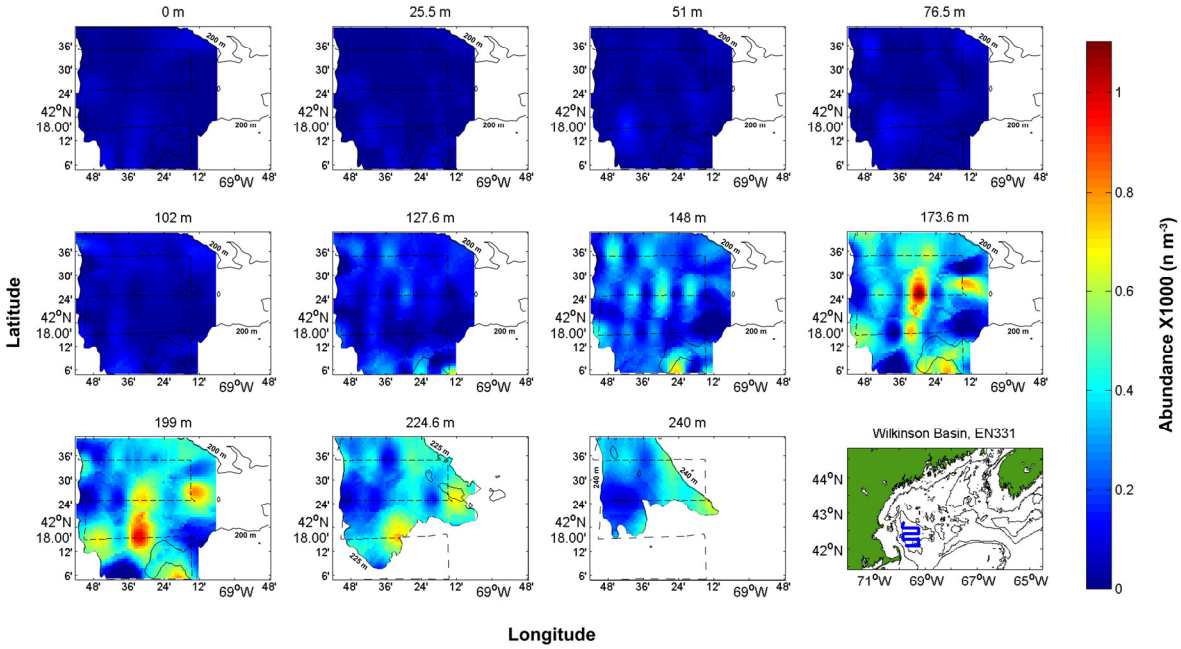


**Fig. 4.2.** *Calanus finmarchicus* abundance in Wilkinson Basin during December 1999 plotted at 25 m intervals. Isobaths (solid line) and cruise track (dashed line) were superimposed for reference.

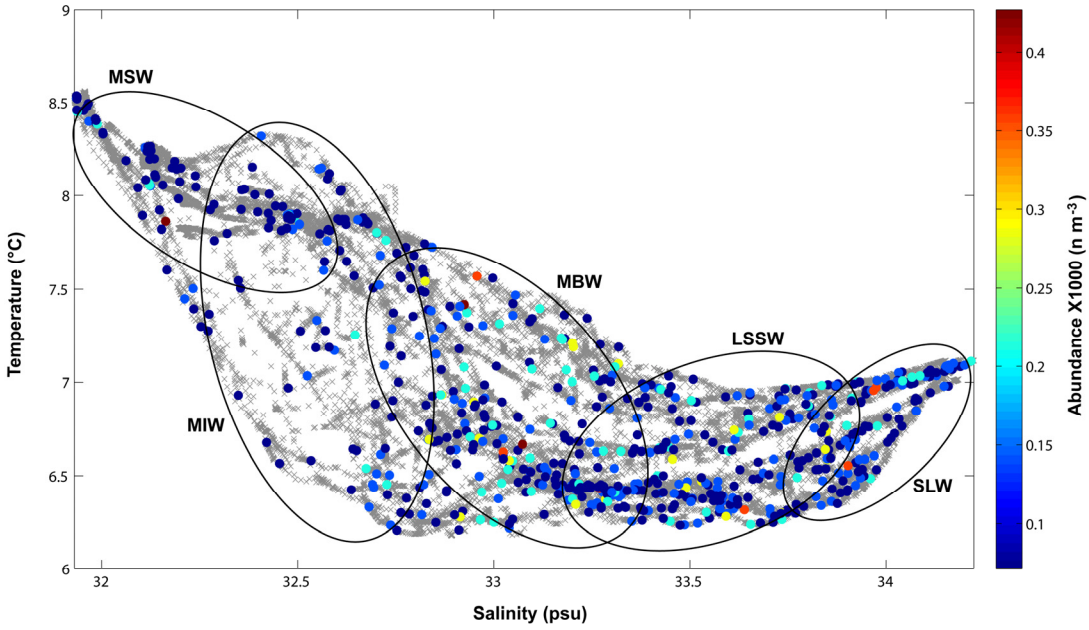


**Fig. 4.3.** TSP plot for Wilkinson Basin during December 1998. *Calanus finmarchicus* abundances are shown in color-coded dots. Temperature-Salinity points are plotted in grey X marks. MSW=Maine Surface Water; MIW=Maine Intermediate Water; MBW= Maine Bottom Water; LSSW=Labrador Subarctic Slope Water; SLW=Slope Water.

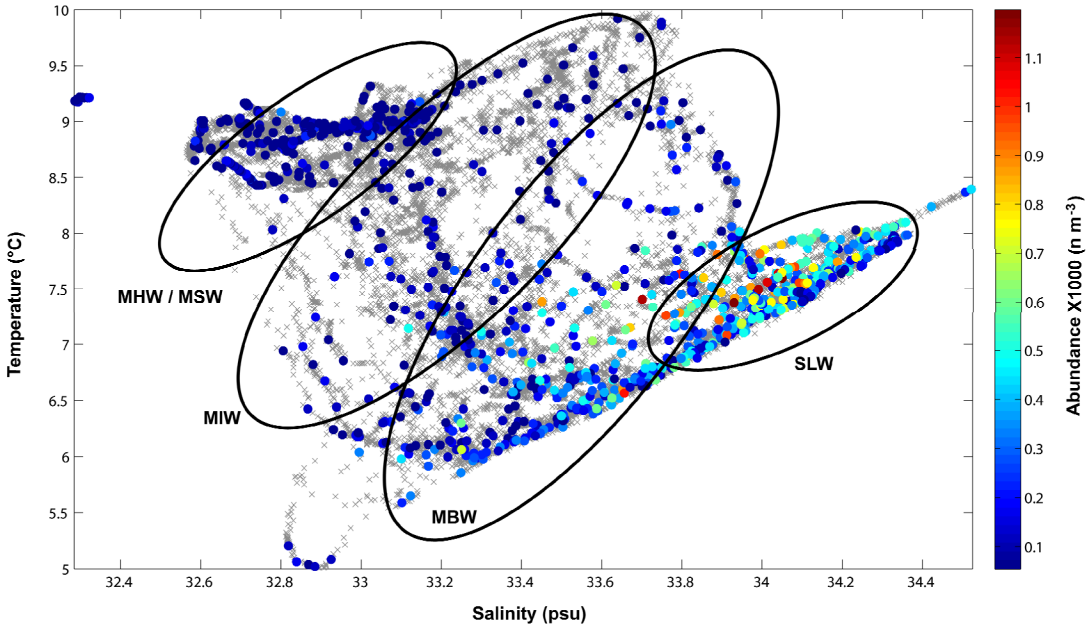


**Fig. 4.4.** TSP plot for Wilkinson Basin during December 1999. *Calanus finmarchicus* abundances are shown in color-coded dots. Temperature-Salinity points are plotted in grey X marks. MHW=Maine Hot Water; MSW=Maine Surface Water; MIW=Maine Intermediate Water; MBW= Maine Bottom Water; SLW=Slope Water.

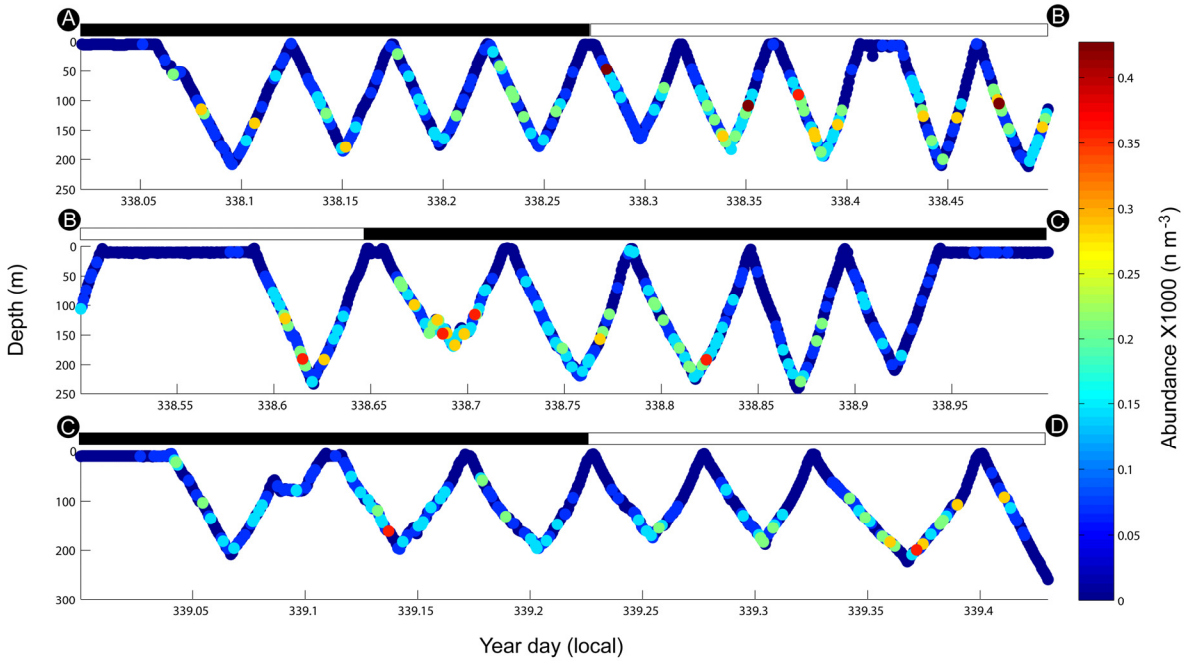


**Figure 4.5.** Diurnal vertical distribution of *Calanus finmarchicus* in Wilkinson Basin during December 1998 along BIOMAPER-II track. Bars on top of each subplot represent day (white) and night (black) periods. Capital letters at the beginning and end of each panel correspond to the sections of the Wilkinson Basin, OC334 cruise track in Fig. 2.6.

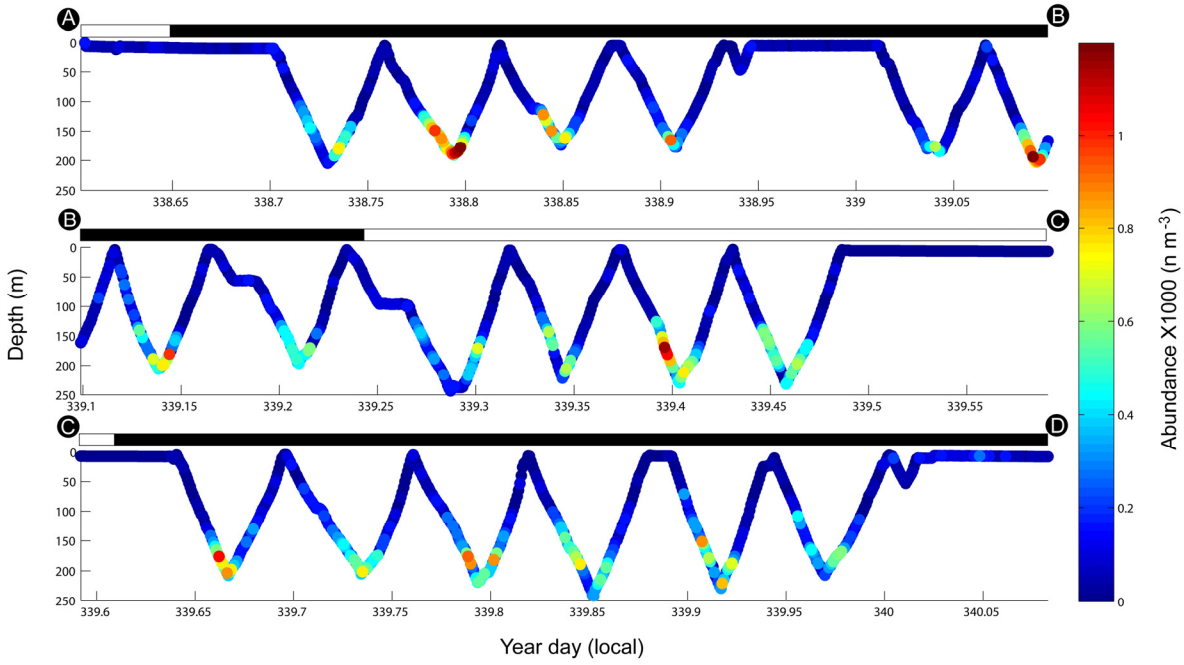


**Figure 4.6.** Diurnal vertical distribution of *Calanus finmarchicus* in Wilkinson Basin during December 1999 along BIOMAPER-II track. Bars on top of each subplot represent day (white) and night (black) periods. Capital letters at the beginning and end of each panel correspond to the sections of the Wilkinson Basin, EN331 cruise track in Fig. 2.6.

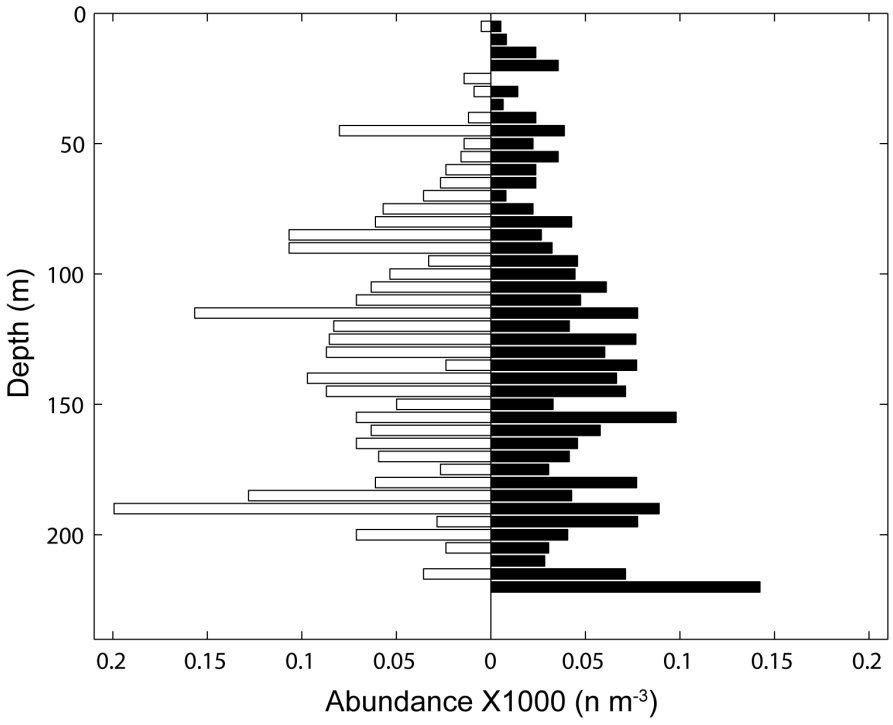


**Figure 4.7.** Vertical distribution of *C. finmarchicus* in Wilkinson Basin during December 1998 during day (empty horizontal bars, left) and night (black bars, right) periods.

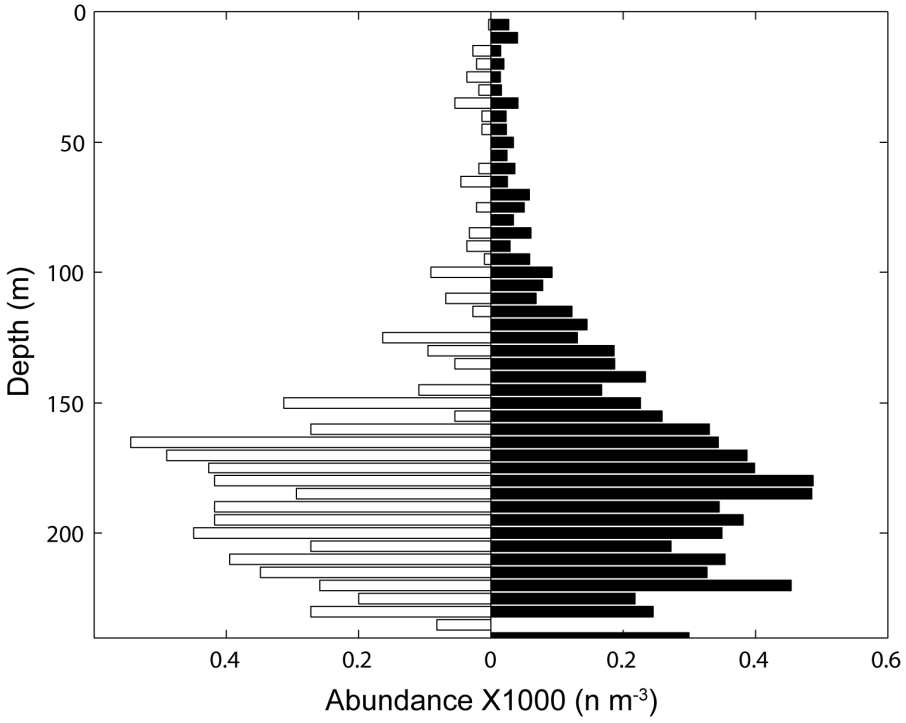


**Figure 4.8.** Vertical distribution of *C. finmarchicus* in Wilkinson Basin during December 1999 during day (empty horizontal bars, left) and night (black bars, right) periods.

### 4.3.2 Jordan Basin

*Calanus finmarchicus* in Jordan Basin (JB) was more abundant during December 1999 than in December 1998 ($p<0.001$), with abundances in 1999 being up to 4 times higher than in 1998. Minimum observed abundances were approximately five times greater in December 1999 than in December 1998. During December 1999 abundance values up to 1,362 n $m^{-3}$ (mean±standard deviation 144.2 ± 244.9 n $m^{-3}$) were observed, while December 1998 abundance values up to 427 n $m^{-3}$ (mean±standard deviation 30.6 ± 59.0 n $m^{-3}$) were observed. Moreover, spatial and depth distribution patterns also differed between both dates.

During December 1998, the distribution of *C. finmarchicus* in JB was patchy. Patches were discrete in size and sparsely distributed in space and depth (Fig. 4.9). Interestingly, the most conspicuous patches were located in the western portion of JB. One of two large, dense patches was observed at 0 m and didn't extend beyond 25 m. The second large dense patch was observed at ~125 m and extended slightly beyond 175 m depth (Fig. 4.9), with its core (~200 n $m^{-3}$) located at ~150 m depth. The densest values (427 n $m^{-3}$) were attributed to the larger patch found at the surface (0-25). However, both patches were mostly dominated by abundance values of ~150 n $m^{-3}$. Background levels of *C. finmarchicus* (~50 n $m^{-3}$) were widespreaded in JB from 100 m down to 200 m but were almost absent in the eastern JB in waters shallower than 100 m. Relatively small patches appeared scattered in between the two larger patches, with no apparent pattern.

On December 1999, *C. finmarchicus* was present in numbers up to ~200 n $m^{-3}$ in waters shallower than ~150 m. From 150 to 240 m, JB was practically packed with a dense "cloud" of *C. finmarchicus* (Fig. 4.10). The cores (containing abundances up to 1,362 n $m^{-3}$) of several patches could be readily identified scattered along and across JB in this depth range. However, it was not clear where the borders of such patch were located, as most core areas were interconnected by abundances of ~500 n $m^{-3}$.

There seemed to be a relationship between the distribution pattern observed in *C. finmarchicus* abundances and water masses for both December 1998 and 1999. During December 1998, the highest abundance values of *C. finmarchicus* were associated with MSW and the SSLW-SLW interface (Fig. 4.11). In contrast, during December 1999 almost all of the high abundance values were found in the SLW (Fig. 4.12). Some high abundance values were also observed associated to the MBW. However, these observations were in the proximity to the boundary of the later with the contiguous SLW.

There was no evidence of vertical migration during either December 1998 or December 1999. During December 1998 there were more dense patches of *C. finmarchicus* from 0-25 m during the nighttime sections than in daylight sections (Figs. 4.13 and 4.15). No pattern of vertical activity was observed during December 1999, as most patches were clustered below 150 m deep during both day and night sections (Figs. 4.14 and 4.16). In both years, the cruise track never repeated coverage of the same sections during day or night making it impossible to directly compare vertical distributions for the same location.

**4.3.3 Georges Basin/Northeast Channel**

Due to the difference in areas covered by the cruise surveys during December 1998 and December 1999, no direct comparison on *C. finmarchicus* distributions in Georges Basin could be evaluated. Moreover, only a portion of Georges Basin was surveyed during December 1998, while the December 1999 cruise included Georges Basin and part of the Northeast Channel.

Despite different spatial coverage, it was clear that during December 1999 *C. finmarchicus* was more abundant than at the same time one year earlier ($p<0.001$). During December 1999, *C. finmarchicus* abundances in Georges Basin ranged between ~55 and ~1,035 n $m^{-3}$ (mean±standard deviation 29.3 ± 87.3 n $m^{-3}$) while during December 1998 *C. finmarchicus* abundances varied between ~71 and ~214 n $m^{-3}$ (mean±standard deviation 10.4 ± 29.8 n $m^{-3}$).

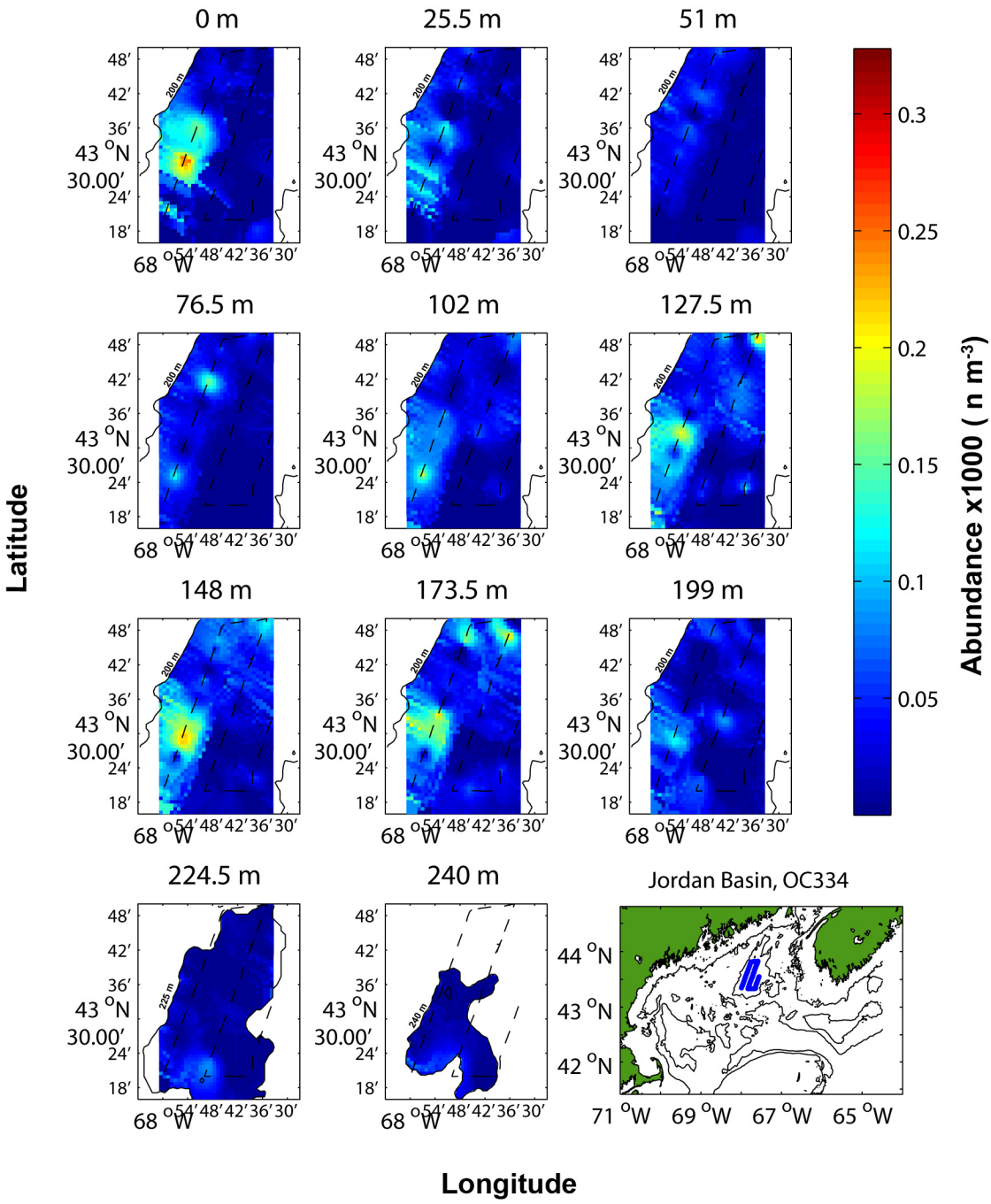


**Fig. 4.9.** *Calanus finmarchicus* abundance in Jordan Basin during December 1998 plotted at 25 m intervals. Isobaths (solid line) and cruise track (dashed line) were superimposed for reference. Areas outside the 200m, 225m and 240 m isobaths and away from the cruise track were cropped out due to the high error variance in those areas.

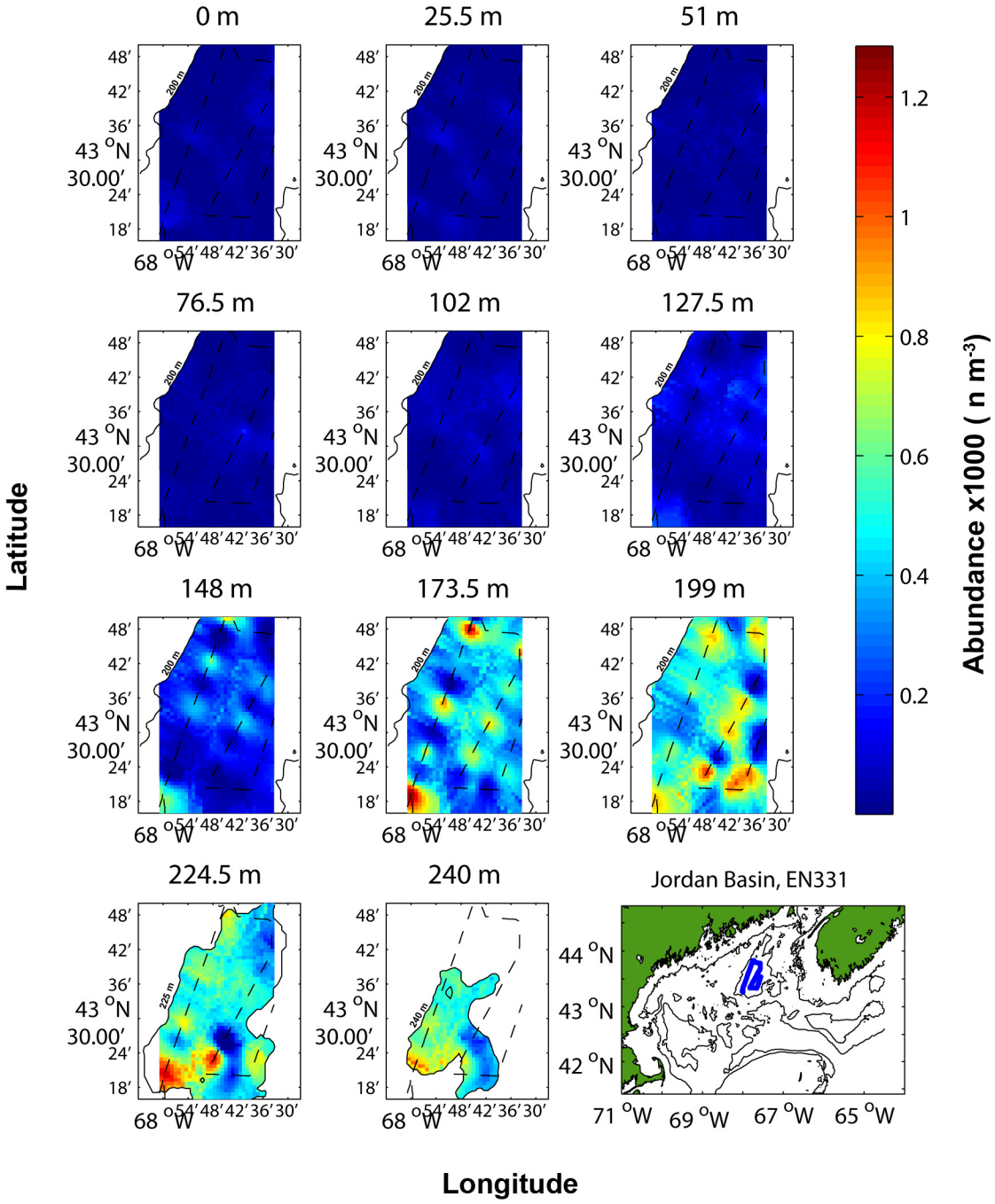


**Fig. 4.10.** *Calanus finmarchicus* abundance in Jordan Basin during December 1999 plotted at 25 m intervals. Isobaths (solid line) and cruise track (dashed line) were superimposed for reference. Areas outside the 200m, 225m and 240 m isobaths and away from the cruise track were cropped out due to the high error variance in those areas.

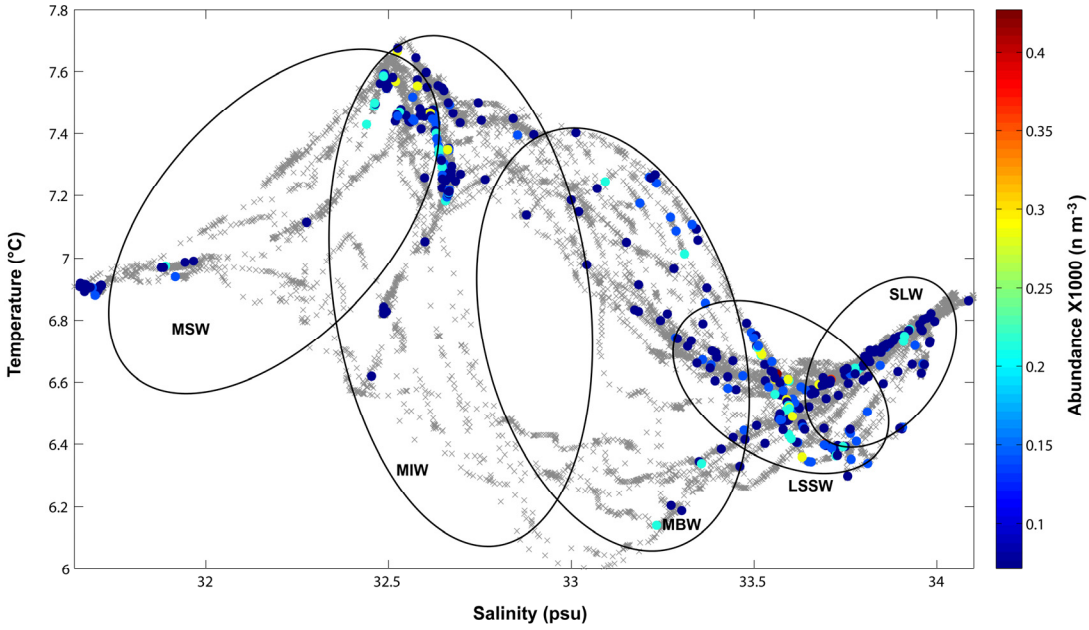


**Fig. 4.11.** TSP plot for Jordan Basin during December 1998. *Calanus finmarchicus* abundances are shown in color-coded dots. Temperature-Salinity points are plotted in grey X marks. MSW=Maine Surface Water; MIW=Maine Intermediate Water; MBW= Maine Bottom Water; SSLW=Subarctic Slope Water; SLW=Slope Water.

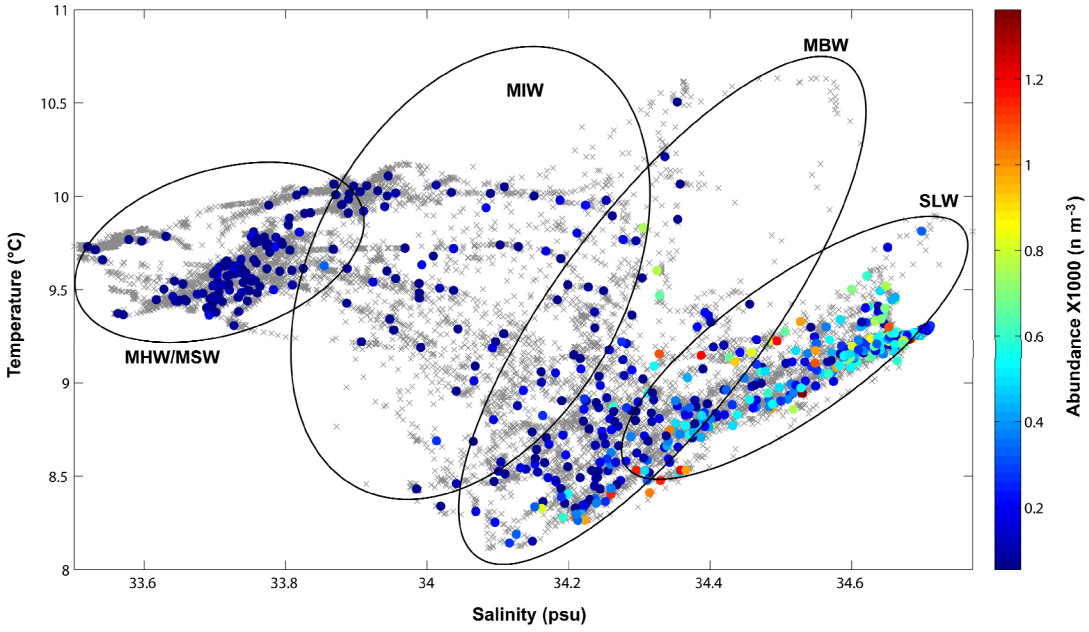


**Fig. 4.12.** TSP plot for Jordan Basin during December 1999. *Calanus finmarchicus* abundances are shown in color-coded dots. Temperature-Salinity points are plotted in grey X marks. MHW/MSW=Maine Surface Water-Maine Hot Water complex; MIW=Maine Intermediate Water; MBW= Maine Bottom Water; SLW=Slope Water.

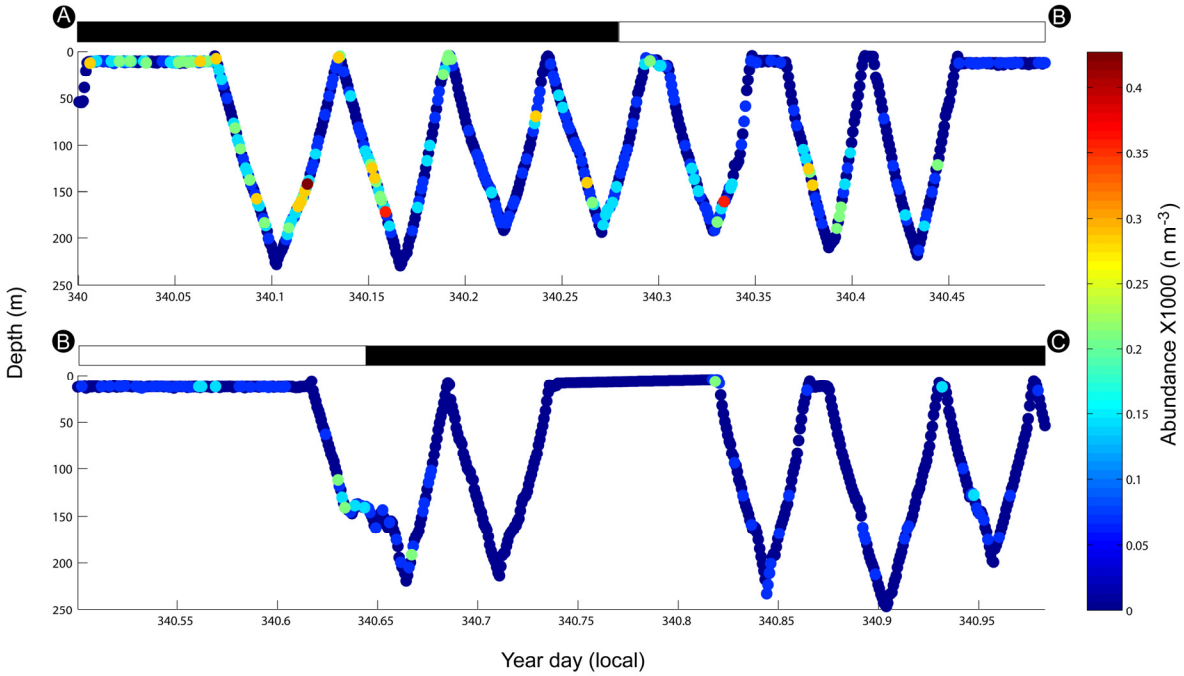


**Fig. 4.13.** Diurnal vertical distribution of *Calanus finmarchicus* in Jordan Basin during December 1998. The path of BIOMAPER-II is depicted with a white solid line. Bars on top of each subplot represent day (white) and night (black) periods. Capital letters at the beginning and end of each panel correspond to the sections of the Jordan Basin, OC334 cruise track in Fig. 2.6.

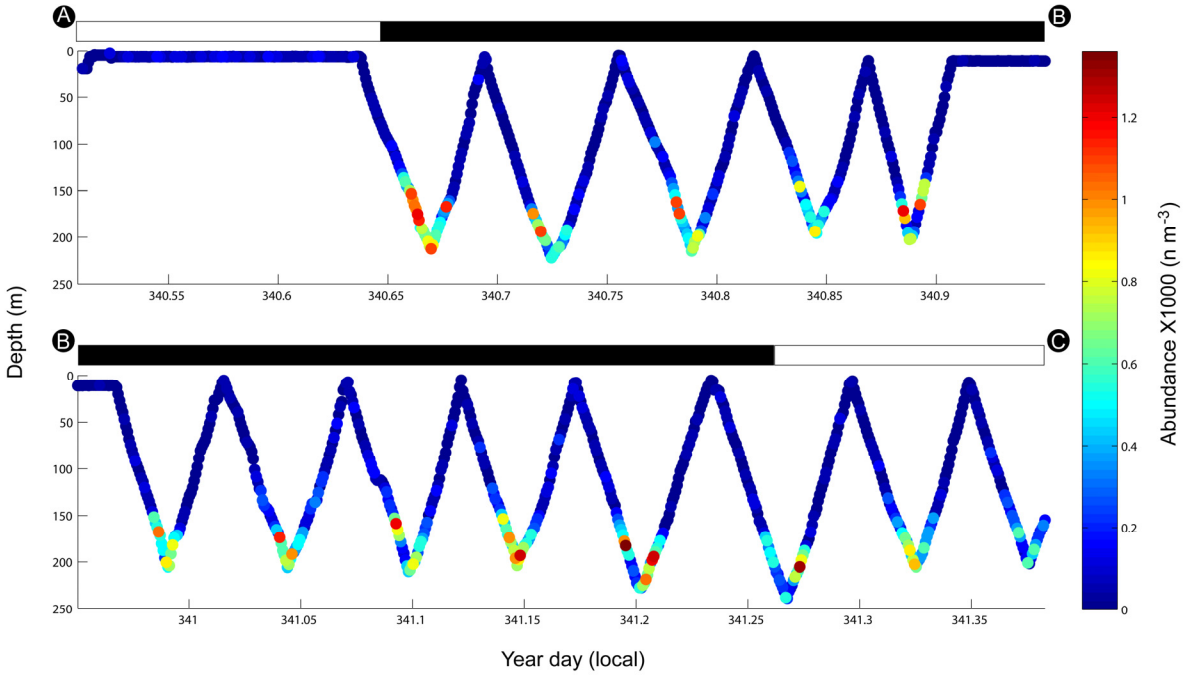


**Fig. 4.14.** Diurnal vertical distribution of *Calanus finmarchicus* in Jordan Basin during December 1999. The path of BIOMAPER-II is depicted with a white solid line. Bars on top of each subplot represent day (white) and night (black) periods. Capital letters at the beginning and end of each panel correspond to the sections of the Jordan Basin, EN331 cruise track in Fig. 2.6.

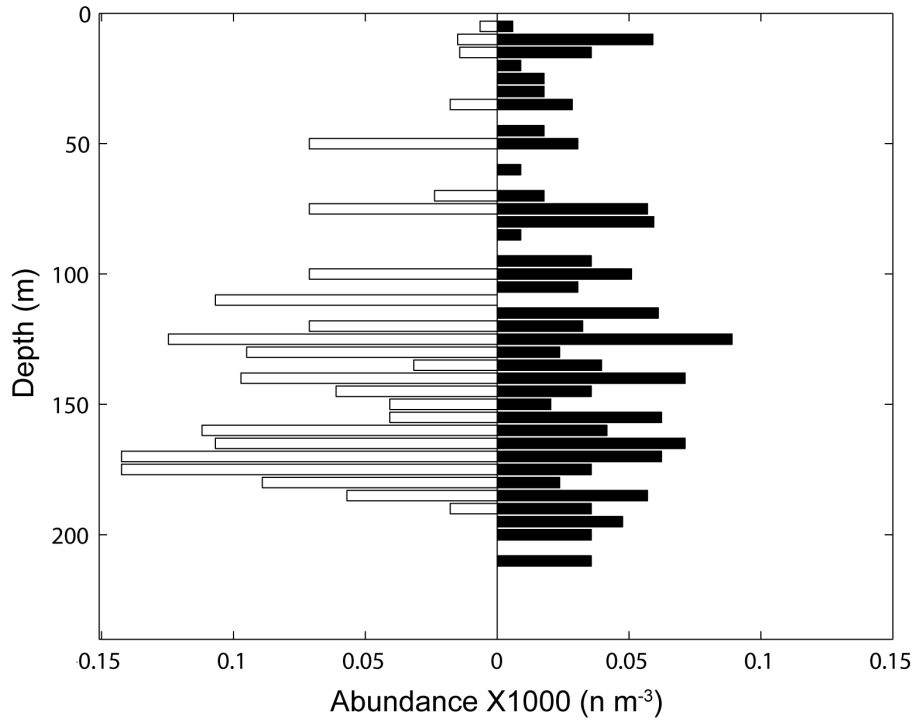


**Figure 4.15.** Vertical distribution of *C. finmarchicus* in Jordan Basin during December 1998 during day (empty horizontal bars, left) and night (black bars, right) periods.

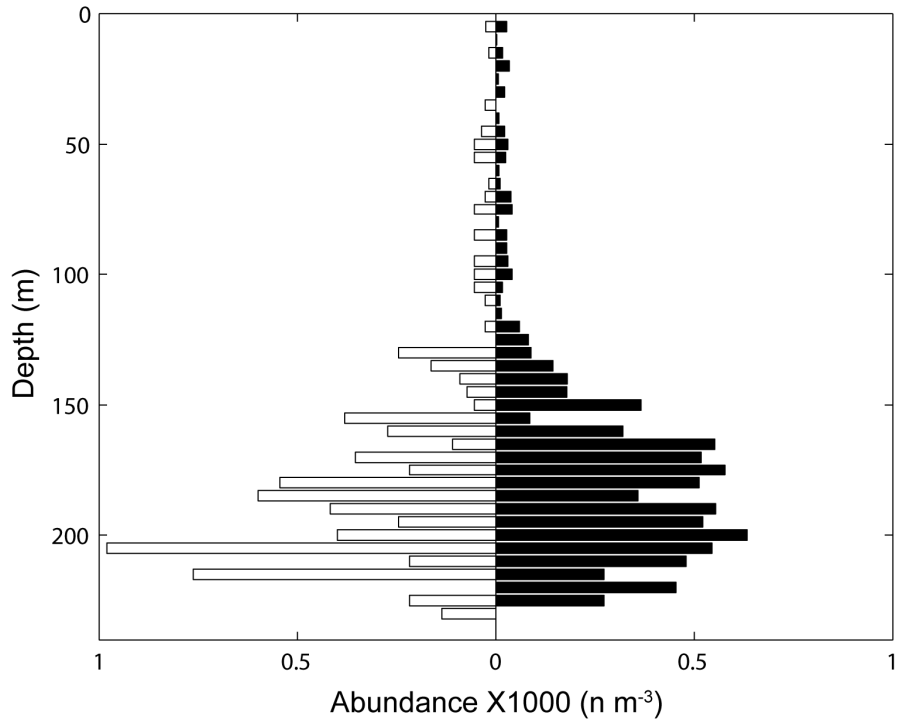


**Figure 4.16.** Vertical distribution of *C. finmarchicus* in Jordan Basin during December 1999 during day (empty horizontal bars, left) and night (black bars, right) periods.

In December 1998, *C. finmarchicus* was more abundant in the western portion of the Georges Basin transect. Patches in the western portion were more clustered while those observed in the eastern portion of the basin were more scattered (Fig. 4.17). Also, the densest patches in the western side were found closer to the bottom (~200-250 m) while low abundance patches were observed below this depth in the eastern side.

Although dense patches of *Calanus finmarchicus* were located in the western side of Georges Basin during December 1999, they were few in number and smaller in size compared with the other patches found in the northeastern part of the basin. The largest and densest patches of *C. finmarchicus* were located in the Northeast Channel (NEC) and in the area that connects the NEC with Georges Basin (Fig. 4.18). Almost without exception, all dense patches of *C. finmarchicus* during December 1999 were located below 125 m depth.

The TSP plot revealed that the highest *C. finmarchicus* abundances (214 n $m^{-3}$) were associated with the interface between the MBW and the LSSW in Georges Basin during December 1998 (Fig. 4.19). Relatively low abundances (~80 n $m^{-3}$) were associated to the other three water masses. From these three, the SLW contained *C. finmarchicus* in abundances up to 130 n $m^{-3}$. During December 1999, the highest (~450-1,035 n $m^{-3}$) abundances of *C. finmarchicus* were associated with the SLW (Fig. 4.20). Lower abundances were associated with the MSW and the MBW, and very few observations were associated with the MIW. Observations of *C. finmarchicus* in the LSSW were located in the boundary layer between this water mass and the SLW.

No diel vertical migration pattern was observed for *C. finmarchicus* in December 1998 (Figs. 4.17 and 4.22). However, low abundance patches (below ~50 n $m^{-3}$) were present in the upper 100 m depth in the night section (Fig. 4.17) more than during the day section. No vertical activity was observed in *C. finmarchicus* during December 1999, as most of the dense patches were found at depth during night periods (Figs. 21 and 23). Low abundances were observed during day time. This, however, may be due to spatial distribution differences.

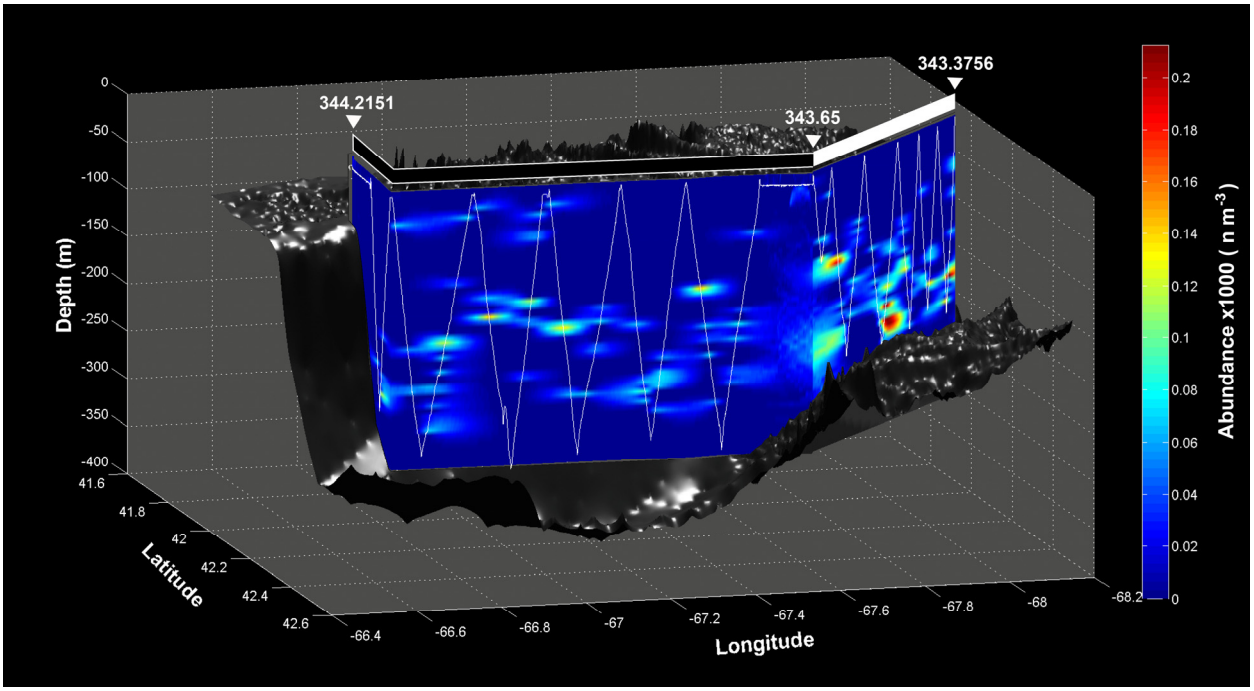


**Figure 4.17.** *Calanus finmarchicus* distribution in Georges Basin during December 1998. The top bar represents the day (white) and night (black) portions of the transect. The dark grey surface represents the bathymetry of the basin. Georges Bank is behind the "curtain" so that the east is to the left of the graph (X-ordinate) and south is towards the back of the graph (Y-ordinate). White solid line represents the trajectory of BIOMAPER-II.

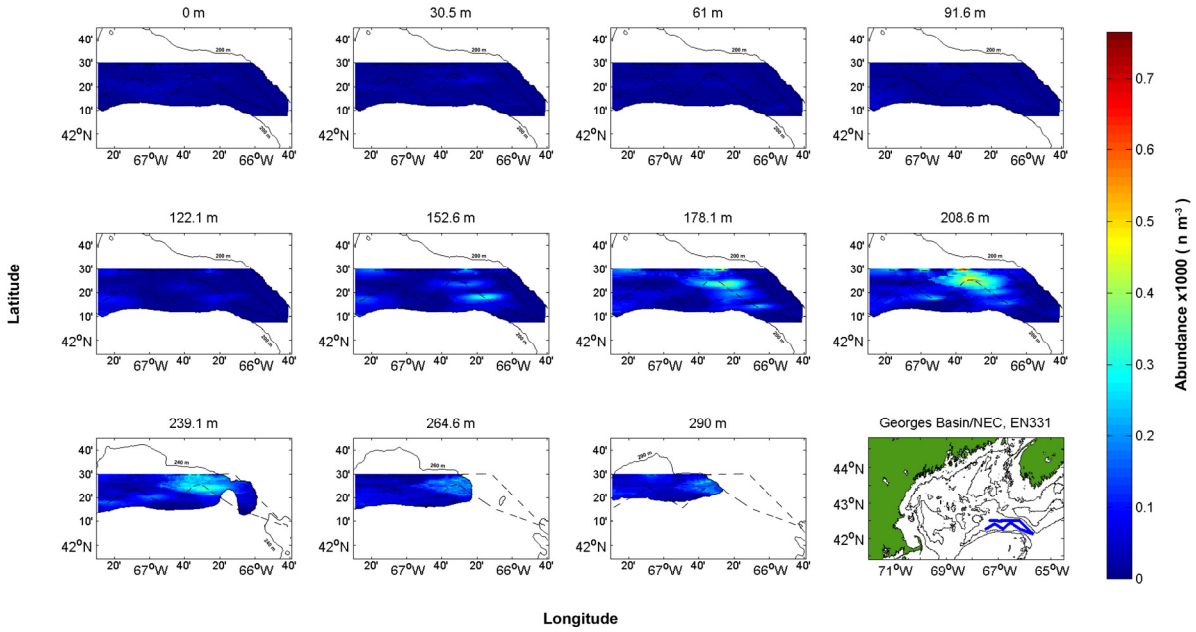


**Figure 4.18.** *Calanus finmarchicus* abundance in Georges Basin/Northeast Channel during December 1999 plotted at ~30 m intervals. Isobaths (solid line) and cruise track (dashed line) were superimposed for reference.

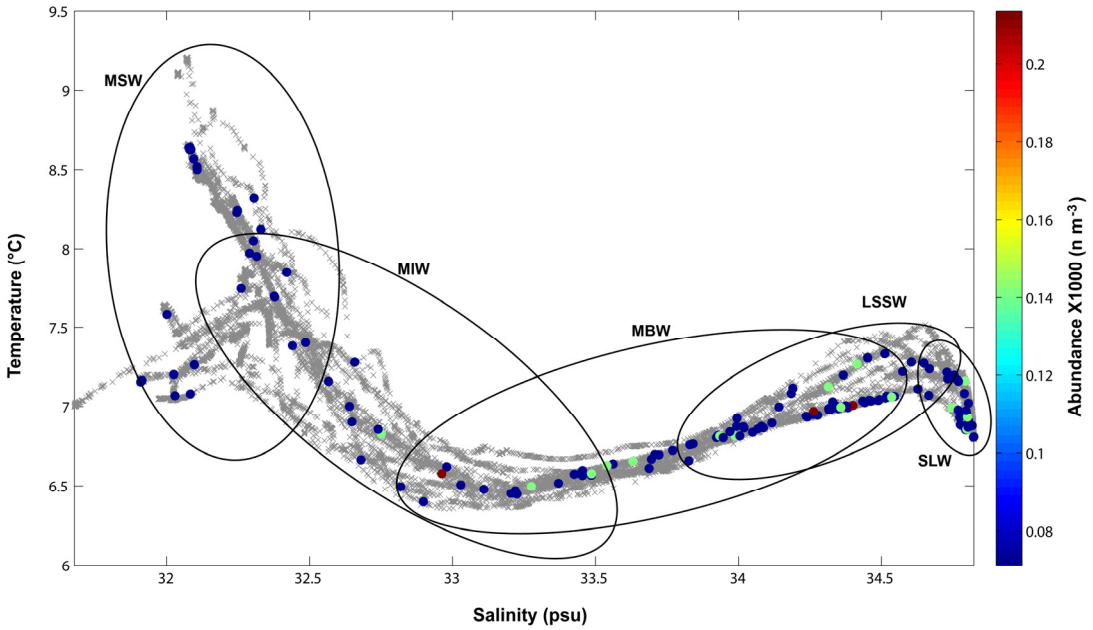


**Figure 4.19.** TSP plot for Georges Basin during December 1998. *Calanus finmarchicus* abundances are shown in color-coded dots. Temperature-Salinity points are plotted in grey X marks. MSW=Maine Surface Water; MIW=Maine Intermediate Water; MBW=Maine Bottom Water; LSSW=Labrador Subarctic Slope Water; SLW=Slope Water.

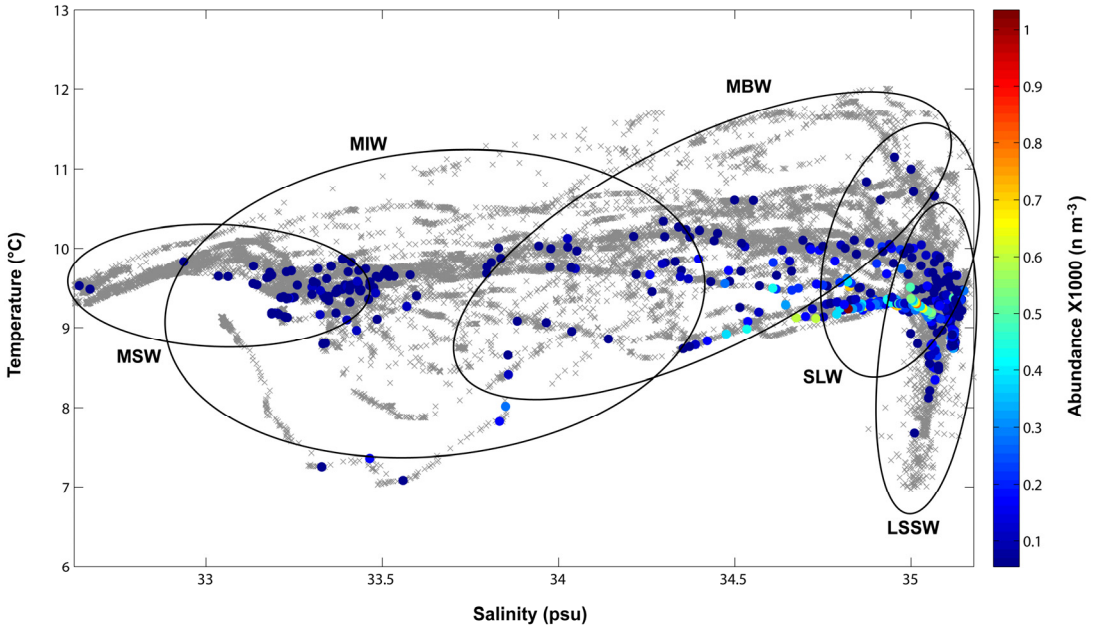


**Figure 4.20.** TSP plot for Georges Basin/Northeast Channel during December 1999. *Calanus finmarchicus* abundances are shown in color-coded dots. Temperature-Salinity points are plotted in grey X marks. MSW=Maine Surface Water; MIW=Maine Intermediate Water; MBW=Maine Bottom Water; LSSW=Labrador Subarctic Slope Water; SLW=Slope Water.

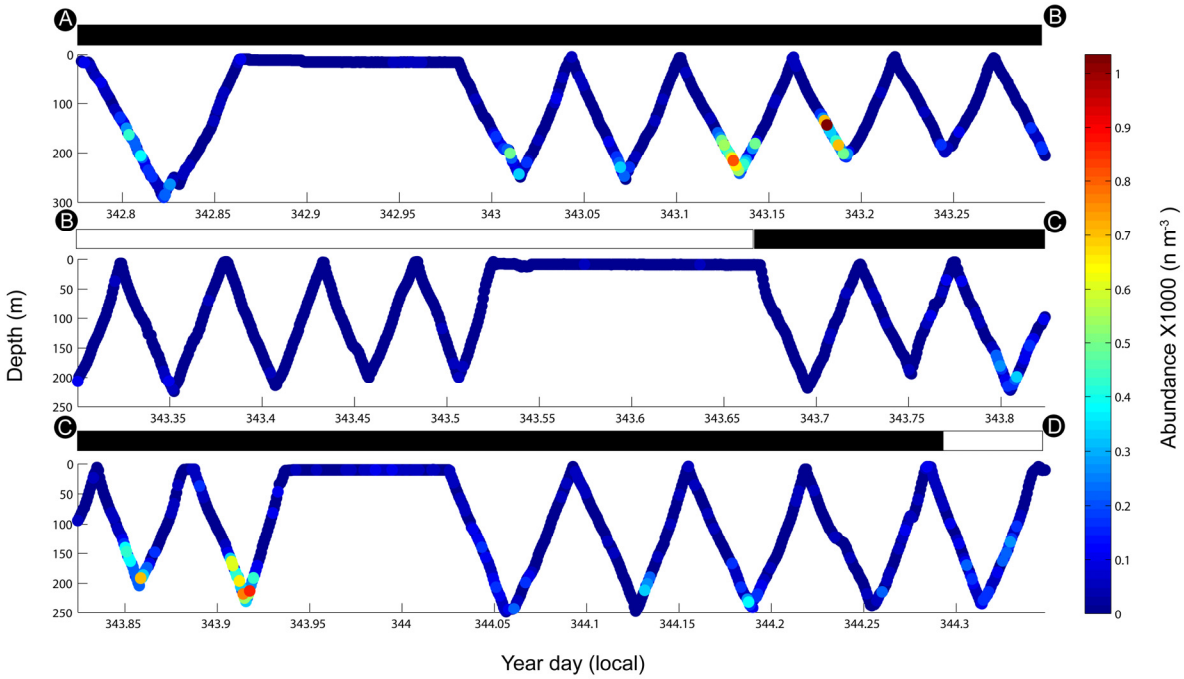


**Figure 4.21. .** Diurnal vertical distribution of *Calanus finmarchicus* in Georges Basin/Northeast Channel during December 1999 along BIOMAPER-II track. Bars on top of each subplot represent day (white) and night (black) periods. Capital letters at the beginning and end of each panel correspond to the sections of the Jordan Basin, EN331 cruise track in Fig. 2.6.

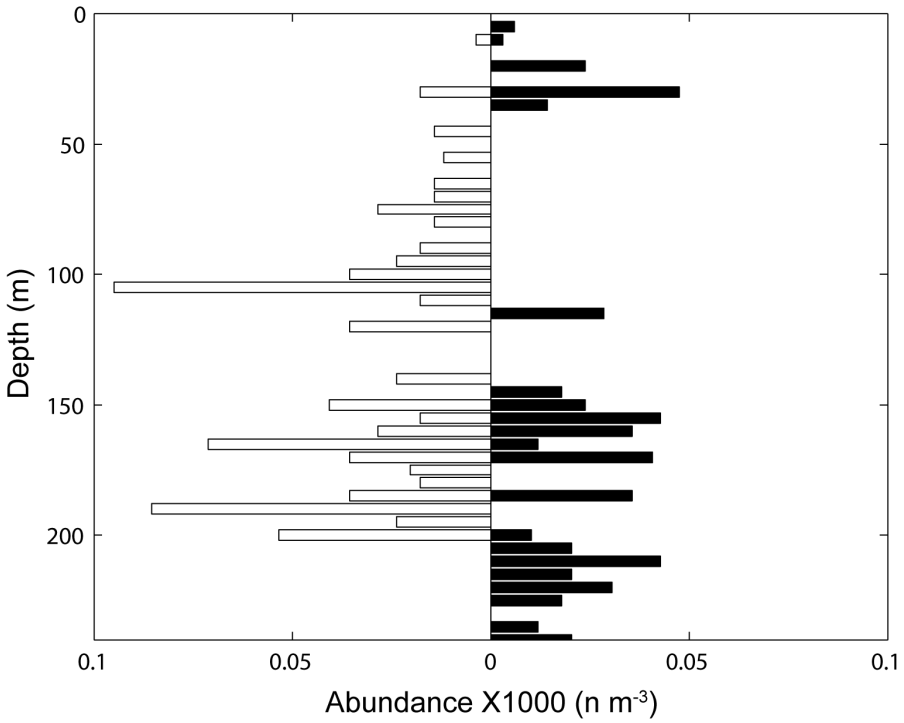


**Figure 4.22.** Vertical distribution of *C. finmarchicus* in Georges Basin Basin during December 1998 during day (empty horizontal bars, left) and night (black bars, right) periods.

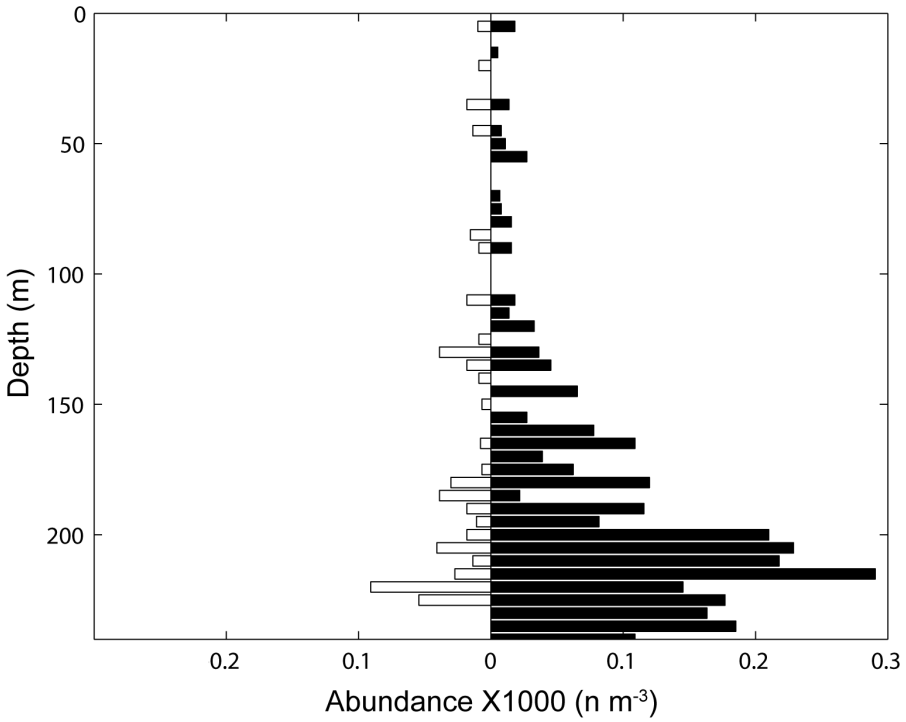


**Figure 4.23.** Vertical distribution of *C. finmarchicus* in Georges Basin/Northeast Channel during December 1999 during day (empty horizontal bars, left) and night (black bars, right) periods.

## 4.4 Discussion

### 4.4.1 Inter-Annual Differences

The GOM experienced two modes of the North Atlantic Oscillation (NAO) index during 1998 and 1999. A positive correlation has been reported between *Calanus finmarchicus* abundances and the general state of the NAO. This positive relationship is thought to be an important factor in controlling *C. finmarchicus* abundance in the GOM (Greene and Pershing, 2000; Conversi et al., 2001). During December 1998, *C. finmarchicus* were considerably less abundant than during December 1999. Although biological factors may also contribute to this interannual difference, the high abundances of *C. finmarchicus* occurred during a period when the NAO was positive while low abundances coincided with the predominantly negative NAO year of 1998. This observation is in agreement with the expected correlation between the NAO and *C. finmarchicus* abundance fluctuations.

During December 1998 the deep basins were occupied by the Labrador Slope Water (LSSW). The extended presence of this nutrient-poor water mass in the deep basins could have resulted in a lower production of *C. finmarchicus* earlier that year, a condition probably reflected in the low abundance of diapausing *C. finmarchicus* in the deep basins of the Gulf by December 1998. Not only is the LSSW poor in nutrients, but is also thought to be depauperate in *C. finmarchicus* (Greene and Pershing, 2000). My observations agree with this report, since lower abundances of *C. finmarchicus* were observed during December 1998, when the LSSW was present in all deep basins of the GOM. The dominance of this *Calanus*-depleted water in the deep basins may have contributed to the low abundances observed during December 1998.

During the positively NAO year of 1999, the remnants of the LSSW were found in the Northeast Channel, but not in the deep basins (MERCINA, 2001). By December 1999 the GOM had returned to its normal conditions, and regular nutrient-rich SLW was found in all basins. The high abundances of diapausing *C. finmarchicus* observed during December 1999 may have been the result of high production rates of *C. finmarchicus* in the GOM earlier in 1999.

The Slope Water (SLW) enters the Gulf of Maine via the Northeast Channel. This advection is thought to occur in during intense outbursts during winter (Ramp et al., 1985). During the SLW advection pulses, *C. finmarchicus* is thought to enter the GOM within the SLW packets. Once the newly advected SLW enters the Gulf, it accumulates in Georges Basin and it is later transferred to the other deep basins. This water mass transport is thought to follow the mean cyclonic circulation of the Gulf (Brown and Irish, 1993; Warn-Varnas et al., 2006), passing from Georges to Jordan Basin, then on to Wilkinson Basin. However, SLW exchange can occur directly from Georges Basin to Wilkinson Basin following a deep (below 75 m) pathway from southwestern Georges Basin to eastern Wilkinson Basin (Brooks, 1985). By this means it is possible that *C. finmarchicus* advected into the Georges Basin via the Northeast Channel, could be transported on to Wilkinson Basin directly.

During this study, at least two SLW pulses were presumably indentified in the GOM during December 1999. Pulse events in this work were identified by visually observing the presence of SLW extending from the known source regions to the interior of the deep basins. One additional indication of been an advected water is the presence of high densities of *Calanus finmarchicus*, whose diapausing expatriate populations are known to enter during such events. One pulse was positively identified entering through the northeastern side of the Northeast Channel and probably reached the northern Georges Basin (Chapter 3; Fig. 3.17). It was in these same areas were *C. finmarchicus* was found in high abundance patches. The high abundances of *C. finmarchicus* observed in Georges Basin during December 1999 may have been directly related to newly advected *C. finmarchicus*.

The second pulse of SLW was observed in Wilkinson Basin during December 1999. This pulse of water with the characteristics of SLW was observed in southeast Wilkinson Basin from ~120 to 150 m (Chapter 3; Fig. 3.4). High abundances of *C. finmarchicus* were also found at these depths and location (Fig. 4.2). Although these patches of *C. finmarchicus* could have been advected within this pulse of SLW, the largest abundances and patches of *C. finmarchicus* were actually found below 150 m. The large abundances of diapausing *C. finmarchicus* observed during December 1999 could have been the result of high production earlier in 1999 (deepest diapausing population) combined with the presumably newly advected *C. finmarchicus* within the SLW.

Water exchange rates inside the deep basins are in the order of 10-12 months (Christensen et al., 1996; Xue et al., 2000). The fact that SLW was identified in a particular basin does not necessarily mean it was recently advected. The vertical position of the water mass could also indicate if a particular water mass is a remnant of a previously advected water mass or not. For example, the SLW was observed shallower (usually from above sill depths) during December 1999 than during December 1998 (Chapter III).

*Calanus finmarchicus* found above the basin sill depths (~190-200 m) are suspected to be advected away from that particular basin and would either be lost or transported into another basin (Johnson et al., 2006). Although no SLW advection pulse was identified in Jordan Basin during December 1999, the large abundances found above the sill depth of the basin may have been the result of one or more such events rather than the result of the locally produced *C. finmarchicus* earlier that year. Evidence supporting this hypothesis is that high densities of *C. finmarchicus* in Jordan Basin were found almost homogeneously across and along the basin, reflecting the possible accumulation of *C. finmarchicus* in the basin at those depths (Fig. 4.8). One more confirmatory observation comes from the fact that in all cases, the temperature-salinity-plankton plots associated the SLW with *C. finmarchicus* high abundances (Figs. 4.4, 4.10 and 4.16).

Although during December 1998 TSP plots showed some relationship between *C. finmarchicus* to the SLW, the copepod was also found in the other water masses in high abundances. The clear association of *C. finmarchicus* with the newly advected SLW observed in the three deep basins during December 1999 was not observed during December 1998. Since no SLW advection events were evident in either basin during December 1998 it is safe to assume that no significant advection of *C. finmarchicus* from outside of the GOM occurred during this period. The high values observed in the deep basins and associated with the SLW during December 1998 were more likely diapausing *C. finmarchicus* and not of exogenous origin as in the case of December 1999. Differences in advected *C. finmarchicus* could be one explanation for the differences observed in its abundances between December 1999 and 1998.

**4.4.2 Regional and Inter-Basin Distribution Patterns**

Johnson et al. (2006) modeled the retention and dispersion rates of diapausing *C. finmarchicus* in the GOM and found that Wilkinson Basin had the highest retention rate while Georges and Jordan basins had the lowest. Advection of *C. finmarchicus* could therefore be another factor contributing to the regional differences in *C. finmarchicus* abundances. During

both studied periods, *C. finmarchicus* was always more abundant in Wilkinson Basin and Jordan basins. Georges Basin consistently showed the lowest abundances within each period. My results were in close agreement with the results obtained from the Johnson et al (2006) model.

While advection of water masses into the GOM occurs mainly through the northeast portion of the NEC, waters from the GOM exit through the southwest area of the NEC (Ramp et al., 1985). Further, in simulation runs Johnson et al. (2006) report that passive particles seeded in Georges Basin left the GOM through the western Northeast Channel and across the Northeast Peak of Georges Bank. During December 1998 and 1999, lower *Calanus finmarchicus* abundances were found in the southeastern Georges Basin compared to the higher abundances in the north of the basin. *Calanus finmarchicus* in the southeastern Georges Basin, close to the exit of the NEC could have been advected in to the North Atlantic or the neighboring Georges Bank during December 1998 and 1999. That may help explaining why low abundances of *C. finmarchicus* were observed in this region during both studied periods.

Dense patches of *Calanus finmarchicus* during December 1998 were mostly found in the south and southwestern areas of Wilkinson and Jordan basins. The lowest abundances were located in the northern areas. This distribution pattern closely reflected the mean circulation of the GOM (Johnson et al., 2006). If no *C. finmarchicus* were being advected during this low abundance period, one would expect to see lower abundances to the northeast areas of the basins. Further, the diapausing *C. finmarchicus* would be subject to the local counterclockwise gyres and therefore be carried away from the northeast and been accumulated in these areas while not been replenish in the northeastern regions.

No similar distribution pattern was observed during December 1999. This was probably due in part to the potential advection of expatriate *C. finmarchicus* replenishing the basins from the Atlantic Ocean through the NEC.

### 4.4.3 Inter-Annual Vertical Distributions

The duration of diapause by *Calanus finmarchicus* has been estimated to last between 3.5 and 5.5 months (Saumweber, 2006). *Calanus finmarchicus* usually enters diapause on late summer-early fall (Miller, 2004) and resurfaces in late winter. However, in some instances resurfacing can happen in late fall and early winter (Durbin et al., 1997; Durbin et al., 2000). Judging from the shallower and broader vertical distribution of *C. finmarchicus*, this seemed to be the case during December 1998. This observation may suggest that a portion of the population was already coming out of diapause during the early winter of 1998.

There is an ongoing discussion on the factors affecting onset and termination of dipause with no general consensus to date (Irigoien, 2004; Saumweber and Durbin, 2006; Johnson et al., 2008). However, the lipid accumulation window hypothesis (Johnson et al., 2008) may explain the presence of dense patches of *C. finmarchicus* in surface 50 m waters during December 1998. Saumweber and Durbin (2006) also suggested that energy limitation may have an important role in the length of diapause. According to the lipid accumulation window hypothesis, the length of diapause could be controlled by the quantity of lipid reserve (wax esters) built up before entering diapause. The theory also suggests that once a copepod has consumed a certain portion of the lipid storage it must become active and migrate towards the surface and resume its development.

Under this hypothesis one would expect that during poor food-availability conditions *C. finmarchicus* would not be able to build up enough lipid storage to overwinter. Since the LSSW dominated the deep basins during critical developing time for the spring and summer of 1998, one would expect that diapausing *C. finmarchicus* found in December 1998 didn't meet their threshold lipid storage requirements. Without enough lipid storage to diapause, *C. finmarchicus* during late fall in December 1998 would have been forced to ascend earlier than its normal timing of late winter (Davis, 1987). I didn't measure oil sacs and could not compare the oil sac size of the presumably active *C. finmarchicus* with the ones of the diapausing *C. finmarchicus* in

the deep basins. However, differences in oil sac sizes among surficial and deep individuals is a plausible possibility given the environmental circumstances experienced by *C. finmarchicus* prior to December 1998. The VPR images lack sufficient resolution to perform measurements of the oil sac and even if resolution had been adequate, the orientations of individuals were usually unfavorable for such measurements.

Waters in the GOM were colder during December 1998 than during December 1999 (Chapter III). The broader distribution of *C. finmarchicus* in the water column during December 1998 may have been in response to the broader expanse of cooler temperatures present in the water column. During December 1998, when temperatures across the water column were warmer than during December 1999, diapausing *C. finmarchicus* was found clustered at depths in the deep basins where temperatures were several degrees cooler than in the surface. If diapause depth is associated with a certain thermal threshold it may also explain why animals were distributed more broadly in the water column during December 1998 when the waters were colder and more narrowly distributed during December 1999, when surface waters were warmer.

**4.5 References**


Avent, S. R., S. M. Bollens, M. Butler, E. Horgan, and R. Rountree. 2001. Planktonic hydroids on Georges Bank: ingestion and selection by predatory fishes. Deep Sea Research Part II: Topical Studies in Oceanography **48**: 673-684.

Beardsley, R. C., A. W. Epstein, C. Chen, K. F. Wishner, M. C. Macaulay, and R. D. Kenney. 1996. Spatial variability in zooplankton abundance near feeding right whales in the Great South Channel. Deep Sea Research Part II: Topical Studies in Oceanography **43**: 1601-1625.

Bigelow, H. B. 1924. Plankton of the offshore waters of the Gulf of Maine. Bulletin of the Bureau of Fisheries **40**: 1-509.

Brown, W. S. and J. D. Irish. 1993. The annual variation of water mass structure in the Gulf of Maine: 1986-1987." Journal of Marine Research **51**: 53-107.

Chu, D. 2004. EasyKrig 3.0. http://globec.whoi.edu/software/kriging/easy_krig/easy_krig.html.

Conversi, A., S. Piontkovski, and S. Hameed. 2001. Seasonal and interannual dynamics of *Calanus finmarchicus* in the Gulf of Maine (Northeastern US shelf) with reference to the North Atlantic Oscillation. Deep Sea Research Part II: Topical Studies in Oceanography **48**: 519-530.

Davis, C. S. 1987. Zooplankton life cycles. In: Backus, R. H. and D. W. Bourne (eds.) Georges Bank. Cambridge, Ma, MIT Press**:** 256-267.

Durbin, E. G., S. L. Gilman, R. G. Campbell, and Ann G. Durbin. 1995. Abundance, biomass, vertical migration and estimated development rate of the copepod *Calanus finmarchicus* in the southern Gulf of Maine during late spring. Continental Shelf Research **15**: 571-591.

Durbin, E. G., J. A. Runge, R. G. Campbell, P. R. Garrahan, M. C. Casas, and S. Plourde. 1997. Late fall-early winter recruitment of *Calanus finmarchicus* on Georges Bank. Marine Ecology Progress Series **151**: 103-114.

Durbin, E. G., P. R. Garrahan, and M. C. Casas. 2000. Abundance and distribution of *Calanus finmarchicus* on the Georges Bank during 1995 and 1996. ICES Journal of Marine Science **57**: 1664-1685.

Fish, C. J. 1936. The biology of *Calanus finmarchicus* in the Gulf of Maine and Bay of Fundy. Biological Bulletin **70**: 118-141.

Greene, C. H. and A. J. Pershing. 2000. The response of *Calanus finmarchicus* populations to climate variability in the Northeast Atlantic: basin-scale forcing associated with the North Atlantic Oscillation. ICES Journal of Marine Science **57**: 1536-1544.

Greene, C. H. and A. J. Pershing. 2004. Climate and the conservation biology of North Atlantic right whales: the right whale at the wrong time? Frontiers in Ecology and the Environment **2**: 29-34.

Irigoien, X. 2004. Some ideas about the role of lipids in the life cycle of *Calanus finmarchicus.* Journal of Plankton Research **26**: 259-263.

Johnson, C., J. Pringle, and C. Chen. 2006. Transport and retention of dormant copepods in the Gulf of Maine. Deep Sea Research Part II: Topical Studies in Oceanography **53**: 2520-2536.

Johnson, C. L., A. W. Leising, J. A. Runge, E. J. H. Head, P. Pepin, S. Plourde, and E. G. Durbin. 2008. Characteristics of *Calanus finmarchicus* dormancy patterns in the Northwest Atlantic. ICES Journal of Marine Science **65**: 339-350.

Li, X., J. D. J. McGillicuddy, E. G. Durbin, and P. H. Wiebe. 2006. Biological control of the vernal population increase of *Calanus finmarchicus* on Georges Bank. Deep Sea Research Part II: Topical Studies in Oceanography **53**: 2632-2655.

Lynch, D. R., W. C. Gentleman, D. J. McGillicuddy Jr., and C. S. Davis. 1998. Biological/physical simulations of *Calanus finmarchicus* population dynamics in the Gulf of Maine. Marine Ecology Progress Series **169**: 189-210.

Meise, C. J. and J. E. O'Reilly. 1996. Spatial and seasonal patterns in abundance and age-composition of *Calanus finmarchicus* in the Gulf of Maine and on Georges Bank. Deep-Sea Research II **43**: 1473-1501.

MERCINA. 2001. Oceanographic responses to climate in the Northwest Atlantic. Oceanography **14**: 76-82.

Miller, C. B. 2004. Biological Oceanography. Malden, MA, Blackwell Publishing. 402 p.

Ohman, M. D., K. Eiane, E. G. Durbin, J. A. Runge, and H. J. Hirche. 2004. A comparative study of *Calanus finmarchicus* mortality patterns at five localities in the North Atlantic. ICES Journal of Marine Sciences **61**: 687-697.

Pershing, A. J., C. H. Greene, J. W. Jossi, L. O'Brien, J. K. T. Brodziak, and B. A. Bailey. 2005. Interdecadal variability in the Gulf of Maine zooplankton community, with potential impacts on fish recruitment. ICES Journal of Marine Science. **62**: 1511-1523.

Ramp, S. R., R. J. Schlitz, and W. R. Wright. 1985. The deep flow through the Northeast Channel, Gulf of Maine. Journal of Physical Oceanography **15**: 1790-1808.

Saumweber, W. J. and E. G. Durbin. 2006. Estimating potential diapause duration in *Calanus finmarchicus*. Deep Sea Research Part II: Topical Studies in Oceanography **53**: 2597-2617.

Wishner, K. F., J. R. Schoenherr, R. Beardsley, and C. Chen. 1995. Abundance, distribution and population structure of the copepod *Calanus finmarchicus* in a springtime right whale feeding area in the southwestern Gulf of Maine. Continental Shelf Research **15**: 475-507.

Warn-Varnas, A., A. Gangopadhyay, J. A. Hawkins, and A. R. Robinson. 2005. Wilkinson Basin area water masses: a revisit with EOFs. Continental Shelf Research **25**: 277-296.

# CHAPTER V

# DISTRIBUTIONS OF INVERTEBRATE PREDATORS OF *CALANUS FINMARCHICUS*

## 5.1 Introduction

*Calanus finmarchicus* has been recognized as an important food source for commercially important fish species of the Gulf of Maine (GOM), and in general in the North Atlantic. Charismatic species, such as the basking shark (*Cetorhinus maximus*) and right whales (*Eubalaena glacialis*) also feed on *C. finmarchicus* (Durbin et al., 1995; Kenney et al., 1995; Wishner et al., 1995; Beardsley et al., 1996). Further, the production of right whale calves is believed to be dependent on the production of *C. finmarchicus* (Greene and Pershing, 2004).

However, *C. finmarchicus* is also consumed by members of the plankton. In other areas of the North Atlantic, studies have documented predation pressure by medusae, euphausiids (*Meganyctiphanes norvegica*) and shrimps (Gislason et al., 2007) on *C. finmarchicus*. In the GOM, *C. finmarchicus* is a common prey item in the diets of siphonophores (mainly *Nanomia cara*, *Agalma* sp.), medusae, ctenophores (*Mertensia* sp. and other cydippid and lobate taxa), chaetognaths (*Sagitta elegans*), euphausiids (primarily *Meganyctiphanes norvegica)*, and larger copepods (mainly *Euchaeta norvegica*) (Rogers et al., 1978; Mills, 1995; Sullivan and Meise, 1996; Dalsgaard et al., 2003; Rossi et al., 2008).

Published reports documenting the relationships between invertebrate predators and *C. finmarchicus* are scarce. Further, fewer works have directly addressed the feeding behavior of invertebrate predators (Rogers et al., 1978; Rossi et al., 2008). Because siphonophores, medusae and ctenophores, are reported to be voracious predators of copepods, these organisms have received a considerable degree of attention (Mills, 1995; Mills, 2001; Rossi et al., 2008; Youngbluth et al., 2008). Mills (1995) found that siphonophores and medusae are highly selective carnivores, which feed selectively on copepods. In some areas of the North Sea, copepod-eating siphonophores are thought to be responsible for reducing copepod population near to zero (Greve, 1994). The physonect siphonophore *Nanomia cara* is thought to

have significant effects on both its competitors and prey when it reaches densities 10-100 colonies $m^{-3}$ (Rossi et al., 2008).

Direct impact assessments on *C. finmarchicus* by siphonophores or other gelatinous taxa in the GOM are not known to be available. However, Mills (1995) believes that siphonophores, medusae and ctenophores may have an important role in driving the ecology in areas where they occur in large quantities. Moreover, gelatinous plankton may further impact fish recruitment. Mills (1995) commented on the possibility of a direct correlation of poor recruitment of yellowtail flounder, silver hake, redfish, and cod following blooms of *Nanomia cara* in the GOM. It is not clear whether this poor recruitment was caused by direct predation by the siphonophore, or due to competition for the same prey items.

In this chapter I explore the spatial (small- to basin-scale) and temporal (inter-annual) distributions of six invertebrate predators of *C. finmarchicus* in Wilkinson, Jordan and Georges Basins during December 1998 and December 1999. Possible relationships between these predators' abundance and their spatial distribution patterns with hydrological conditions are also discussed.

**5.2 Methods**

Environmental Sensor System (ESS) data from BIOMAPER-II was processed as reported in chapter II. Abundances were calculated in 60-s bins along the VPR track and Kriged using EasyKrig V3.0 tool box from Matlab. Best variogram/correlogram parameters used during Kriging are reported in Appendix B. Abundance estimates for siphonophores, medusae and euphausiids were calculated as described in chapter II. Kruskal-Wallis, a non-parametric version of the one-way ANOVA, was utilized to study differences in predator's abundances between studied periods in the three deep basins of the Gulf of Maine. Non-parametric techniques were utilized because data didn't meet normal distribution criteria, even when transformed using diverse methods (i.e. square root, log10). When significant differences were found, post-hoc pair-wise comparison tests were performed to investigate which groups were significantly

different from others. Temperature-salinity-plankton (TSP) plots were constructed using ESS data from BIOMAPER-II and non-Kriged estimated abundances. Water masses identified by cluster analysis were superimposed in the TSP plots to study the possible relationship between predators abundance and hydrological conditions in the Gulf of Maine during December 1998 and 1999.

**5.3 Results**

Six potential predators were studied in the three deep basins of the Gulf of Maine during December 1998 and 1999. One predator group was consisted of gelatinous plankton (siphonophores, ctenophores and medusae), the second group was composed of crustaceans (euphausiids and the predatory copepod *Euchaeta norvegica*), and the last one contained chaetognaths.

The abundances of *C. finmarchicus* invertebrate predators were significantly different for each of the three deep basins when compared across years. The pair-wise tests showed that siphonophores were significantly more abundant in December 1998 than in December 1999 in all three deep basins (Wilkinson Basin: $p<0.001$; Jordan Basin: $p<0.001$; Georges Basin: $p<0.001$). The very low abundance of ctenophores and medusae during December 1999 did not allow to statistically test for differences. However, as a group, gelatinous plankton was more abundant during December 1998 than during December 1999 in all three deep basins of the Gulf of Maine (Table 5.1). On the other hand, euphausiids (Wilkinson Basin: $p<0.001$; Jordan Basin: $p<0.05$; Georges Basin: $p<0.001$) and *E. norvegica* (Wilkinson Basin: $p<0.001$; Jordan Basin: $p<0.001$) were significantly more abundant during December 1999 than during December 1998 (Table 5.2). No statistical tests were performed for chaetognaths, as this group had extremely low abundances during December 1998. However, chaetognaths were more abundant during December 1999 than during December 1998 (Table 5.2).

Gelatinous plankton (siphonophores, ctenophores and medusae) were usually more abundant in Wilkinson Basin than in Jordan and Georges Basins during December 1998 and

December 1999 ($p<0.001$; Table 5.3). Georges Basin and Jordan Basin consistently showed no statistical differences in gelatinous plankton. Because of low abundances of ctenophore and medusae during December 1999, spatial patterns could not be statistically tested. Crustacean plankton was consistently greater in Wilkinson Basin than Jordan Basin ($p<0.05$; Table 5.4). Crustacean plankton in Jordan Basin had either no statistical differences or it was statistically lower than in Georges Basin. Chaetognaths were consistently greater in Georges Basin than in the other basins, and there were no statistical differences between Wilkinson and Jordan Basin ($p<0.001$; Table 5.4).

### 5.3.1 Siphonophores

#### 5.3.1.1 Wilkinson Basin

Siphonophores were less abundant during December 1999 than during December 1998 ($p<0.001$). During December 1998, siphonophores (*Nanomia cara*, *Agalma* sp.) were found widely distributed throughout Wilkinson Basin in densities below 10 $m^{-3}$. However, denser patches (15 – 35 $m^{-3}$) were present in scattered areas of the Basin. Vertically, siphonophores showed a bimodal distribution. The densest patches were found in the upper 75 m and then from 175 to 200 m. However, the deeper patches were less frequent and abundances at depth generally did not surpass densities of 25 $m^{-3}$ (Fig.5.1). High abundance patches (up to 13 $m^{-3}$) appeared dispersed horizontally and vertically within the basin with no apparent pattern. The highest density patches were located at 25.5, 148, 173, and 240 m at different locations.. The largest patch occurred at 240 m depth at the center of Wilkinson Basin (Fig. 5.2).

TSP plots showed that siphonophores appeared evenly distributed across the five water masses identified during December 1998. However, higher abundance (19-39 $m^{-3}$) observations were observed in association with MSW and SLW masses (Fig. 5.3). During December 1999 the TSP plot for siphonophores suggested that high abundance (10-15.8 $m^{-3}$) observations were not clearly related to specific water masses (Fig. 5.4) although most of these observations were

found in areas affected by MHW-MSW and SLW masses. Low (<6 $m^{-3}$) abundance observations were found associated with MIW and MBW masses.

Vertical distribution maps from December 1998 and 1999 indicated that siphonophores exhibited horizontal and vertical variability in their distributions (Figs. 5.5 and 5.6). Most of the densest patches appeared close to the surface during night time, although lower abundances were scattered in the water column. Interestingly, few dense patches were surveyed during day time at the surface during December 1998 (Figs. 5.5, top and bottom panels) and December 1999 (Fig. 5.6 middle panel). Low abundance patches appeared progressively deeper in the water column over the course of the day during both periods. While the color-coded scatter plots reveal spatial distributions, histograms of abundances compiled for day and night provide a more effective means of assessing potential vertical migration patterns. Siphonophore vertical distribution during December 1998 and 1999 showed some evidence of nocturnal vertical migration. During both periods, higher siphonophore abundances increased towards the surface during night time, while higher abundances increased towards depth during day time (Figs.5.7 and 5.8). However, that majority of the survey was conducted during the night and the observed vertical pattern may have been biased by spatial heterogeneity.

**Table 5.1.** Mean (1STD) abundance (n $m^{-3}$) of gelatinous plankton in the three deep basins of the Gulf of Maine during cruises OC334 (December 1998) and EN331 (December 1999). Pair-wise tests marked with an asterisk were significant at the 95 confidence level.

| Taxa | Deep Basin | December 1998 | December 1999 | Pair-wise test |
|---|---|---|---|---|
| Siphonophores | Wilkinson Basin | 2.4 (4.9) | 0.55 (1.9) | Dec.1998>Dec. 1999 |
| | Jordan Basin | 3.6 (10.6) | 0.065 (0.31) | Dec.1998>Dec. 1999 |
| | Georges Basin/NEC | 4.2 (9.1) | 0.36 (2.0) | Dec.1998>Dec. 1999 |
| Ctenophores | Wilkinson Basin | 13.9 (38.4) | ----- | N/A |
| | Jordan Basin | 7.9 (25.4) | ----- | N/A |
| | Georges Basin/NEC | 10 (31.7) | ----- | N/A |
| Medusae | Wilkinson Basin | 3.2 (13.9) | ----- | N/A |
| | Jordan Basin | 1.4 (9.0) | ----- | N/A |
| | Georges Basin/NEC | 3.1 (14.8) | ----- | N/A |

**Table 5.2.** Mean (1STD) abundance (n $m^{-3}$) of crustacean plankton and chaetognaths in the three deep basins of the Gulf of Maine during cruises OC334 (December 1998) and EN331 (December 1999). Pair-wise tests marked with an asterisk were significant at the 95 confidence level.

| Taxa | Deep Basin | December 1998 | December 1999 | Pair-wise test |
|---|---|---|---|---|
| Euphausiids | Wilkinson Basin | 1.9 (10.4) | 3.5 (14.9) | Dec. 1998<Dec. 1999* |
| | Jordan Basin | 1.1 (7.8) | 1.7 (10.0) | Dec. 1998<Dec. 1999* |
| | Georges Basin/NEC | 1.2 (8.5) | 3.9 (15.2) | Dec. 1998<Dec. 1999* |
| *E. norvegica* | Wilkinson Basin | 2.3 (13.5) | 6.1 (19.7) | Dec. 1998<Dec. 1999* |
| | Jordan Basin | 1.3 (9.9) | 4.1 (17.8) | Dec. 1998<Dec. 1999* |
| | Georges Basin/NEC | ----- | 2.7 (13.5) | N/A |
| Chaetognaths | Wilkinson Basin | ----- | 1.4 (9.3) | N/A |
| | Jordan Basin | ----- | 2.3 (13.2) | N/A |
| | Georges Basin/NEC | ----- | 7.6 (23.5) | N/A |

**Table 5.3.** Mean (1STD) abundance (n $m^{-3}$) of gelatinous plankton in the three deep basins of the Gulf of Maine during cruises OC334 (December 1998) and EN331 (December 1999). Pair-wise tests marked with an asterisk were significant at the 95 confidence level. WB=Wilkinson Basin; JB=Jordan Basin; GB=Georges Basin; NEC=Northeast Channel.

| Taxa | Period | Deep Basin | | | Pair-wise test |
|---|---|---|---|---|---|
| | | WB | JB | GB/NEC | |
| Siphonophores | Dec. 1998 | 2.4 (4.9) | 3.6 (10.6) | 4.2 (9.1) | WB=GB>JB* |
| | Dec. 1999 | 0.55 (1.9) | 0.065 (0.31) | 0.36 (2.0) | WB>JB=GB* |
| Ctenophores | Dec. 1998 | 13.9 (38.4) | 7.9 (25.4) | 10.0 (31.7) | WB>JB=GB* |
| | Dec. 1999 | ----- | ----- | ----- | N/A |
| Medusae | Dec. 1998 | 3.2 (13.9) | 1.4 (9.0) | 3.1 (14.8) | GB=WB>JB=GB* |
| | Dec. 1999 | ----- | ----- | ----- | N/A |

**Table 5.4.** Mean (1STD) abundance (n $m^{-3}$) of crustacean plankton and chaetognaths in the three deep basins of the Gulf of Maine during cruises OC334 (December 1998) and EN331 (December 1999). Pair-wise tests marked with an asterisk were significant at the 95 confidence level. WB=Wilkinson Basin; JB=Jordan Basin; GB=Georges Basin; NEC=Northeast Channel.

| Taxa | Period | Deep Basin | | | Pair-wise test |
|---|---|---|---|---|---|
| | | WB | JB | GB/NEC | |
| Euphausiids | Dec. 1998 | 1.9 (10.4) | 1.1 (7.8) | 1.2 (8.5) | GB=WB>JB=GB* |
| | Dec. 1999 | 3.5 (14.9) | 1.7 (10.0) | 3.9 (15.2) | WB=GB>JB* |
| *E. norvegica* | Dec. 1998 | 2.3 (13.5) | 1.3 (9.9) | ----- | WB>JB* |
| | Dec. 1999 | 6.1 (19.7) | 4.1 (17.8) | 2.7 (13.5) | WB>JB=GB* |
| Chaetognaths | Dec. 1998 | ----- | ----- | ----- | N/A |
| | Dec. 1999 | 1.4 (9.3) | 2.3 (13.2) | 7.6 (23.5) | GB>WB=JB* |

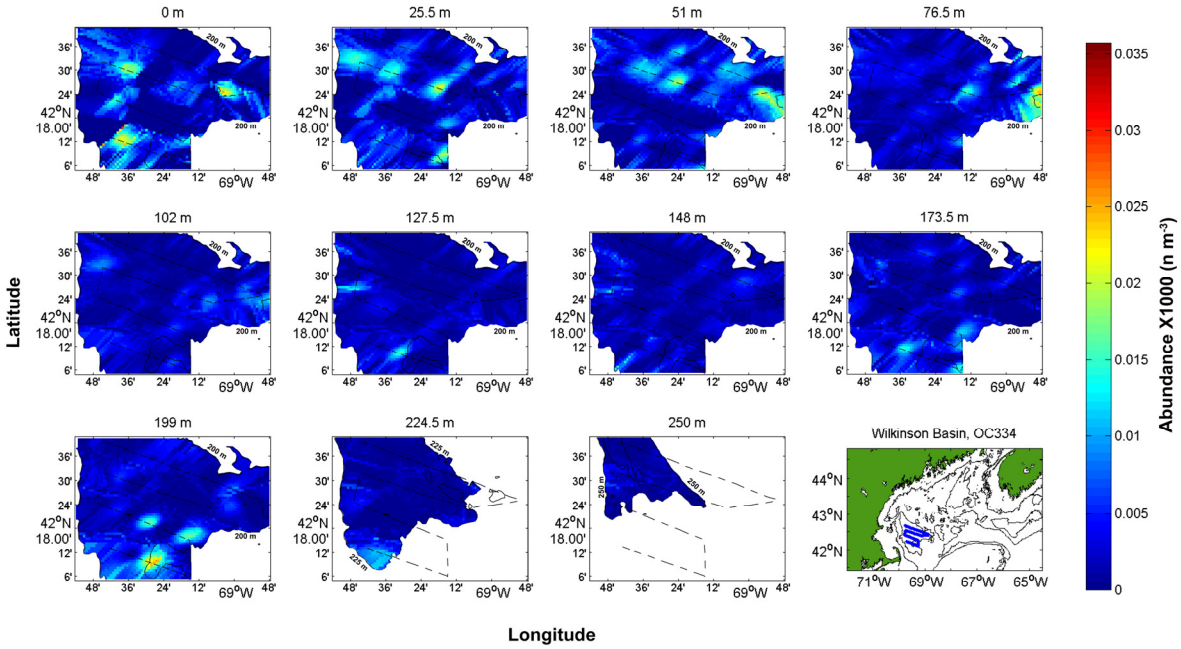


**Figure 5.1.** Siphonophores abundance in Wilkinson Basin during December 1998 plotted at 25 m intervals. Isobaths (solid lines) and cruise track (dashed line) were superimposed for reference.

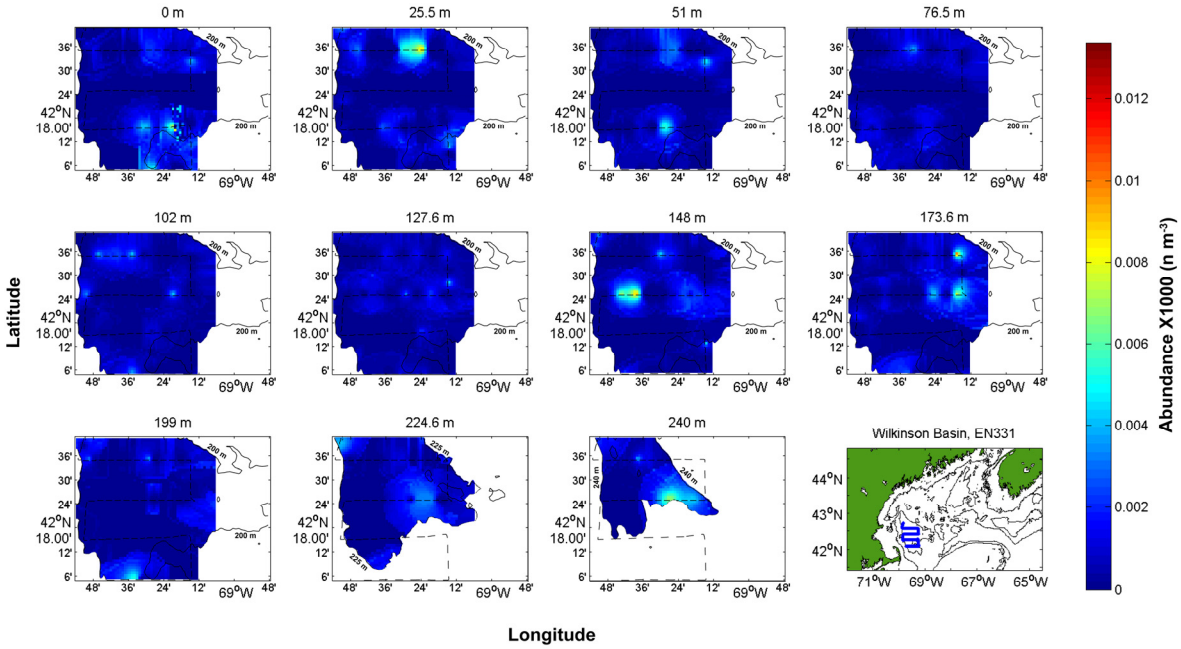


**Figure 5.2.** Siphonophores abundance in Wilkinson Basin during December 1999 plotted at 25 m intervals. Isobaths (solid lines) and cruise track (dashed line) were superimposed for reference.

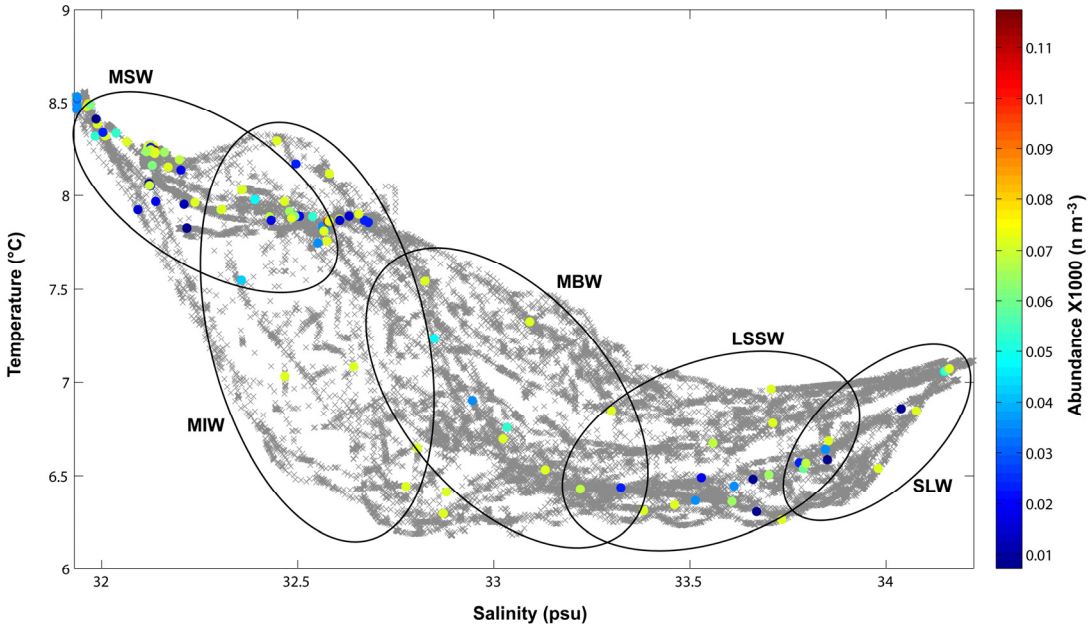


**Figure 5.3.** TSP plot for Wilkinson Basin during December 1998. Siphonophores abundances are shown in color-coded dots. Temperature-Salinity points are plotted in grey X marks. MSW=Maine Surface Water; MIW=Maine Intermediate Water; MBW= Maine Bottom Water; LSSW=Labrador Subarctic Slope Water; SLW=Slope Water.

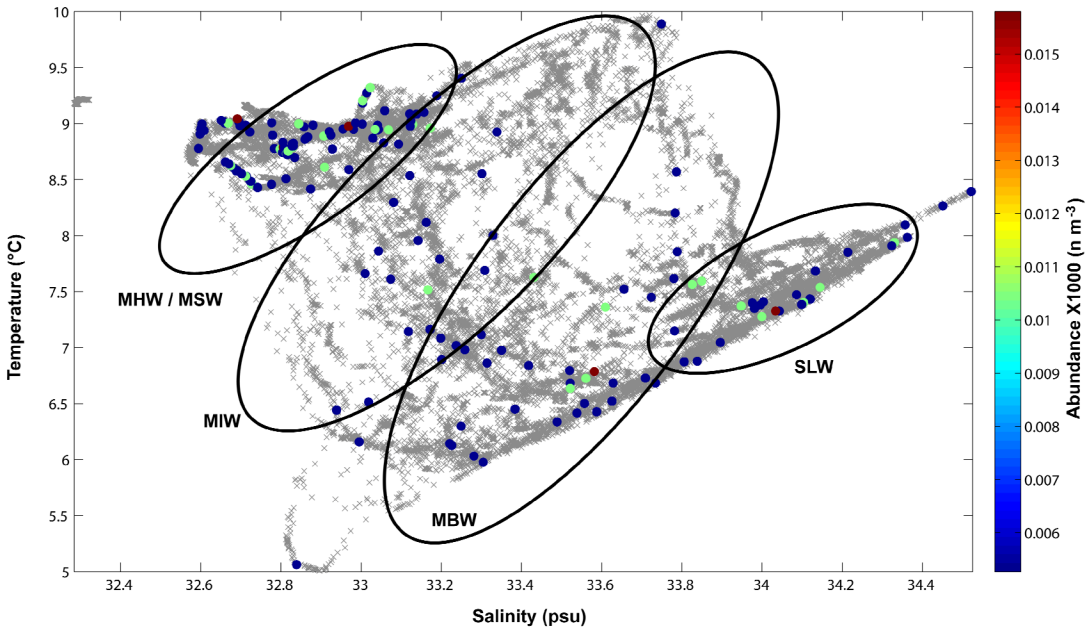


**Figure 5.4.** TSP plot for Wilkinson Basin during December 1999. Siphonophores abundances are shown in color-coded dots. Temperature-Salinity points are plotted in grey X marks. MHW=Maine Hot Water; MSW=Maine Surface Water; MIW=Maine Intermediate Water; MBW= Maine Bottom Water; SLW=Slope Water.

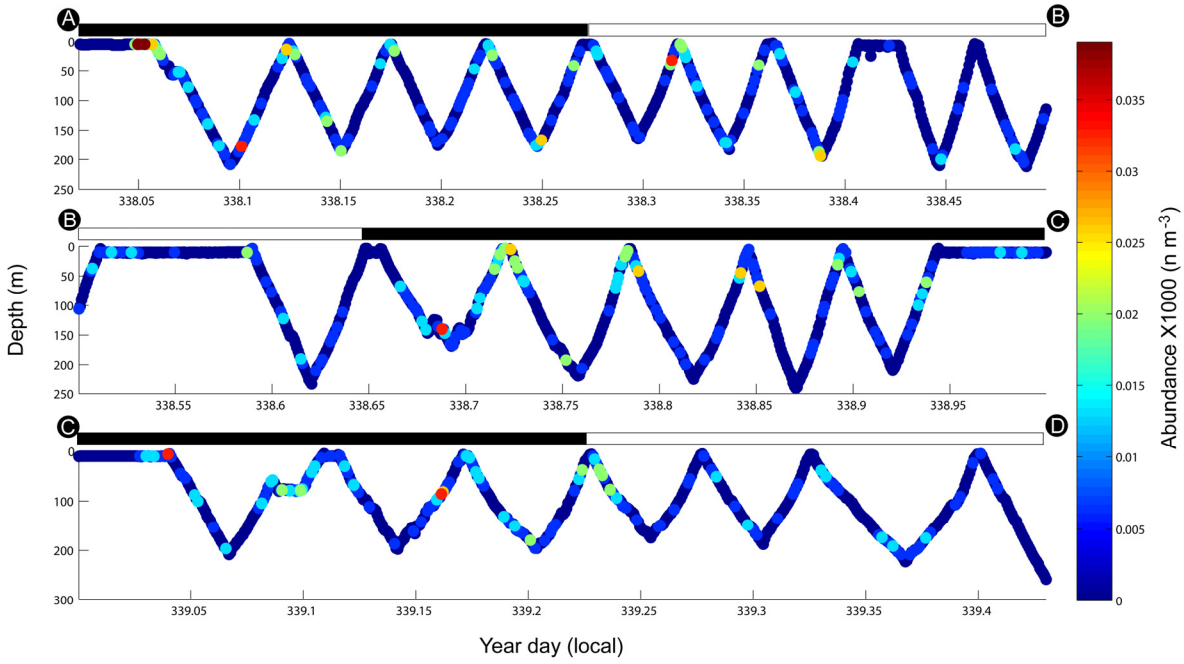


**Figure 5.5.** Diurnal vertical distribution of siphonophores in Wilkinson Basin during December 1998 along BIOMAPER-II track. Bars on top of each subplot represent day (white) and night (black) periods. Capital letters at the beginning and end of each panel correspond to the sections of the Wilkinson Basin, OC334 cruise track in Fig. 2.6.

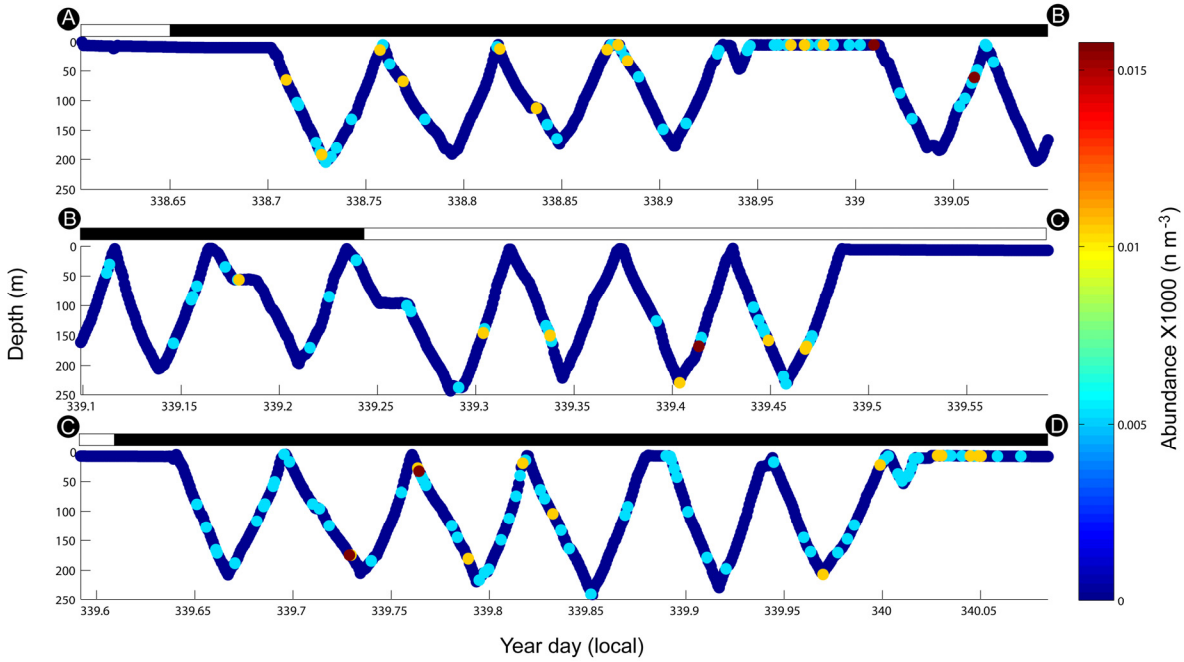


**Figure 5.6.** Diurnal vertical distribution of siphonophores in Wilkinson Basin during December 1999 along BIOMAPER-II track. Bars on top of each subplot represent day (white) and night (black) periods. Capital letters at the beginning and end of each panel correspond to the sections of the Wilkinson Basin, EN331 cruise track in Fig. 2.6.

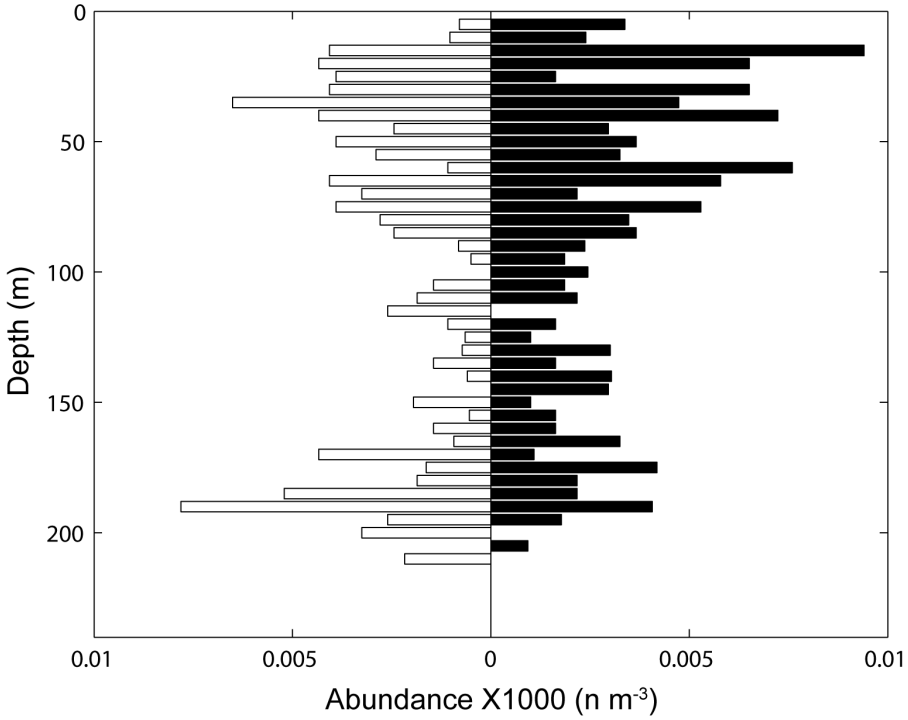


**Figure 5.7.** Vertical distribution of siphonophores in Wilkinson Basin during December 1998 during day (open horizontal bars, left) and night (black bars, right) periods.

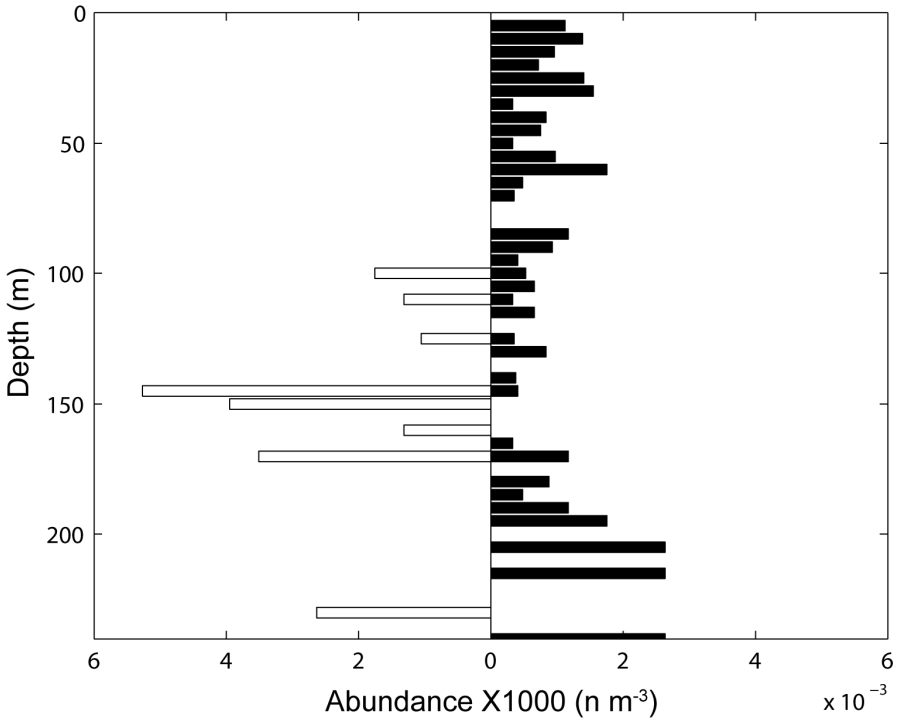


**Figure 5.8.** Vertical distribution of siphonophores in Wilkinson Basin during December 1999 during day (open horizontal bars, left) and night (black bars, right) periods.

#### 5.3.1.2 Jordan Basin

Siphonophore abundances in Jordan Basin were considerably higher during December 1998 than December 1999 ($p<0.001$). Siphonophore abundances observed during December 1999 were almost negligible with a maximum of only 3 $m^{-3}$. In contrast, abundances up to 93 $m^{-3}$ were observed during December 1998.

During December 1998, siphonophores were widely and evenly distributed in Jordan Basin at all depths at concentrations of 20 $m^{-3}$. The densest siphonophore patches were located between 173 m and 200 m deep (Fig. 5.9) in the northern half of the basin. Few siphonophores were observed in December 1999. However, siphonophores during December 1999 were patchily and sparsely distributed at all depths and along and across Jordan Basin with no apparent spatial pattern (Fig. 5.10).

TSP plots suggested a relationship between siphonophores distributions and water masses present in Jordan Basin. During December 1998, siphonophores were associated mostly with the LSSW and with the boundary between the MSW and MIW (Fig. 5.11). Despite the few observations of siphonophores in December 1999, most siphonophore observations were associated to the MHW/MSW complex and to the SLW (Fig. 5.12). Some observations were made in the MBW as well, but very close to the SLW nonetheless.

There seemed to be evidence of siphonophore diel vertical migration in Jordan Basin during December of both years. During December 1998, siphonophores were scattered vertically at night, while during day their abundances increased with increasing depth (Figs. 5.13 and 5.15). Despite the low siphonophores abundance on December 1999, there seemed to be differences in vertical distributions (Figs. 5.14). After dusk, small patches of siphonophores appeared progressively shallower (Fig. 5.14 top panel) while before dawn, most patches appeared progressively deeper (Fig. 5.14, bottom panel). The distributional pattern in December 1999 was similar to that of the previous year, with siphonophores scattered in the water column at night while aggregated at depths below ~140 m during day time (Fig. 5.16).

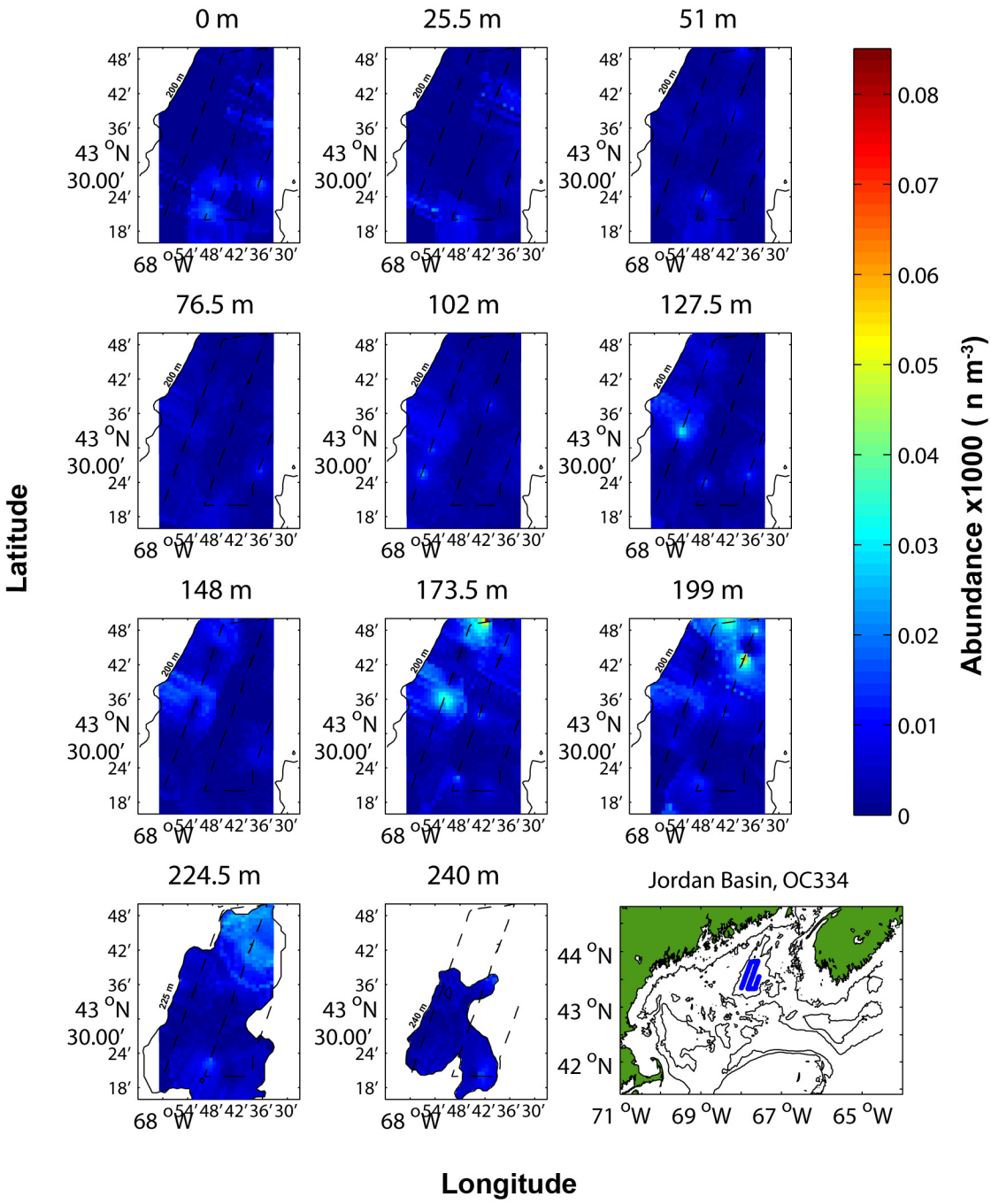


**Figure 5.9.** Siphonophore abundance in Jordan Basin during December 1998 plotted at 25 m intervals. Isobaths (solid lines) and cruise track (dashed line) were superimposed for reference.

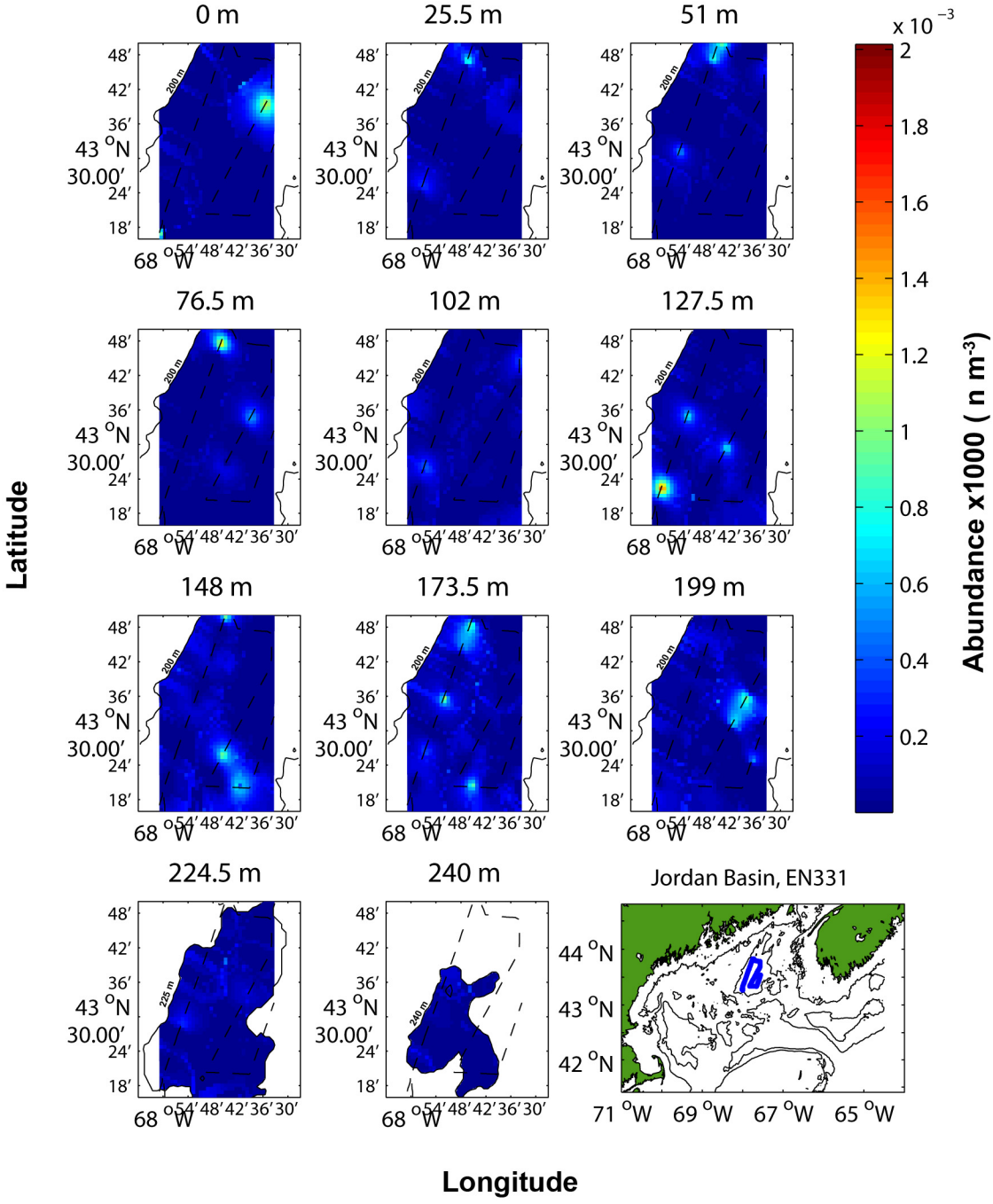


**Figure 5.10.** Siphonophore abundance in Jordan Basin during December 1999 plotted at 25 m intervals. Isobaths (solid lines) and cruise track (dashed line) were superimposed for reference.

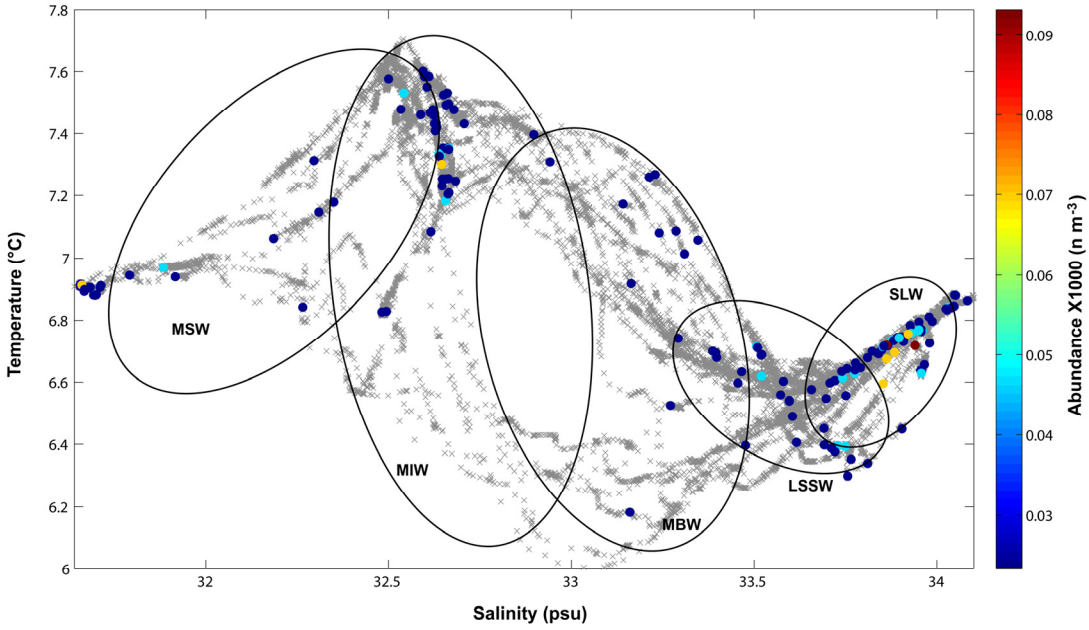


**Figure 5.11.** TSP plot for Jordan Basin during December 1998. Siphonophore abundances are shown in color-coded dots. Temperature-Salinity points are plotted in grey X marks. MSW=Maine Surface Water; MIW=Maine Intermediate Water; MBW= Maine Bottom Water; LSSW=Labrador Subarctic Slope Water; SLW=Slope Water.

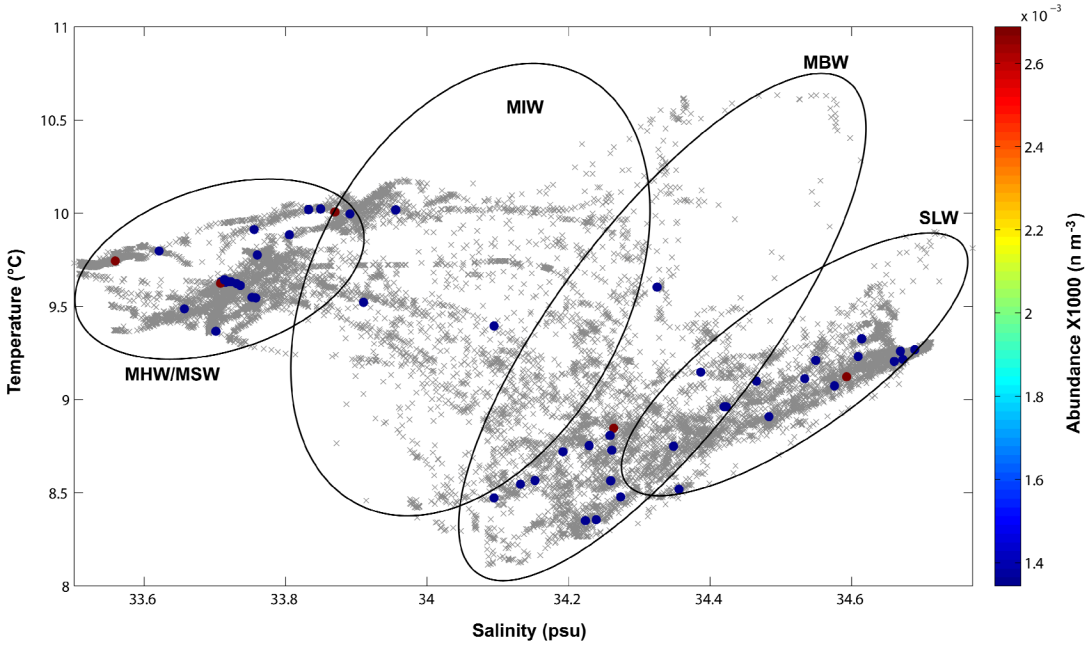


**Figure 5.12.** TSP plot for Jordan Basin during December 1999. Siphonophore abundances are shown in color-coded dots. Temperature-Salinity points are plotted in grey X marks. MHW=Maine Hot Water; MSW=Maine Surface Water; MIW=Maine Intermediate Water; MBW= Maine Bottom Water; SLW=Slope Water.

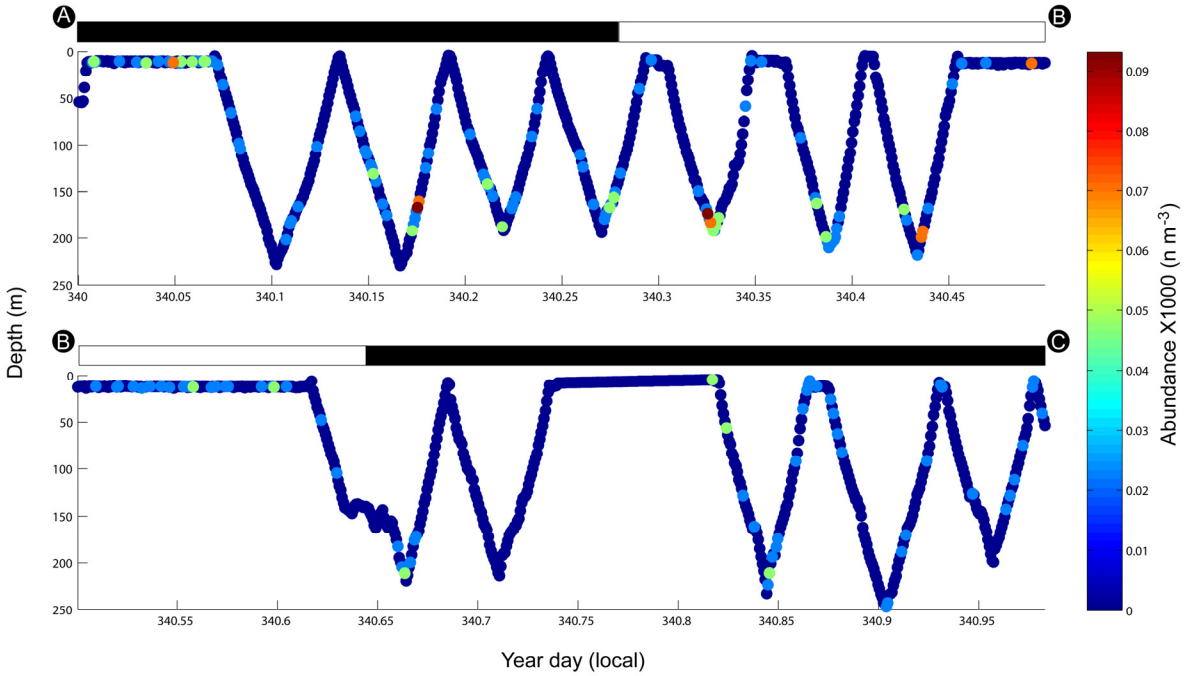


**Figure 5.13.** Diurnal vertical distribution of siphonophores in Jordan Basin during December 1998 along BIOMAPER-II track. Bars on top of each subplot represent day (white) and night (black) periods. Capital letters at the beginning and end of each panel correspond to the sections of the Jordan Basin, OC334 cruise track in Fig. 2.6.

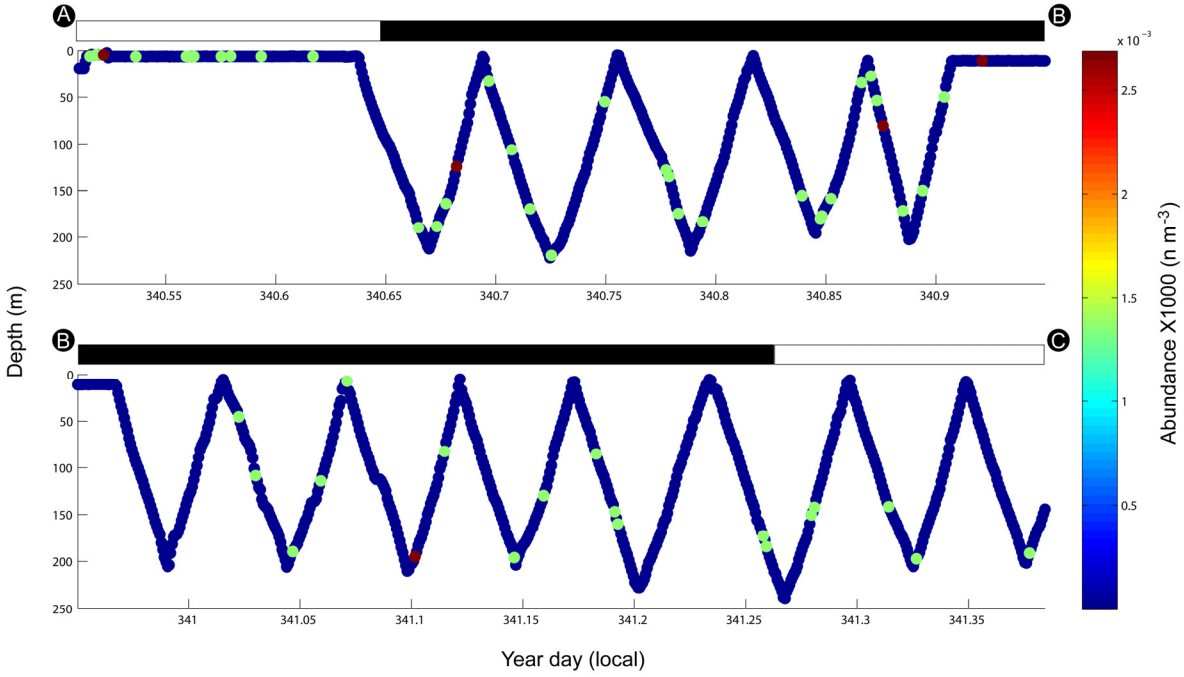


**Figure 5.14.** Diurnal vertical distribution of siphonophores in Jordan Basin during December 1999 along BIOMAPER-II track. Bars on top of each subplot represent day (white) and night (black) periods. Capital letters at the beginning and end of each panel correspond to the sections of the Jordan Basin, EN331 cruise track in Fig. 2.6.

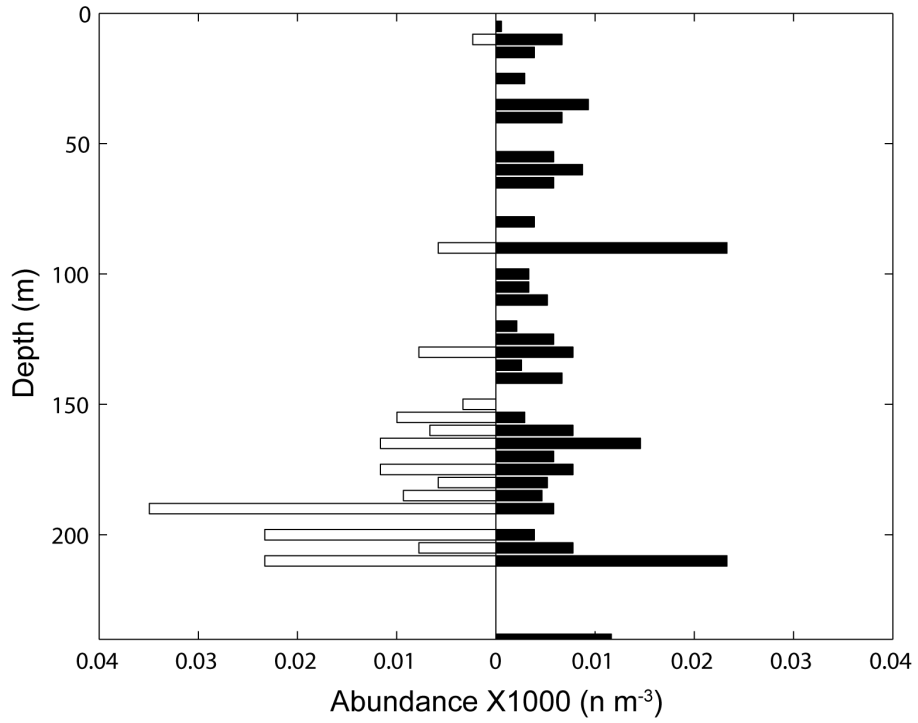


**Figure 5.15.** Vertical distribution of siphonophores in Jordan Basin during December 1998 during day (open horizontal bars, left) and night (black bars, right) periods.

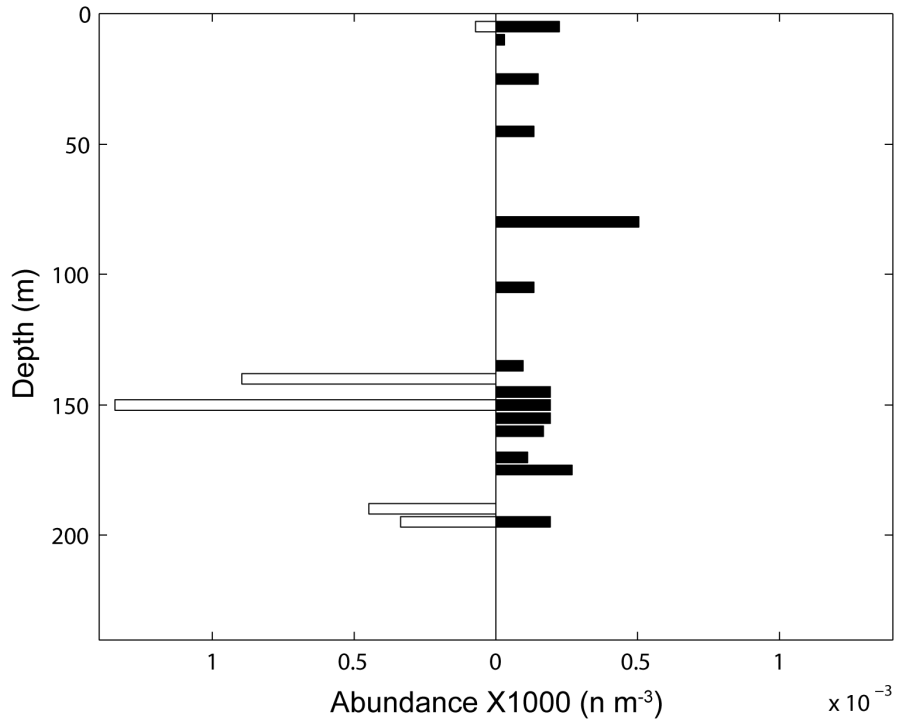


**Figure 5.16.** Vertical distribution of siphonophores in Jordan Basin during December 1999 during day (open horizontal bars, left panel) and night (black bars, right panel) periods.

#### 5.3.1.3 Georges Basin/Northeast Channel

Siphonophores in Georges Basin were more abundant during December 1998 than during December 1999 ($p<0.001$). During December 1998, siphonophores abundance ranged from ~11 to ~86 $m^{-3}$ (mean±standard deviation 4.2±9.1). On December 1999, siphonophores abundances varied between ~9 and ~42 $m^{-3}$ (mean±standard deviation 0.36±2.0).

During December 1998, siphonophores patches were scattered in the water column along the entire transect. However, the densest patches resolved by Kriging were found in the upper 100 m and to the west of the Georges Basin transect. A dense aggregation of siphonophores was also observed between 150 and 200 m depth in the western portion of the transect (right side on Fig. 5.17).

During December 1999, siphonophores were more abundant in Georges Basin than in the Northeast Channel (NEC). The densest and largest aggregations of siphonophores were found in the westernmost portion of Georges Basin and below 150 m depth. A large patch was also located below 200 m in the northeast portion of Georges Basin, close to the NEC area. Fewer and smaller siphonophores patches were observed in the NEC and the eastern Georges Basin, where they were mostly scattered along the entire water column (Fig. 5.18).

During December 1998, siphonophores largest abundances were associated to the MSW in Georges Basin (Fig. 5.19). The MIW and the MBW had the lowest siphonophores abundances. The LSSW and the SLW were also associated to medium-high siphonophores abundances. During December 1999, the largest abundance values were associated with the SLW. The MIW and the MBW had several siphonophores observations of low abundance, while the MSW and the LSSW had almost no observations of siphonophores (Fig. 5.20).

No diel movement was apparent in siphonophores during December 1998. The largest patches though, were found at the surface during the day transect (Figs. 5.17 and 5.22). During December 1999, siphonophores were scattered at night in the water column while during day time siphonophores were found at depths greater than 150 m (Figs. 5.21 and 5.23).

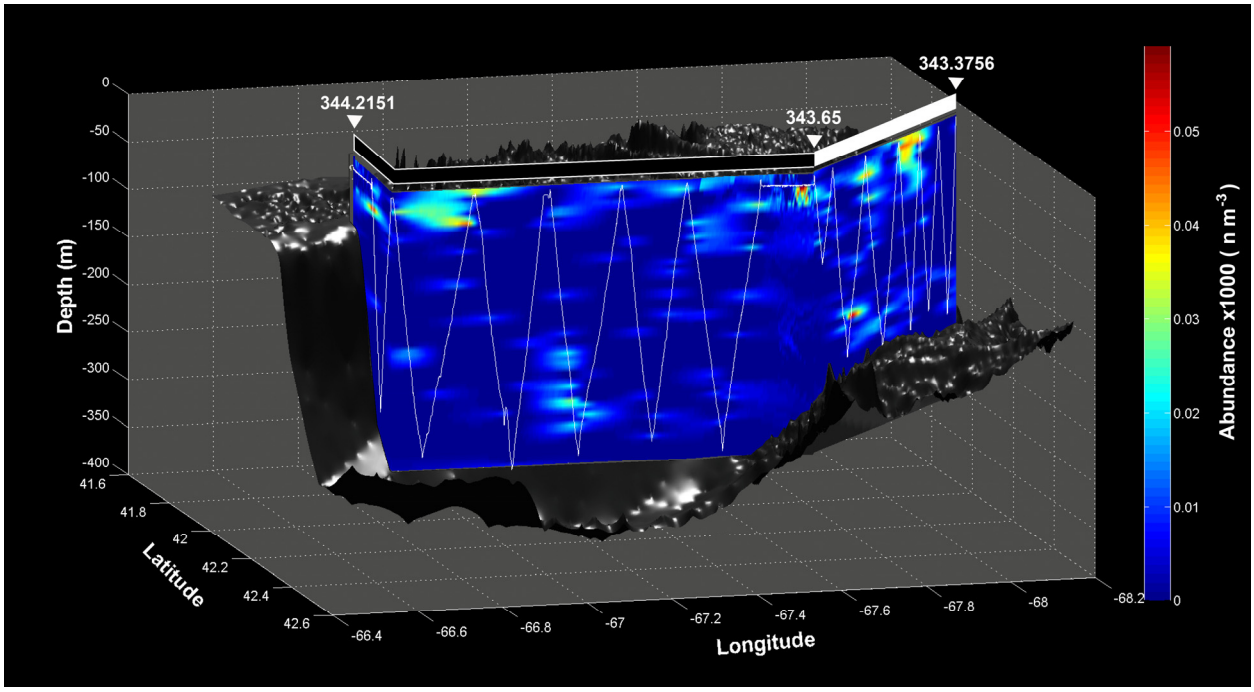


**Figure 5.17.** Siphonophore distribution in Georges Basin during December 1998. The top bar represents the day (white) and night (black) portions of the transect. The dark grey surface represents the bathymetry of the basin. Georges Bank is behind the "curtain" so that the east is to the left of the graph (X-ordinate) and south is towards the back of the graph (Y-ordinate).

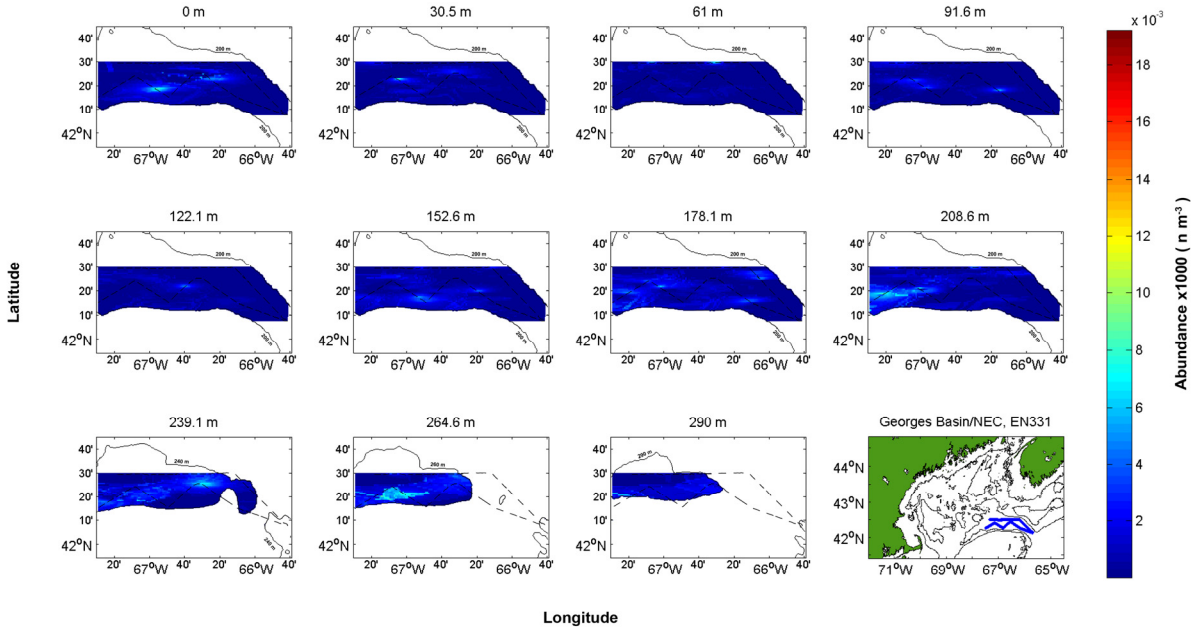


**Figure 5.18.** Siphonophores abundance in Georges Basin/NE Channel during December 1999 plotted at 30 m intervals. Isobaths (solid lines) and cruise track (dashed line) were superimposed for reference.

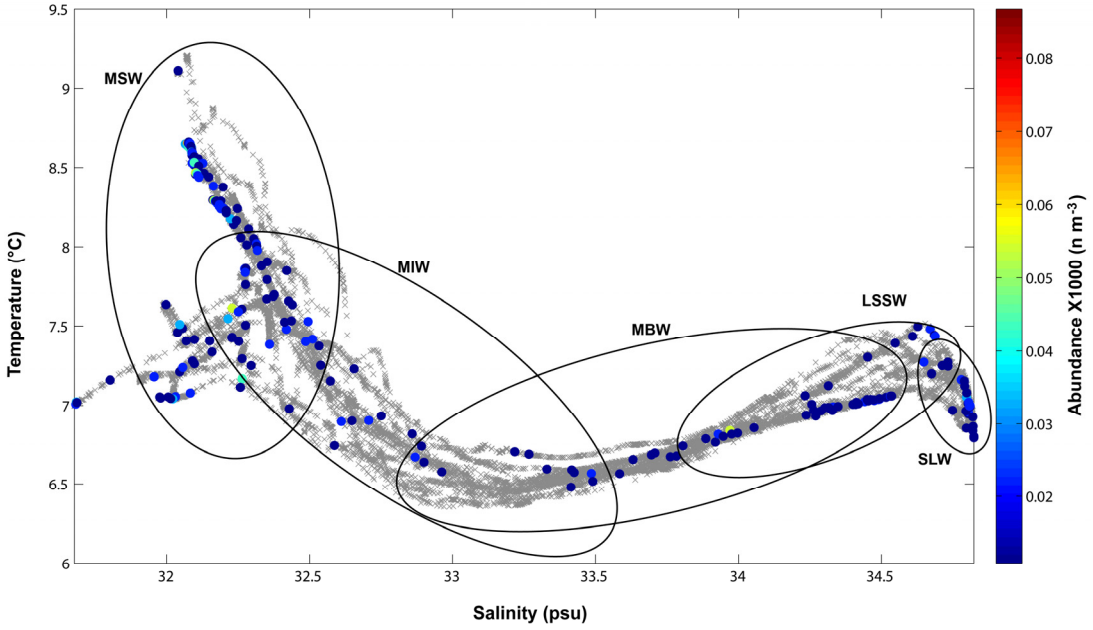


**Figure 5.19.** TSP plot for Georges Basin during December 1998. Siphonophore abundances are shown in color-coded dots. Temperature-Salinity points are plotted in grey X marks. MSW=Maine Surface Water; MIW=Maine Intermediate Water; MBW= Maine Bottom Water; LSSW=Labrador Subarctic Slope Water; SLW=Slope Water.

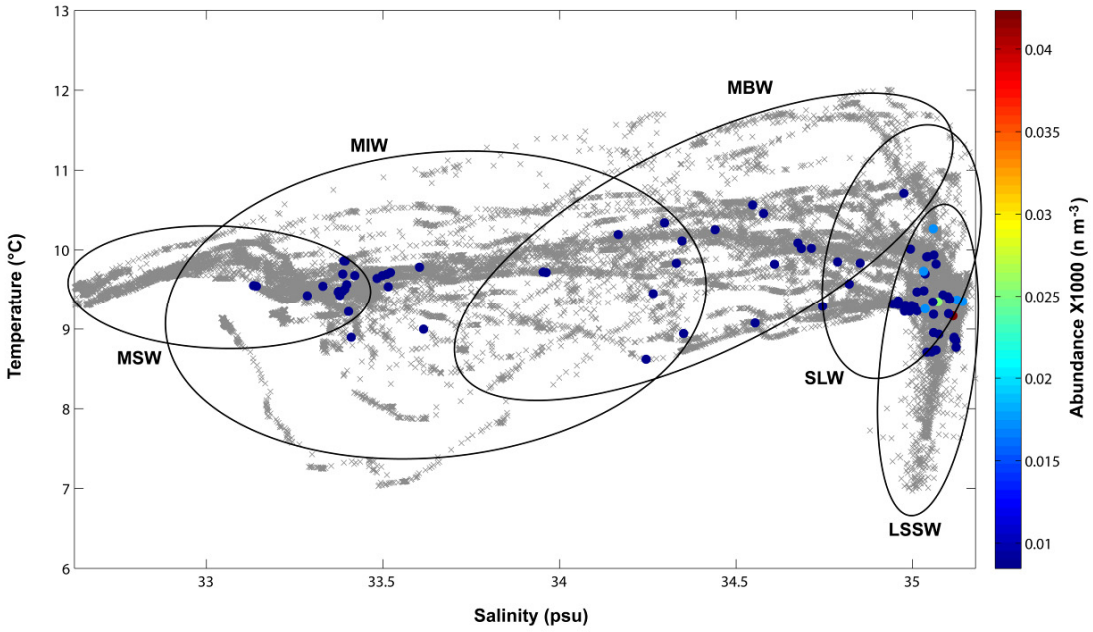


**Figure 5.20.** TSP plot for Georges Basin/NE Channel during December 1999. Siphonophore abundances are shown in color-coded dots. Temperature-Salinity points are plotted in grey X marks. MSW=Maine Surface Water; MIW=Maine Intermediate Water; MBW= Maine Bottom Water; LSSW=Labrador Subarctic Slope Water; SLW=Slope Water.

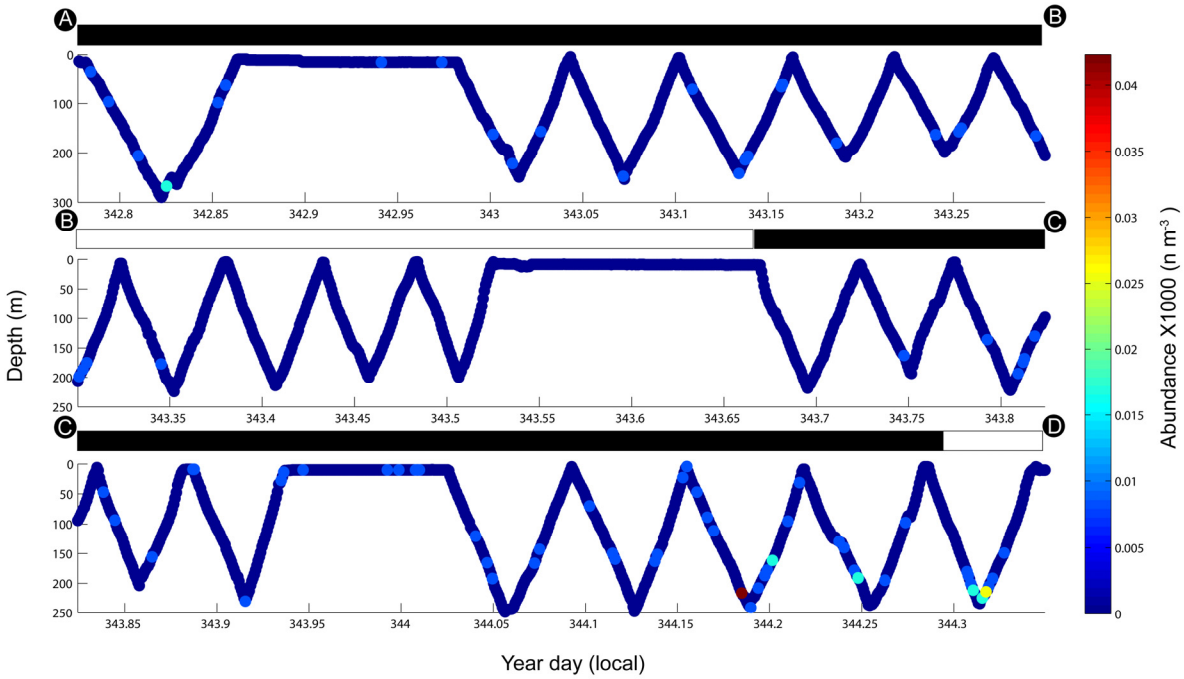


**Figure 5.21.** Diurnal vertical distribution of siphonophores in Georges Basin/NE Channel during December 1999 along BIOMAPER-II track. Bars on top of each subplot represent day (white) and night (black) periods. Capital letters at the beginning and end of each panel correspond to the sections of the Georges Basin/NE Channel, EN331 cruise track in Fig. 2.6.

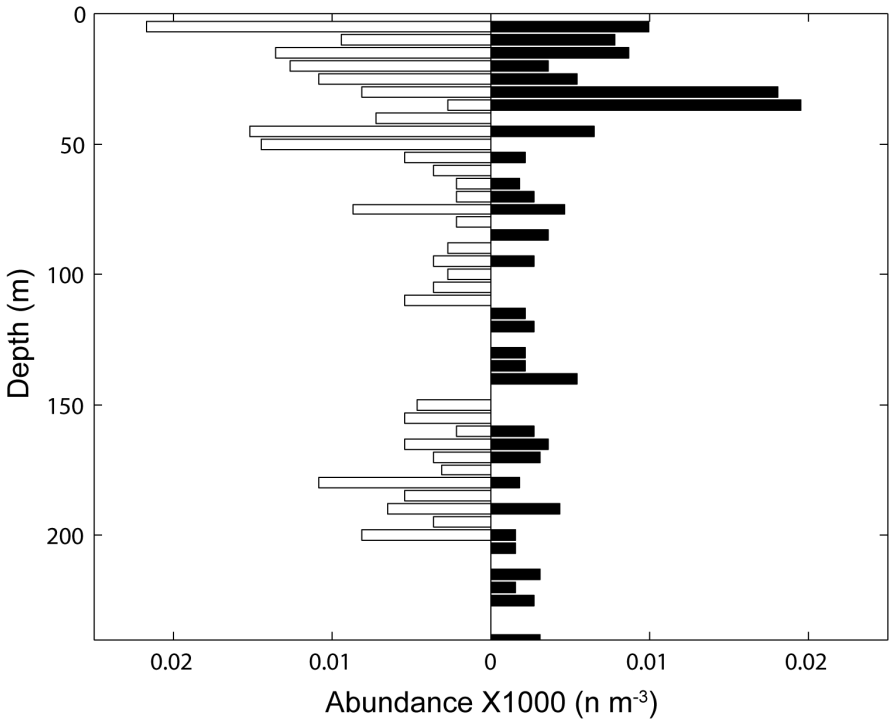


**Figure 5.22.** Vertical distribution of siphonophores in Georges Basin during December 1998 during day (empty horizontal bars, left) and night (black bars, right) periods.

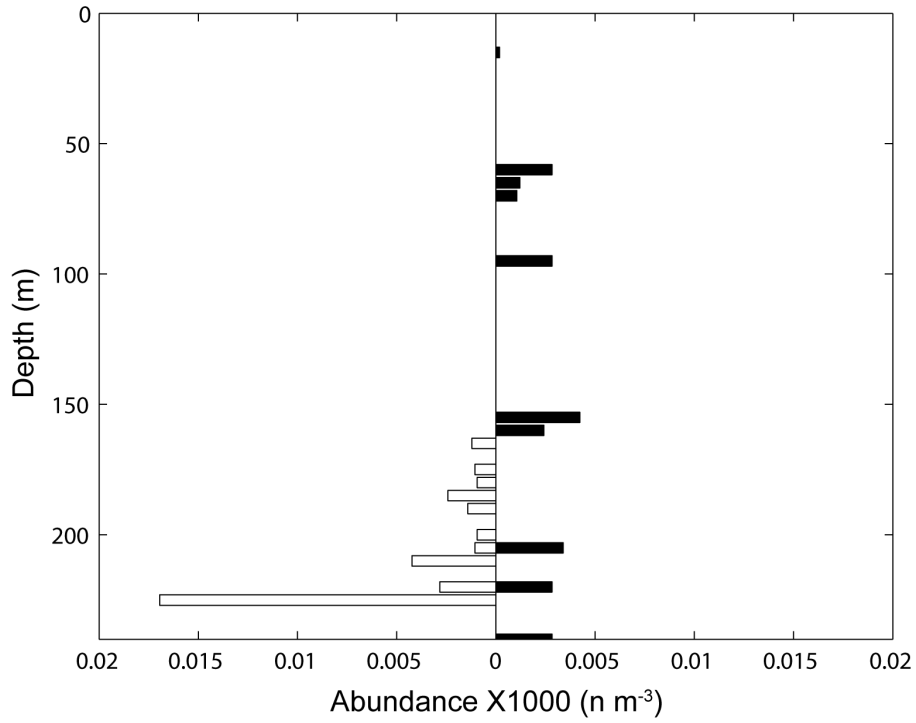


**Figure 5.23.** Vertical distribution of siphonophores in Georges Basin/NE Channel during December 1999 during day (open horizontal bars, left panel) and night (black bars, right panel) periods.

### 5.3.2 Ctenophores

#### 5.3.2.1 Wilkinson Basin

During December 1998 ctenophores (genus *Mertensia* and other cydippid and lobate taxa) were observed mainly in the first 75 m depth and seemed to be dispersed throughout the basin with patches of abundance of approximately 70 $m^{-3}$. The greatest abundance during December 1998 was observed in a single patch in the first 25 m depth and close to the center of Wilkinson Basin (Fig. 5.24). Three more patches of density ~150 $m^{-3}$ were observed at the center of the basin along the third and fourth legs, at depths 25 and 50m.

Few observations of ctenophores (4 ROIs) were made during December 1999 in Wilkinson Basin. Their very patchy (present or absent) distribution made it difficult to examine their overall spatial pattern and no conclusions about distributional patterns could be drawn. Observations of higher abundance patches during December 1998 were generally associated with warm, low salinity waters characteristic of MSW (Fig. 5.25). During 1998 some high

abundance observations were also located in the other three water masses identified in Wilkinson Basin. No obvious association between ctenophore distributions and water masses could be identified during December 1999 because few ctenophores were observed.

There was little evidence of diel vertical movements for ctenophores in Wilkinson Basin during December 1998. Similar vertical distributions were observed in ctenophores during day and night periods (Figs. 5.26 and 5.27). However, the larger, densest patches were observed at the surface right before midnight (Fig. 5.26). During day time, patches were smaller in size, had lower abundances and were scattered throughout the water column. Due to its discrete nature, not enough data were available to draw conclusions on ctenophores diel activity during December 1999.

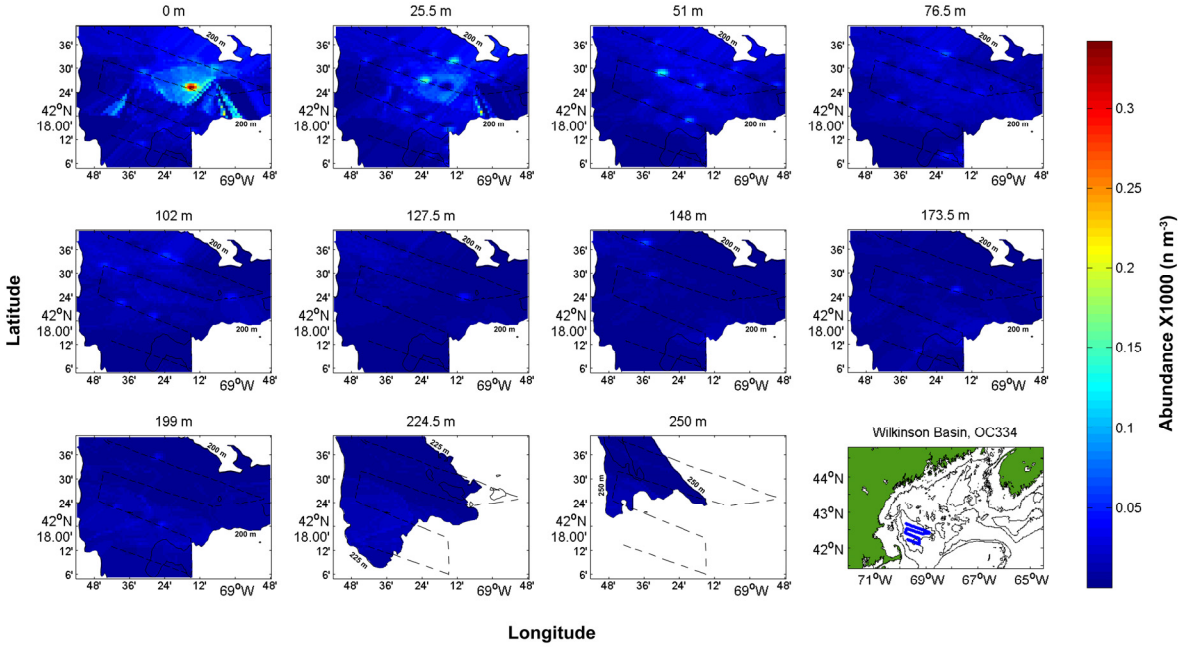


**Figure 5.24.** Ctenophores abundance in Wilkinson Basin during December 1998 plotted at ~25 m intervals. Isobaths (solid lines) and cruise track (dashed line) were superimposed for reference.

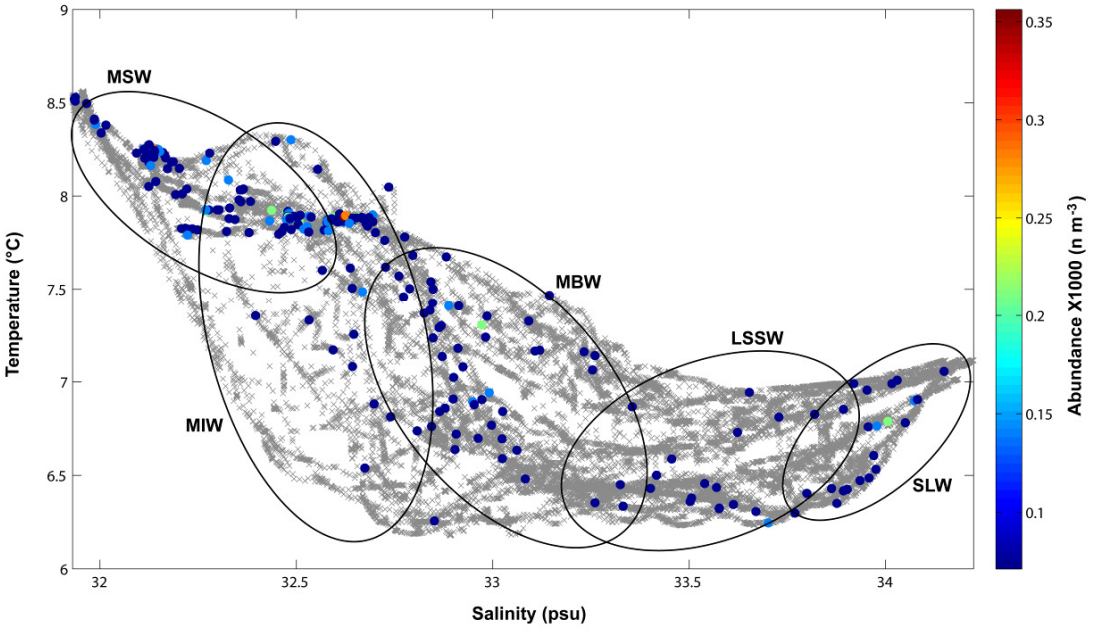


**Figure 5.25.** TSP plot for Wilkinson Basin during December 1998. Ctenophore abundances are shown in color-coded dots. Temperature-Salinity points are plotted in grey X marks. MSW=Maine Surface Water; MIW=Maine Intermediate Water; MBW= Maine Bottom Water; LSSW=Labrador Subarctic Slope Water; SLW=Slope Water.

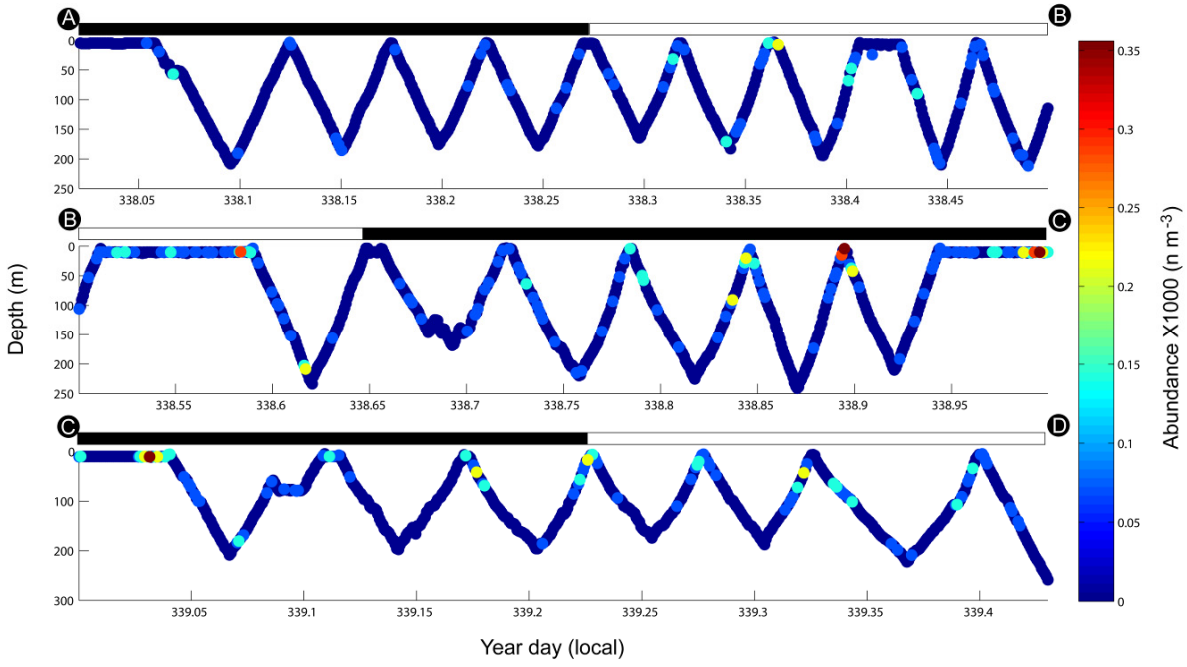


**Figure 5.26.** Diurnal vertical distribution of ctenophores in Wilkinson Basin during December 1998 along BIOMAPER-II track. Bars on top of each subplot represent day (white) and night (black) periods. Capital letters at the beginning and end of each panel correspond to the sections of the Wilkinson Basin, OC334 cruise track in Fig. 2.6.

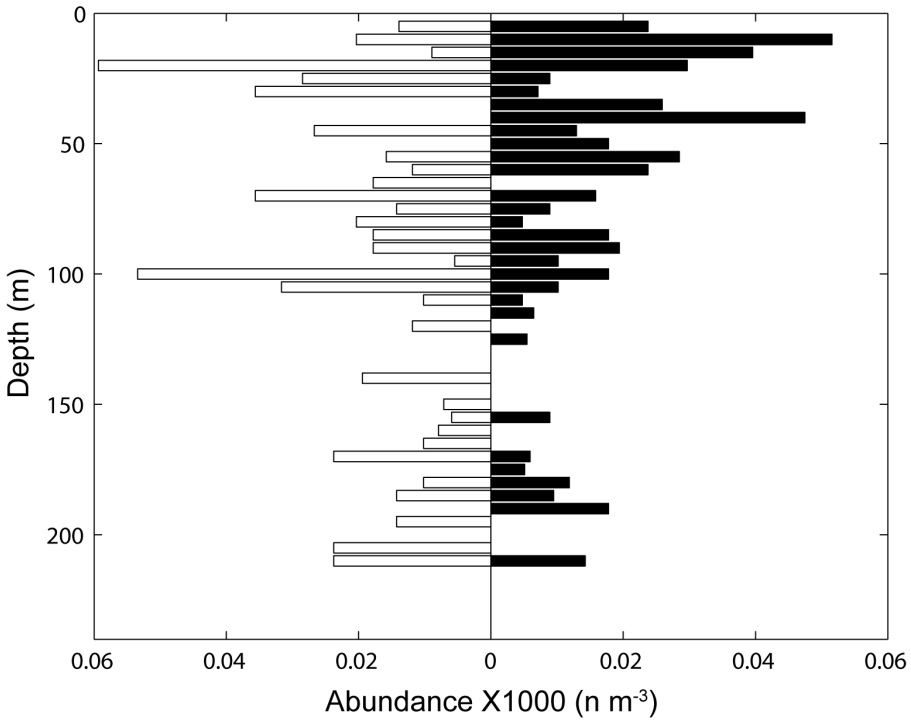


**Figure 5.27.** Vertical distribution of ctenophores in Wilkinson Basin during December 1998 during day (open horizontal bars, left) and night (black bars, right) periods.

#### 5.3.2.2 Jordan Basin

Ctenophores in Jordan Basin were more abundant during December 1998 than during December 1999. Only 3 individual ctenophores were identified by the VPR during December 1999. Maximum ctenophore abundance value during 1998 was 213 $m^{-3}$ (mean±standard deviation 7.9±25.4). However, most abundance observations were on the order of ~70 $m^{-3}$.

During December 1998, ctenophores were clustered mainly in three patches from 0 to 25 m. The largest patch was located at the surface (0 m) and to the SW half of Jordan Basin (Fig. 5.28). The other two large patches were located in the eastern half of Jordan Basin and at the surface (0 m). Ctenophores were found in scattered throughout Jordan Basin in small numbers (~23 $m^{-3}$). It seemed that almost no ctenophore observations were made in the second leg of the transect (Figure 5.28, second dashed line from left to right) on cruise OC334 during December 1998.

December 1998 TSP plot for cetnophores revealed that the highest abundance values were related with the MSW, with close proximity to the MIW. Also some high observations were associated to the fresher, cooler LSSW (Fig. 5.29).

No solid evidence of ctenophore vertical migration was observed during December 1998 in Jordan Basin. High abundances were observed at the surface and at depth during day and night periods (Figs. 5.30 and 5.31). However, more large patches were observed at the surface during the day section than during night sections. Interestingly, the densest patches observed during the night sections were found close to midnight, at the beginning of the transect (Fig. 5.30 top panel) and towards dusk (Fig. 5.30 bottom panel). Because few ctenophores were observed, no results on hydrology and plankton distribution could be reported for ctenophores in Jordan Basin during December 1999.

**5.3.2.3 Georges Basin/Northeast Channel**

During December 1998, ctenophore abundances in Georges Basin ranged between 71 and 356 $m^{-3}$ (mean±standard deviation 10.0±31.7). During this period, ctenophores were mainly found in the upper 100 m. Below 100 m, ctenophores were only found in a few scattered patches elsewhere in the basin (Fig. 5.32). No conclusions on ctenophores could be drawn for December 1999 because of insufficient data.

According to the TSP plot for ctenophores, during December 1998 almost all of the observations were associated to the MSW and MIW (Fig. 5.33). Although abundances as high as 71 $m^{-3}$ were observed in the MBW, LSSW and SLW those observations were very scattered and lacked a defined pattern.

No diel vertical movement was apparent in Georges Basin during December 1998. Patches of ctenophores were found in similar abundances at the surface during day and night periods in Georges Basin during December 1998 (Figs. 5.32 and 5.34). Although higher abundances were related to patches found in day time (Fig. 5.34), it is possible this was more related to spatial distribution rather than an indication of vertical diel activity (Fig. 5.32).

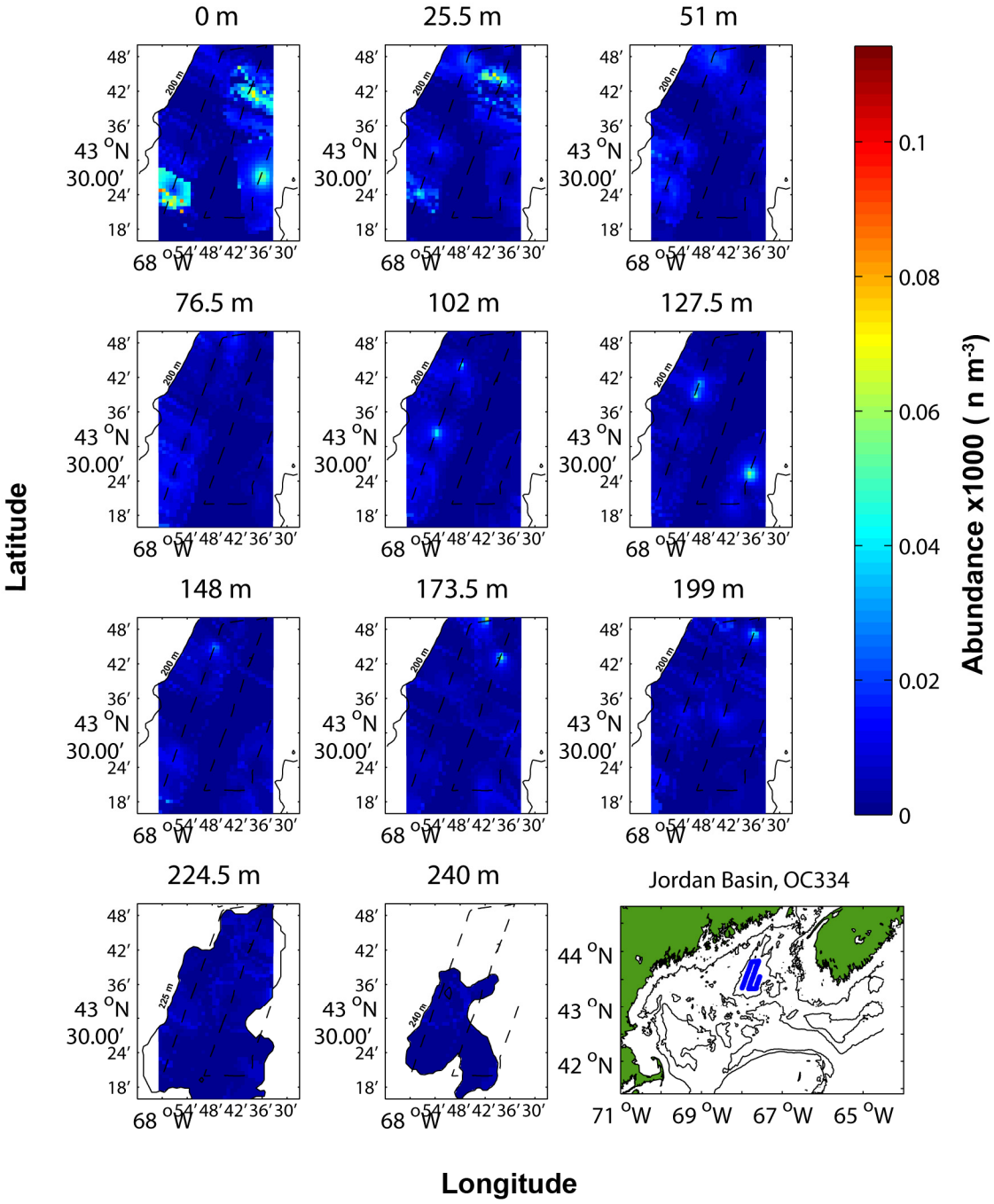


**Figure 5.28.** Ctenophores abundance in Jordan Basin during December 1998 plotted at ~25 m intervals. Isobaths (solid lines) and cruise track (dashed line) were superimposed for reference.

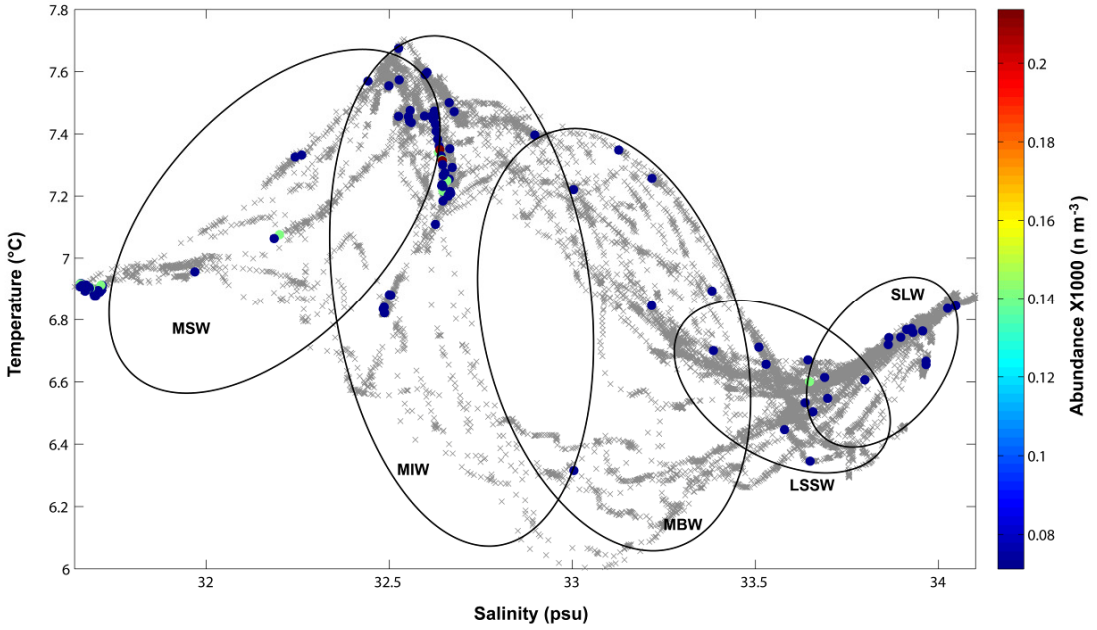


**Figure 5.29.** TSP plot for Jordan Basin during December 1998. Ctenophores abundances are shown in color-coded dots. Temperature-Salinity points are plotted in grey X marks. MSW=Maine Surface Water; MIW=Maine Intermediate Water; MBW= Maine Bottom Water; LSSW=Labrador Subarctic Slope Water; SLW=Slope Water.

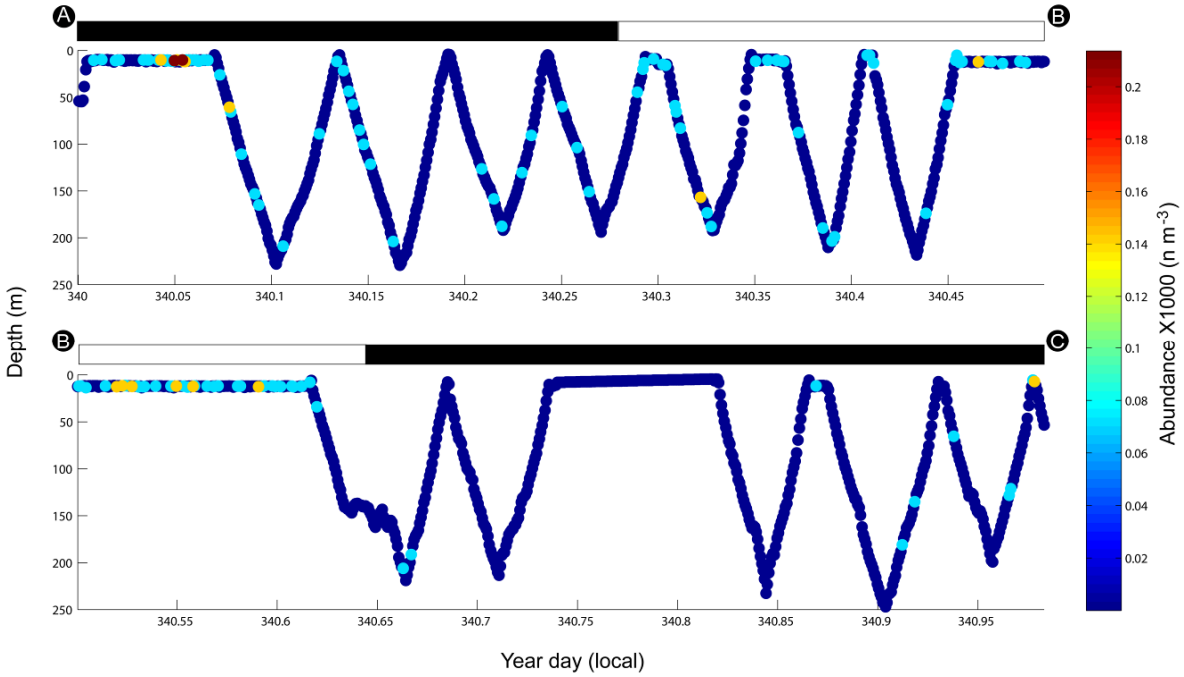


**Figure 5.30.** Diurnal vertical distribution of ctenophores in Jordan Basin during December 1998 along BIOMAPER-II track. Bars on top of each subplot represent day (white) and night (black) periods. Capital letters at the beginning and end of each panel correspond to the sections of the Jordan Basin, OC334 cruise track in Fig. 2.6.

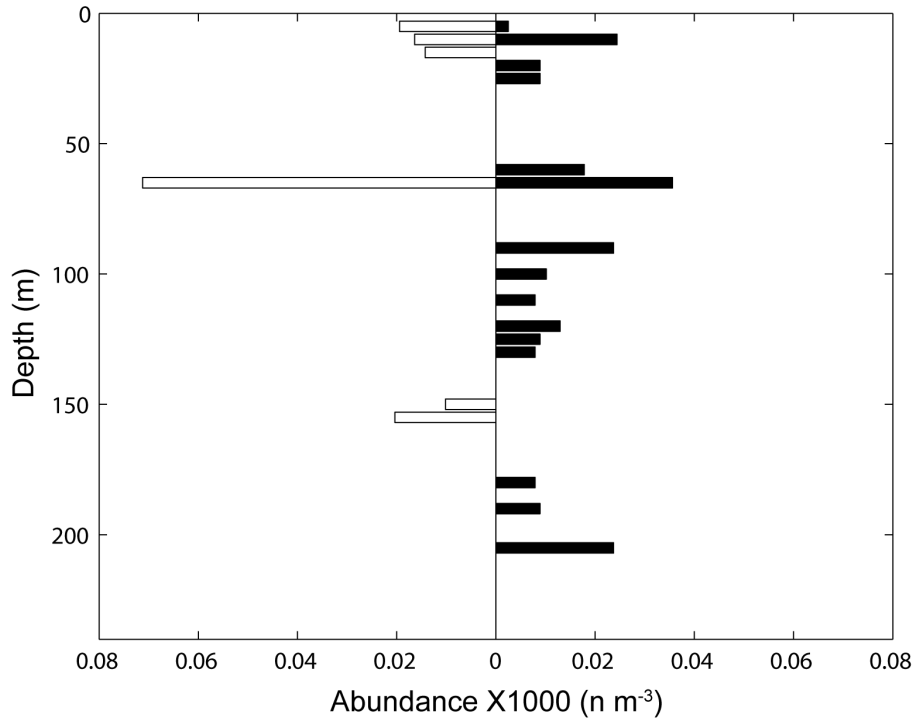


**Figure 5.31.** Vertical distribution of ctenophores in Jordan Basin during December 1998 during day (open horizontal bars, left) and night (black bars, right) periods.

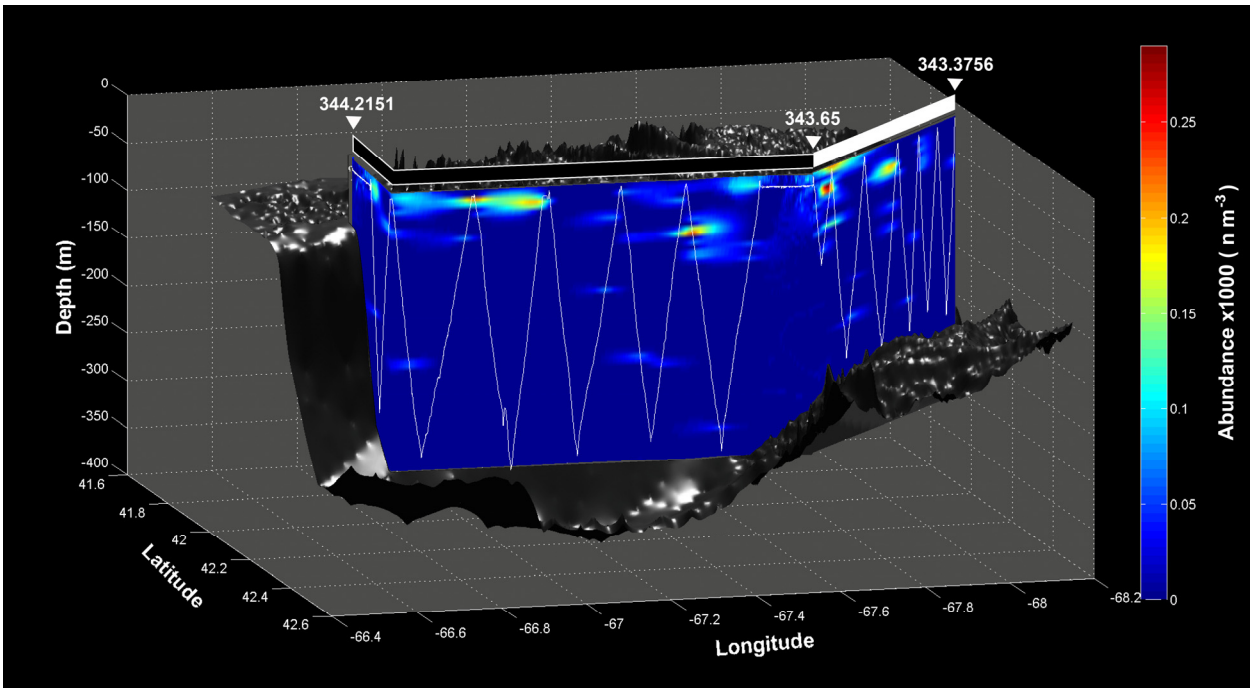


**Figure 5.32.** Ctenophore distribution in Georges Basin during December 1998. The top bar represents the day (white) and night (black) portions of the transect. The dark grey surface represents the bathymetry of the basin. Georges Bank is behind the “curtain” so that the east is to the left of the graph (X-ordinate) and south is towards the back of the graph (Y-ordinate).

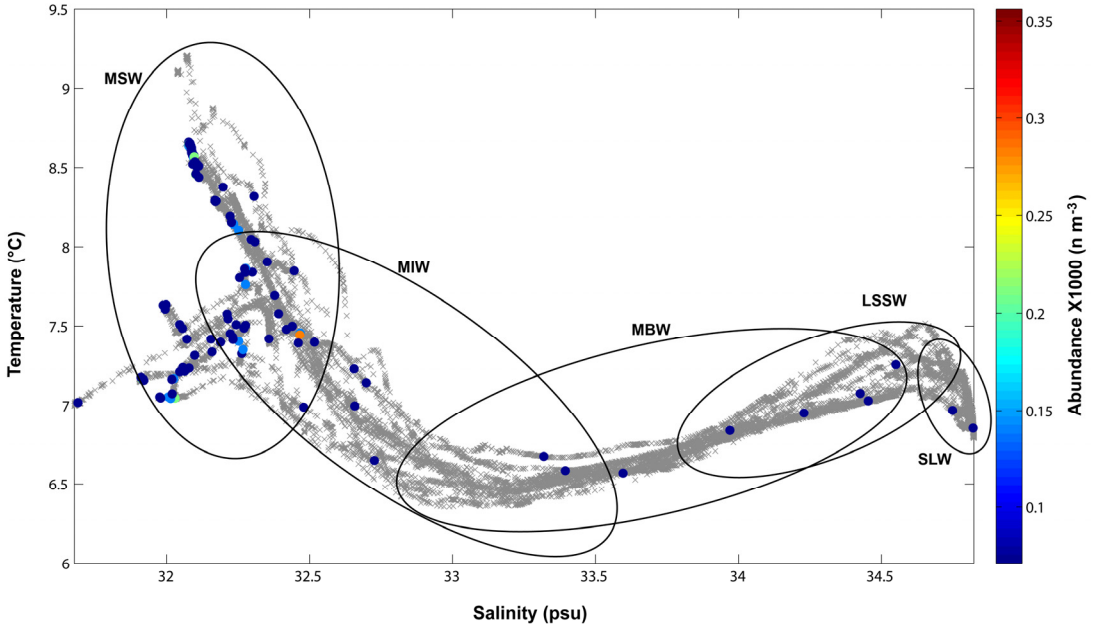


**Figure 5.33.** TSP plot for Georges Basin during December 1998. Ctenophore abundances are shown in color-coded dots. Temperature-Salinity points are plotted in grey X marks. MSW=Maine Surface Water; MIW=Maine Intermediate Water; MBW= Maine Bottom Water; LSSW=Labrador Subarctic Slope Water; SLW=Slope Water.

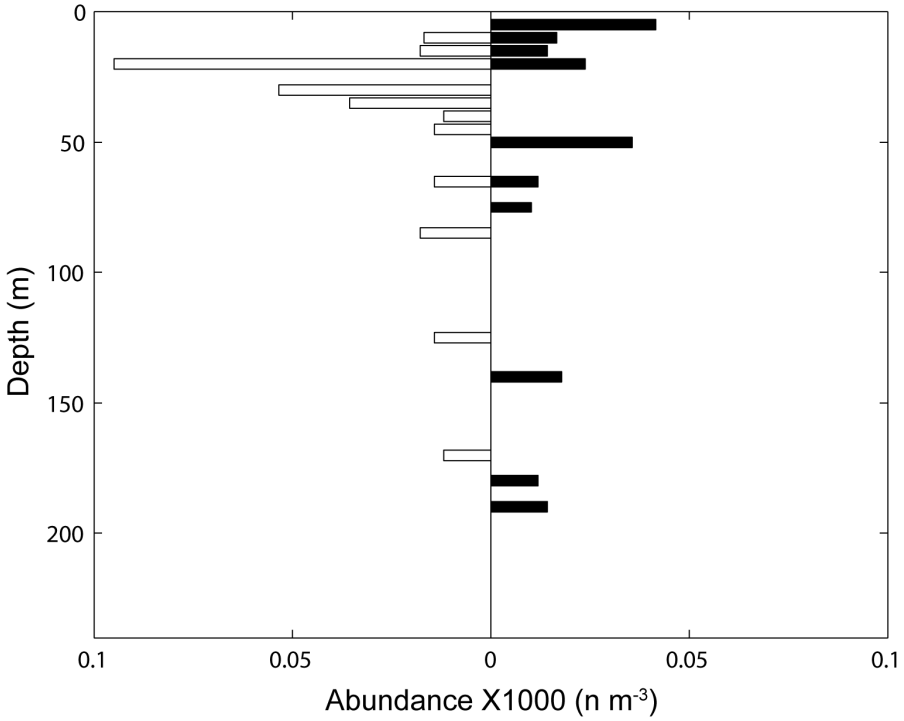


**Figure 5.34.** Vertical distribution of ctenophores in Georges Basin during December 1998 during day (open horizontal bars, left) and night (black bars, right) periods.

### 5.3.3 Medusae

#### 5.3.3.1 Wilkinson Basin

As in the case of ctenophores, more than one species of medusae were included in this category. Different sizes and medusae shapes were observed, but I did not attempt to differentiate among them because many of the observations were of only part of the animal, which complicated identification. Moreover, the relatively low image resolution generally obscured critical taxonomic features. During December 1998, medusae appeared dispersed throughout the entire basin densities smaller than 10 $m^{-3}$ (mean±standard deviation 3.2±13.9); however, the largest and most abundant patches (> 70 $m^{-3}$) were found in the upper 75 m (Fig. 5.35). From 75 m to 250 m small patches of similar abundance (~20-65 $m^{-3}$) were scattered in the basin.

Medusae were found in all five water masses at abundances up to 75 $m^{-3}$ during December 1998. However, most of the high abundance observations seemed to be associated with the MSW and LSSW (Fig. 5.36).

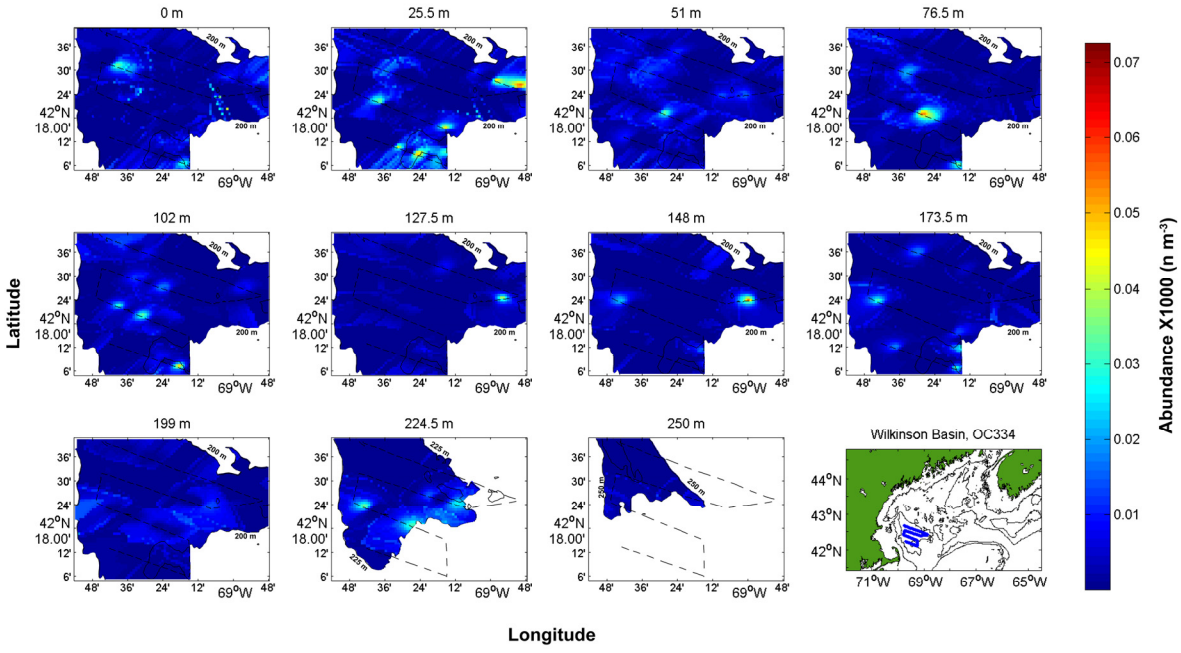


**Figure 5.35.** Medusae abundance in Wilkinson Basin during December 1998 plotted at ~25 m intervals. Isobaths (solid lines) and cruise track (dashed line) were superimposed for reference.

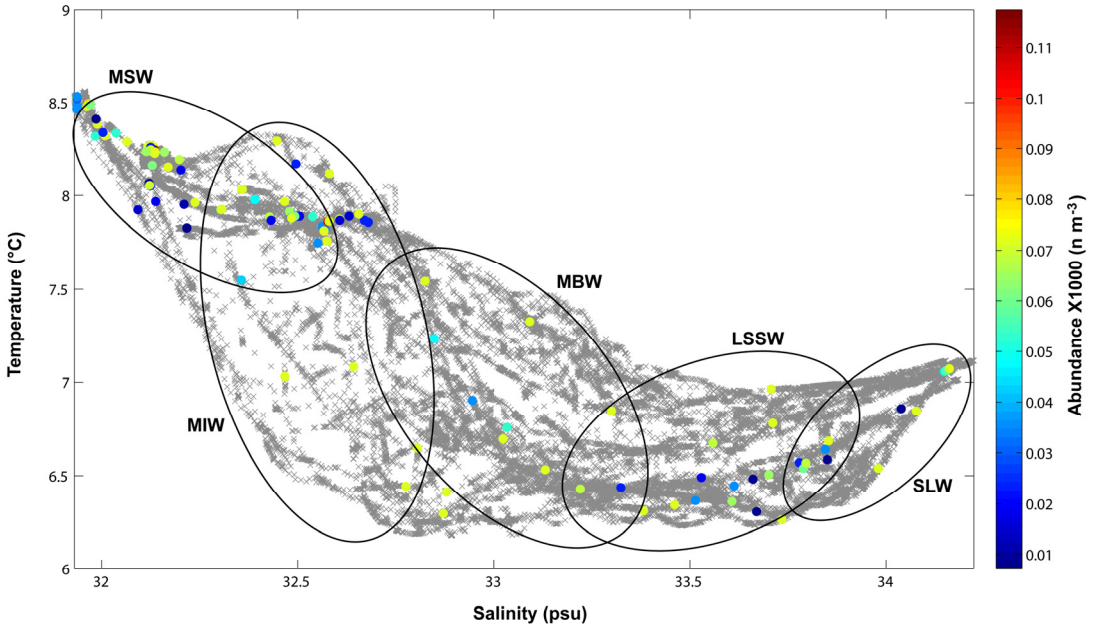


**Figure 5.36.** TSP plot for Wilkinson Basin during December 1998. Medusae abundances are shown in color-coded dots. Temperature-Salinity points are plotted in grey X marks. MSW=Maine Surface Water; MIW=Maine Intermediate Water; MBW= Maine Bottom Water; LSSW=Labrador Subarctic Slope Water; SLW=Slope Water.

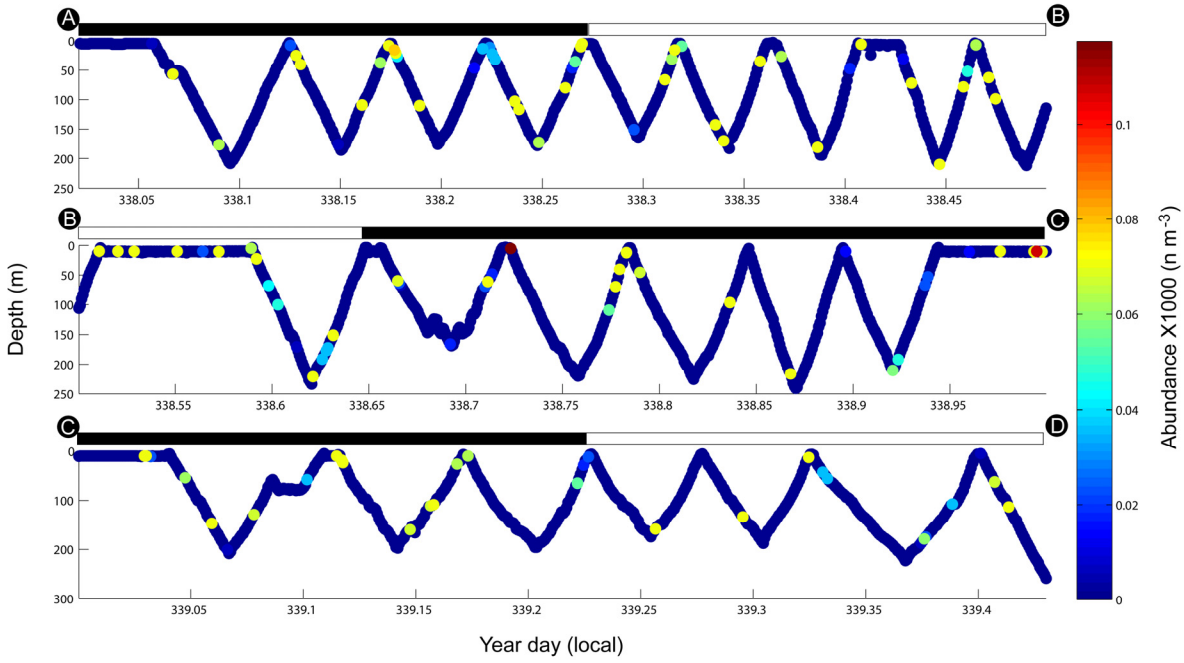


**Figure 5.37.** Diurnal vertical distribution of medusae in Wilkinson Basin during December 1998 along BIOMAPER-II track. Bars on top of each subplot represent day (white) and night (black) periods. Capital letters at the beginning and end of each panel correspond to the sections of the Wilkinson Basin, OC334 cruise track in Fig. 2.6.

No diel vertical migration by medusae was detected during December 1998. Dense patches were observed at similar depths during the day and night periods (Figs. 5.37 and 5.38). It should be noted that most observations of medusae were made during night time and it was difficult to separate any diel migration pattern from differences in medusae spatial distribution in Wilkinson Basin during December 1998.

Only 16 medusae were recorded in Wilkinson Basin during December 1999 and abundance overestimation was a potential issue when using these few observations because the full size of most organisms could not be determined. No data for medusae for this period was reported due to abundance estimation uncertainties.

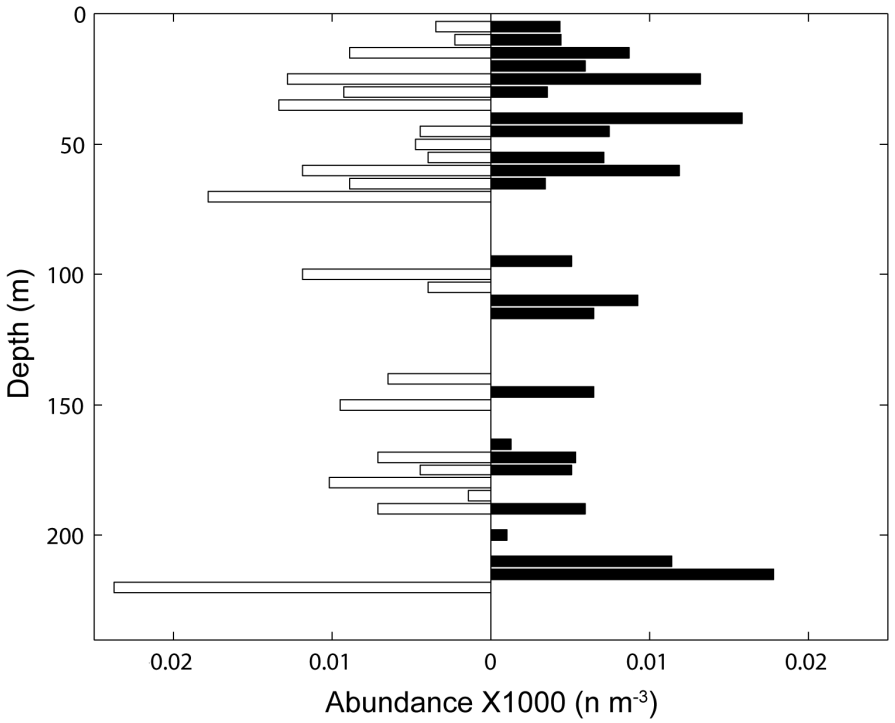


**Figure 5.38.** Vertical distribution of medusae in Wilkinson Basin during December 1998 during day (open horizontal bars, left) and night (black bars, right) periods.

#### 5.3.3.2 Jordan Basin

Medusae were more abundant in Jordan Basin during December 1998 than during December 1999. During December 1998, the maximum abundance for medusae was 107 $m^{-3}$ (mean±standard deviation 1.4±9.0). However, most abundance observations were scattered between 18 and 80 $m^{-3}$. Only 5 individual medusae were recorded by the VPR during December 1999, making it difficult to draw conclusions for medusae for this cruise.

During December 1998, medusae were patchily distributed in Jordan Basin. The most conspicuous patch was found at the surface (0 m) at the center of the western half of Jordan Basin (Fig. 5.39). Seven smaller patches occurred at different depths. Four of them occurred in the western half of Jordan Basin between 50 and 100 m, but no apparent spatial pattern was observed for the other three, which were found between ~150 and ~175 m (Fig. 5.39). The maximum abundance at the core of most patches inferred from the Kriged data was 63 $m^{-3}$. Medusae were also found in low abundances (~15 $m^{-3}$) mostly around the main patches. No medusae data were Kriged for December 1999, due to their sparse and discrete nature.

The medusae TSP plot for December 1998 showed a relationship between abundance distribution and hydrographic data. During December 1998, highest medusae abundances were associated with the MSW, the MSW-MIW interface, and the SLW (Fig. 5.40). The densest patch was associated with the warm, fresh waters of the MSW. Few observations of relatively large values (~65 $m^{-3}$) were found in the MIW and MBW masses. No results on water masses and abundance relationships could be drawn for medusae during December 1999.

Despite the fact that highly abundant patches occurred at the surface and at depth during day and night sections (Fig. 5.41), there was some evidence of vertical migration of medusae during December 1998. Greater abundances were found in waters deeper than150 m during day time while larger abundances were found in surface waters above 65 m during night time (Fig. 5.42). This might be an indication of vertical diel migration by medusae in Jordan Basin during December 1998.

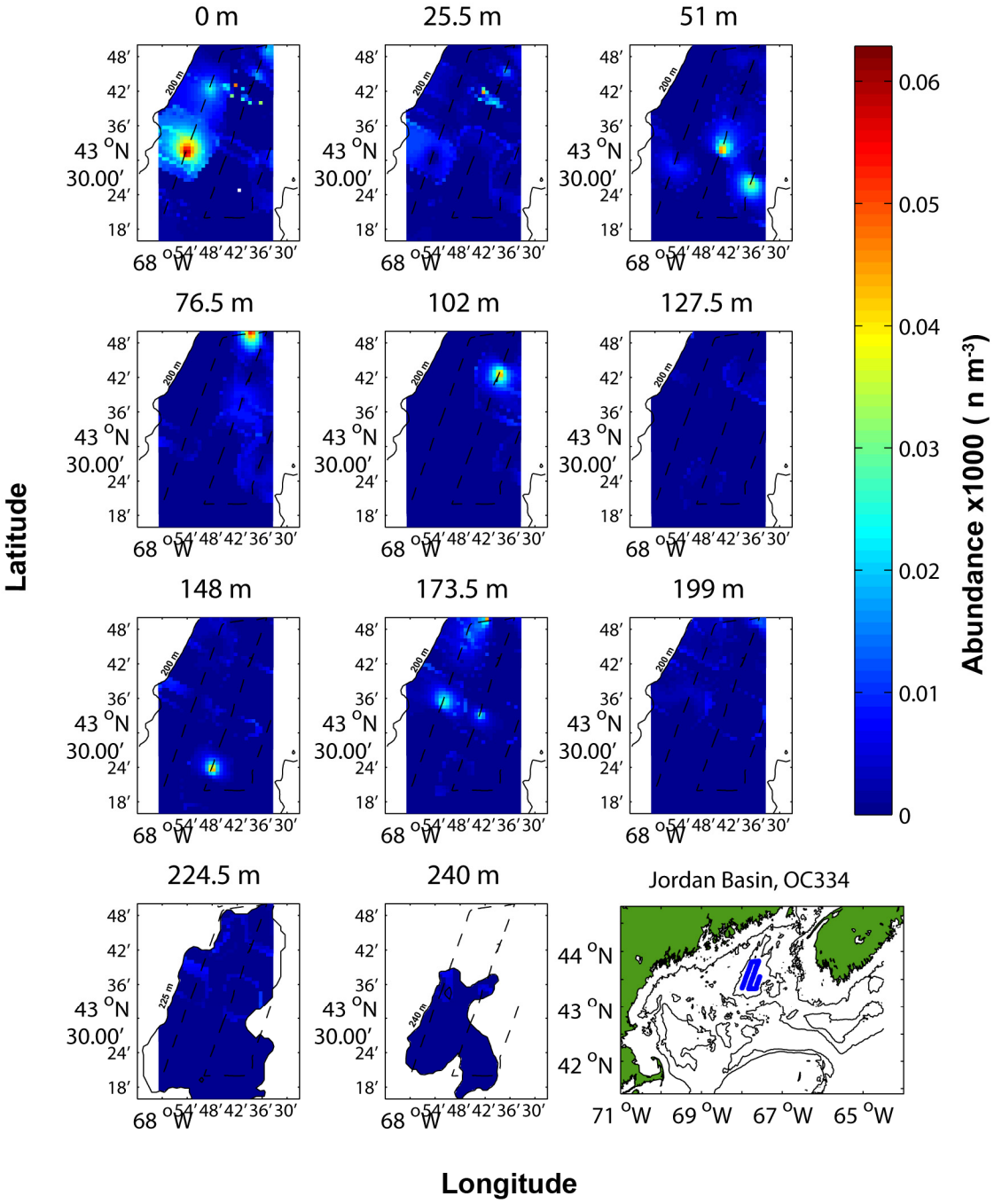


**Figure 5.39.** Medusae abundance in Jordan Basin during December 1998 plotted at ~25 m intervals. Isobaths (solid lines) and cruise track (dashed line) were superimposed for reference.

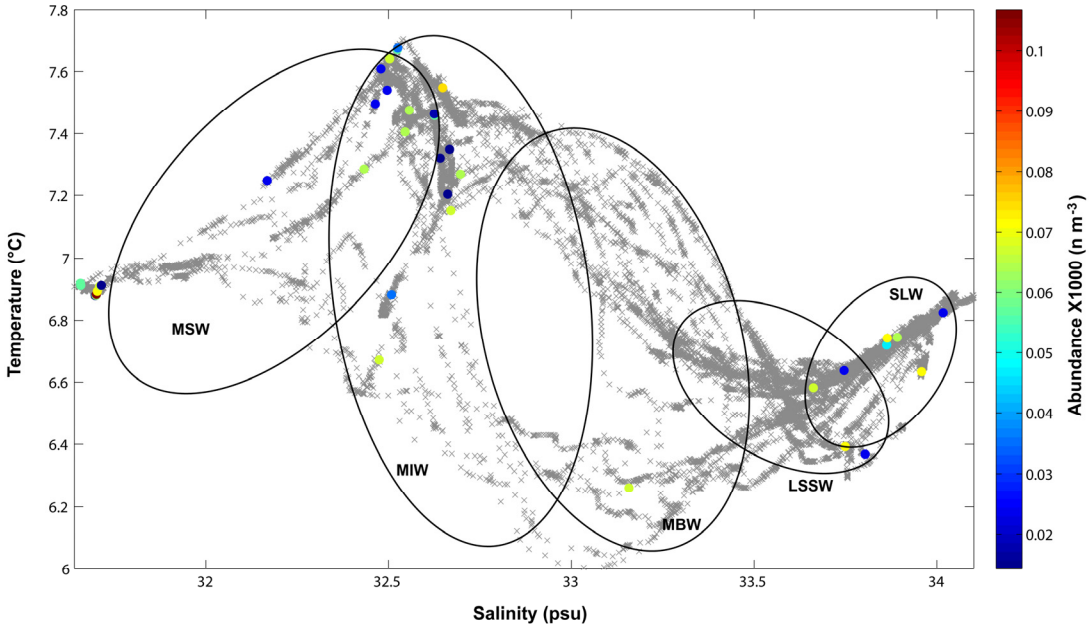


**5.40.** TSP plot for Jordan Basin during December 1998. Medusae abundances are shown in color-coded dots. Temperature-Salinity points are plotted in grey X marks. MSW=Maine Surface Water; MIW=Maine Intermediate Water; MBW= Maine Bottom Water; LSSW=Labrador Subarctic Slope Water; SLW=Slope Water.

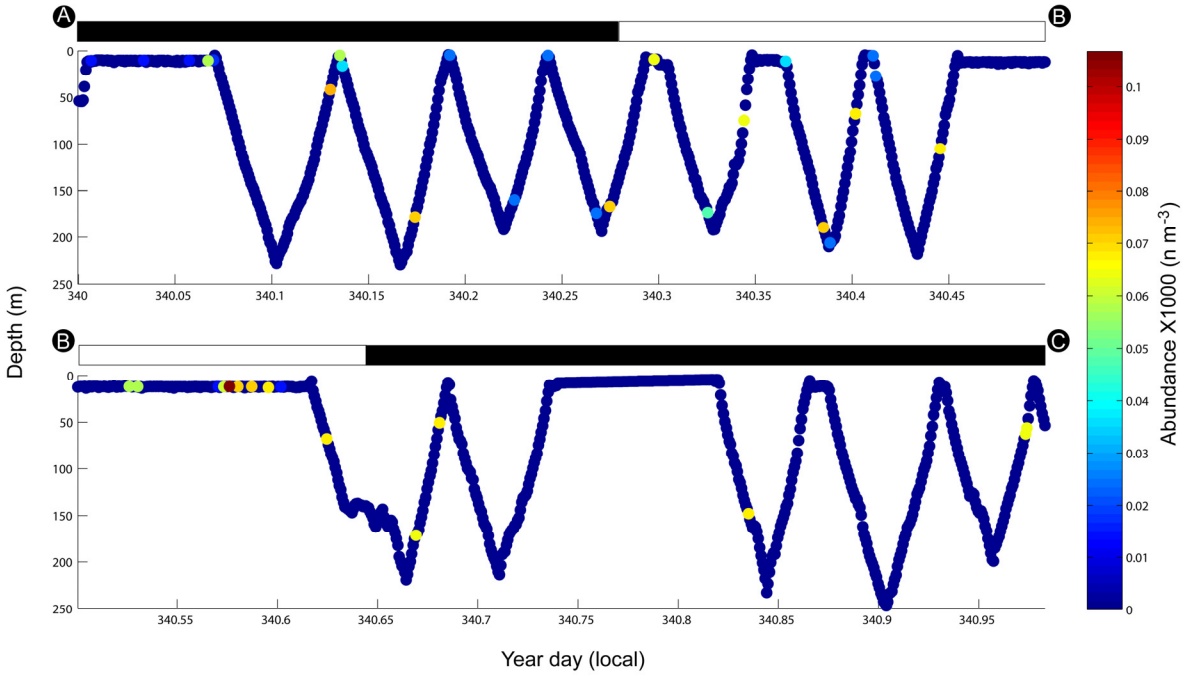


**Figure 5.41.** Diurnal vertical distribution of medusae in Jordan Basin during December 1998 along BIOMAPER-II track. Bars on top of each subplot represent day (white) and night (black) periods. Capital letters at the beginning and end of each panel correspond to the sections of the Jordan Basin, OC334 cruise track in Fig. 2.6.

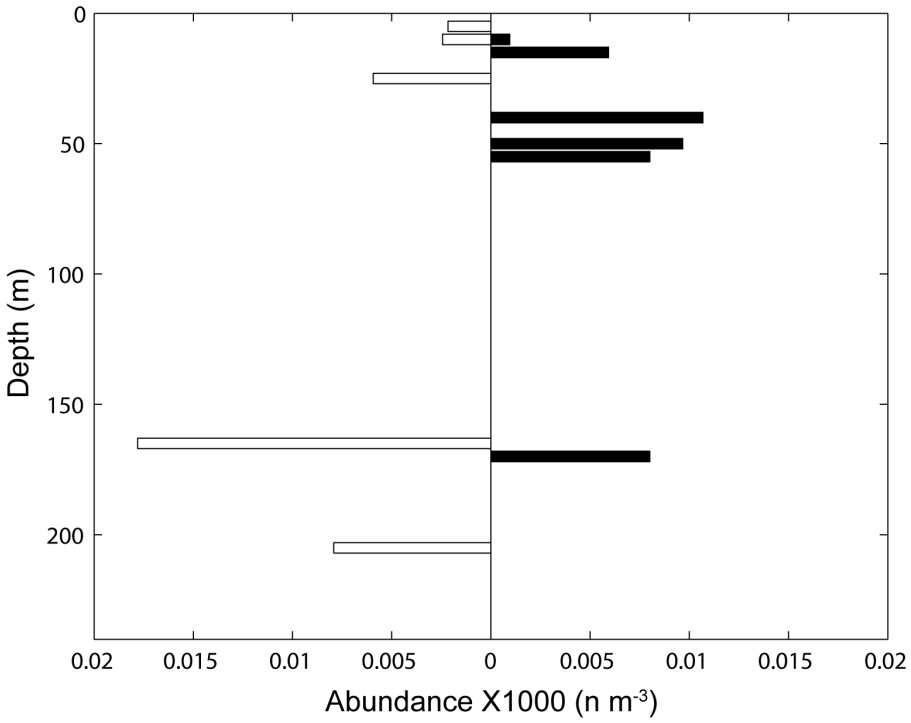


**Figure 5.42.** Vertical distribution of medusae in Jordan Basin during December 1998 during day (open horizontal bars, left) and night (black bars, right) periods.

#### 5.3.3.3 Georges Basin/Northeast Channel

During December 1998, medusae abundances in Georges Basin ranged from 12 to 142 $m^{-3}$ (mean±standard deviation 3.1±14.8). Despite their high abundance, medusae were clustered in few scattered patches found in the upper 150 m along the transect with most concentrated in the western portion of the Georges Basin (Fig. 5.43). Very few medusae were observed below 150 m. Only eight individual medusae were recorded by the VPR during December 1999. Therefore, no results could be drawn for this group in December 1999.

Most of the medusae observations were related to the Maine Surface Water close to the interface with the Maine Intermediate Water (Fig. 5.44). Abundances in the order of ~60 $m^{-3}$ were observed in the MBW, LSSW and SLW but these observations were very sparse.

There was no evidence of medusae diel activity in Georges Basin during December 1998. Similar abundances were observed during day and night periods (Fig. 5.45).

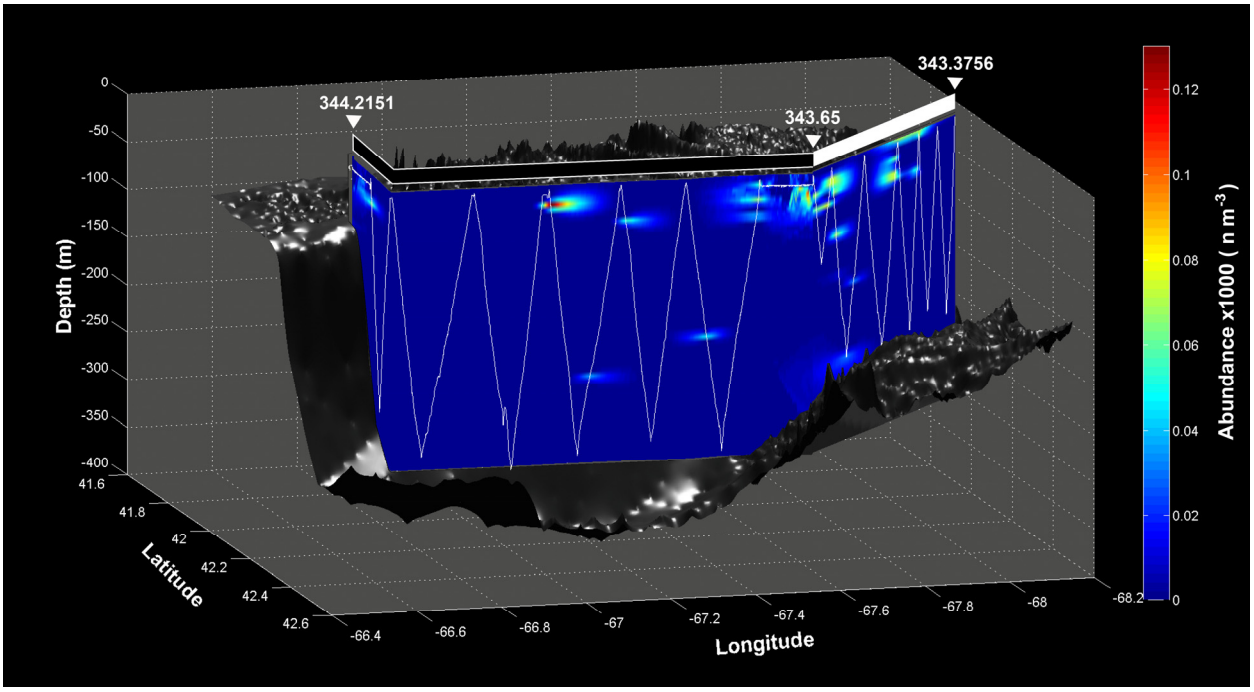


**Figure 5.43.** Medusae distribution in Georges Basin during December 1998. The top bar represents the day (white) and night (black) portions of the transect. The dark grey surface represents the bathymetry of the basin. Georges Bank is behind the "curtain" so that the east is to the left of the graph (X-ordinate) and south is towards the back of the graph (Y-ordinate).

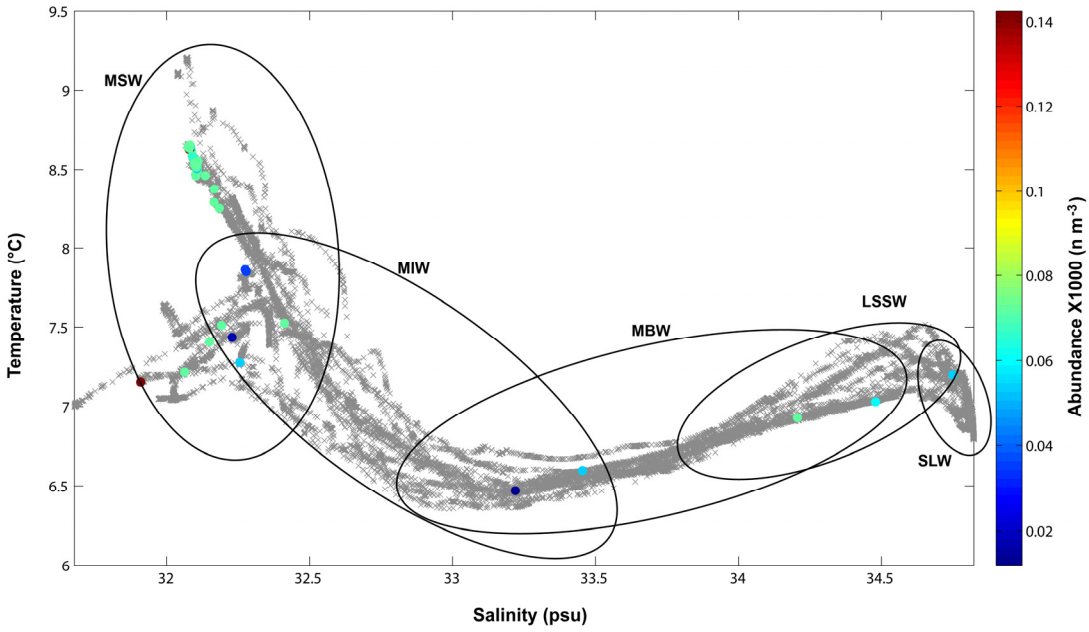


**Figure 5.44.** TSP plot for Georges Basin during December 1998. Medusae abundances are shown in color-coded dots. Temperature-Salinity points are plotted in grey X marks. MSW=Maine Surface Water; MIW=Maine Intermediate Water; MBW= Maine Bottom Water; LSSW=Labrador Subarctic Slope Water; SLW=Slope Water.

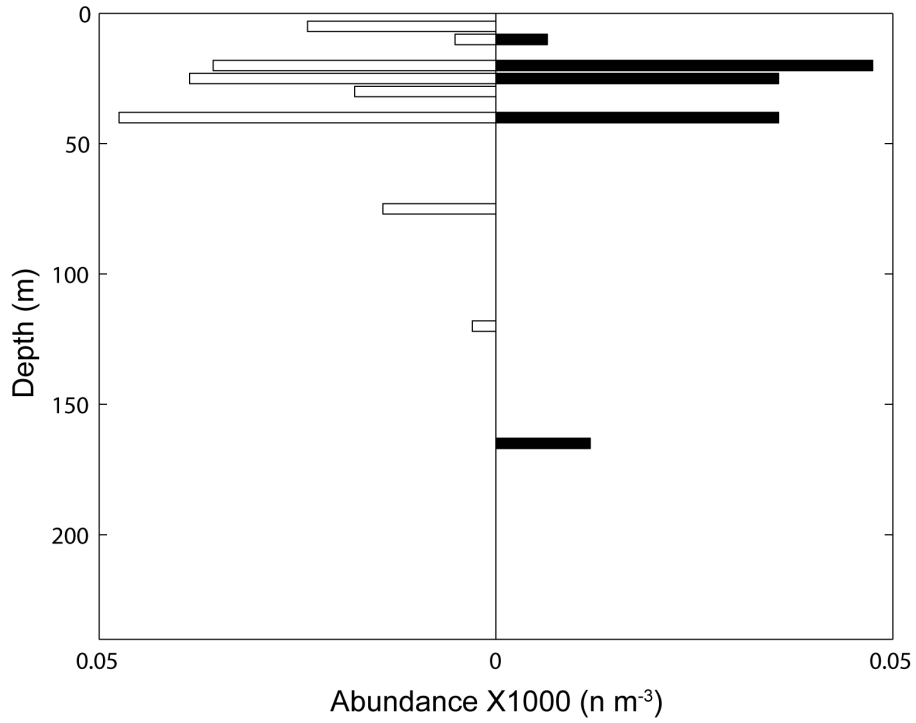


**Figure 5.45.** Vertical distribution of medusae in Jordan Basin during December 1998 during day (empty horizontal bars, left) and night (black bars, right) periods.

### 5.3.4 Euphausiids

#### 5.3.4.1 Wilkinson Basin

Euphausiids in Wilkinson Basin were more abundant in December 1999 than December 1998 ($p<0.001$). During December 1998, euphausiids (mainly *Meganyctiphanes norvegica*) appeared dispersed across Wilkinson Basin in small, low-abundance patches (mean±standard deviation 1.9±10.4). From 0 to ~150 m depth, patches of maximum abundance of approximately 50-55 $m^{-3}$ were found on the northeast corner of the Basin (Fig. 5.46). Patches of 20 $m^{-3}$ and lower occurred at all depths in the entire basin. A single, high-abundance (up to 120 $m^{-3}$ in its core) patch of *M. norvegica* was present around 225 m deep. During December 1999, the greatest euphausiids abundances (104 $m^{-3}$) in Wilkinson Basin were observed in the upper 75 m (mean±standard deviation 3.5±14.9). Maximum euphausiid abundances during December 1999 were in the order of 140 $m^{-3}$ (Fig. 5.47). In contrast, patches on December 1998 rarely surpassed abundances of 40 $m^{-3}$, with only one patch reaching 120 $m^{-3}$.

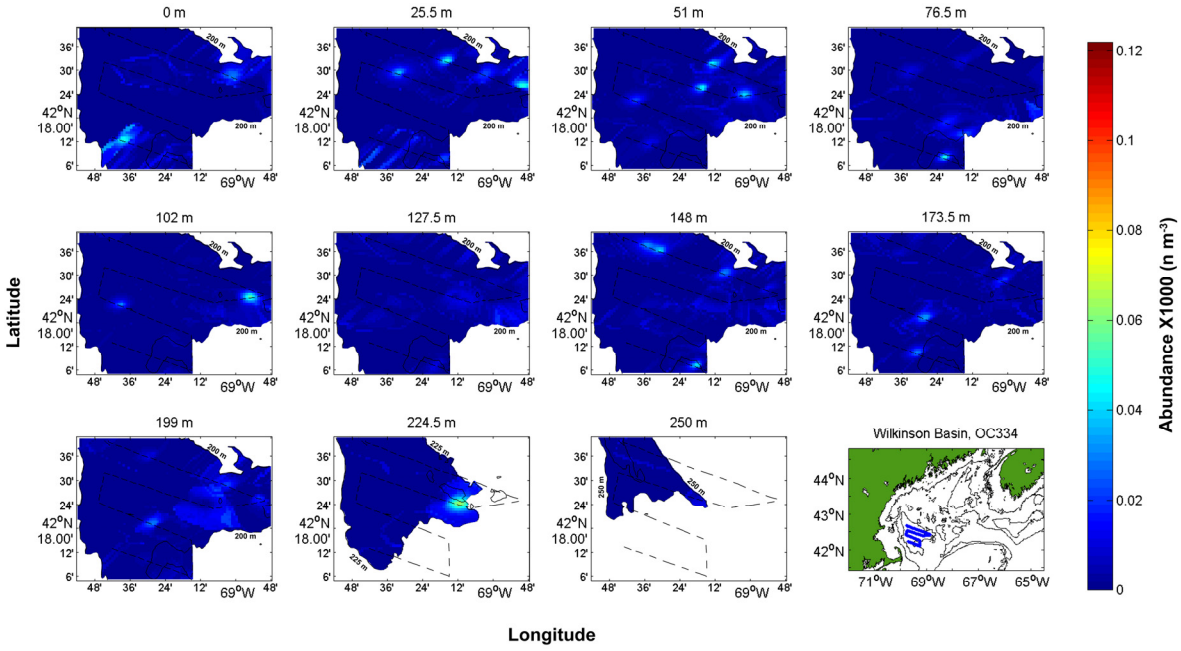


**Figure 5.46.** Euphausiid abundance (n $m^{-3}$) in Wilkinson Basin during December 1998 plotted at ~25 m intervals. Isobaths (solid lines) and cruise track (dashed line) were superimposed for reference.

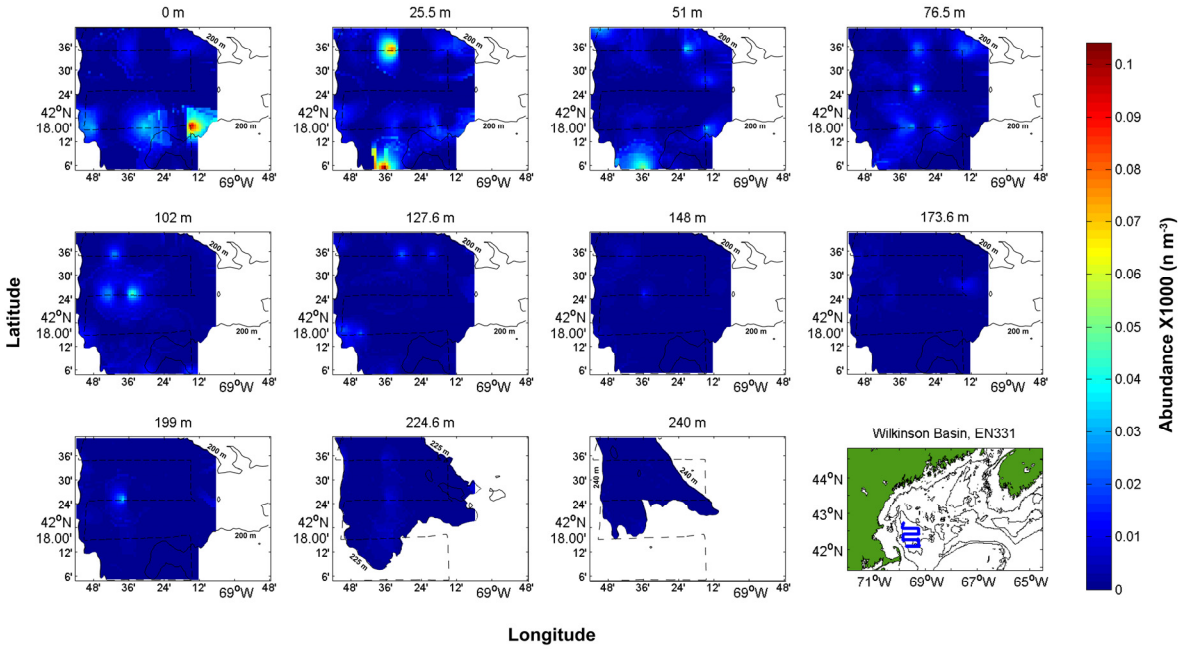


**Figure 5.47.** Euphausiid abundance (n $m^{-3}$) in Wilkinson Basin during December 1999 plotted at ~25 m intervals. Isobaths (solid lines) and cruise track (dashed line) were superimposed for reference.

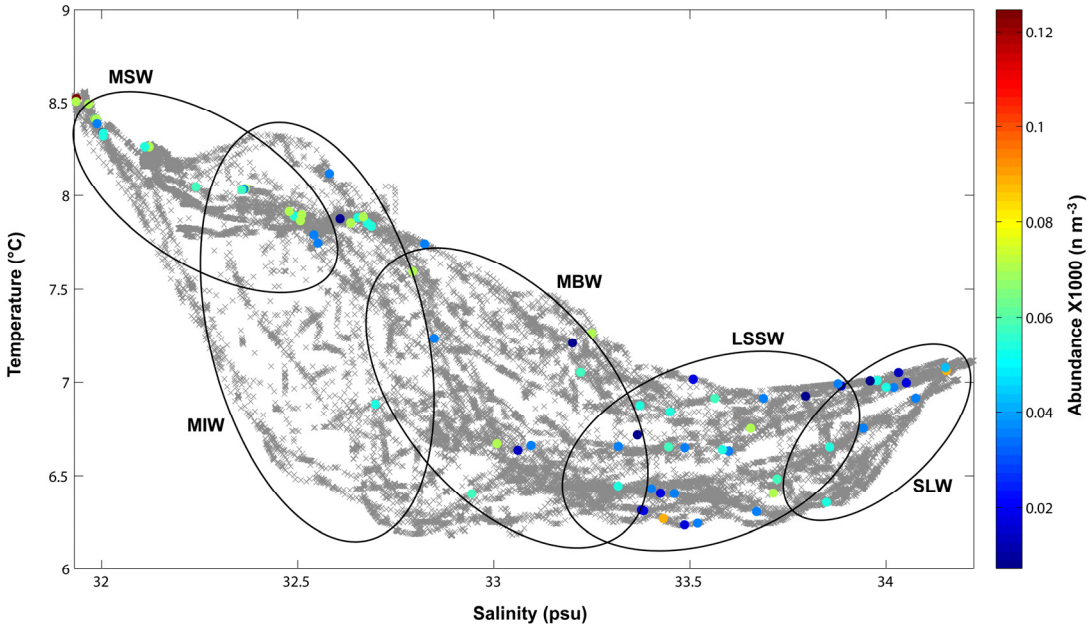


**Figure 5.48.** TSP plot for Wilkinson Basin during December 1998. Euphausiid abundances are shown in color-coded dots. Temperature-Salinity points are plotted in grey X marks. MSW=Maine Surface Water; MIW=Maine Intermediate Water; MBW= Maine Bottom Water; LSSW=Labrador Subarctic Slope Water; SLW=Slope Water.

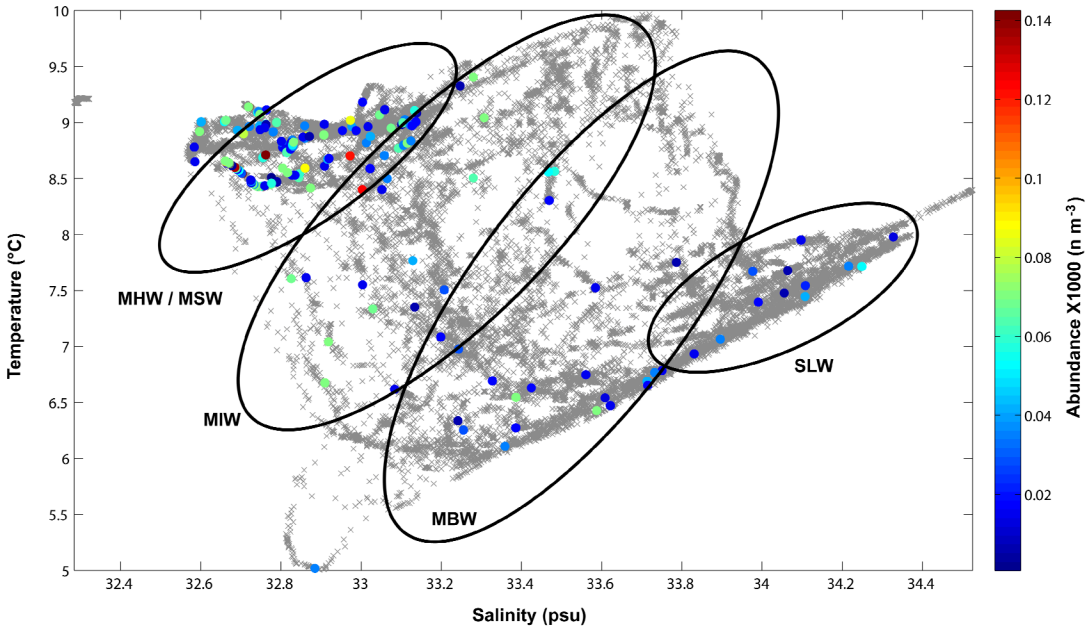


**Figure 5.49.** TSP plot for Wilkinson Basin during December 1999. Euphausiid abundances are shown in color-coded dots. Temperature-Salinity points are plotted in grey X marks. MHW=Maine Hot Water; MSW=Maine Surface Water; MIW=Maine Intermediate Water; MBW= Maine Bottom Water; SLW=Slope Water.

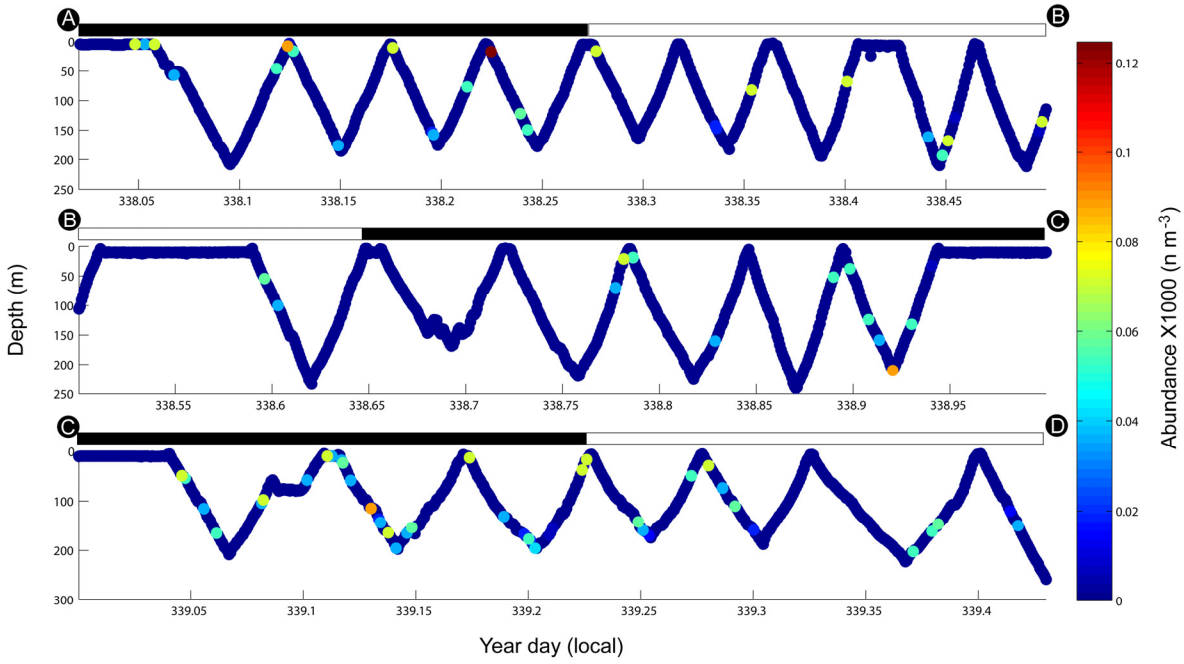


**Figure 5.50.** Diurnal vertical distribution of euphausiids in Wilkinson Basin during December 1998 along BIOMAPER-II track. Bars on top of each subplot represent day (white) and night (black) periods. Capital letters at the beginning and end of each panel correspond to the sections of the Wilkinson Basin, OC334 cruise track in Fig. 2.6.

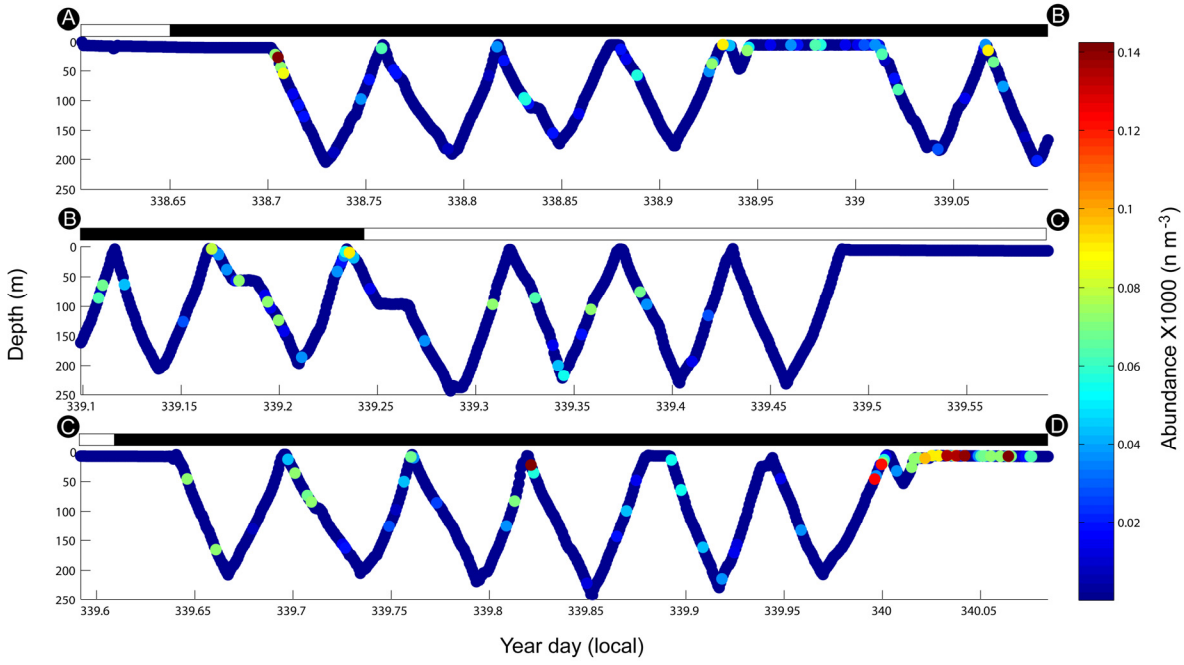


**Figure 5.51.** Diurnal vertical distribution of euphausiids in Wilkinson Basin during December 1999 along BIOMAPER-II track. Bars on top of each subplot represent day (white) and night (black) periods. Capital letters at the beginning and end of each panel correspond to the sections of the Wilkinson Basin, EN331 cruise track in Fig. 2.6.

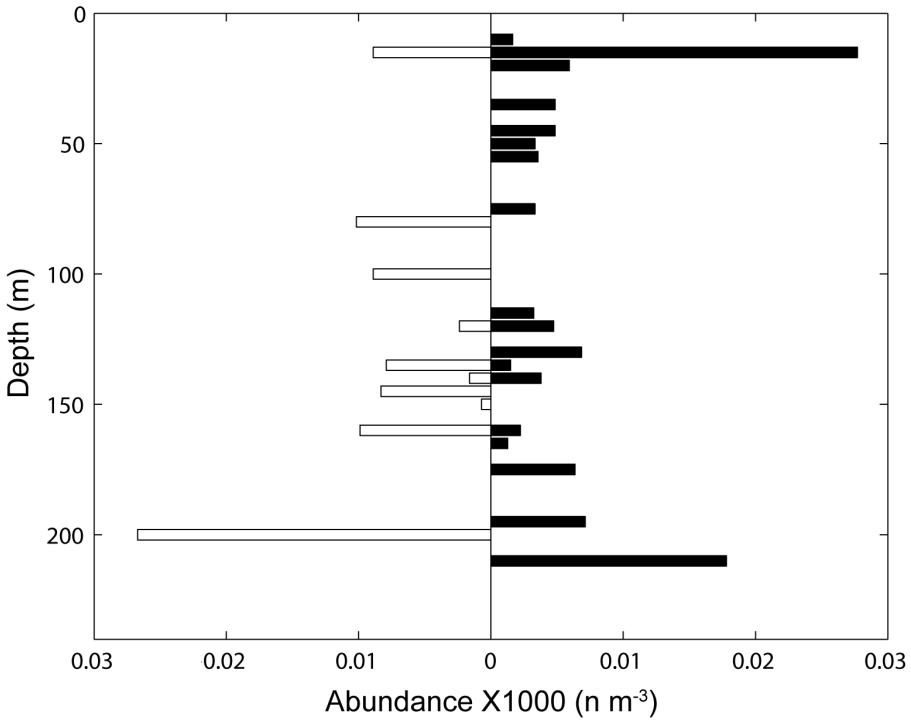


**Figure 5.52.** Vertical distribution of euphausiids in Wilkinson Basin during December 1998 during day (open horizontal bars, left) and night (black bars, right) periods.

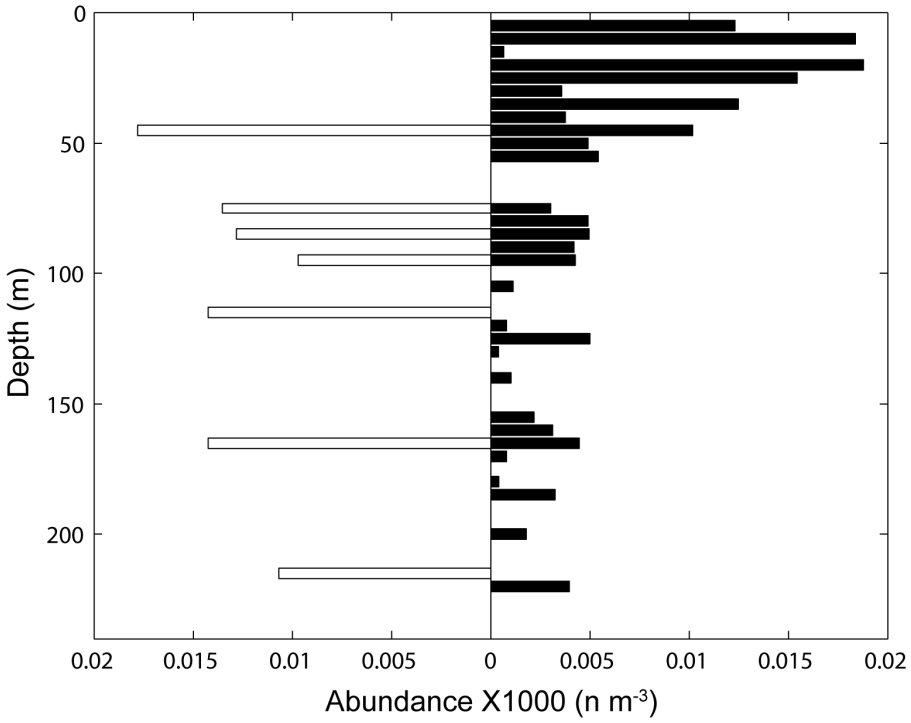


**Figure 5.53.** Vertical distribution of euphausiids in Wilkinson Basin during December 1999 during day (empty horizontal bars, left) and night (black bars, right) periods.

In December 1998, euphausiid abundances didn't show a clear relationship between abundances and water masses (Fig. 5.48). In general, higher abundance observations were associated with the MSW (> 120 $m^{-3}$) and LSSW (up to 90 $m^{-3}$). On December 1999, when euphausiids were more plentiful, a clearer relationship was observed between euphausiids abundance and water masses (Fig. 5.49). Most observations and peak abundances (70-142 $m^{-3}$) were associated with the MHW/MSW masses. Concentrations of 70 $m^{-3}$ and lower appeared scattered in the other three water masses with no apparent pattern.

Euphausiids during December 1998 showed higher abundances at surface (0-100 m) during night time while they were found in larger numbers below 100 m during day time (Figs. 5.51 and 5.52). During December 1999, larger high-abundance patches were found above 50 m during night segments (Fig. 5.51). Higher abundances were found during day time at depths below 50 m than during night time (Fig. 5.53). Although this pattern may be due to spatial heterogeneity, it may also indicate diel vertical migration of euphausiids.

**5.3.4.2 Jordan Basin**

Euphausiids in Jordan Basin showed higher abundance values during December 1999 than during December 1998 ($p<0.05$). Maximum calculated abundances during December 1999 were 164 $m^{-3}$, while the highest abundance during December 1998 was ~82 $m^{-3}$. However, during December 1998 euphausiids were clustered in few large dense patches (Fig. 5.54) while during December 1999 they were more scattered in numerous small patches across and at depths in Jordan Basin (Fig. 5.55).

During December 1998, euphausiids were found almost exclusively in a single large patch that extended from the surface to almost 50 m depth (Fig. 5.54). The patch was located to the northwest of Jordan Basin and the maximum abundance at its core was ~75 $m^{-3}$. During December 1999, euphausiids appeared widely scattered in the basin (Fig. 5.55). Euphausiids during December 1999 were found in dense patches from 0 m down to 100 m deep with abundance values of ~60 $m^{-3}$ at their core (Fig. 5.55).

TSP plots showed a relationship between euphausiid abundances and hydrographic features in Jordan Basin. Euphausiids in December 1998 were almost exclusively found in association with the MSW, close to the boundary with the MIW (Fig. 5.56). During December 1999, euphausiids were also clustered in the MHW/MSW complex. However, some high abundance values were found in the MIW, MBW and SLW, but were scattered and showed no clustering pattern (Fig. 5.57).

No clear evidence of euphausiids vertical migration was observed for either period. However, the high abundances found in Jordan Basin during December 1998 were observed in the top 50 m during dark periods (Figs. 5.58 and 5.60): one before dawn (Fig. 5.58, top panel) and the second close to midnight (Fig. 5.58, bottom panel). No euphausiids vertical migration pattern was evident during December 1999 either (Fig. 5.59). However, high abundances during day were located below 45 m depth while euphausiids were more scattered in the water column by night (Fig. 5.61). Interestingly, with abundances during night decreased with increasing depth while abundances during day increased with increasing depth (Fig. 5.61).

**5.3.4.3 Georges Basin/Northeast Channel**

Euphausiid abundance in Georges Basin was slightly greater during December 1999 than during December 1998 ($p<0.001$). During December 1999, euphausiids abundance varied between ~4 and 140 $m^{-3}$ while during December 1998 euphausiids in Georges Basin were found at all depths with abundances ranging between 7 and 127 $m^{-3}$.

During December 1998, the largest aggregations of euphausiids resolved by Kriging were found in waters deeper than 150 m in the western side of the Georges Basin transect (right side in Fig. 5.62). In the center of the transect, and towards the eastern portion of Georges Basin, euphausiid patches were located from 150 m and above (Fig. 5.62). During December 1999, euphausiids found in Georges Basin and the Northeast Channel (NEC) where located along and across the transect without apparent spatial pattern. However, the larger patches were observed in the first 50 m (Fig. 5.63) to the east of Georges Basin, close to the NEC.

Other large patches were found close to 200 m depth in the Northeast Channel, but no euphausiids were recorded in the 90 m sampled below that depth.

During December 1998, euphausiids in Georges Basin were associated to different water masses, depending on the location of the patches inside the basin. Euphausiid patches found in the western Georges Basin, appeared to be associated with the MBW and the LSSW (Fig. 5.64). Patches found in the eastern Georges Basin were associated mainly with the MSW and in the upper limit of the MIW, close to the interface between the MSW. Very few observations were made in the lower limit of the MIW (Fig. 5.64). During December 1999, euphausiid high abundances (40-140 $m^{-3}$) were associated with the MSW and to a lesser degree with MIW, MBW and SLW (Fig. 5.65). Euphausiids were virtually absent from the LSSW in December 1999.

The different depth location of patches between day and night transects suggested diel activity in euphausiids in Georges Basin during December 1998. Patches registered at night time were found deeper and patches appeared to be located at progressively shallower depths at dusk and then deeper again close to twilight (Fig. 5.62). The vertical distribution plot (fig. 5.67) further supports the evidence of euphausiids diel migration during December 1998 with higher abundances towards the surface at night and higher abundances towards the bottom at day.

No apparent vertical migration was observed for euphausiids during December 1999 (Figure 5.66). However, most euphausiids were observed during night time, and considerably fewer observations were made during day time (Figs. 5.66 and 5.68). Further, a bimodal pattern was evident for euphausiids during December 1999. From 0 to 140 m, higher abundances were found shallower at night, while higher abundances during day were found deeper (Fig. 5.68). The same pattern was observed for the interval from 140 to ~210 m depth. Although this may suggest spatial differences, it could indicate different euphausiids populations showing different

behavior. While *Meganyctiphanes norvegica* was the main identified species, other unidentified species were also included in the euphausiids data set.

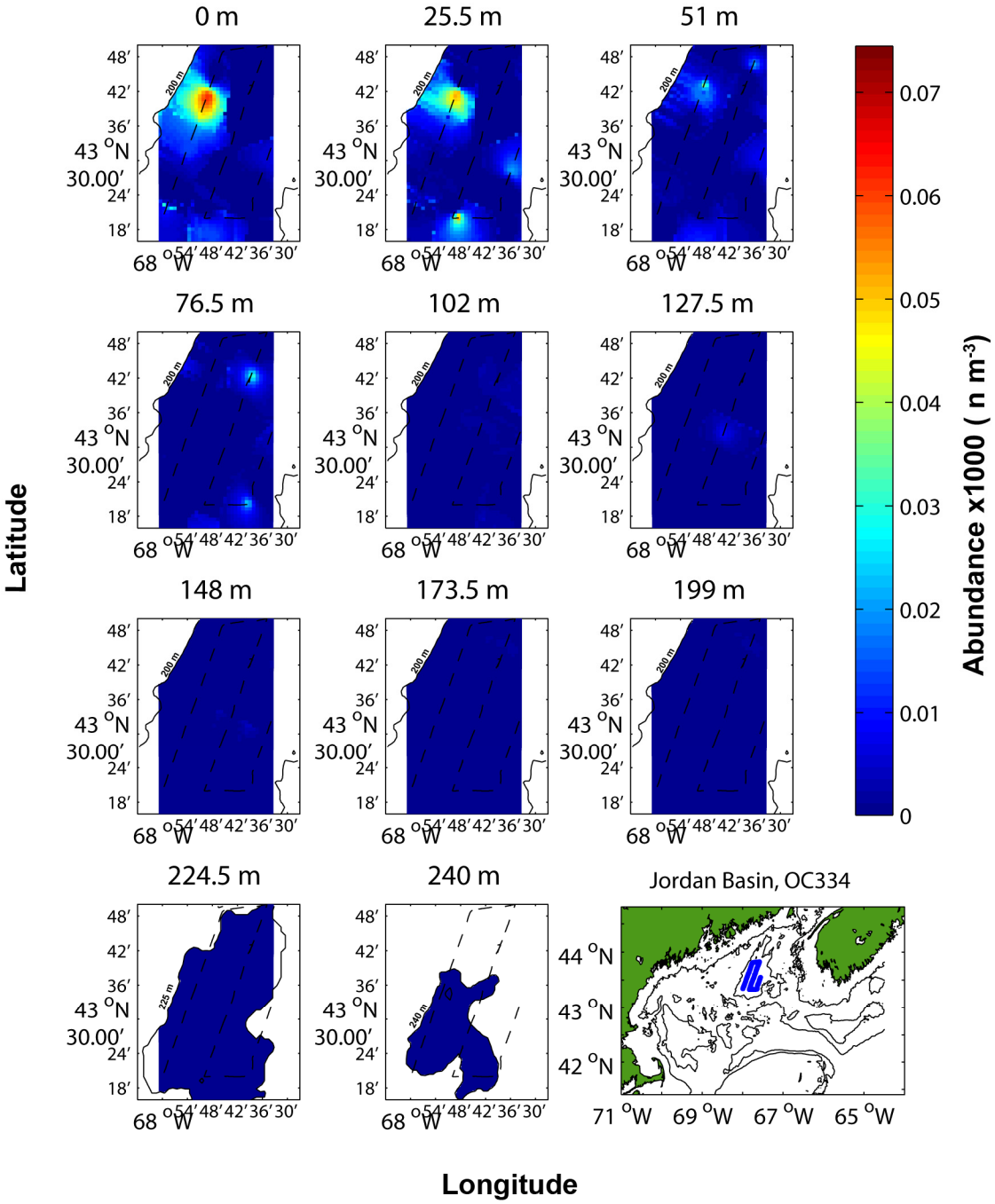


**Figure 5.54.** Euphausiid abundance in Jordan Basin during December 1998 plotted at ~25 m intervals. Isobaths (solid lines) and cruise track (dashed line) were superimposed for reference.

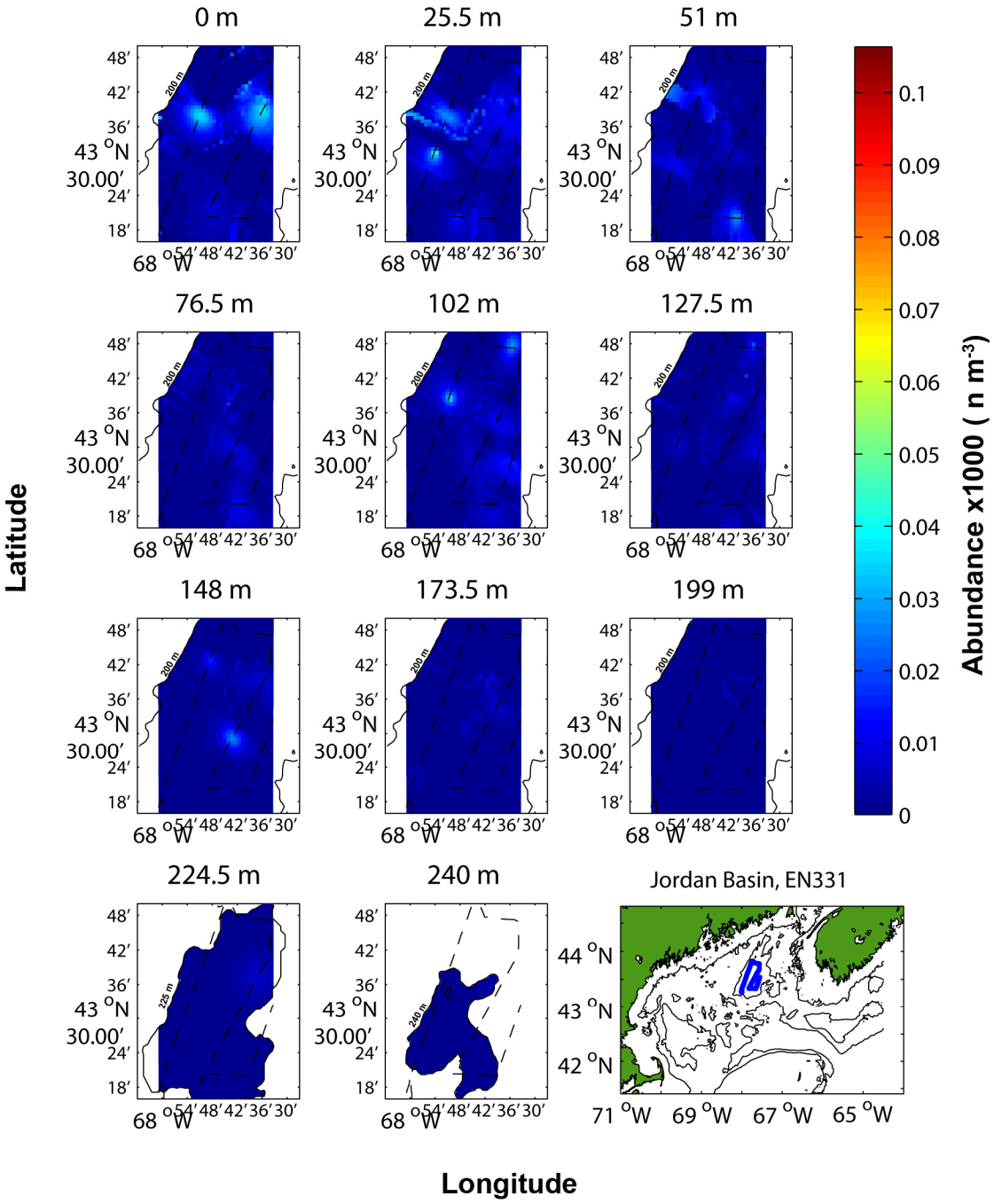


**Figure 5.55.** Euphausiid abundance (n $m^{-3}$) in Jordan Basin during December 1999 plotted at ~25 m intervals. Isobaths (solid lines) and cruise track (dashed line) were superimposed for reference.

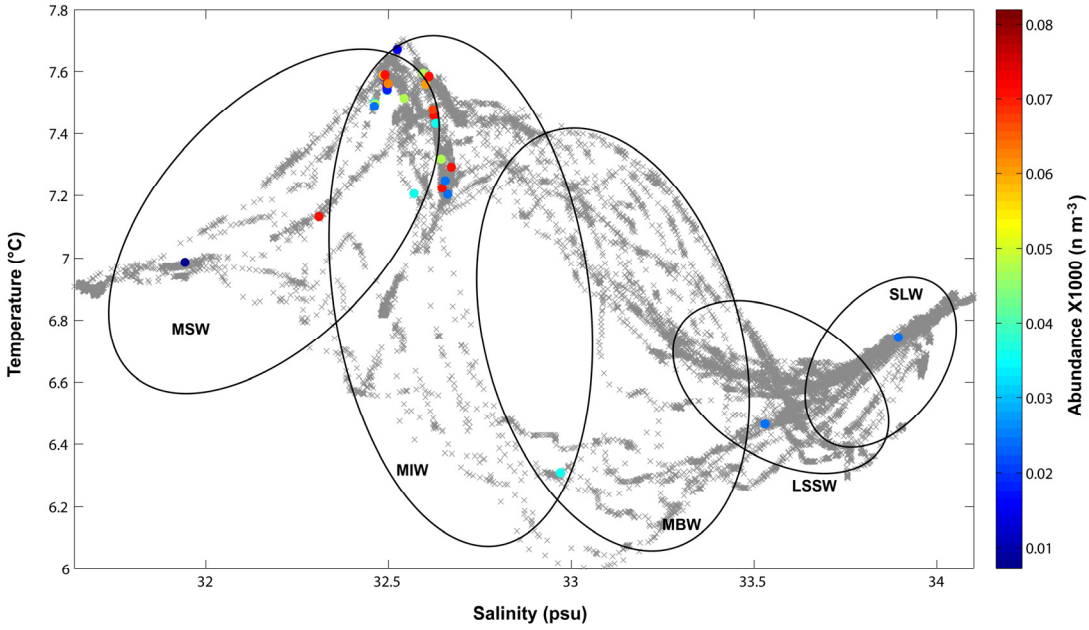


**Figure 5.56.** TSP plot for Jordan Basin during December 1998. Euphausiid abundances are shown in color-coded dots. Temperature-Salinity points are plotted in grey X marks. MSW=Maine Surface Water; MIW=Maine Intermediate Water; MBW= Maine Bottom Water; LSSW=Labrador Subarctic Slope Water; SLW=Slope Water.

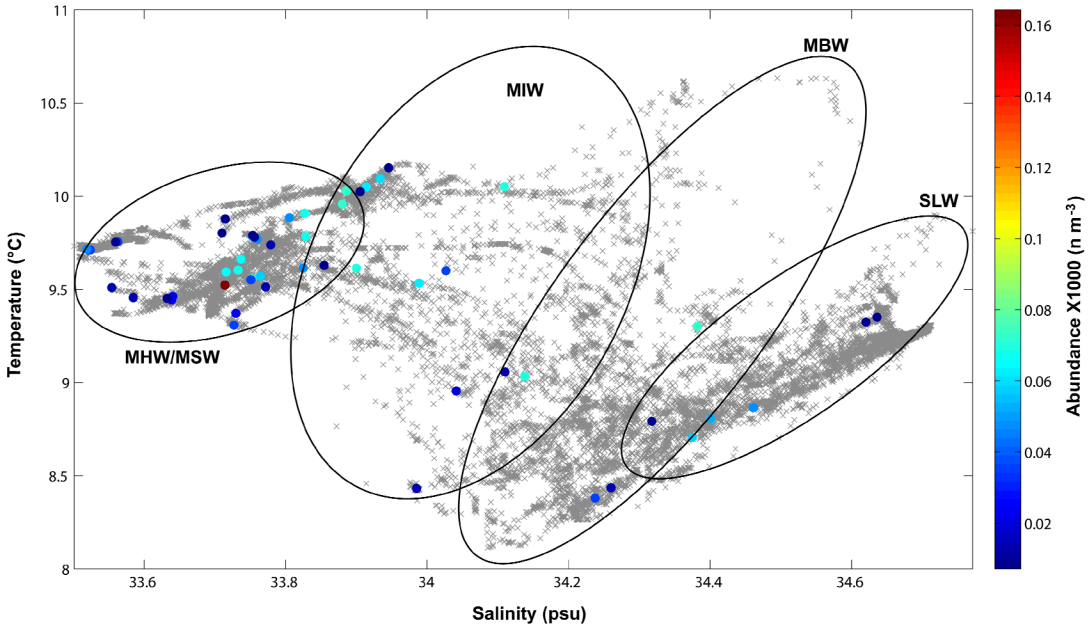


**Figure 5.57.** TSP plot for Jordan Basin during December 1999. Euphausiids abundances are shown in color-coded dots. Temperature-Salinity points are plotted in grey X marks. MHW=Maine Hot Water; MSW=Maine Surface Water; MIW=Maine Intermediate Water; MBW= Maine Bottom Water; SLW=Slope Water.

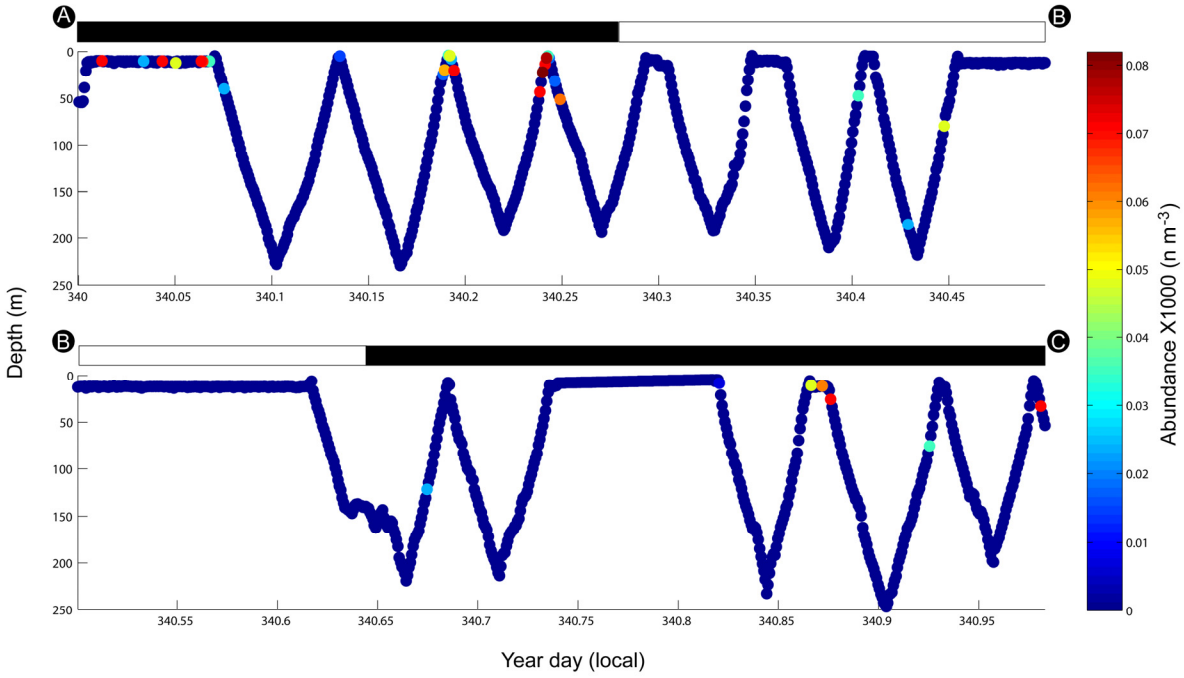


**Figure 5.58.** Diurnal vertical distribution of euphausiids in Jordan Basin during December 1998 along BIOMAPER-II track. Bars on top of each subplot represent day (white) and night (black) periods. Capital letters at the beginning and end of each panel correspond to the sections of the Jordan Basin, OC334 cruise track in Fig. 2.6.

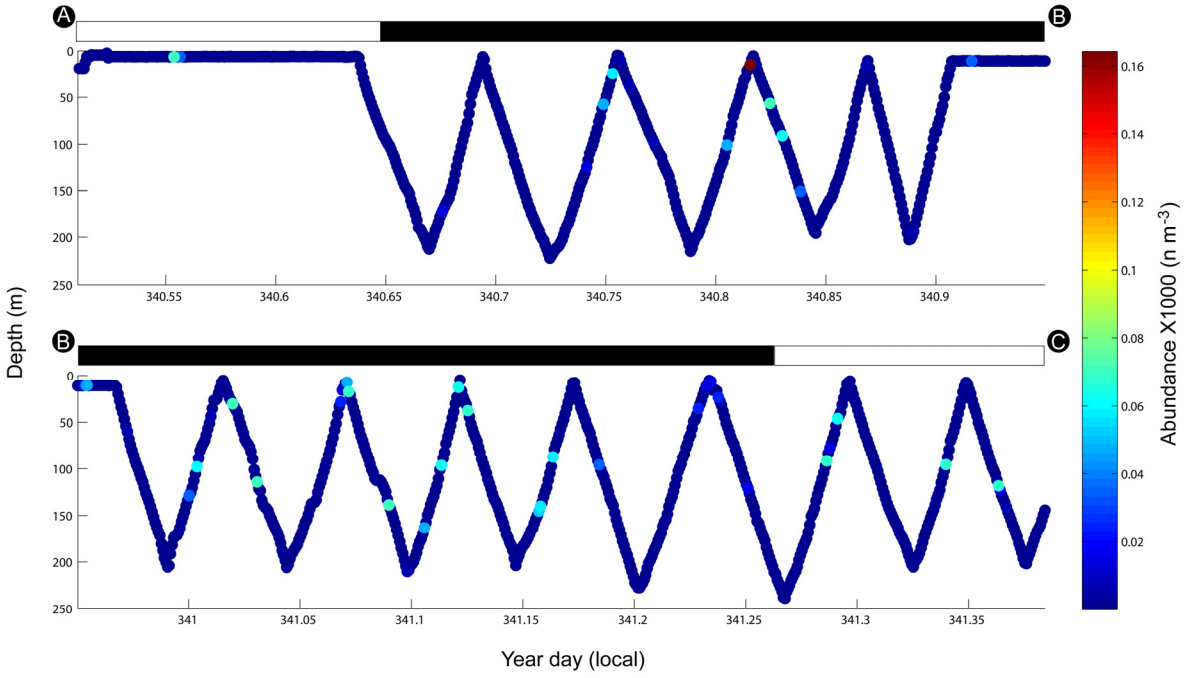


**Figure 5.59.** Diurnal vertical distribution of euphausiids in Jordan Basin during December 1999 along BIOMAPER-II track. Bars on top of each subplot represent day (white) and night (black) periods. Capital letters at the beginning and end of each panel correspond to the sections of the Jordan Basin, EN331 cruise track in Fig. 2.6.

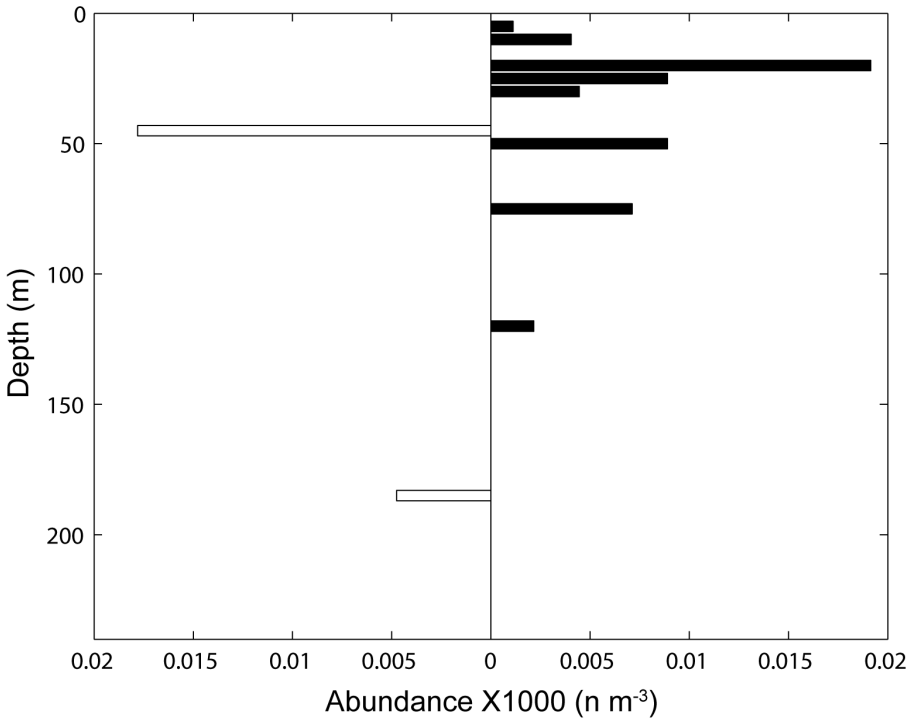


**Figure 5.60.** Vertical distribution of euphausiids in Jordan Basin during December 1998 during day (empty horizontal bars, left) and night (black bars, right) periods.

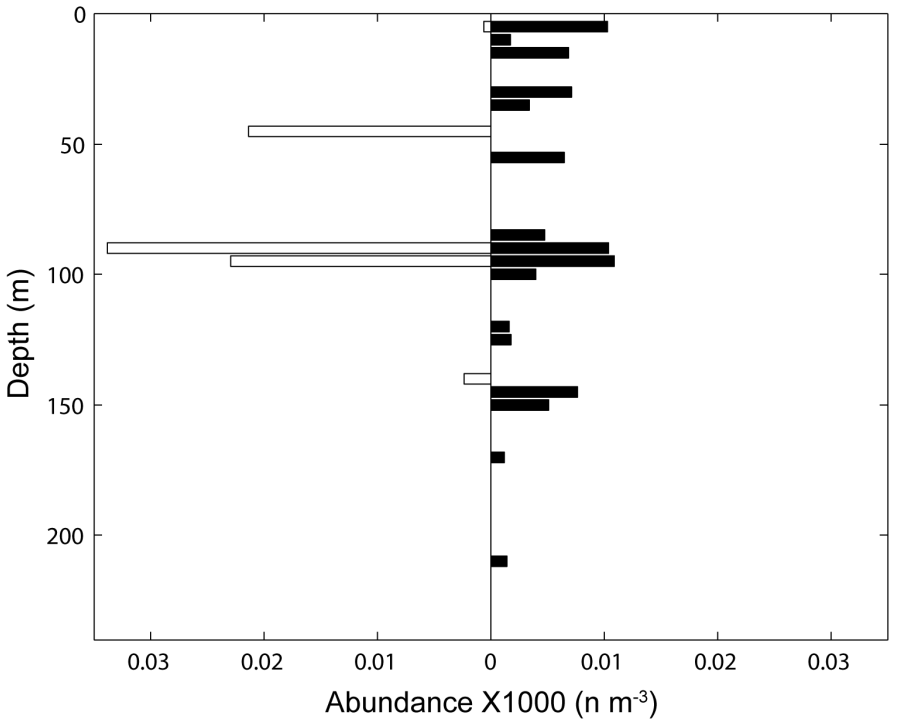


**Figure 5.61.** Vertical distribution of euphausiids in Jordan Basin during December 1999 during day (empty horizontal bars, left) and night (black bars, right) periods.

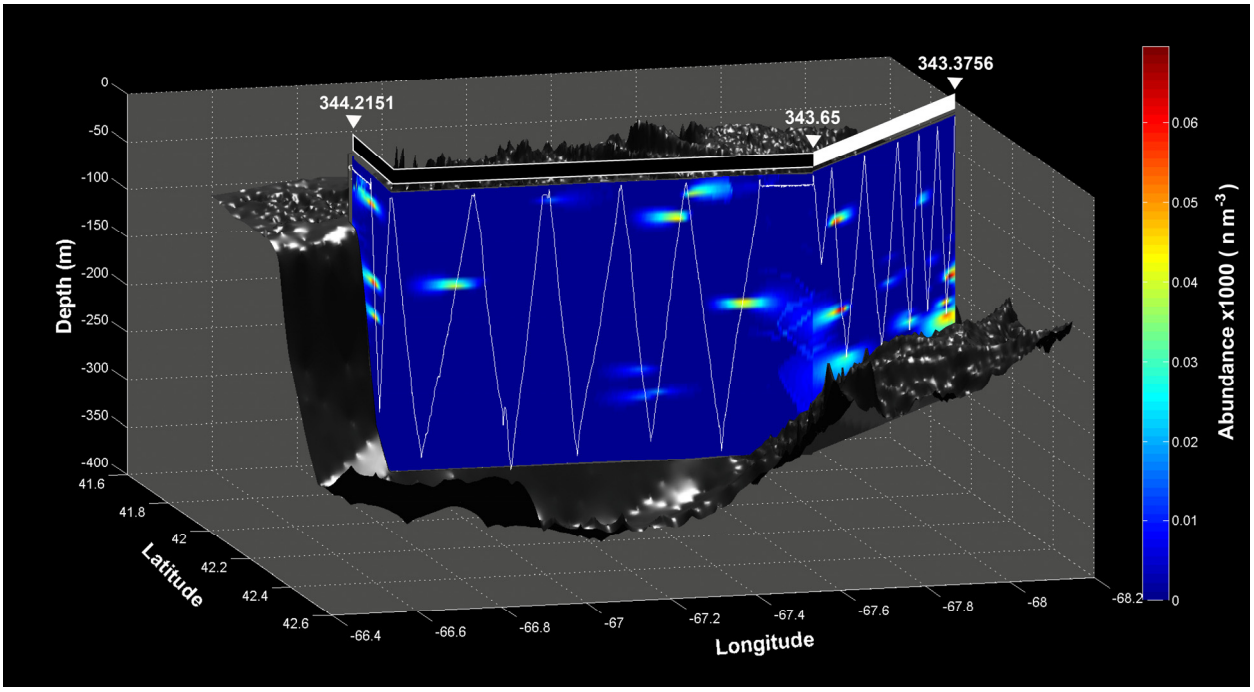


**Figure 5.62.** Euphausiid distribution in Georges Basin during December 1998. The top bar represents the day (white) and night (black) portions of the transect. The dark grey surface represents the bathymetry of the basin. Georges Bank is behind the "curtain" so that the east is to the left of the graph (X-ordinate) and south is towards the back of the graph (Y-ordinate).

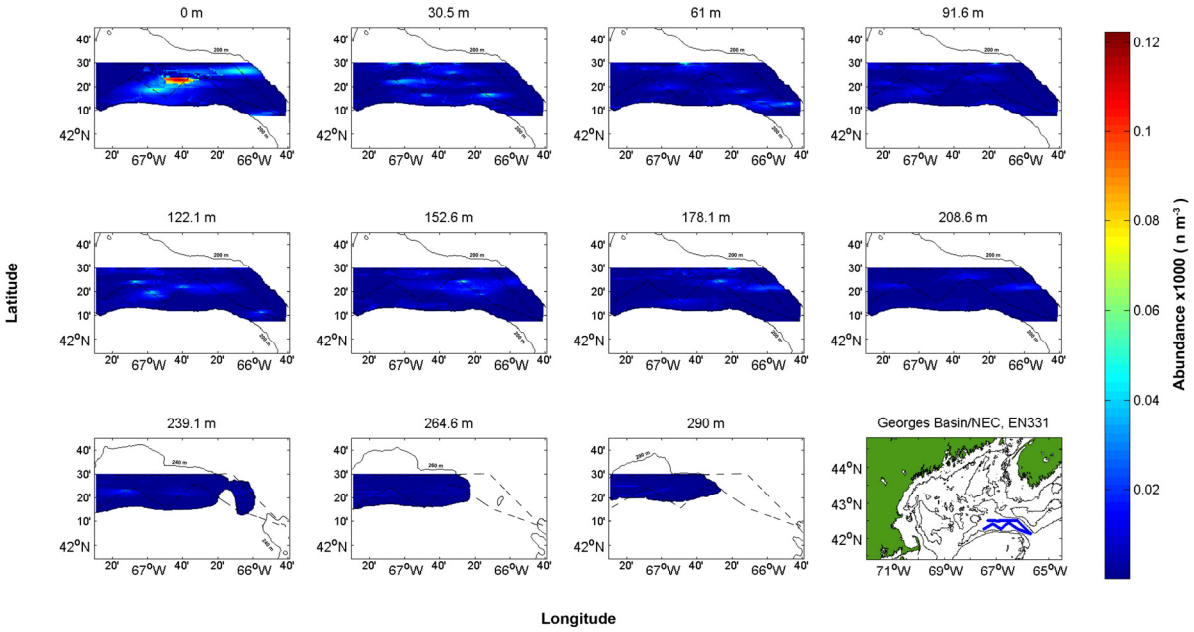


**Figure 5.63.** Euphausiids abundance (n $m^{-3}$) in Georges Basin/NE Channel during December 1999 plotted at ~30 m intervals. Isobaths (solid lines) and cruise track (dashed line) were superimposed for reference.

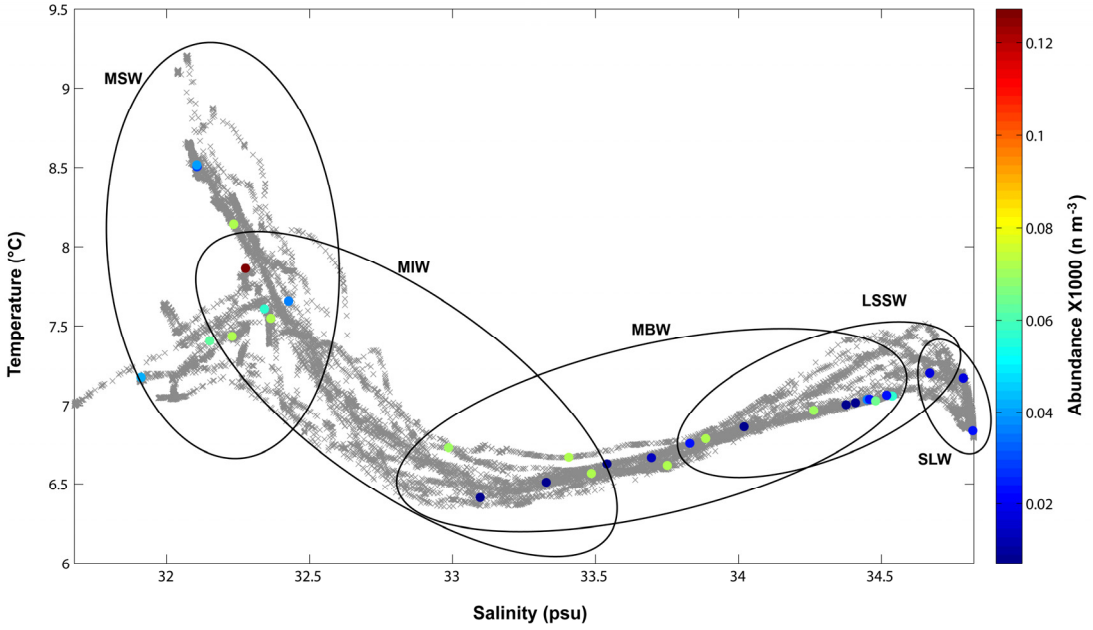


**Figure 5.64.** TSP plot for Georges Basin during December 1998. Euphausiid abundances are shown in color-coded dots. Temperature-Salinity points are plotted in grey X marks. MSW=Maine Surface Water; MIW=Maine Intermediate Water; MBW= Maine Bottom Water; LSSW=Labrador Subarctic Slope Water; SLW=Slope Water.

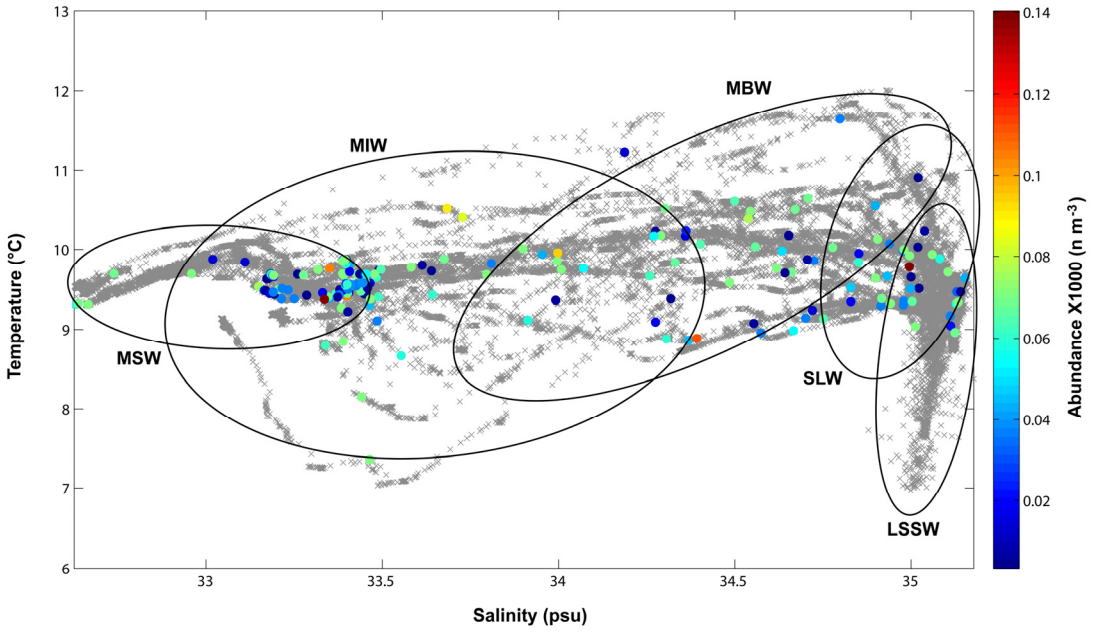


**Figure 5.65.** TSP plot for Georges Basin/NE Channel during December 1999. Euphausiid abundances are shown in color-coded dots. Temperature-Salinity points are plotted in grey X marks. MSW=Maine Surface Water; MIW=Maine Intermediate Water; MBW= Maine Bottom Water; LSSW=Labrador Subarctic Slope Water; SLW=Slope Water.

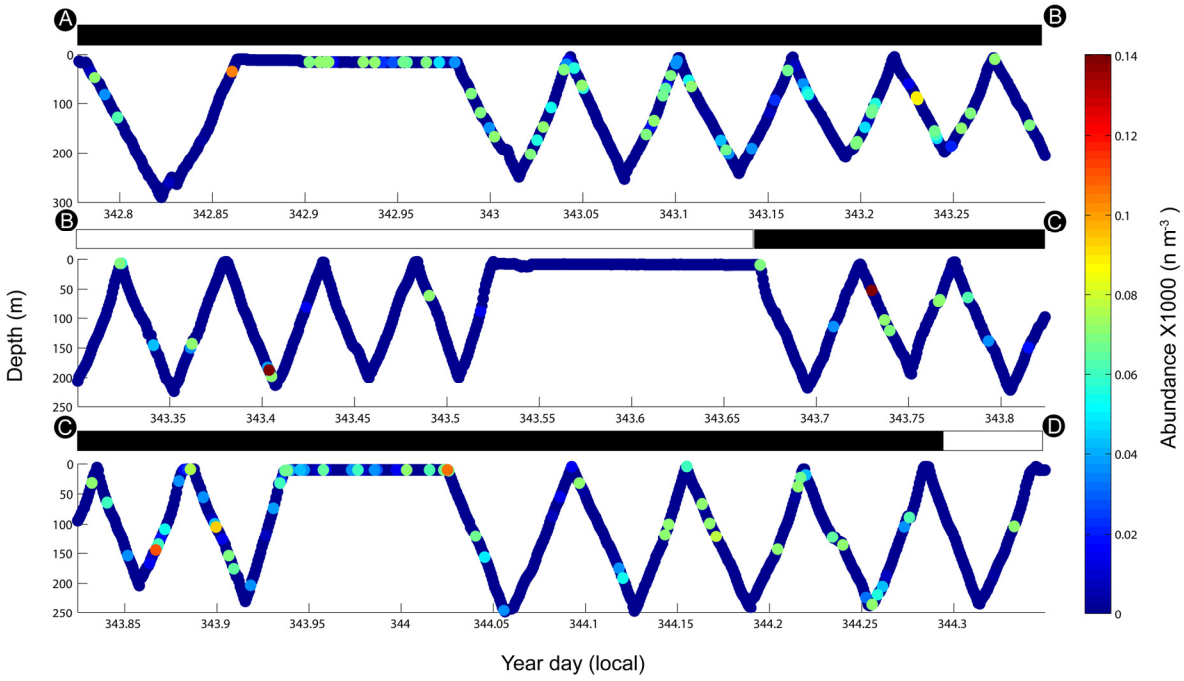


**Figure 5.66.** Diurnal vertical distribution of euphausiids in Georges Basin/NE Channel during December 1999 along BIOMAPER-II track. Bars on top of each subplot represent day (white) and night (black) periods. Capital letters at the beginning and end of each panel correspond to the sections of the Wilkinson Basin, EN331 cruise track in Fig. 2.6.

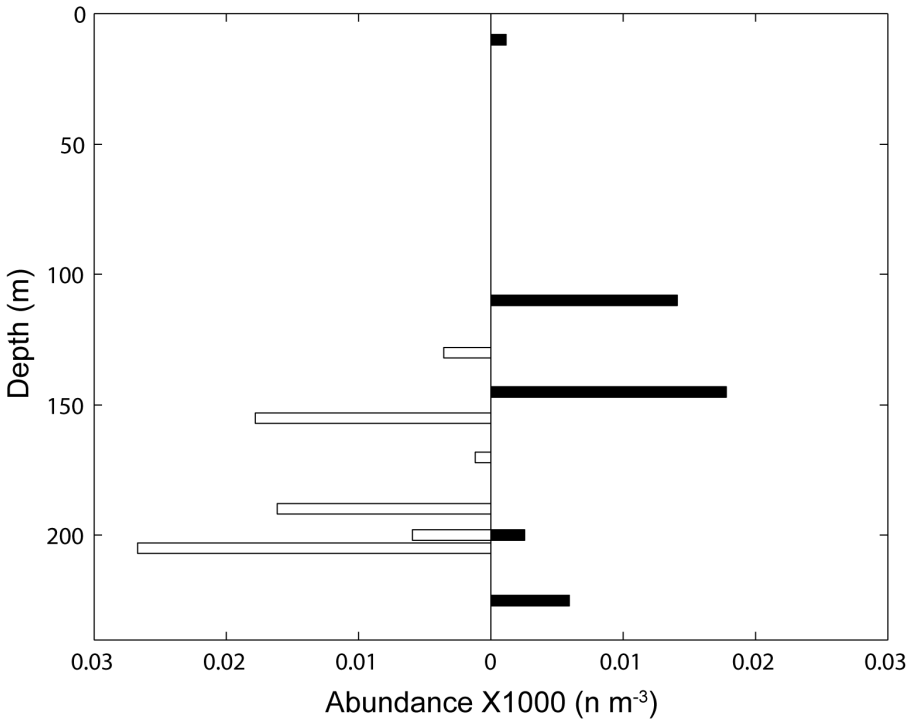


**Figure 5.67.** Vertical distribution of euphausiids in Georges Basin during December 1998 during day (open horizontal bars, left) and night (black bars, right) periods.

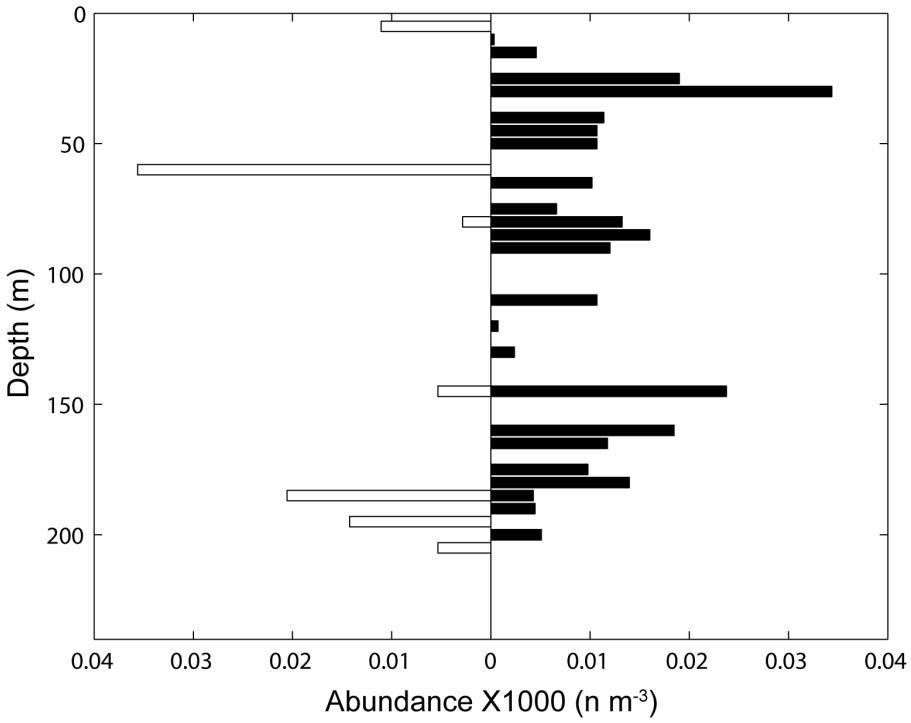


**Figure 5.68.** Vertical distribution of euphausiids in Georges Basin/NE Channel during December 1999 during day (open horizontal bars, left) and night (black bars, right) periods.

### 5.3.5 *Euchaeta norvegica*

#### 5.3.5.1 Wilkinson Basin

The large copepod *Euchaeta norvegica* was readily differentiated from *C. finmarchicus* and other copepods due to its large body size, and its characteristic fan-shaped legs (Fig. 2.2P). *Euchaeta norvegica* was more abundant in Wilkinson Basin during December 1999 than on December 1998. During 1998, *E. norvegica* was widely dispersed in low-abundance patches from 100 to 225 m depth. The patch with the highest abundance (~130 $m^{-3}$ in its core) was observed at 225 m in the western region of Wilkinson Basin (Fig. 5.69). At the surface and towards the easternmost part of the basin, there was evidence of another patch with a maximum concentration of 80 $m^{-3}$ at its core.

During December 1999, *E. norvegica* was widely distributed at all depths at abundances of 40 $m^{-3}$ or less. The highest abundances (120 $m^{-3}$) were observed in patches located in the upper 25 m and again below 200 m in the center of Wilkinson Basin (Fig. 5.70).

Although less marked during December 1998, the distributions of *Euchaeta norvegica* were related to hydrological conditions during both periods. During December 1998, the highest concentrations of *E. norvegica* (up to 213 $m^{-3}$) were associated to the SLW mass (Fig. 5.71). *Euchaeta norvegica* highest abundances in December 1999 were associated both to the MHW/MSW (up to 110 $m^{-3}$) and to the SLW (up to 160 $m^{-3}$) masses (Fig. 5.72). Fewer observations of *E. norvegica* were associated with MSW and MIW during December 1999 than during December 1998.

There was no clear evidence of vertical migration by *E. norvegica* during December 1998 as evidenced by similar *E. norvegica* vertical distributions during day and night sections (Figs. 5.73 and 5.75). During December 1999 the highest abundance patches of *E. norvegica* were observed in surface and deep waters during the night sections (Figs. 5.74 and 5.76). However, most of the recorded patches in the day section were located below 100 m depth while *E. norvegica* was scattered in the first 150 m at night (Fig. 6.76).

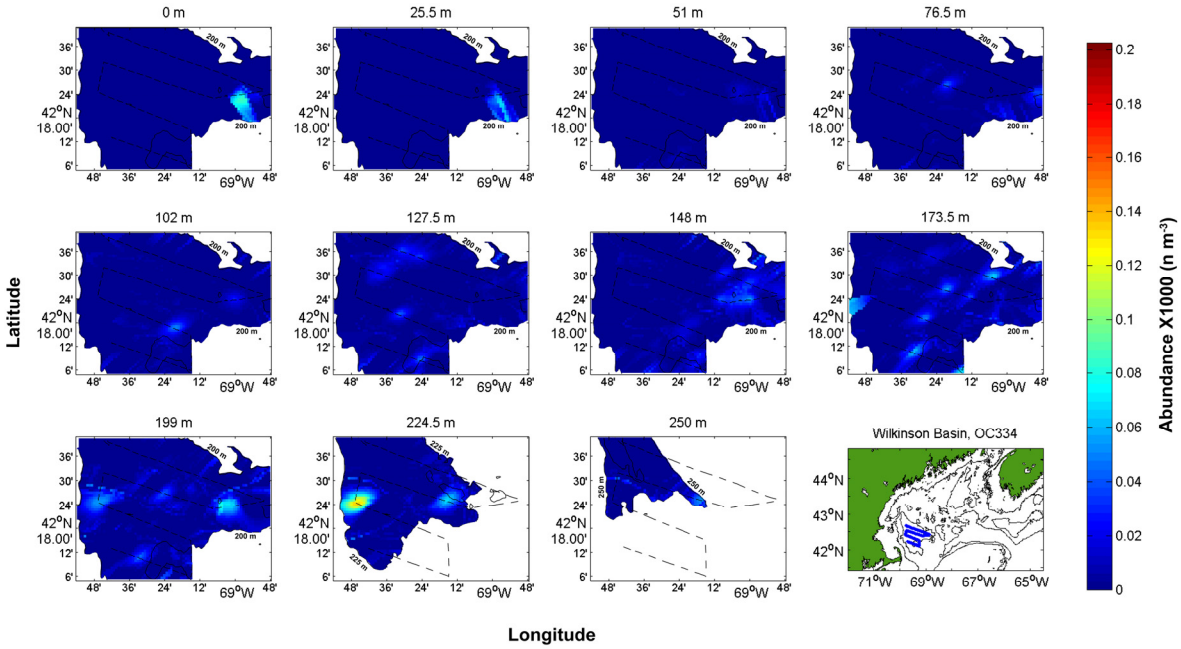


**Figure 5.69.** *Euchaeta norvegica* abundance in Wilkinson Basin during December 1998 plotted at ~25 m intervals. Isobaths (solid lines) and cruise track (dashed line) were superimposed for reference.

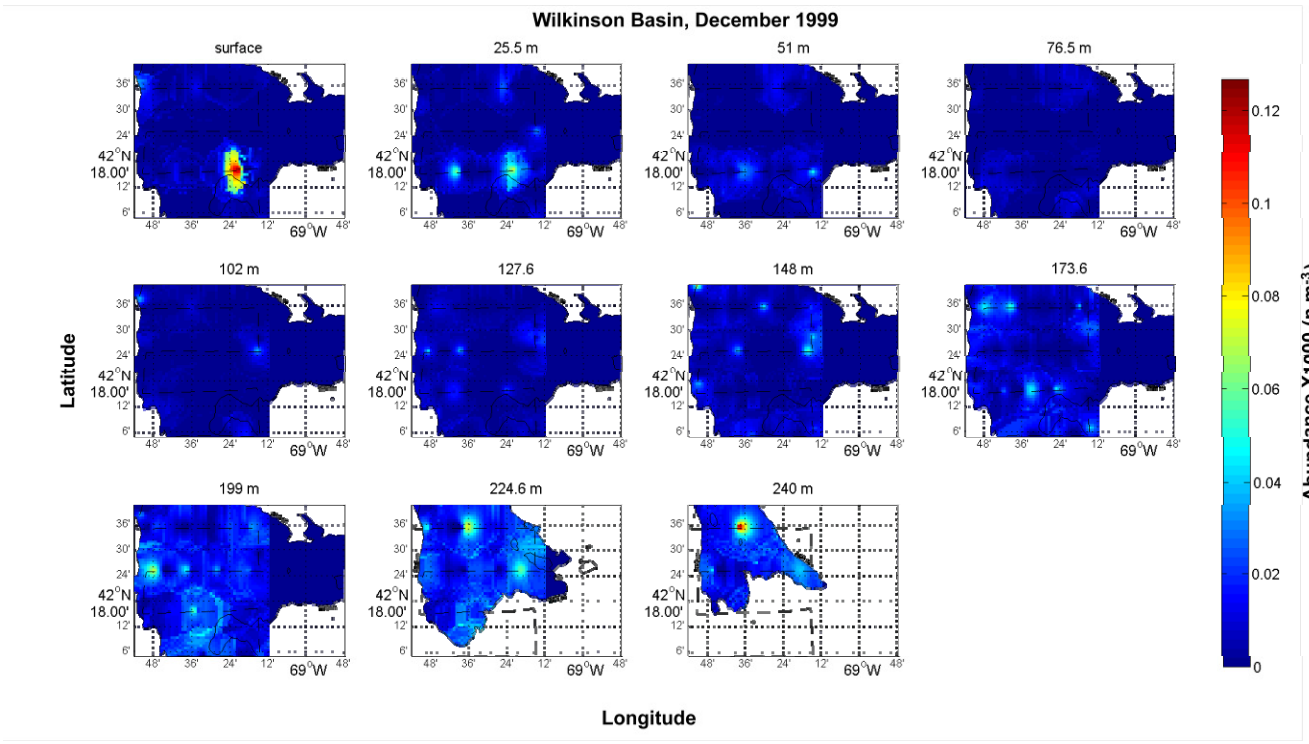


**Figure 5.70.** *Euchaeta norvegica* abundance in Wilkinson Basin during December 1999 plotted at ~25 m intervals. Isobaths (solid lines) and cruise track (dashed line) were superimposed for reference.

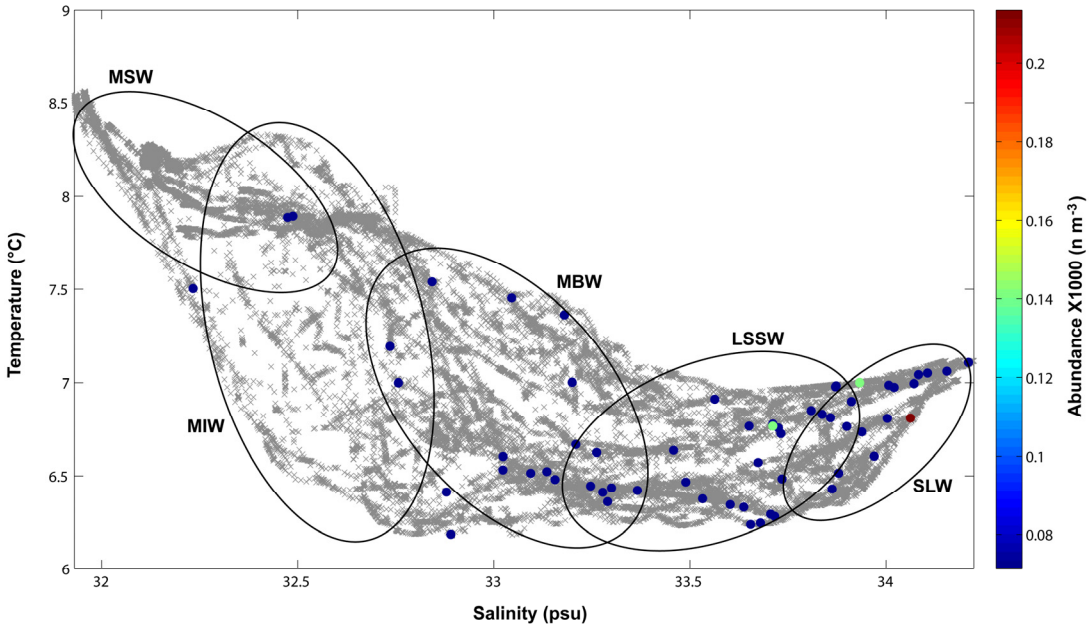


**Figure 5.71.** TSP plot for Wilkinson Basin during December 1998. *Euchaeta norvegica* abundances are shown in color-coded dots. Temperature-Salinity points are plotted in grey X marks. MSW=Maine Surface Water; MIW=Maine Intermediate Water; MBW= Maine Bottom Water; LSSW=Labrador Subarctic Slope Water; SLW=Slope Water.

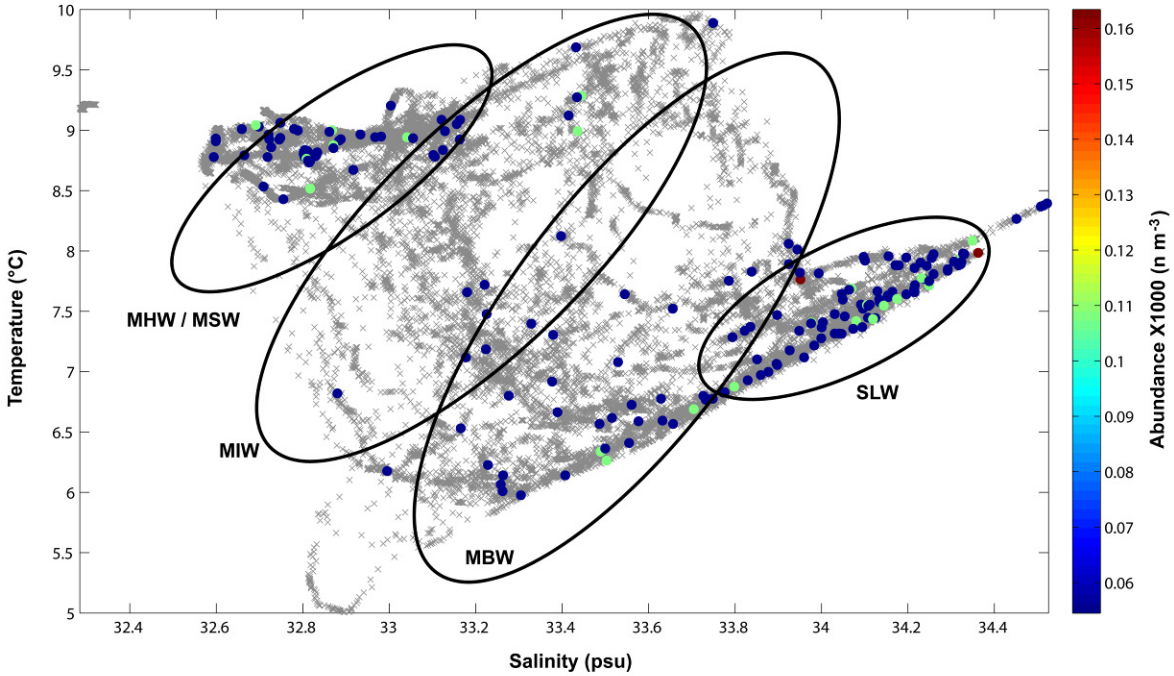


**Figure 5.72.** TSP plot for Wilkinson Basin during December 1999. *Euchaeta norvegica* abundances are shown in color-coded dots. Temperature-Salinity points are plotted in grey X marks. MHW=Maine Hot Water; MSW=Maine Surface Water; MIW=Maine Intermediate Water; MBW= Maine Bottom Water; SLW=Slope Water.

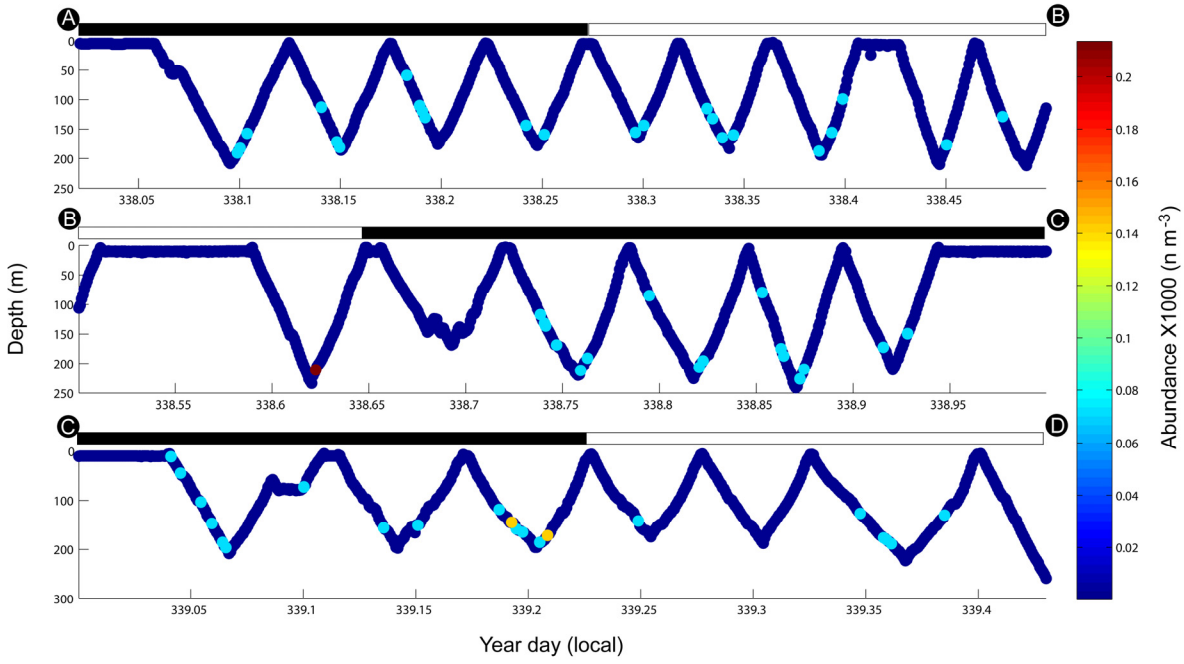


**Figure 5.73.** Diurnal vertical distribution of *Euchaeta norvegica* in Wilkinson Basin during December 1998 along BIOMAPER-II track. Bars on top of each subplot represent day (white) and night (black) periods. Sections correspond to the Wilkinson Basin, OC334 track in Fig. 2.6.

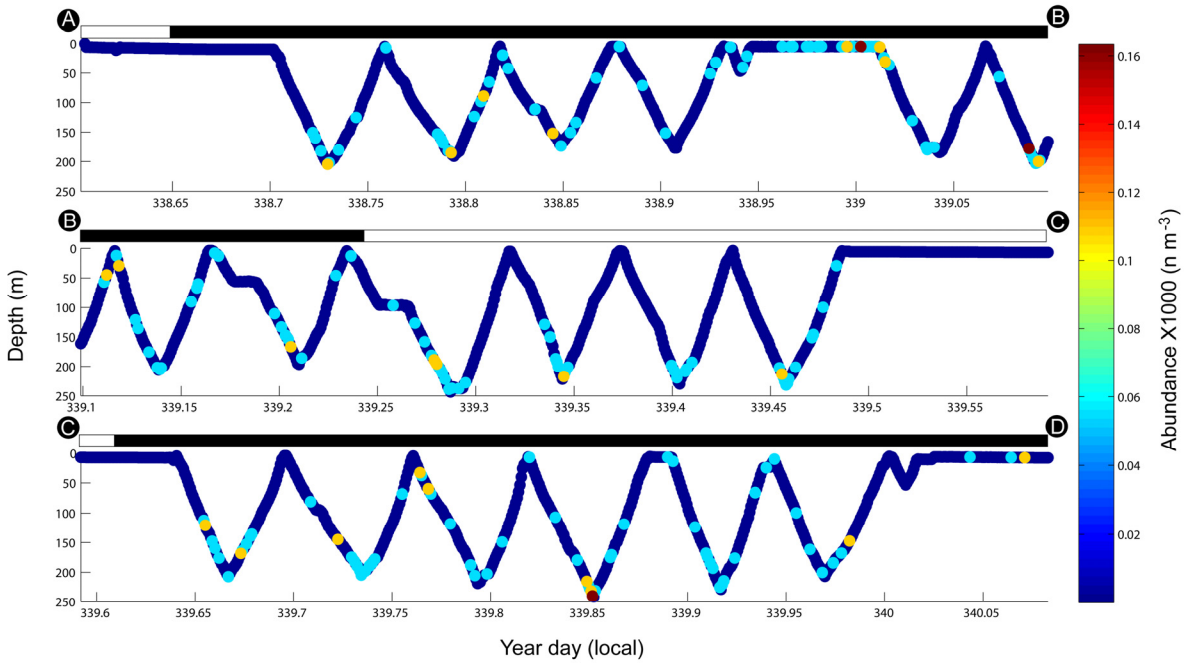


**Figure 5.74.** Diurnal vertical distribution of *Euchaeta norvegica* in Wilkinson Basin during December 1999 along BIOMAPER-II track. Bars on top of each subplot represent day (white) and night (black) periods. Capital letters at the beginning and end of each panel correspond to the sections of the Wilkinson Basin, EN331 cruise track in Fig. 2.6.

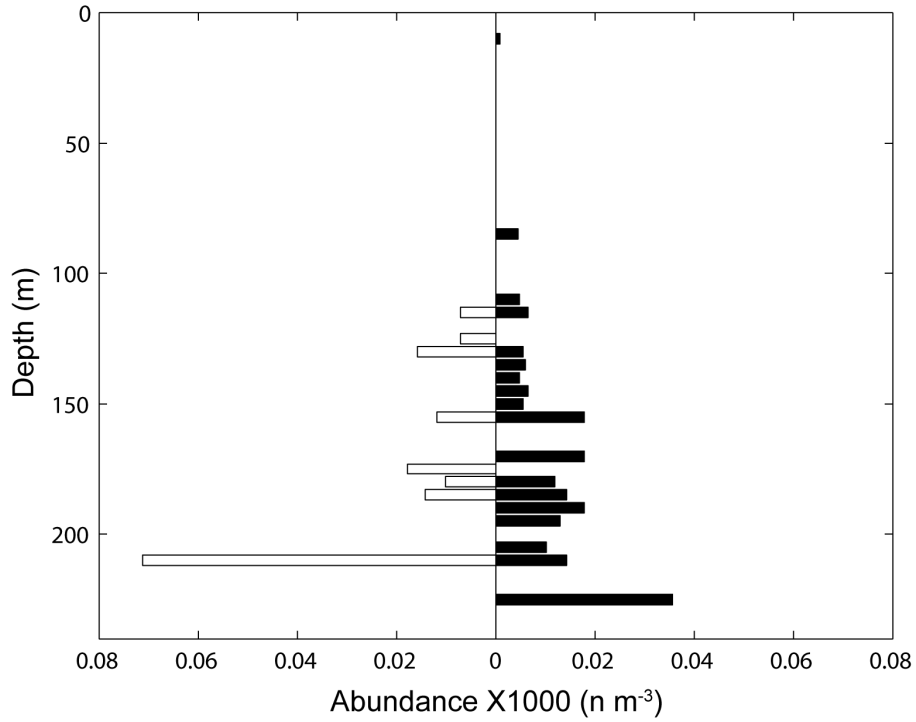


**Figure 5.75.** Vertical distribution of *Euchaeta norvegica* in Wilkinson Basin during December 1998 during day (open horizontal bars, left) and night (black bars, right) periods.

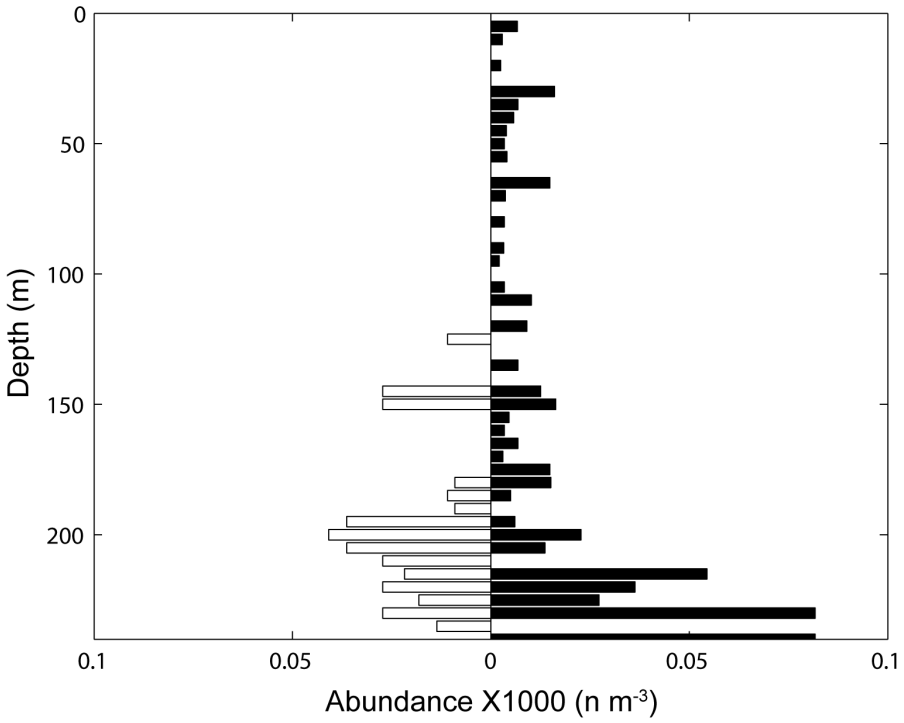


**Figure 5.76.** Vertical distribution of *Euchaeta norvegica* in Wilkinson Basin during December 1999 during day (open horizontal bars, left) and night (black bars, right) periods.

#### 5.3.5.2 Jordan Basin

*Euchaeta norvegica* was more abundant in December 1999 than in December 1998 ($p<0.001$). In December 1998, *E. norvegica* abundances ranged from ~70 to 142 $m^{-3}$ (mean±standard deviation 1.3±9.9 $m^{-3}$). During December 1999, *E. norvegica* abundances ranged from ~50 to 272 $m^{-3}$ (mean±standard deviation 4.1±17.8 $m^{-3}$), however, most values ranged between ~50 and ~100 $m^{-3}$. Like euphausiids, *E. norvegica* was clustered in few large dense patches during December 1998 (Fig. 5.77).

During December 1999 *E. norvegica* was more scattered in numerous small patches across and at depths in Jordan Basin (Fig. 5.78). Although spatial patterns differed between both dates, it was interesting to observe that the highest abundant patches during both dates were located in deep (200-240 m) waters (Figs. 5.83 and 5.84).

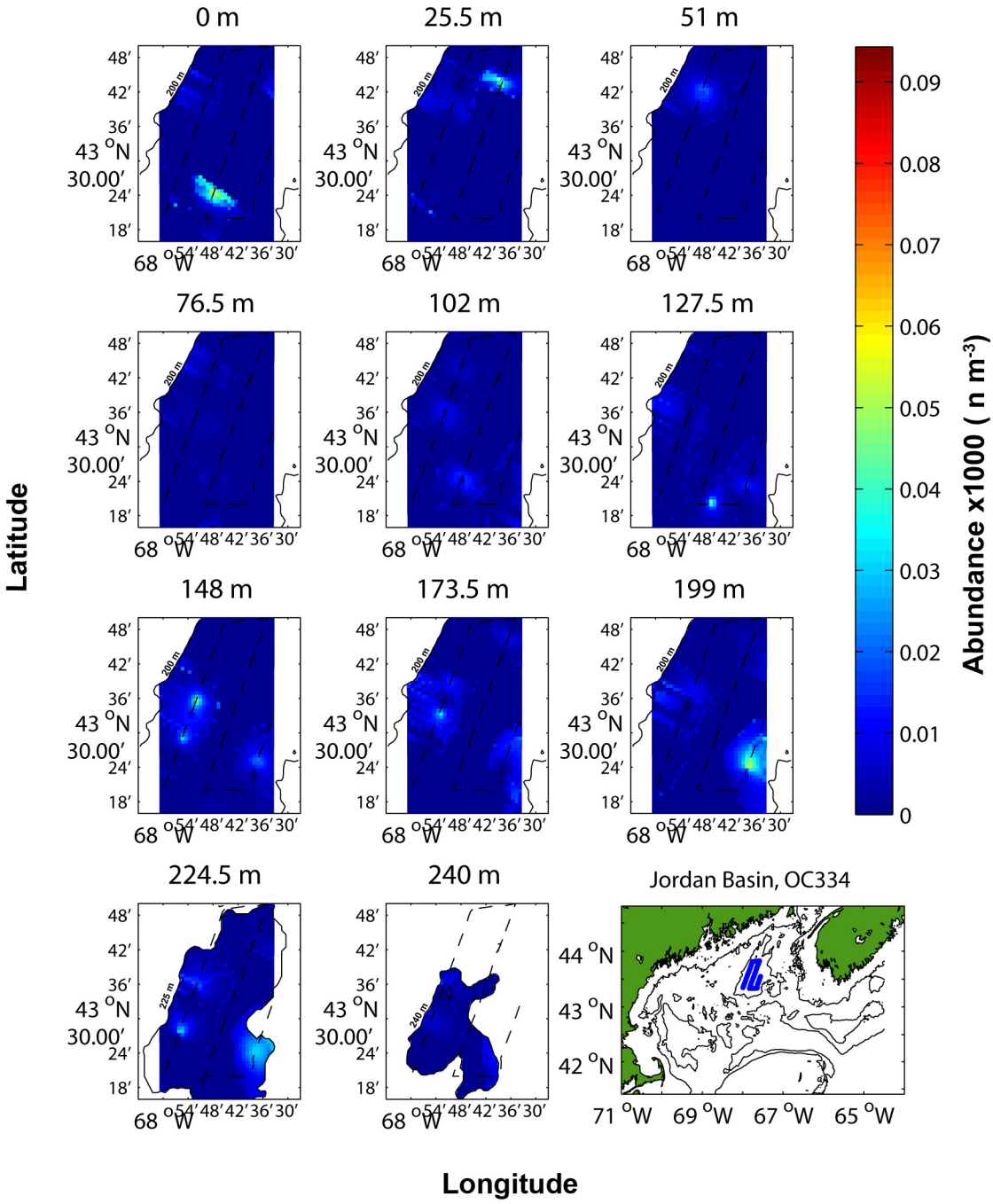


**Figure 5.77.** *Euchaeta norvegica* abundance in Jordan Basin during December 1998 plotted at ~25 m intervals. Isobaths (solid lines) and cruise track (dashed line) were superimposed for reference.

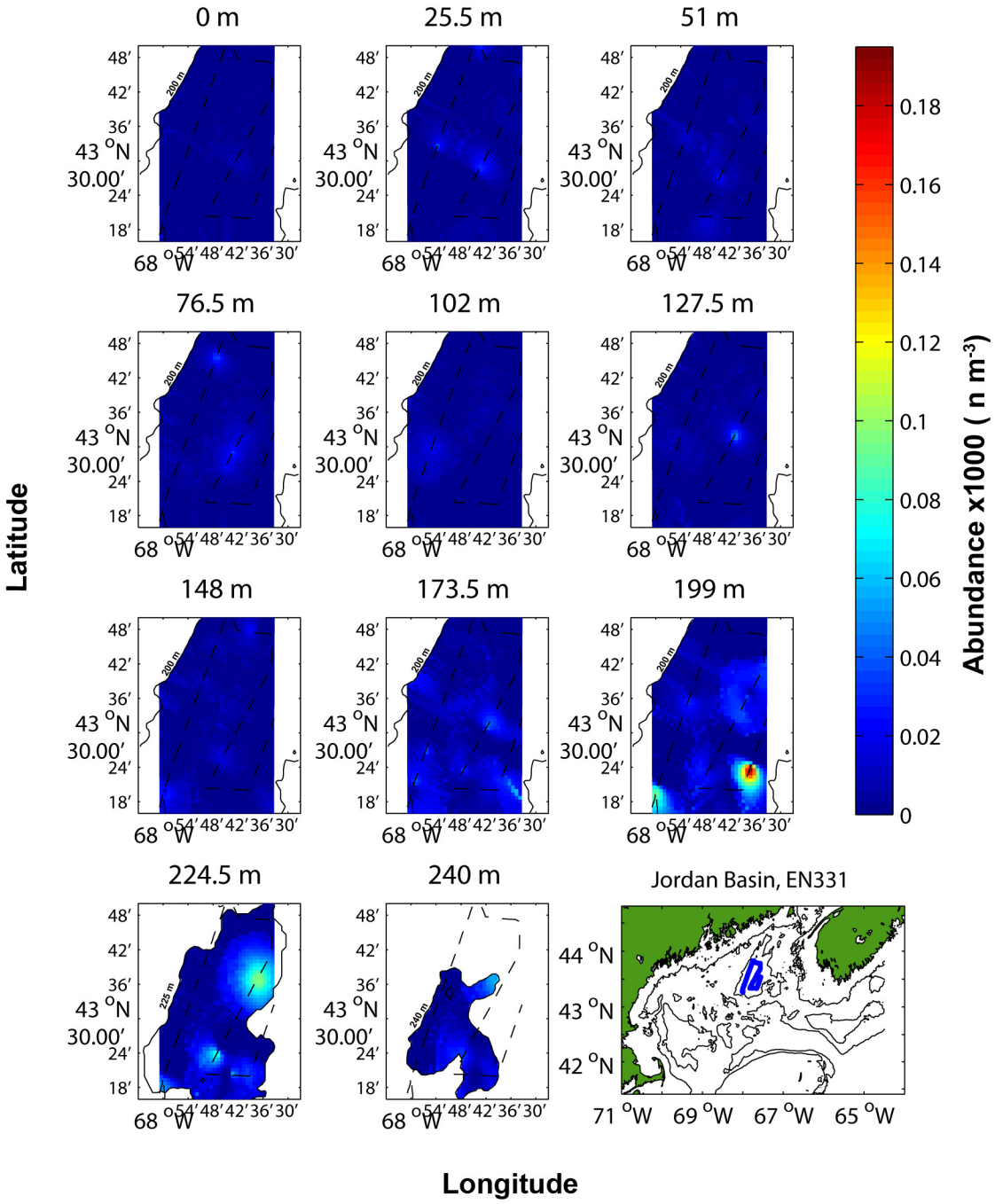


**Figure 5.78.** *Euchaeta norvegica* abundance (n $m^{-3}$) in Jordan Basin during December 1999 plotted at ~25 m intervals. Isobaths (solid lines) and cruise track (dashed line) were superimposed for reference

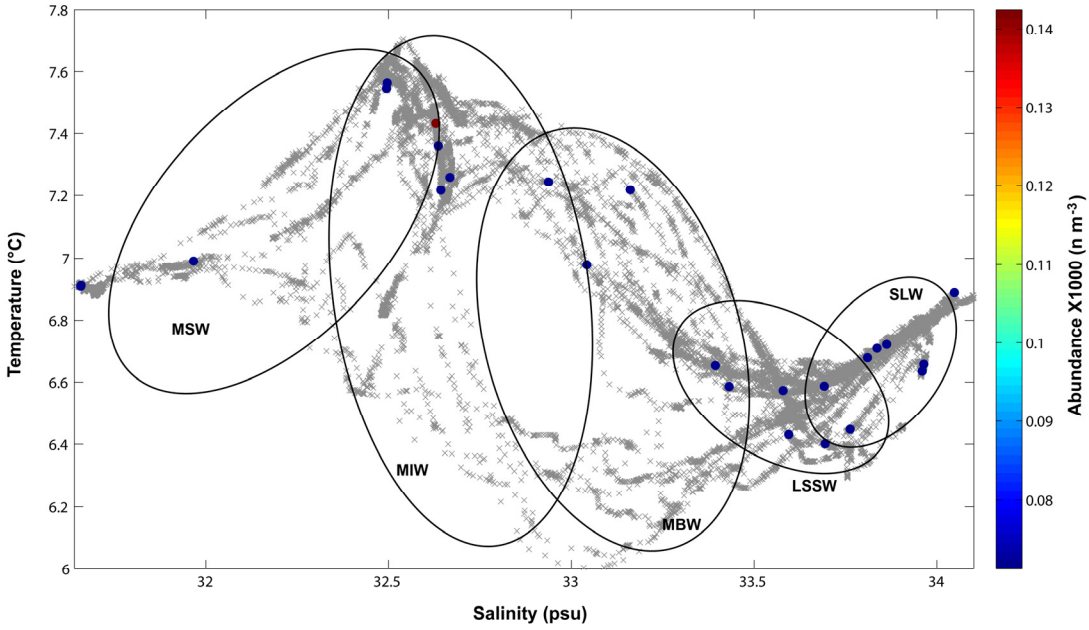


**Figure 5.79.** TSP plot for Jordan Basin during December 1998. *Euchaeta norvegica* abundances are shown in color-coded dots. Temperature-Salinity points are plotted in grey X marks. MSW=Maine Surface Water; MIW=Maine Intermediate Water; MBW= Maine Bottom Water; LSSW=Labrador Subarctic Slope Water; SLW=Slope Water.

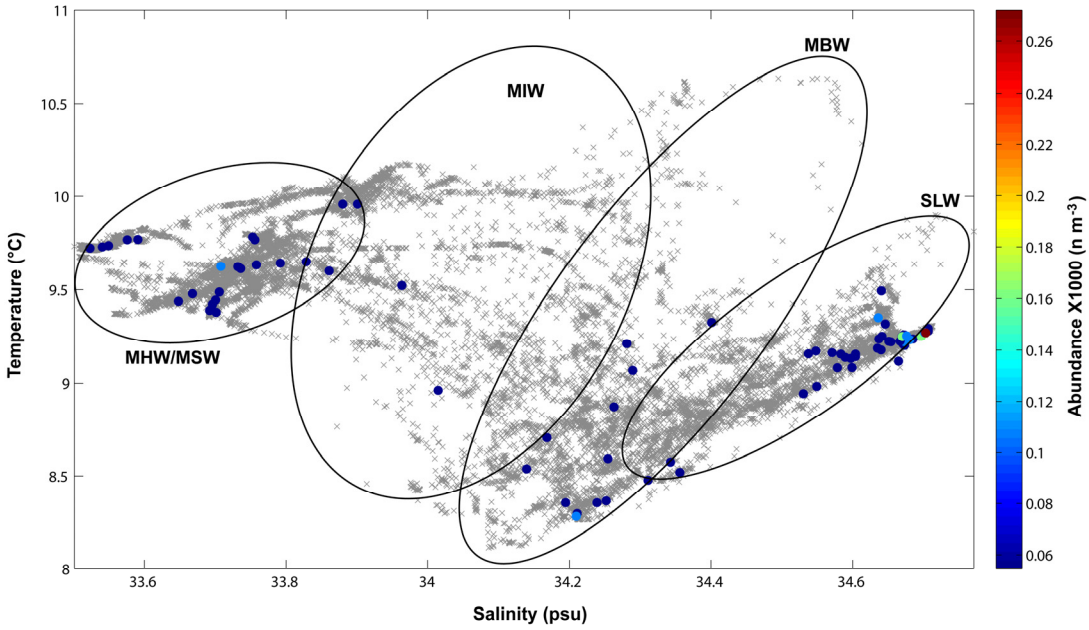


**Figure 5.80.** TSP plot for Jordan Basin during December 1999. *Euchaeta norvegica* abundances are shown in color-coded dots. Temperature-Salinity points are plotted in grey X marks. MHW=Maine Hot Water; MSW=Maine Surface Water; MIW=Maine Intermediate Water; MBW= Maine Bottom Water; SLW=Slope Water.

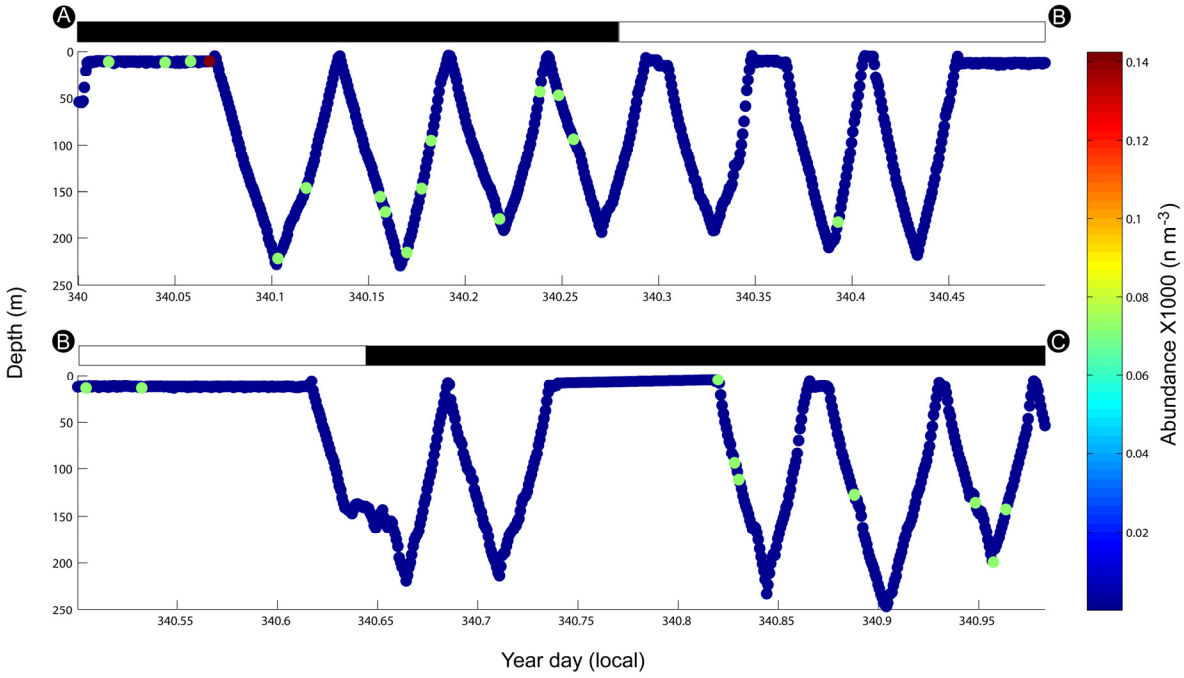


**Figure 5.81.** Diurnal vertical distribution of *Euchaeta norvegica* in Jordan Basin during December 1998 along BIOMAPER-II track. Bars on top of each subplot represent day (white) and night (black) periods. Capital letters at the beginning and end of each panel correspond to the sections of the Jordan Basin, OC334 cruise track in Fig. 2.6.

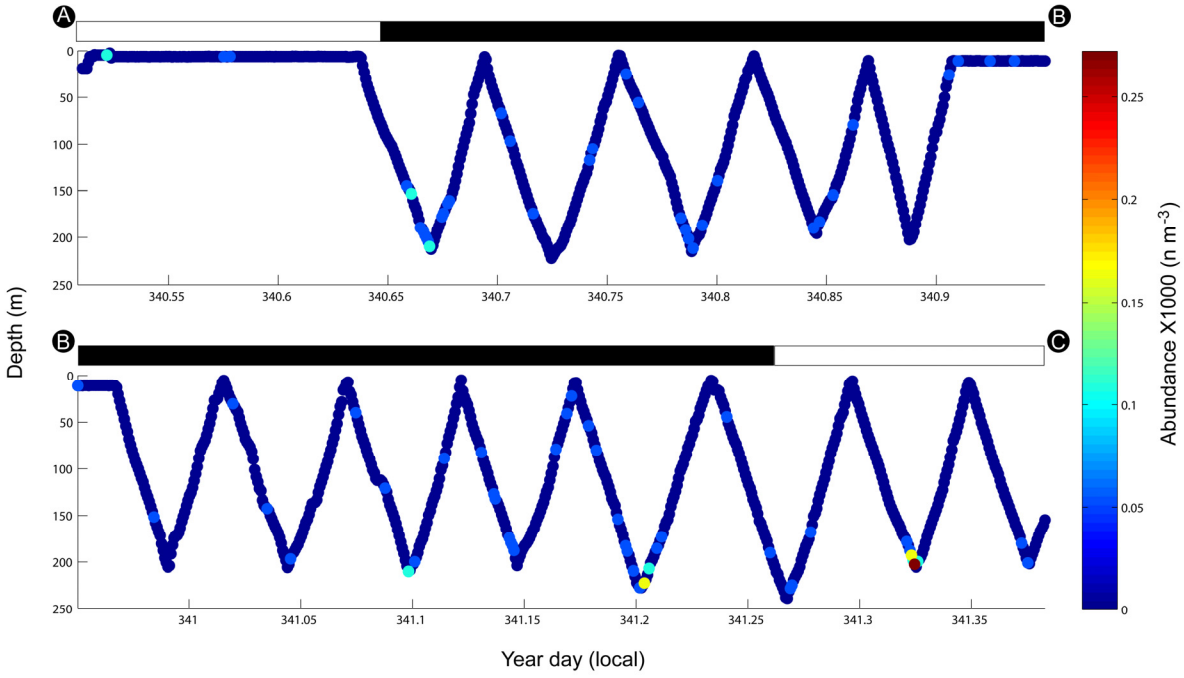


**Figure 5.82.** Diurnal vertical distribution of *Euchaeta norvegica* in Jordan Basin during December 1999 along BIOMAPER-II track. Bars on top of each subplot represent day (white) and night (black) periods. Capital letters at the beginning and end of each panel correspond to the sections of the Jordan Basin, EN331 cruise track in Fig. 2.6.

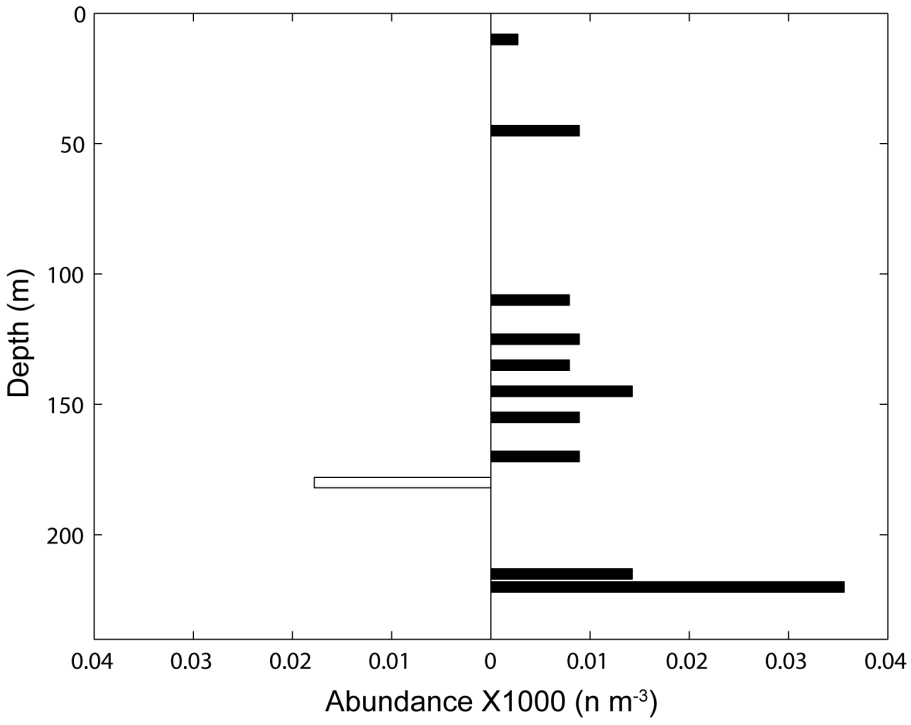


**Figure 5.83.** Vertical distribution of *Euchaeta norvegica* in Jordan Basin during December 1998 during day (open horizontal bars, left) and night (black bars, right) periods.

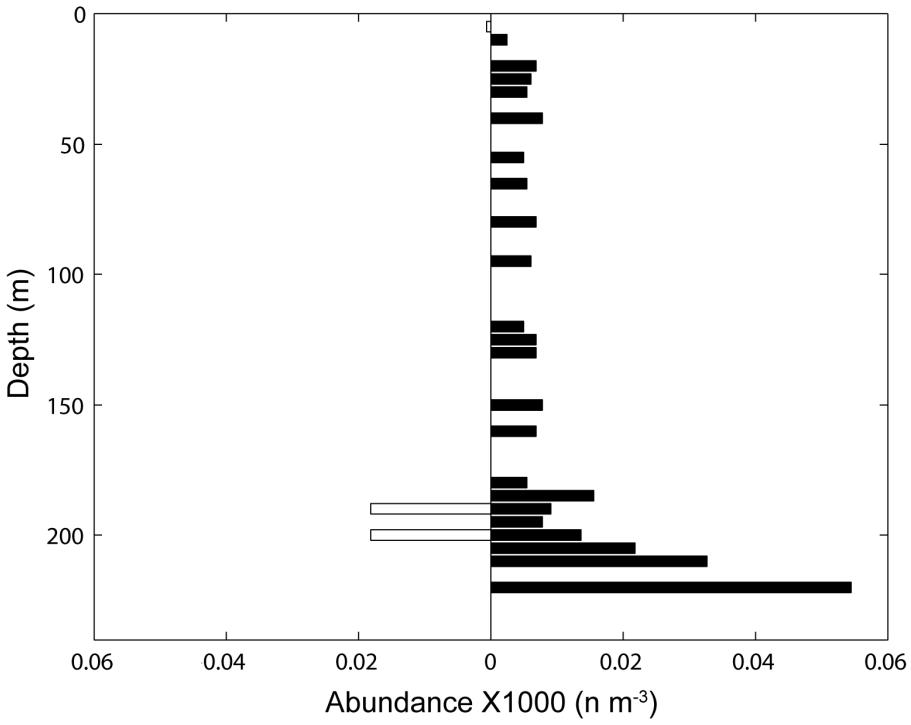


**Figure 5.84.** Vertical distribution of *Euchaeta norvegica* in Jordan Basin during December 1999 during day (open horizontal bars, left) and night (black bars, right) periods.

During December 1998, the densest patches of *E. norvegica* showed a bimodal distribution; dense patches were apparent from 0-25 m at the south and north of Jordan Basin and a single large patch in the southeast corner of the basin from 200-225 m (Fig. 5.77). Small abundances (~21 $m^{-3}$) occurred scattered at different depths in Jordan Basin. During December 1999, two notably large patches were observed in the eastern half of Jordan Basin (Fig. 5.78). The first one was located southeast at 200 m deep, and the second located northeast at 225 m deep. The first patch was smaller in size compared to the second patch, but it accounted for the higher abundances. During December 1999 *Euchaeta norvegica* occurred broadly in small abundances (~40 $m^{-3}$) across Jordan Basin from 175-240 m and in waters shallower than 175 m (Fig. 5.78).

There was not a clear relationship between water masses and abundance features during December 1998 (Fig. 5.79). *Euchaeta norvegica* abundance distributions were more clearly related with water masses during December 1999. Most observations during December 1999 formed clusters in the MHW/MSW complex and in the SLW. However, the highest abundance values were associated with the SLW (Fig. 5.80).

No clear evidence of vertical migration could be detected in *E. norvegica* during December 1998 or December 1999 (Figs. 5.81 and 5.82). *E. norvegica* was found widely dispersed in the water column during night time during both years, while its highest abundances during day time were observed at depths greater than 150 m (Figs. 5.83 and 5.84). Although this may be the result of spatial heterogeneity, this may also indicate some vertical migration activity in *E. norvegica* during December 1998 and December 1999.

**5.3.5.3 Georges Basin/Northeast Channel**

During December 1999, *E. norvegica* abundances in Georges Basin ranged between ~55 and 163 $m^{-3}$. *Euchaeta norvegica* was scattered at the center of Georges Basin between 150 and ~225 m depth. During December 1999 one patch of *E. norvegica* was observed at 250 m depth at the center of Georges Basin (Fig. 5.85). Only one very small patch was observed in

the first 15-20 m. No *E. norvegica* patches were resolved by Kriging neither in the rest of Georges Basin nor in the Northeast Channel.

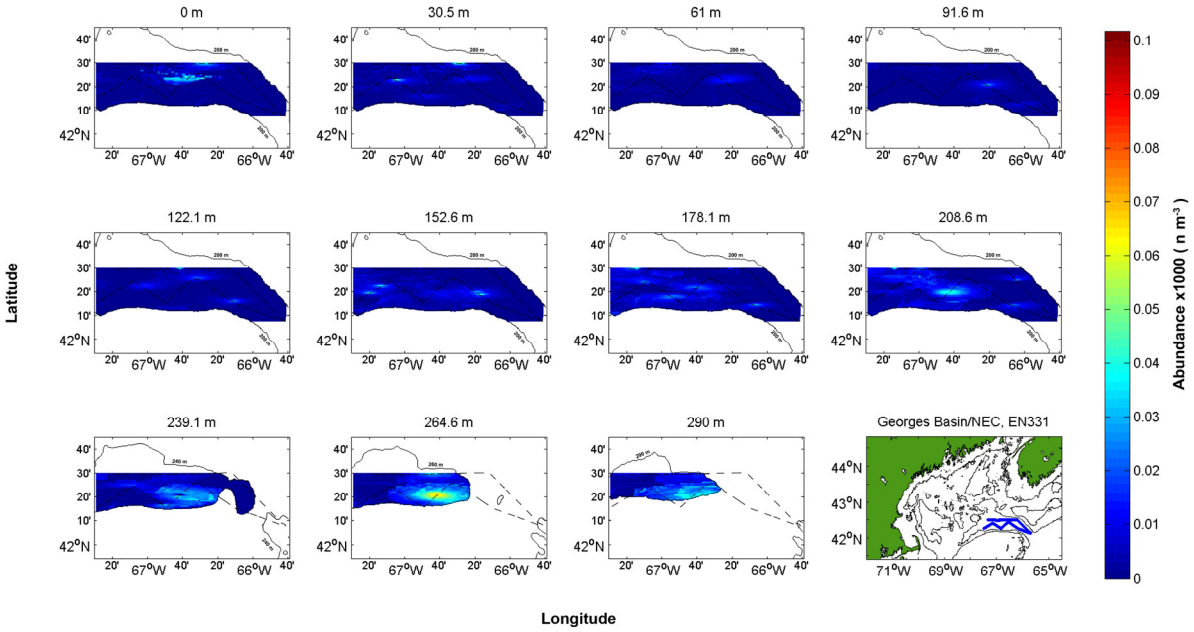


**Figure 5.85.** *Euchaeta norvegica* abundance (n $m^{-3}$) in Georges Basin/NE Channel during December 1999 plotted at ~30 m intervals. Isobaths (solid lines) and cruise track (dashed line) were superimposed for reference.

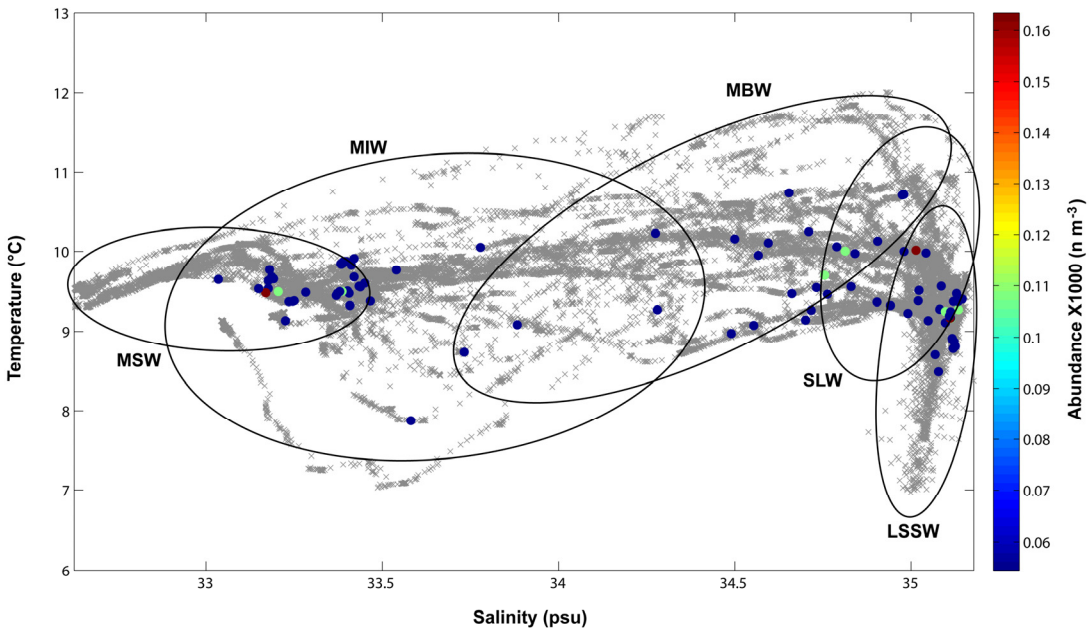


**Figure 5.86.** TSP plot for Georges Basin/NE Channel during December 1999. *Euchaeta norvegica* abundances are shown in color-coded dots. Temperature-Salinity points are plotted in grey X marks. MSW=Maine Surface Water; MIW=Maine Intermediate Water; MBW= Maine Bottom Water; LSSW=Labrador Subarctic Slope Water; SLW=Slope Water.

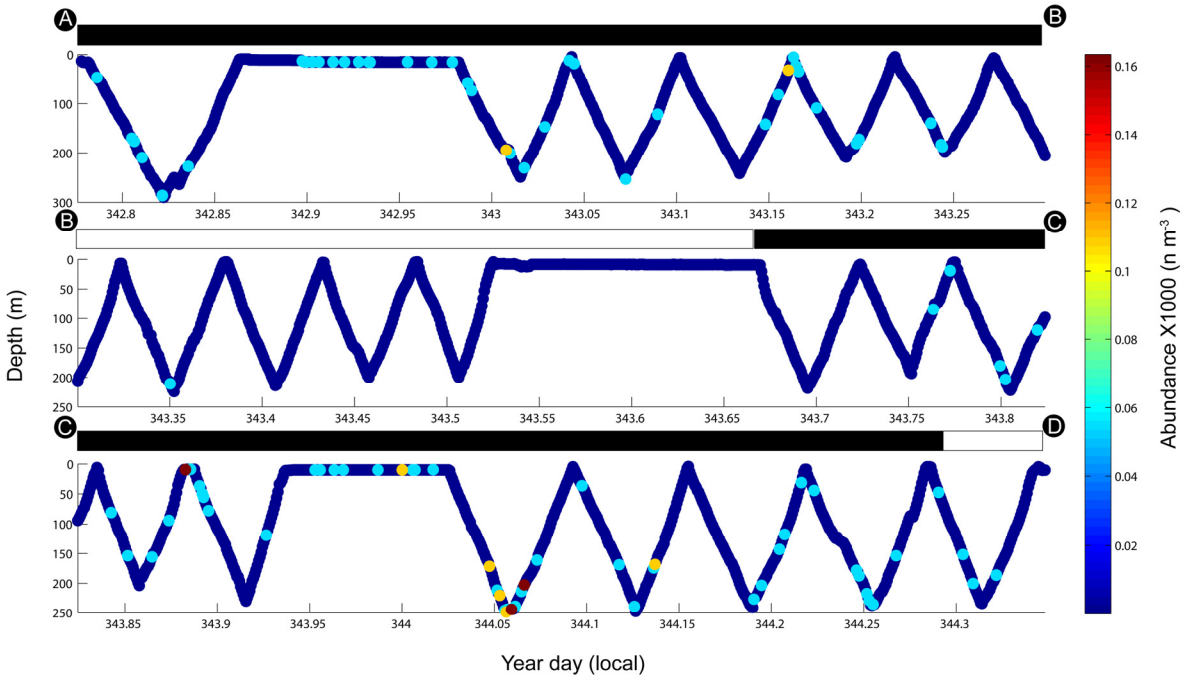


**Figure 5.87.** Diurnal vertical distribution of *Euchaeta norvegica* in Georges Basin/NE Channel during December 1999 along BIOMAPER-II track. Bars on top of each subplot represent day (white) and night (black) periods. Capital letters at the beginning and end of each panel correspond to the sections of the Wilkinson Basin, EN331 cruise track in Fig. 2.6.

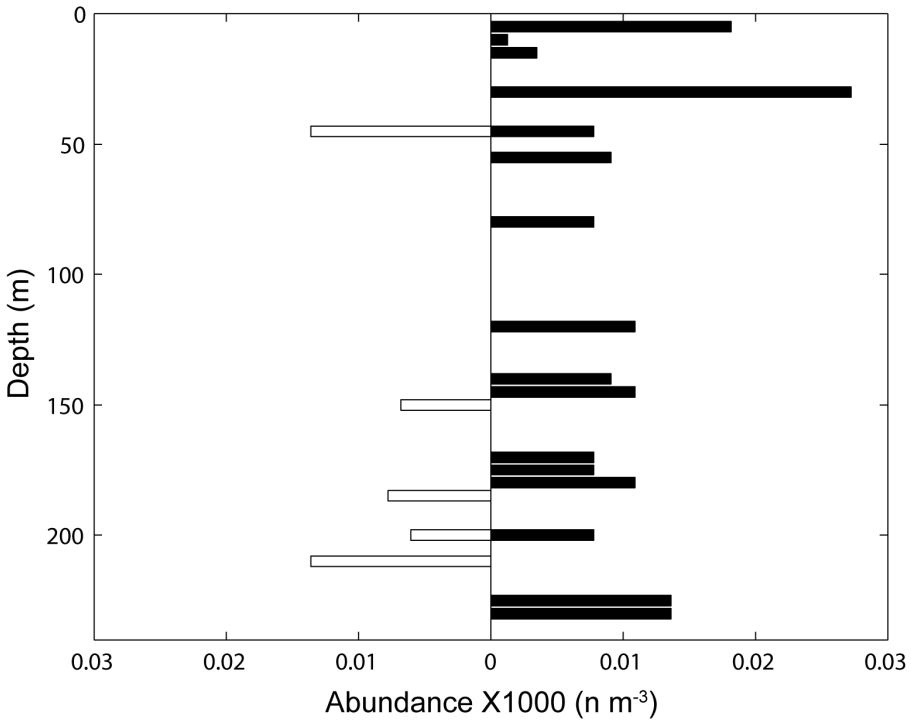


**Figure 5.88.** Vertical distribution of *Euchaeta norvegica* in Georges Basin/NE Channel during December 1999 during day (open horizontal bars, left) and night (black bars, right) periods.

According to the TSP plot for *Euchaeta norvegica*, during December 1999 its greater abundances were mainly related with the SLW, close to its boundary with the LSSW (Fig. 5.86). *Euchaeta norvegica* was sometimes observed in high abundances associated with the MSW. To a lesser extent, *E. norvegica* was associated with the MBW. Very few *E. norvegica* observations were made in the MIW.

Although the diel vertical distribution of *Euchaeta norvegica* could be due to spatial heterogeneity, it is important to mention that during December 1999 most observations were made during night periods (Figs. 5.87 and 5.88). Very few observations were made during day time. However, no other diel pattern was observed for this taxon during the surveyed period.

During December 1998, only 11 *Euchaeta norvegica* individuals were recorded in Georges Basin. Due to the discrete nature of these data, no results could be drawn for this taxon.

### 5.3.6 Chaetognaths

#### 5.3.6.1 Wilkinson Basin

Chaetognaths were more abundant during December 1999 than during December 1998. Chaetognaths were scarce in Wilkinson Basin during December 1998; only eight individuals were observed during that period. During December 1999 chaetognaths were mostly found at shallow depths (0-80 m). The densest patches were found in the upper 50 m depth (Fig. 5.89). Only two dense patches recorded at 0 m and 25 m reached abundances greater than 80 $m^{-3}$ at their core. During December 1999, chaetognaths in Wilkinson Basin were virtually absent in waters deeper than 150 m. During this period, chaetognaths observations were associated with the MSW and were virtually absent in the other three water masses (Fig. 5.90).

Chaetognaths did not appear to migrate vertically during December 1999. Fewer observations were made during day time (Figs. 5.91 and 5.92). However, while during night chaetognaths were found scattered in the water column from 0 to 100 m, denser observations were concentrated between 50 and 100 m during day (Fig. 5.92).

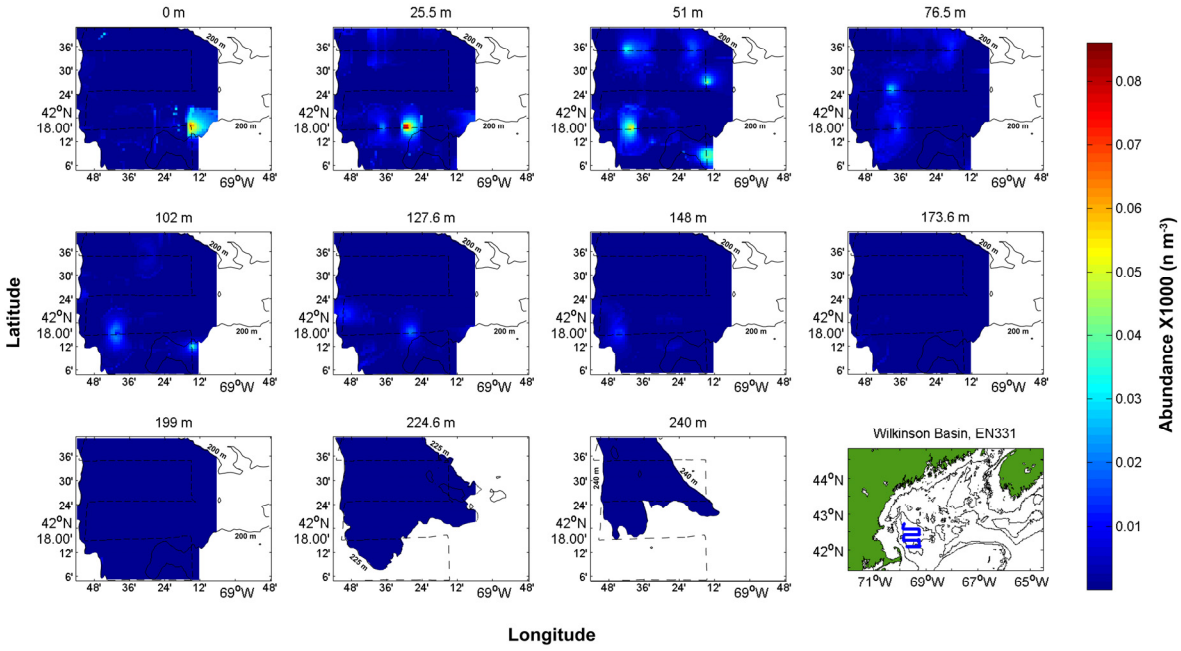


**Figure 5.89.** Chaetognaths abundance in Wilkinson Basin during December 1999 plotted at ~25 m intervals. Isobaths (solid lines) and cruise track (dashed line) were superimposed for reference.

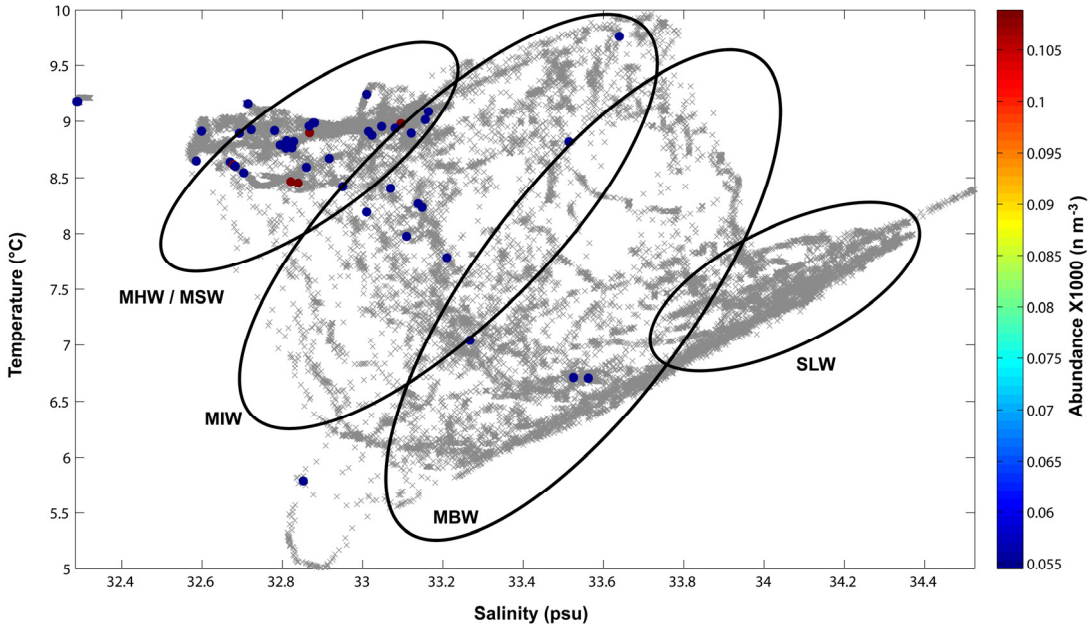


**Figure 5.90.** TSP plot for Wilkinson Basin during December 1999. Chaetognaths abundances are shown in color-coded dots. Temperature-Salinity points are plotted in grey X marks. MHW=Maine Hot Water; MSW=Maine Surface Water; MIW=Maine Intermediate Water; MBW= Maine Bottom Water; SLW=Slope Water.

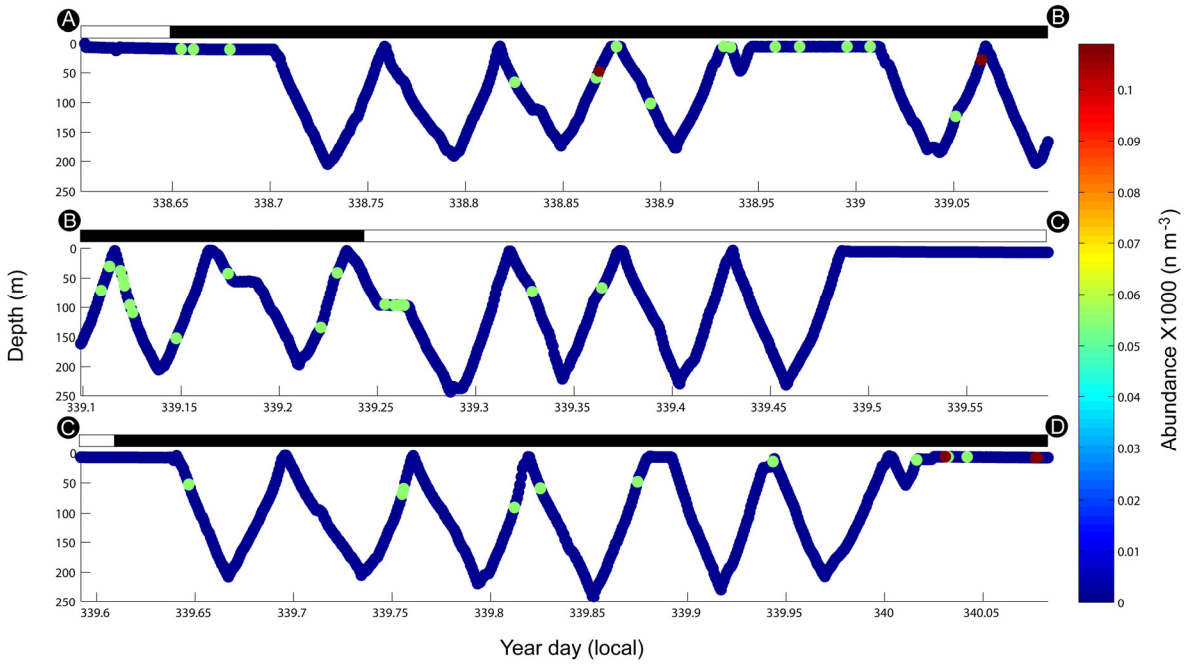


**Figure 5.91.** Diurnal vertical distribution of chaetognaths in Wilkinson Basin during December 1999 along BIOMAPER-II track. Bars on top of each subplot represent day (white) and night (black) periods. Capital letters at the beginning and end of each panel correspond to the sections of the Wilkinson Basin, EN331 cruise track in Fig. 2.6.

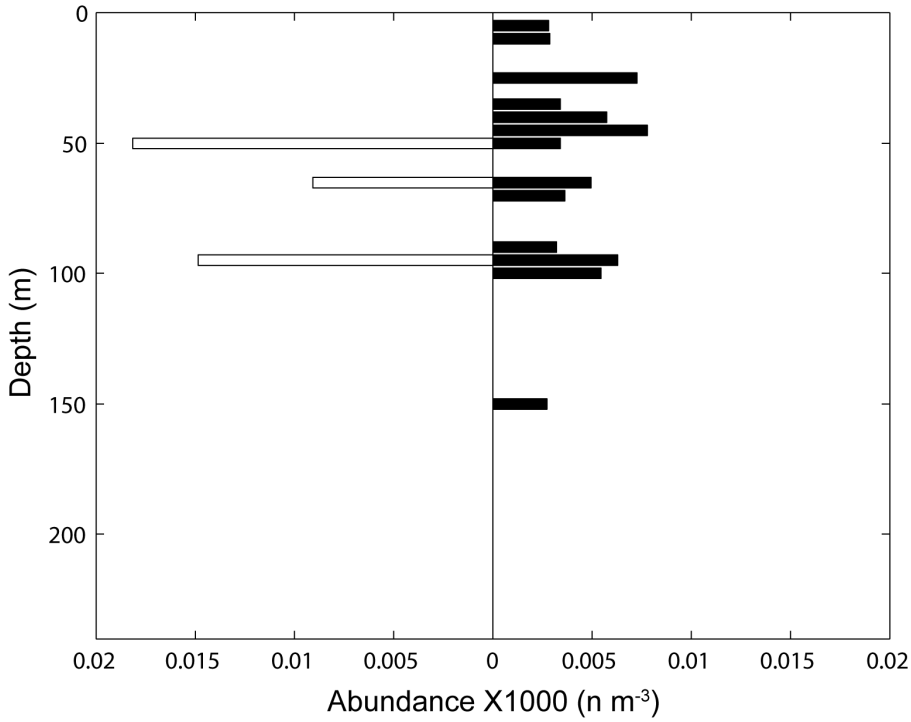


**Figure 5.92.** Vertical distribution of chaetognaths in Wilkinson Basin during December 1999 during day (open horizontal bars, left) and night (black bars, right) periods.

#### 5.3.6.2 Jordan Basin

Chaetognaths were clearly more abundant in December 1999 than during December 1998. Only three individual chaetognaths were recorded by the VPR during December 1998. During December 1999, chaetognaths abundances ranged from 54 to 163 $m^{-3}$ (mean±standard deviation 2.3±13.2 $m^{-3}$). However, most of the observations ranged between 54 and 108 $m^{-3}$.

Chaetognath patches during December 1999 were scattered in the upper 100 m in Jordan Basin (Fig. 5.93). Chaetognaths were practically absent from Jordan Basin in waters deeper than 100 m.

During December 1999, chaetognaths were clearly associated to the MHW/MSW complex (Fig.5.94). Although some high values were observed associated to the MIW, those observations were very close to the boundary of this with the MSW.

No evidence of vertical migration by chaetognaths was observed during December 1999 (Figs. 5.95 and 5.96). And vertical migration for December 1998 could not be evaluated due to insufficient data.

#### 5.3.6.3 Georges Basin/Northeast Channel

During December 1999, chaetognaths showed abundances between 55 and 218 $m^{-3}$ (mean±standard deviation 7.6±23.5 $m^{-3}$). Most of the chaetognath patches were observed in the first 125 m depth, with very few occurrences in deeper waters. Indeed, chaetognaths were virtually absent in George Basin in waters deeper than 125 m. The largest aggregation of chaetognaths was observed in the center of Georges Basin, although some high-abundance chaetognath patches were also observed in the Northeast Channel (Fig. 5.97). Indeed the only high-abundance patches found below 150 m depth were located in the Northeast Channel, close to the boundary of this region and Georges Basin (Fig. 5.97).

According to the TSP plot for chaetognaths, during December 1999 their distribution seemed to be related to specific water masses. During December 1999 chaetognaths higher abundances were associated with the MSW, and to the boundary of this and the MIW (Fig.

5.98). The other high abundance observations made were actually associated to the LSSW which dominated the deep waters of the Northeast Channel during December 1999 (see Chapter III).

No diel vertical activity was observed for chaetognaths during December 1998. High chaetognath abundances were recorded at surface during day and night periods (Figs. 5.99 and 5.100). Also, similar abundance levels were found in waters below 150 m (Fig. 5.100), which corresponded to observations made in the Northeast Channel.

Chaetognaths were scarce during December 1998 in Georges Basin when only 9 individuals were counted and therefore no results could be drawn.

## 5.4 Discussion

### 5.4.1 Inter-Annual Variability

Inter-annual variations in gelatinous predators (siphonophores, ctenophores and medusae) abundance during December 1998 and December 1999 were observed in all deep basins. The same pattern was also consistent in all three basins: gelatinous plankton were generally more abundant in all basins during December 1998 than during December 1999 (Table 5.1; $p<0.05$). Only a few ctenophores were imaged by the VPR in all three basins during December 1999, making it difficult to estimate their abundances.

On the other hand, non-gelatinous predators (*Euchaeta norvegica*, euphausiids and chaetognaths) were all slightly less abundant during December 1998 than during December 1999, in all three deep basins. Few chaetognaths were imaged during December 1998. However, the larger number of imaged chaetognaths (hence their higher abundances) during December 1999 suggests that even though I was not able to estimate their abundance pattern, chaetognath numbers during December 1998 were extremely low.

However, the low number of imaged ctenophores suggests that they were scarce in the Gulf during December 1999. The same was true for medusae. Possible causes for underestimation are discussed below in section 5.4.5.

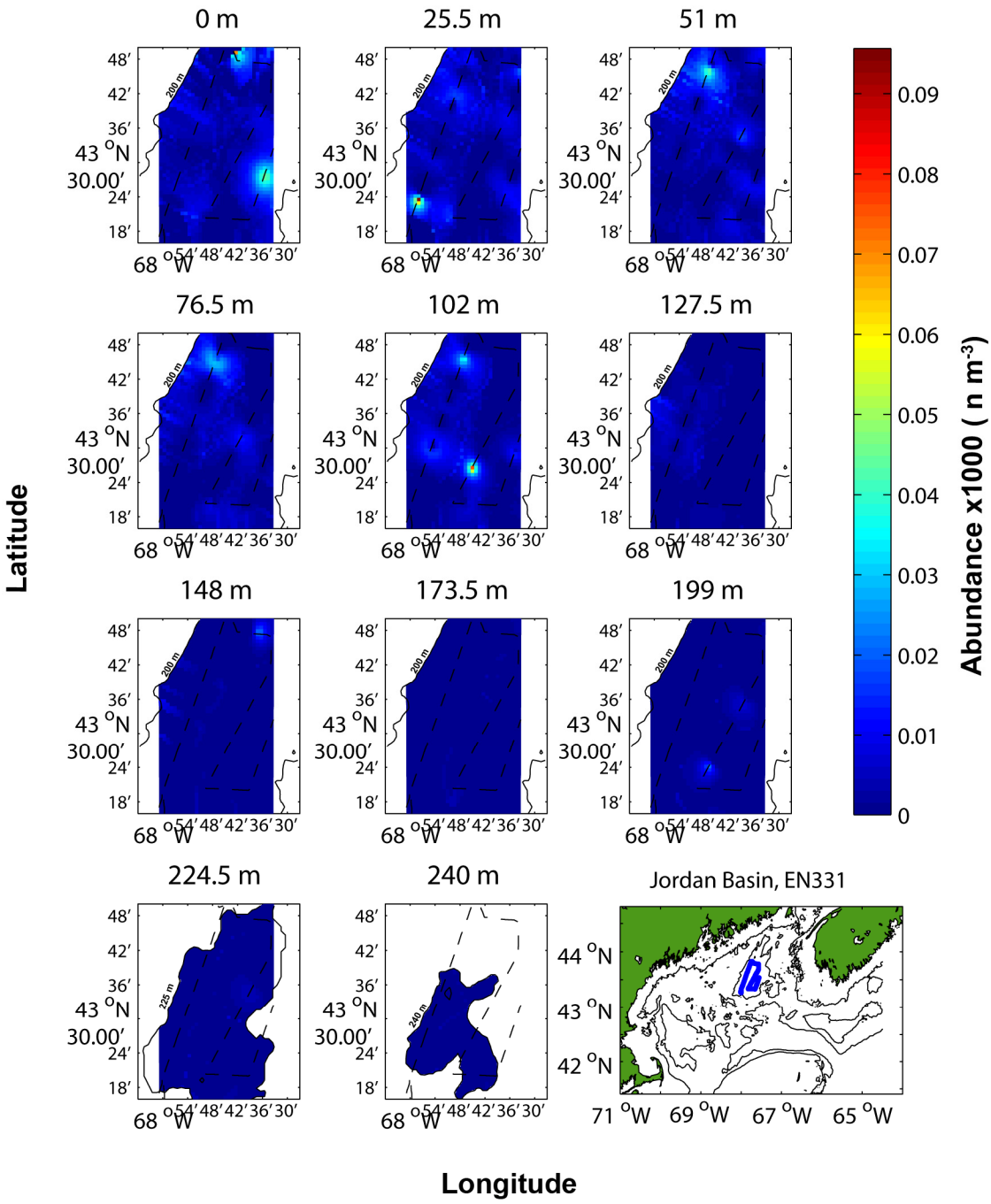


**Figure 5.93.** Chaetognath abundance (n $m^{-3}$) in Jordan Basin during December 1999 plotted at ~25 m intervals. Isobaths (solid lines) and cruise track (dashed line) were superimposed for reference.

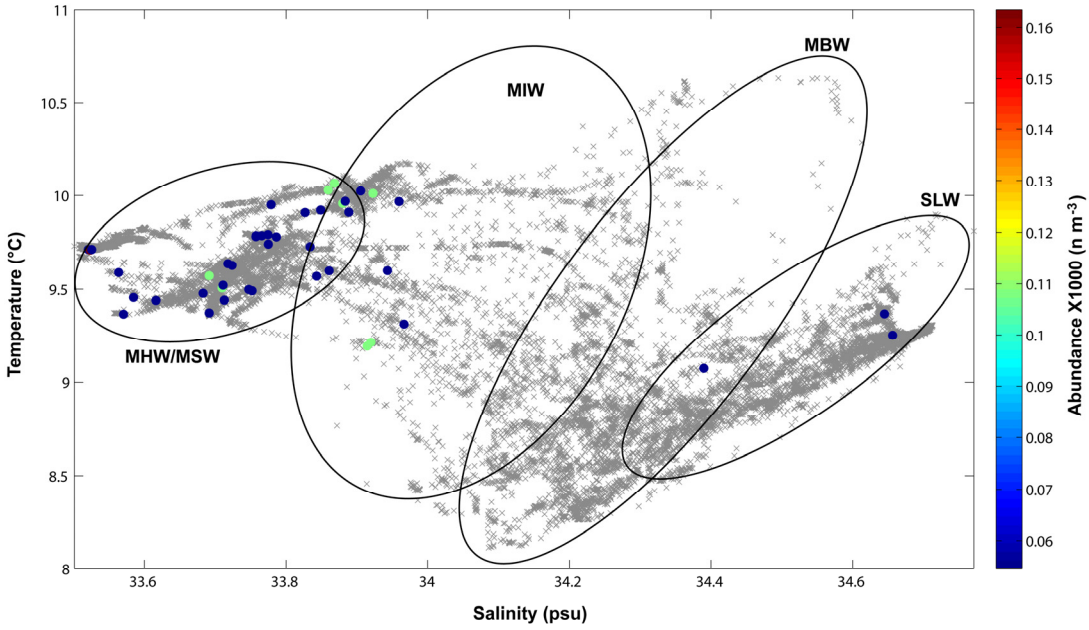


**Figure 5.94.** TSP plot for Jordan Basin during December 1999. Chaetognath abundances are shown in color-coded dots. Temperature-Salinity points are plotted in grey X marks. MHW=Maine Hot Water; MSW=Maine Surface Water; MIW=Maine Intermediate Water; MBW= Maine Bottom Water; SLW=Slope Water.

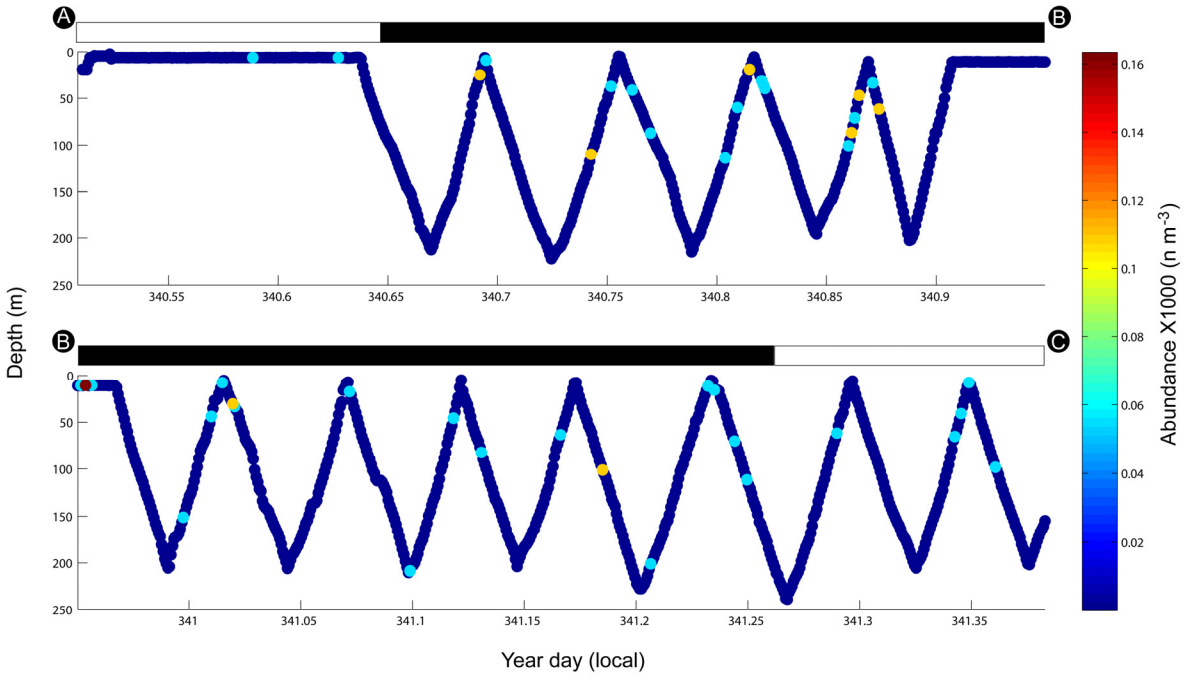


**Figure 5.95.** Diurnal vertical distribution of chaetognaths in Jordan Basin during December 1999 along BIOMAPER-II track. Bars on top of each subplot represent day (white) and night (black) periods. Capital letters at the beginning and end of each panel correspond to the sections of the Jordan Basin 1999 (EN331) cruise track in Fig. 2.6.

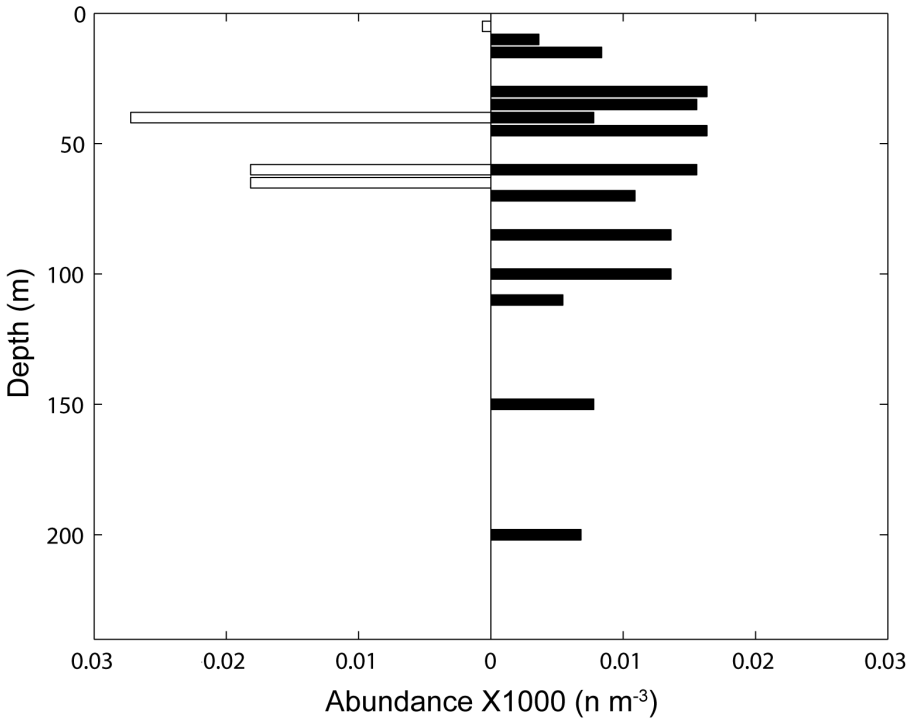


**Figure 5.96.** Vertical distribution of chaetognaths in Jordan Basin during December 1999 during day (open horizontal bars, left) and night (black bars, right) periods.

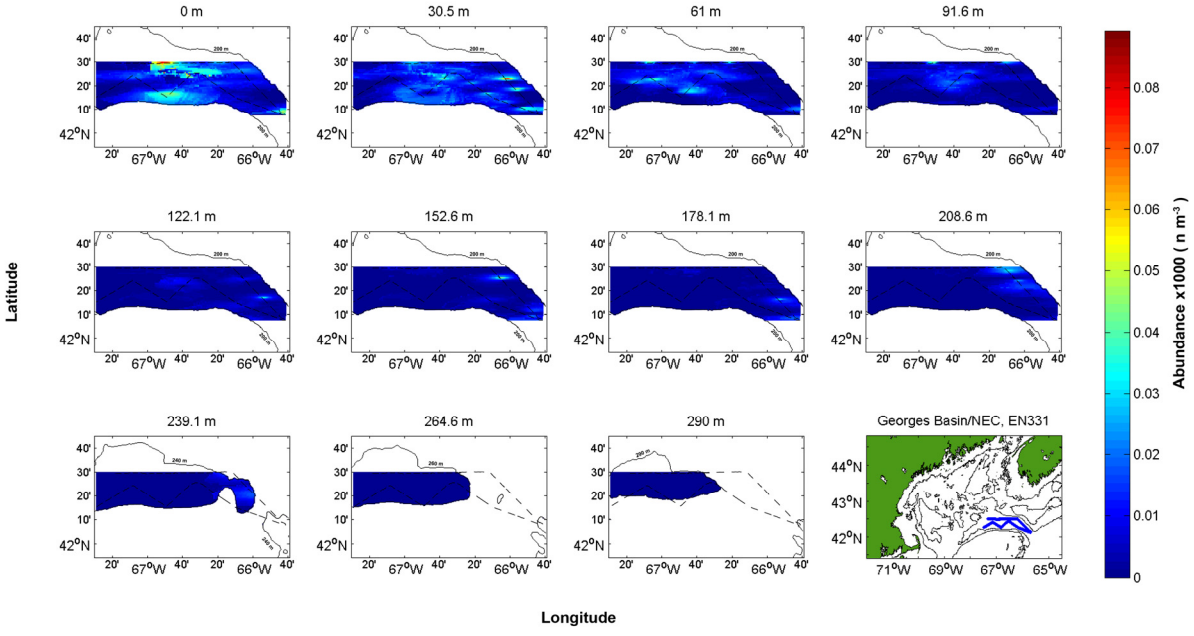


**Figure 5.97.** Chaetognaths abundance (n $m^{-3}$) in Georges Basin/NE Channel during December 1999 plotted at ~30 m intervals. Isobaths (solid lines) and cruise track (dashed line) were superimposed for reference.

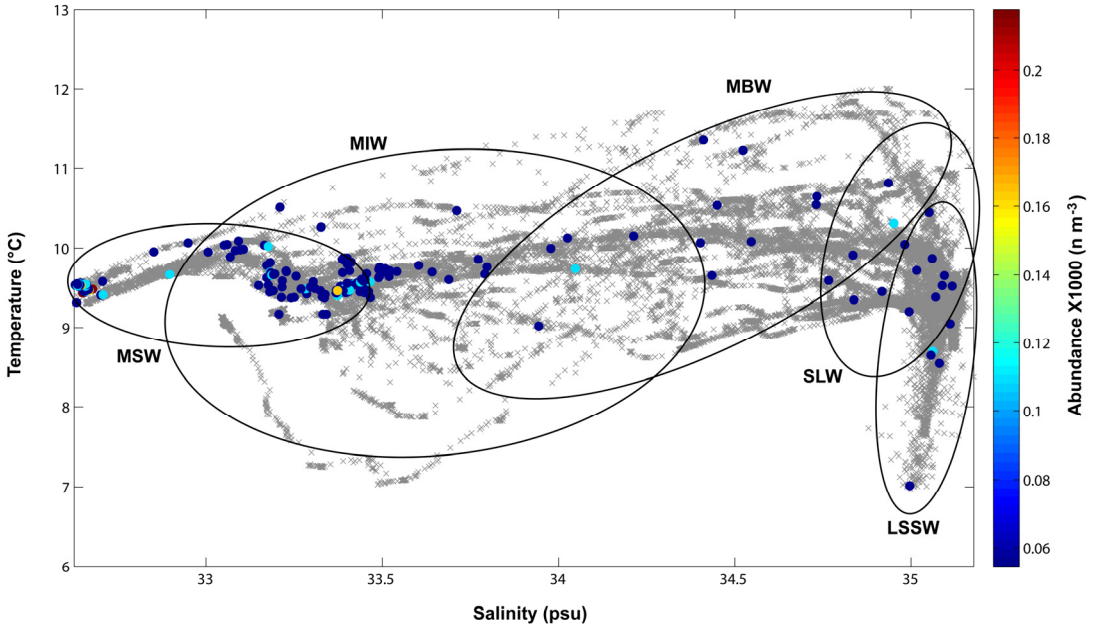


**Figure 5.98.** TSP plot for Georges Basin/NE Channel during December 1999. Chaetognath abundances are shown in color-coded dots. Temperature-Salinity points are plotted in grey X marks. MSW=Maine Surface Water; MIW=Maine Intermediate Water; MBW= Maine Bottom Water; LSSW=Labrador Subarctic Slope Water; SLW=Slope Water.

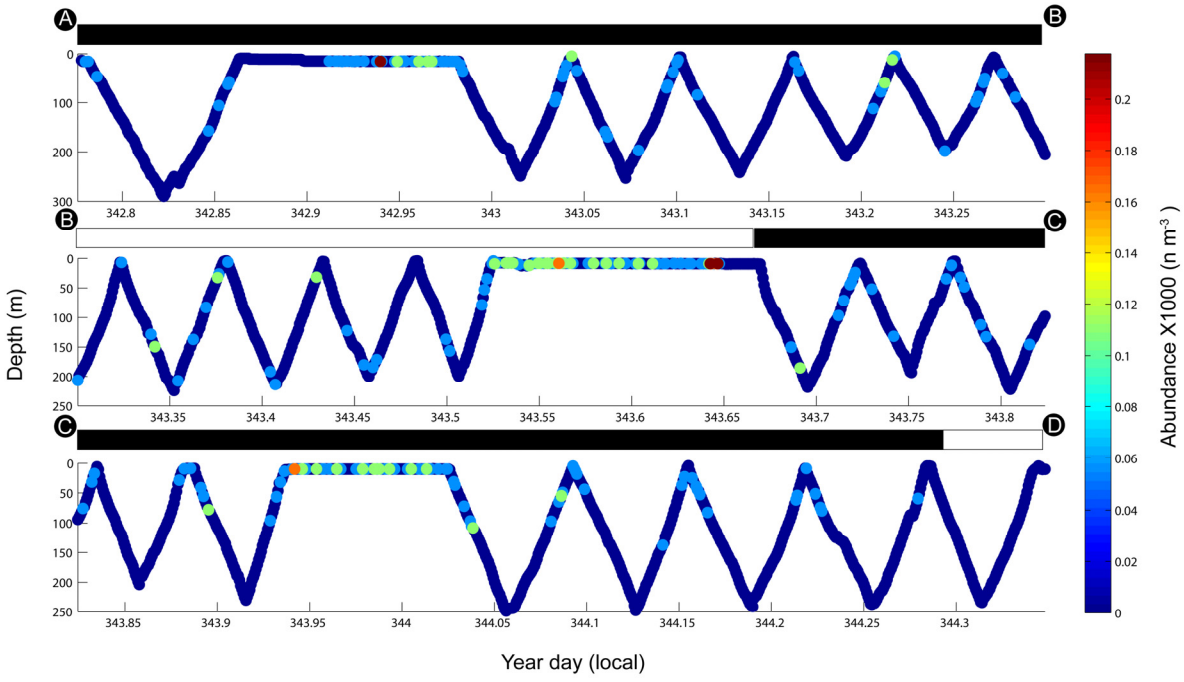


**Figure 5.99.** Diurnal vertical distribution of chaetognaths in Georges Basin/NE Channel during December 1999 along BIOMAPER-II track. Bars on top of each subplot represent day (white) and night (black) periods. Capital letters at the beginning and end of each panel correspond to the sections of the Wilkinson Basin, EN331 cruise track in Fig. 2.6.

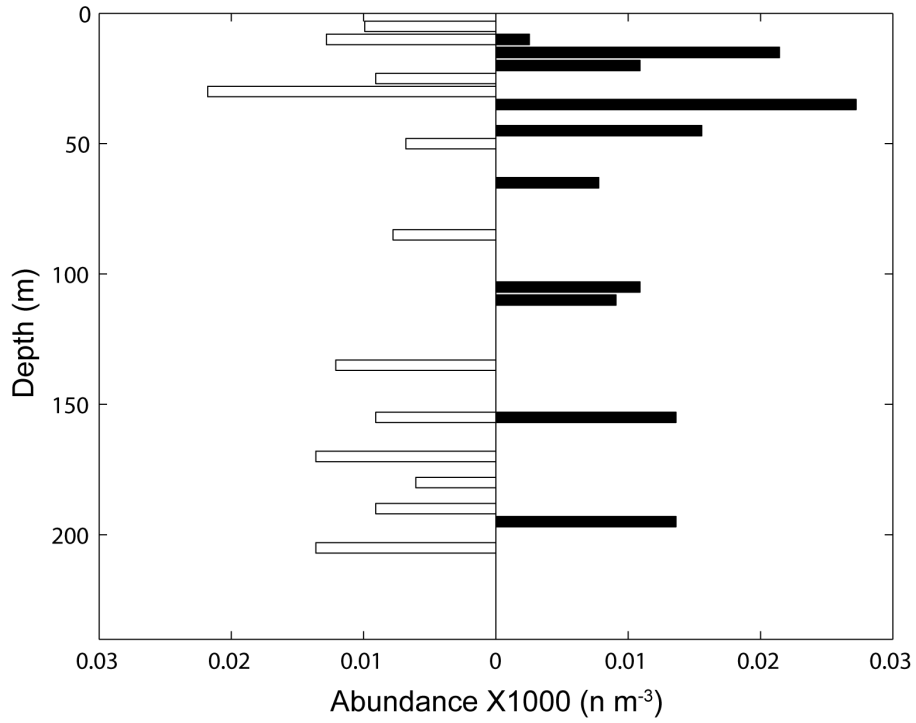


**Figure 5.100.** Vertical distribution of chaetognaths in Georges Basin/NE Channel during December 1999 during day (open horizontal bars, left) and night (black bars, right) periods.

Some authors have commented on the possibility of increasing jellyfish blooms as response to regime shifts in other regions of the world (i.e. Brodeur et. al., 1999, Graham, 2001). How regime shifts affect the inter-annual variances on gelatinous plankton in the Gulf of Maine has not been studied. However, it was clear that during December 1998, when the NAO was in its negative phase, high abundances of siphonophores, medusae, and ctenophores were observed in the deep basins of the Gulf of Maine. Whether these gelatinous plankton were carried into the Gulf of Maine within the LSSW was not clear. High abundances of siphonophores, medusae and ctenophores didn't show an exclusive relationship with the LSSW during December 1998. Indeed, high abundances of gelatinous plankton were observed in the other identified water masses, especially those with warmer temperatures. Further, gelatinous plankton are known to thrive in oligothrophic regions (Mills, 1995). Although not oligothrophic, the LSSW-dominated Gulf of Maine probably was nutrient-poor and conditions were suitable for gelatinous plankton to grow. Numerous siphonulae (siphonophore larvae) were observed during

December 1998 (data not presented), supporting the idea of reproduction of this selective carnivore in the Gulf of Maine during December 1998.

Blooms of *Nanomia cara* have been recorded in the Gulf of Maine in the autumn of 1975-summer of 1976, and early falls of 1992 and 1993 (Rogers et al., 1978; Mills, 1995). An apparent bloom of siphonophores was recorded during the studied period of December 1998. Coincidently, the NAO index during the 1975-1976 and 1992-1993 *N. cara* blooms was weakly positive or weakly negative. As discussed in previous chapters, during 1998 the NAO index was strongly negative. However, in order to test the validity of the above mentioned patterns, a long-term time series for gelatinous plankton remains to be analyzed with respect to atmospherically-driven phenomena, in the same manner it was done for *Calanus finmarchicus* and the NAO index (Greene and Pershing, 2000).

### 5.4.2 Regional and Inter-Basin Distributions

Predators as a whole were more abundant in the northeastern areas of Wilkinson, Jordan and Georges basins during 1998. However, during December 1999 predators showed a more scattered pattern both vertically and especially in all three basins. This pattern could have been affected by the local gyres in the basins. The possibility of vertical migration of some predators could have exposed them to different current velocities therefore affecting their spatial distribution in the basins, causing the differences observed during December 1998 and 1999.

### 5.4.3 Diel Vertical Migration

Diel vertical migration was potentially exhibited by siphonophores during both years. Both Rogers (1978) and Miller (1995) mention that during day time, *N. cara* was invariably below 150 m. Both authors observed *N. cara* vertically migrating towards the surface at night. The pattern observed during December 1998 and 1999 in siphonophores agrees with the previously reported vertical behavior. This pattern though was more apparent in Wilkinson Basin than in the Jordan Basin and Georges Basin/NE Channel.

Vertical diel activity for the other five predators was less apparent. For medusae and cetnophores there was a possibility, but the patterns were not clear. One reason could be that more than one species of ctenophores and medusae were included in each group. If different species show different vertical migration behavior, then the vertical distribution plots may mask the patterns exhibited by individual taxa. This seemed likely for medusae and ctenophores during December 1998 and 1999.

### 5.4.4 Possible Predator Interactions

Siphonophores are known to feed *on Meganyctiphanes norvegica* in the Gulf of Maine (Rossi et al., 2008). The physonect siphonophore *Nanomia cara* is thought to have significant effects on both, competitors and prey when it reaches densities 10-100 colonies $m^{-3}$ (Rossi et al., 2008). Interestingly, siphonophores were more abundant during December 1998, when euphausiids had the lowest abundances. The opposite occurred during December 1999: siphonophores showed low abundances, and euphausiids appeared in larger abundances than the same period in the previous year. It is worth mentioning that euphausiids were more clustered during December 1998 when gelatinous plankton was more abundant. During December 1999, when gelatinous plankton was found in lower numbers, euphausiids were more scattered in the water column. Whether this pattern was the result of predation of euphausiids by siphonophores is not known, but there exists the possibility since siphonophores actively prey on euphausiids (Rossi et al., 2008).

High abundances of euphausiids and the highest abundances of siphonophores were found in the same waters masses during December 1999. This could be an indication of the possible interaction between siphonophores and euphausiids in the deep basins of the Gulf during December 1999. This clustering pattern of siphonophores and euphausiids was less clear during December 1998. Only in one instance, during December 1998, did the clusters of euphausiids and siphonophores co-occur in the same water mass. Therefore, their closest possible interaction during that period was found in the MSW/MIW boundary in Jordan Basin.

Complex interactions can occur between predators. Some medusae species can actually prey on ctenophores, while ctenophores on its part are capable of preying on small siphonophores (Mills, 1995). As will be discussed in the next section, this could explain why dense patches of predators did usually not overlap spatially, although they can be found in similar water masses as was observed in this section.

### 5.4.5 Possible Estimation Errors

The low abundances of chaetognaths observed during December 1998 in all three deep basins of the Gulf could be an underestimation due to the small sampling volume of the VPR. Previous studies have shown that the VPR failed to estimate with certainty abundances for chaetognaths and rare taxa (Benfield et al., 1996). Benfield and colleagues estimated a 95% probability of non-detection by the VPR when chaetognaths abundances were below 1 $m^{-3}$. There was a difference in the volume imaged per frame by the VPR during cruises OC334 (December 1998) and EN331 (December 1999), however the difference was likely too small (1.19 ml) to cause disparities in the abundance estimation for chaetognaths. More likely, it was rather the low abundance of the organism that caused the non-detection by the VPR during December 1998.

Euphausiids and medusae were potentially larger than the field of view of the VPR. Some underestimation of euphausiids and medusae abundances could have occurred for two reasons: 1) they were not detected by the VPR due to the euphausiids avoidance behavior or abundances below detection thresholds; and 2) the subjective method I used to calculate the visible portions of these organisms in the cropped ROIs (refer to chapter II: General Methods). One more possible underestimation error could have occurred during image extraction in the RTVPR. The image processing routines did not always select the entire organisms when creating the ROI and often generated a subsection based when part of the organism contained particularly bright features. Gelatinous plankton were usually better identified when manually searching for unidentified ROIs. When I suspected that a particular ROI was part of a larger

organism, I back calculated the time and frame from the file name and searched for that particular ROI in the raw video material. Much of gelatinous plankton was identified in this way using manual/visual post-extraction processing.

Some errors could have originated during Kriging. Kriging is an interpolation technique, and in most cases it produced an under estimation of abundances. Kriged distributions for euphausiids resulted in some underestimation for December 1999, due to smoothing. In other instances lower abundances of euphausiids were predicted by Kriging in 1999, when they actually were more abundant than in December 1998. However, the raw abundance data showed higher maximum abundances of euphausiids in December 1999 than on December 1998. Despite these artifacts, Kriging was very useful in studying the spatial variation of abundance.

**5.5 References**


Beardsley, R. C., A. W. Epstein, C. Chen, K. F. Wishner, M. C. Macaulay, and R. D. Kenney. 1996. Spatial variability in zooplankton abundance near feeding right whales in the Great South Channel. Deep Sea Research Part II: Topical Studies in Oceanography **43**: 1601-1625.

Benfield, M. C., C. S. Davis, P. H. Wiebe, S. M. Gallager, R. G. Lough, and N. J. Copley. 1996. Video Plankton Recorder estimates of copepod, pteropod and larvacean distributions from a stratified region of Georges Bank with comparative measurements from a MOCNESS sampler. Deep-Sea Research II: Topical Studies in Oceanography **43**: 1925-1945.

Brodeur, R. D., C. E. Mills, J. E. Overland, G. E. Walters, and J. D. Schumacher. 1999. Evidence for a substantial increase in gelatinous zooplankton in the Bering Sea, with possible links to climate change. Fisheries Oceanography **8:** 296-306.

Dalsgaard, J., M. St. John, G. Kattner, D. Müller–Navarra and W. Hagen. 2003. Fatty acid trophic markers in the pelagic marine environment: a review. Advances in Marine Biology **46**: 225-340.

Durbin, E. G., S. L. Gilman, R. G. Campbell, and Ann G. Durbin. 1995. Abundance, biomass, vertical migration and estimated development rate of the copepod *Calanus finmarchicus* in the southern Gulf of Maine during late spring. Continental Shelf Research **15**: 571-591.

Gislason, A., K. Eiane, and P. Reynisson. 2007. Vertical distribution and mortality of *Calanus finmarchicus* during overwintering in oceanic waters southwest of Iceland. Marine Biology **150**: 1253-1263.

Graham, W. M. 2001. Numerical increases and distributional shifts of *Chrysaora quinquecirrha* (Desor) and *Aurelia aurita* (Linné) (Cnidaria: Scyphozoa) in the northern Gulf of Mexico. Hydrobiologia **451**: 97-111.

Greene, C. H. and A. J. Pershing. 2000. The response of *Calanus finmarchicus* populations to climate variability in the Northeast Atlantic: basin-scale forcing associated with the North Atlantic Oscillation. ICES Journal of Marine Science **57**: 1536-1544.

Greene, C. H. and A. J. Pershing. 2004. Climate and the conservation biology of North Atlantic right whales: the right whale at the wrong time? Frontiers in Ecology and the Environment **2**: 29-34.

Greve, W. 1994. The 1989 German Bight invasion of *Muggiaea atlantica*. ICES Journal of Marine Science **51**: 355-358.

Kenney, R. D., H. E. Winn, and M. C. Macaulay. 1995. Cetaceans in the Great South Channel, 1979-1989: right whale (*Eubalaena glacialis*). Continental Shelf Research **15**: 385-414.

Mills, C. E. 1995. Medusae, siphonophores, and ctenophores as planktivorous predators in changing global ecosystems. ICES Journal of Marine Science **52**: 575-581.

Mills, C. E. 2001. Jellyfish blooms: are populations increasing globally in response to changing ocean conditions? Hydrobiologia **451**: 55-68.

Rogers, C. A., D.C. Biggs, and R.A. Cooper. 1978. Aggregation of the siphonophores *Nanomia cara* in the Gulf of Maine: observations from a submersible. Fisheries Bulletin **76**: 281-284.

Rossi, S., M. J. Youngbluth, C. A. Jacoby, F. Pagès, and X. Garrofè. 2008. Fatty acid trophic markers and trophic links among seston, crustacean zooplankton and the siphonophores *Nanomia cara* in Georges Basin and Oceanographer Canyon (NW Atlantic). Scientia Marina **72**: 403-416.

Sullivan, B. K. and C. J. Meise. 1996. Invertebrate predators of zooplankton on Georges Bank, 1977-1987. Deep Sea Research Part II: Topical Studies in Oceanography **43**: 1503-1519.

Wishner, K. F., J. R. Schoenherr, R. Beardsley, and C. Chen. 1995. Abundance, distribution and population structure of the copepod *Calanus finmarchicus* in a springtime right whale feeding area in the southwestern Gulf of Maine. Continental Shelf Research **15**: 475-507.

Youngbluth, M., T. Sørnes, A. Hosia, and L. Stemmann. 2008. Vertical distribution and relative abundance of gelatinous zooplankton, in situ observations near the Mid-Atlantic Ridge. Deep Sea Research Part II: Topical Studies in Oceanography **55**: 119-125.

# CHAPTER VI

# THREE-DIMENSIONAL DISTRIBUTION OF *CALANUS FINMARCHICUS* WITH RESPECT TO POTENTIAL INVERTEBRATE PREDATORS

## 6.1 Introduction

*Calanus finmarchicus* abundances fluctuate on different temporal and spatial scales. Spatial variations may be related to physical parameters like currents (Lynch et al., 1998; Johnson et al., 2006). Phenological responses may also contribute to observed spatial patterns. For example, the asynchronous emergence of diapausing *C. finmarchicus* in different areas of the Gulf of Maine, or even at different latitudes in the North Atlantic, may lead to a patchy distribution (Fish, 1936; Meise and O'Reilly, 1996; Johnson et al., 2008). Spatial variations could also be caused by the presence or absence of predators in different areas (Meise and O'Reilly, 1996). For instance, decrease in *C. finmarchicus* abundances in the Georges Bank area have been related to the presence of the chaetognath *Sagitta* spp. and ctenophores (Davis, 1984; Meise and O'Reilly, 1996).

Seasonal, interannual, and decadal fluctuations in *C. finmarchicus* have been well documented (Greene and Pershing, 2000; Conversi et al., 2001; MERCINA, 2001; Greene et al., 2003). Seasonal variations are linked to the phenology of the species. *Calanus finmarchicus* is more abundant during the spring phytoplankton bloom and for a couple of months after the phytoplankton mean production peak. During fall and winter, production becomes limited due to lack of food and *C. finmarchicus* enters diapause (Meise and O'Reilly, 1996). During this period of arrested development, *C. finmarchicus* survives on the oil storage built up during the spring and summer. Seasonal variations are also thought to be driven by predation (Davis, 1984).

Interannual and decadal fluctuations of *C. finmarchicus* have been related to regime shifts due to atmospheric-driven phenomena, namely the North Atlantic Oscillation (NAO). Oceanographic regime shifts in the NW Atlantic are related to the NAO index. The Gulf of Maine (GOM) is directly affected by oceanic waters that enter through the Northeast Channel. Extraneous water intrusions happen mainly in two modes. The first one is the warm, salty,

nutrient-rich, upper Slope Water (SLW). The second is the invasion of cooler, fresher nutrient-depleted Labrador Subarctic Water (LSSW). The result is an overall warmer Gulf during a positive NAO index, with SLW-dominating deep waters and a colder Gulf during a negative NAO index, with LSSW-dominated deep waters. These regime shifts between the SLW and the LSSW seem to exert some control over biological responses in the shelf ecosystem of the GOM. One such biological reaction is the high or low production of *C. finmarchicus* during positive and negative NAO index modes, respectively (Greene and Pershing, 2000).

In this chapter, I describe the spatial distributions of *C. finmarchicus* with respect to six predators in three deep basins of the GOM during December 1998 and December 1999 in order to study their potential predation affect on diapausing *C. finmarchicus*.

**6.2 Methods**

Composite, three-dimensional plots were constructed using the highest abundances of *C. finmarchicus* and six invertebrate predators during December 1998 and December 1999. Table 6.1 summarizes the definition ranges for high abundance patches for the studied taxa during December 1998 and 1999 for Wilkinson, Jordan and Georges Basin/Northeast Channel. These distributional maps were used to qualitatively examine the relative locations of regions of abundant *C. finmarchicus* patches with respect to high abundance patches of invertebrate predators. It is important to note that high abundance patches were defined differently for each period and basin because of the dramatically different abundances observed between basins and the studied periods.

**6.3 Results**

**6.3.1 Wilkinson Basin**

Taxon-specific distributional patterns suggested that invertebrate predators within Wilkinson Basin were concentrated in locations where *C. finmarchicus* was not particularly abundant. For instance, during December 1998, a composite plot of predators and *C. finmarchicus* revealed highly abundant patches of invertebrate predators that were not located either above, or within patches of *C. finmarchicus* (Fig. 6.1a). Furthermore, when viewed from

above in a way that integrates water-column abundances, the December 1998 data suggest an inverse spatial relationship between high abundance *C. finmarchicus* patches and high abundance patches of some invertebrate predators such as siphonophores, ctenophores, euphausiids, *Euchaeta norvegica* and to some extent – medusae (Fig. 6.1b). Vertically, most high abundance predator patches were located above 100 m depth, while the highly abundant patches of diapausing *C. finmarchicus* occurred deeper in the water column. Some dense patches of medusae appeared on top of *C. finmarchicus* patches, although they were not collocated. However, medusae were also scattered in small dense patches at depths where *C. finmarchicus* was located. Chaetognaths also were located above *C. finmarchicus* patches. It should be mentioned that *C. finmarchicus* occurred in low abundances in between dense patches. However, such low abundances were not plotted in these 3-D composite maps.

**Table 6.1.** Definition ranges for high abundance (n $m^{-3}$) patches of *Calanus finmarchicus* and six invertebrate predators in the deep basins of the GOM during early fall of years 1998 and 1999.

| | December 1998 | | | December 1999 | | |
|---|---|---|---|---|---|---|
| Taxon | Wilkinson | Jordan | Georges | Wilkinson | Jordan | Georges /NEC |
| *C. finmarchicus* | 120-270 | 100-300 | 50-200 | 400-1 100 | 400-1 100 | 100-760 |
| Siphonophores | 13-35 | 15-80 | 3-55 | 4-12 | 1-2 | 3-19 |
| Ctenophores | 100-300 | 40-110 | 40-280 | ----- | ----- | ----- |
| Medusae | 20-70 | 20-60 | 20-120 | ----- | ----- | ----- |
| Euphausiids | 50-120 | 30-70 | 10-60 | 50-100 | 20-100 | 30-122 |
| *E. norvegica* | 50-200 | 30-90 | ----- | 50-120 | 50-195 | 50-100 |
| Chaetognaths | ----- | ----- | ----- | 15-85 | 25-95 | 25-89 |

The inverse spatial relationship observed in December 1998 was not evident on December 1999 (Fig. 6.2b). During December 1999, high abundance patches of *C.*

*finmarchicus* were located below 150 m. Most of the invertebrate predators were found above the residence depth of diapausing *C. finmarchicus* in Wilkinson Basin during December 1999 (Fig. 6.2a). However, below 150 m depth some scattered patches of invertebrate predators occurred inside the *C. finmarchicus* patches. These included chaetognaths, siphonophores, ctenophores, and a large patch of medusae below 200 m in the easternmost part of the basin. In terms of horizontal geographic coordinates, all dense patches of *C. finmarchicus* seemed to coincide with those of invertebrate predators, with the exception of *Euchaeta norvegica*. The densest patches of *E. norvegica* seemed to be collocated with the high density patches of *C. finmarchicus*.

### 6.3.2 Jordan Basin

Composite plots of *C. finmarchicus* and five potential predators showed two different distribution patterns during December 1998 and December 1999 in Jordan Basin. Viewed from above in a 2D perspective, *C. finmarchicus* showed an inverse spatial relationship with four of the potential predators during December 1998. High-abundance patches of siphonophores, ctenophores, *Euchaeta norvegica*, and euphausiids were located in areas where *C. finmarchicus* was absent or in low numbers (Fig. 6.3b). Medusae didn't show the same pattern as the above-mentioned predators. Indeed, when viewed from above, most high-abundance patches of medusae were located above high-abundance *C. finmarchicus* patches (Fig. 6.3b). Chaetognaths were not included in these plots due to the lack of data for this taxon during December 1998. During December 1999, *C. finmarchicus* and its potential predators showed no inverse spatial relationship in the integrated water column view. High-abundance patches of euphausiids, chaetognaths and siphonophores were located on top of highly abundant patches of *C. finmarchicus* (Fig. 6.4b). Ctenophores and medusae were not included in this composite plot due to the sparse number of observations of these taxa during December 1999.

Vertically, *C. finmarchicus* was vertically collocated with high-abundance predator patches during December 1998. High-abundance *C. finmarchicus* patches found between 50

and 100 m were surrounded by large, high-density patches of euphausiids, medusae and ctenophores (Fig. 6.3a). Only siphonophores were observed in large, dense patches surrounding the *C. finmarchicus* overwintering population in the deep waters of Jordan Basin. During December 1999, *C. finmarchicus* was not vertically collocated with most of its potential predators. Only dense patches of *E. norvegica* were collocated at depths with highly abundant *C. finmarchicus* (Fig. 6.4a). High-abundance patches of chaetognaths, euphausiids, and siphonophores during December 1999 were located well above the overwintering depth of *C. finmarchicus* (Fig. 6.4a).

### 6.3.3 Georges Basin/Northeast Channel

During December 1998, *C. finmarchicus* was inversely vertically distributed with respect to ctenophores and medusae. Dense patches of medusae and ctenophores where found well above *C. finmarchicus* patches, and were scarce in deep waters. Euphausiids and siphonophores were generally collocated with high abundances of *C. finmarchicus* in Georges Basin during December 1998. In the southwestern Georges Basin, dense patches of euphausiids were located below the dense patches of *C. finmarchicus* (Fig. 6.5 top panel). However, in south-central Georges Basin, euphausiids were scattered and did not overlap with *C. finmarchicus* dense regions. The continuous high dense patch of siphonophores in waters deeper than 150 m in the southwestern Georges Basin overlapped with *C. finmarchicus* high dense patches. *Calanus finmarchicus* and siphonophores were widely scattered in south-central Georges Basin; however, a slight overlapping was observed in this region in waters deeper than 100 m (Fig. 6.5 top panel). Almost no *C. finmarchicus* were observed in the Northeast Peak region of Georges Bank. However, high abundances of all predators were observed there during December 1998.

Data were insufficient for *Euchaeta norvegica* and chaetognaths. No horizontal spatial relationship could be addressed due to the fact that the transect was linear and no 3-D Kriging was performed for cruise OC334 in Georges Basin.

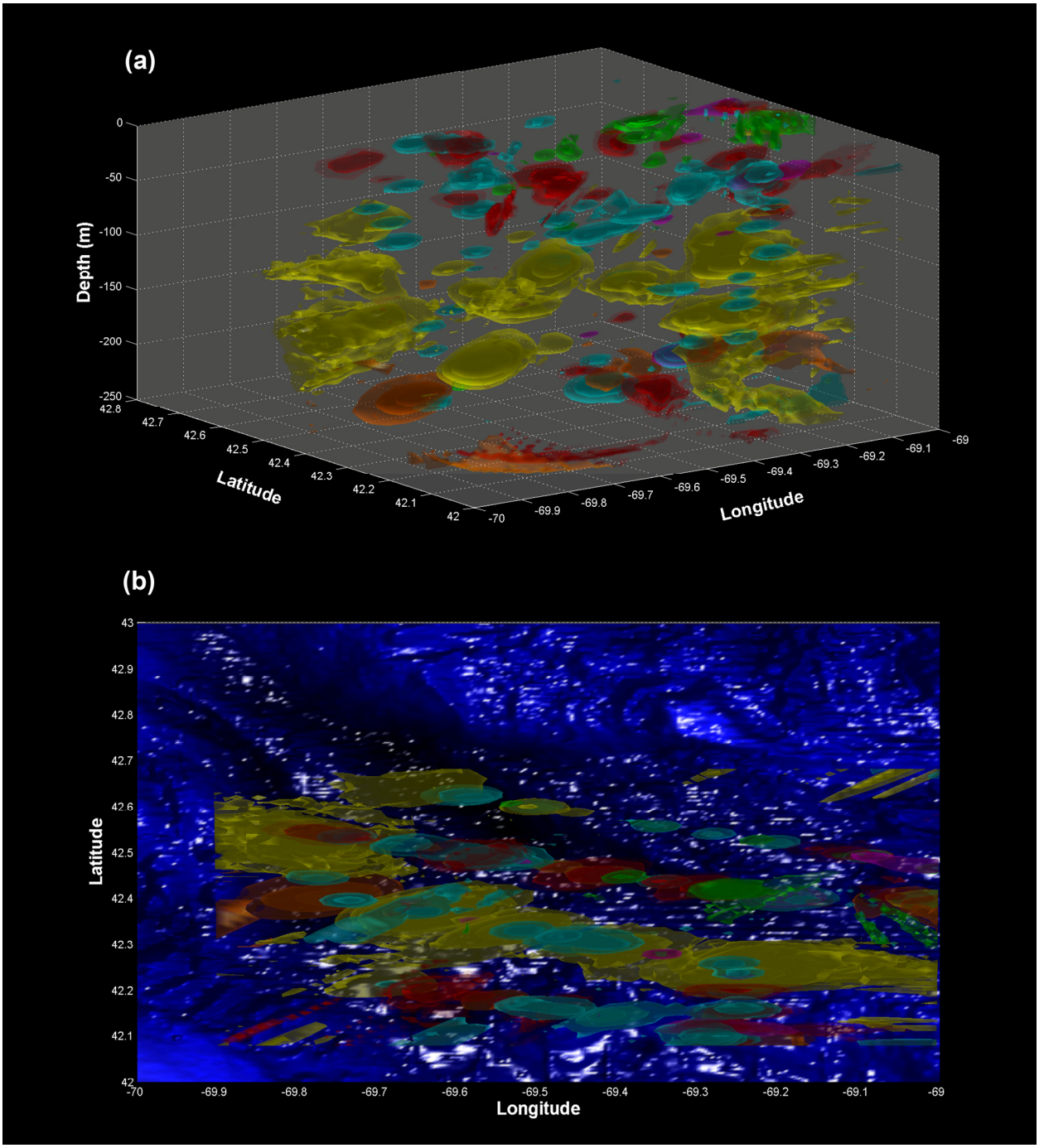


**Figure 6.1.** A) Wilkinson Basin: A three-dimensional composite view from the southwestern of higher abundance patches for *Calanus finmarchicus* (yellow, 120-270 n $m^{-3}$) and five potential invertebrate predators during December 1998: siphonophores (red, 13-35 n $m^{-3}$), ctenophores (green, 100-300 n $m^{-3}$), medusae (cyan, 20-70 n $m^{-3}$), *Euchaeta norvegica* (orange, 50-200 n $m^{-3}$), and euphausiids (magenta, 50-120 n $m^{-3}$). B) Aerial view of the composite map, color-coded as in (A). The bathymetry of Wilkinson Basin was included in the plot for reference.

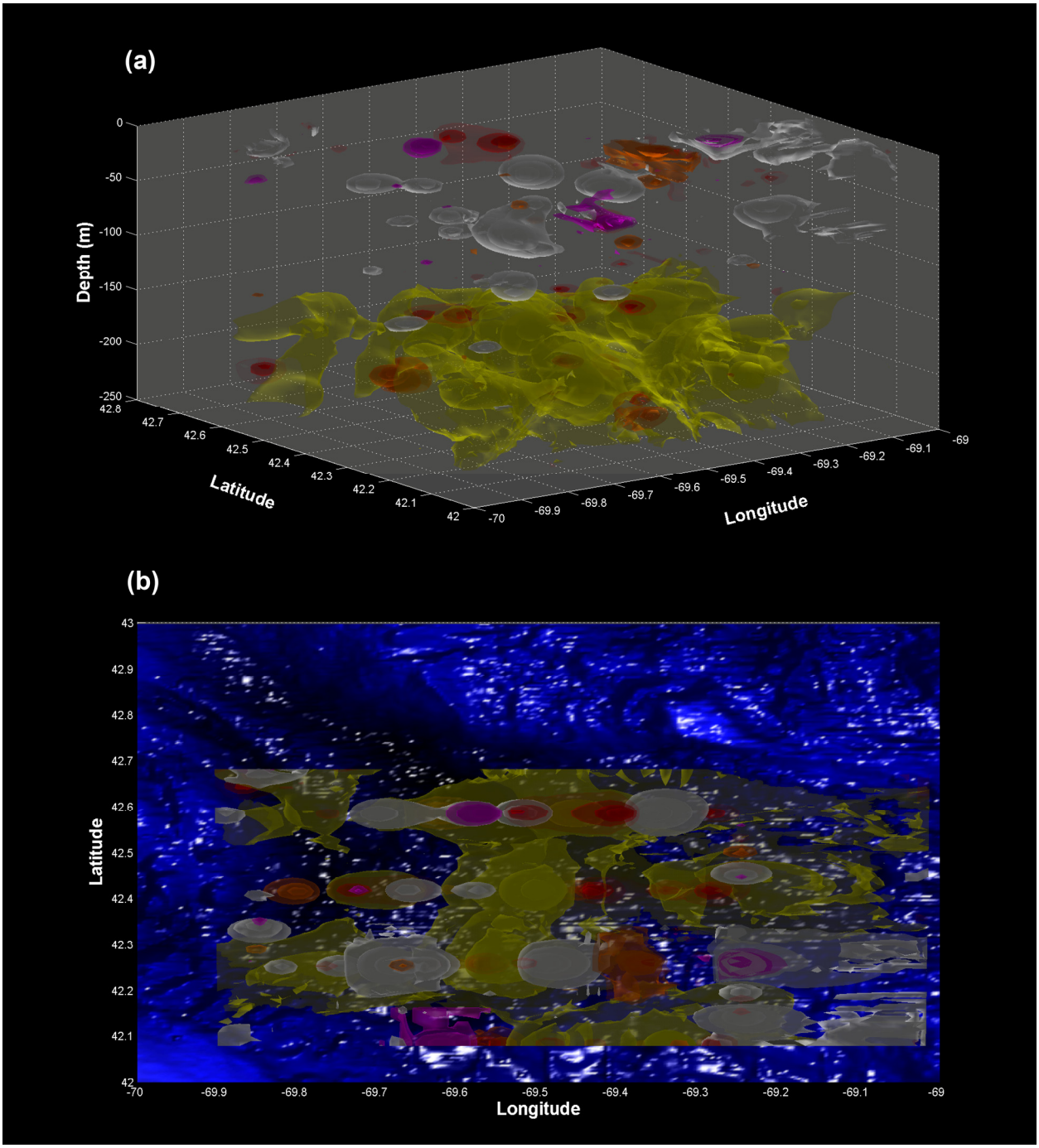


**Figure 6.2.** A) Wilkinson Basin: A three-dimensional composite view from the southwestern of higher abundance patches for *Calanus finmarchicus* (yellow, 400-1,100 n $m^{-3}$) and four potential invertebrate predators during December 1999: siphonophores (red, 4-12 n $m^{-3}$), chaetognaths (white, 15-85 n $m^{-3}$), *Euchaeta norvegica* (orange, 50-120 n $m^{-3}$), euphausiids (magenta, 50-100 n $m^{-3}$). B) Aerial view of the composite map, color-coded as in (A). The bathymetry of Wilkinson Basin was included in the plot for reference.

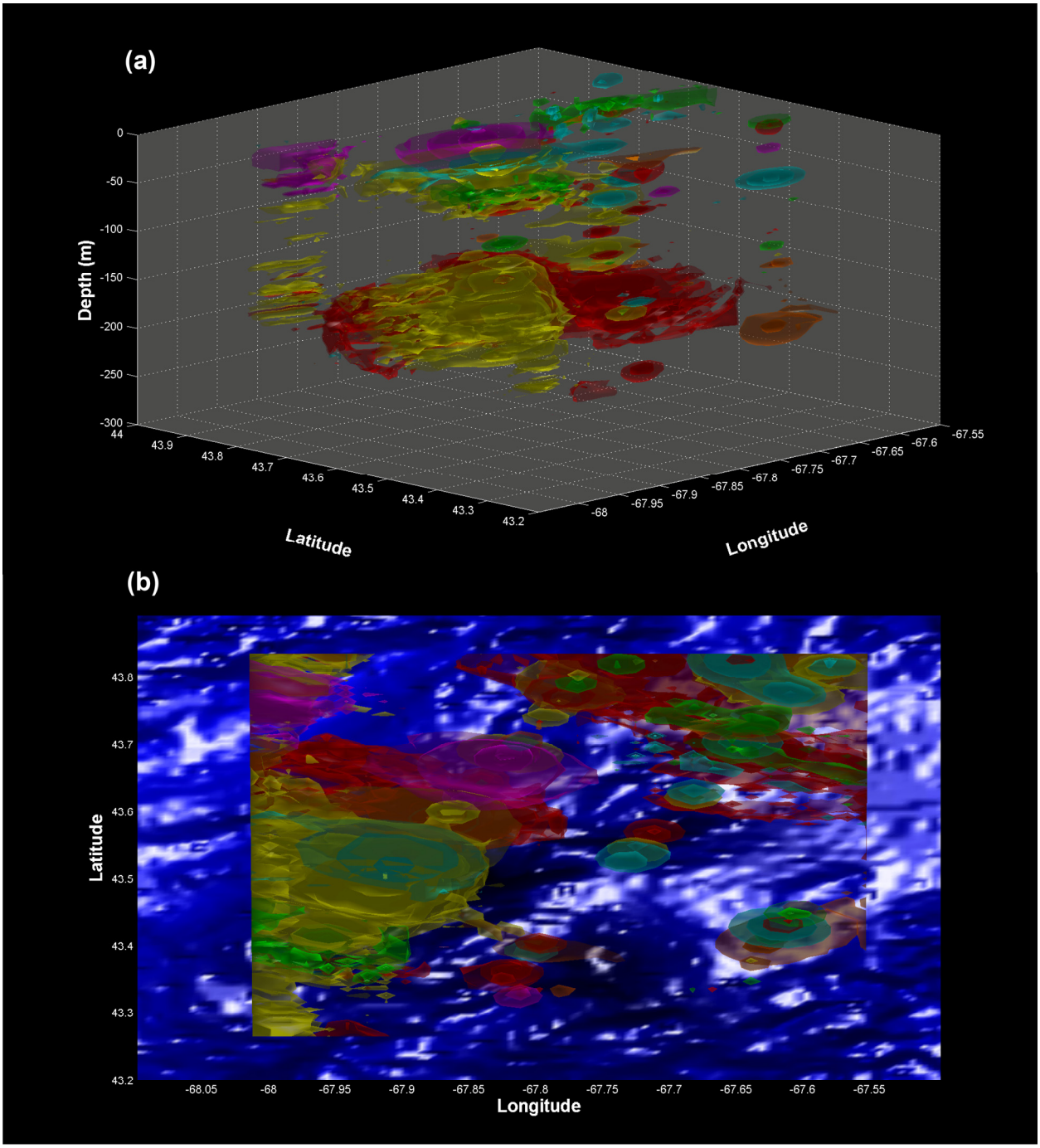


**Figure 6.3.** A) Jordan Basin: A three-dimensional composite view from the southwestern of higher abundance patches for *Calanus finmarchicus* (yellow, 100-300 n $m^{-3}$) and five potential invertebrate predators during December 1998: siphonophores (red, 15-80 n $m^{-3}$), ctenophores (green, 40-110 n $m^{-3}$), medusae (cyan, 20-60 n $m^{-3}$), *Euchaeta norvegica* (orange, 30-90 n $m^{-3}$), euphausiids (magenta, 30-70 n $m^{-3}$). B) Aerial view of the composite map, color-coded as in (A). The bathymetry of Jordan Basin was included in the plot for reference.

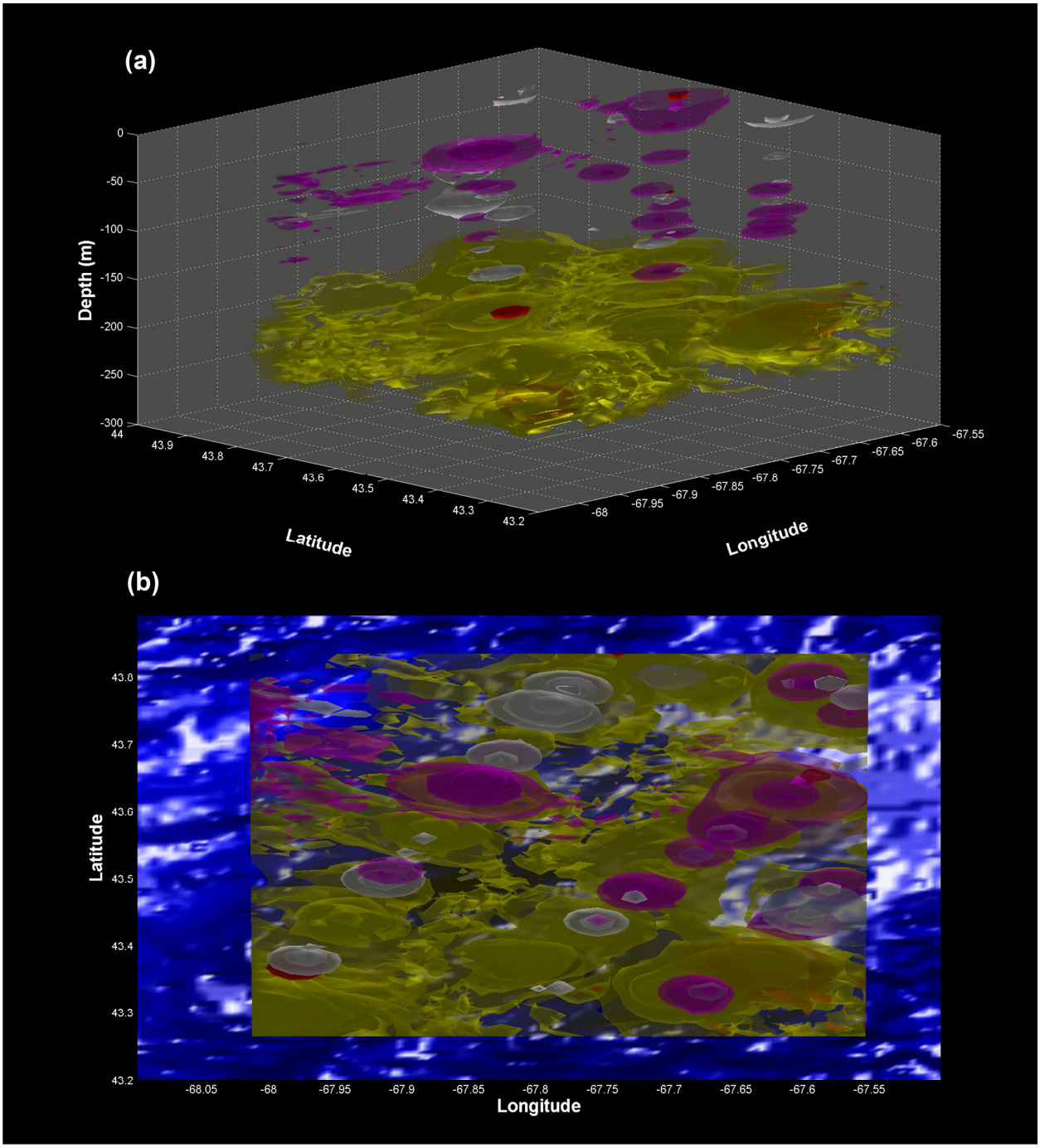


**Figure 6.4.** A) Jordan Basin: A three-dimensional composite view from the southwestern of higher abundance patches for *Calanus finmarchicus* (yellow, 400-1,100 n $m^{-3}$) and four potential invertebrate predators during December 1999: siphonophores (red, 1-2 n $m^{-3}$), chaetognaths (white, 25-95 n $m^{-3}$), *Euchaeta norvegica* (orange, 50-195 n $m^{-3}$), euphausiids (magenta, 20-100 n $m^{-3}$). B) Aerial view of the composite map, color-coded as in (A). The bathymetry of Jordan Basin was included in the plot for reference.

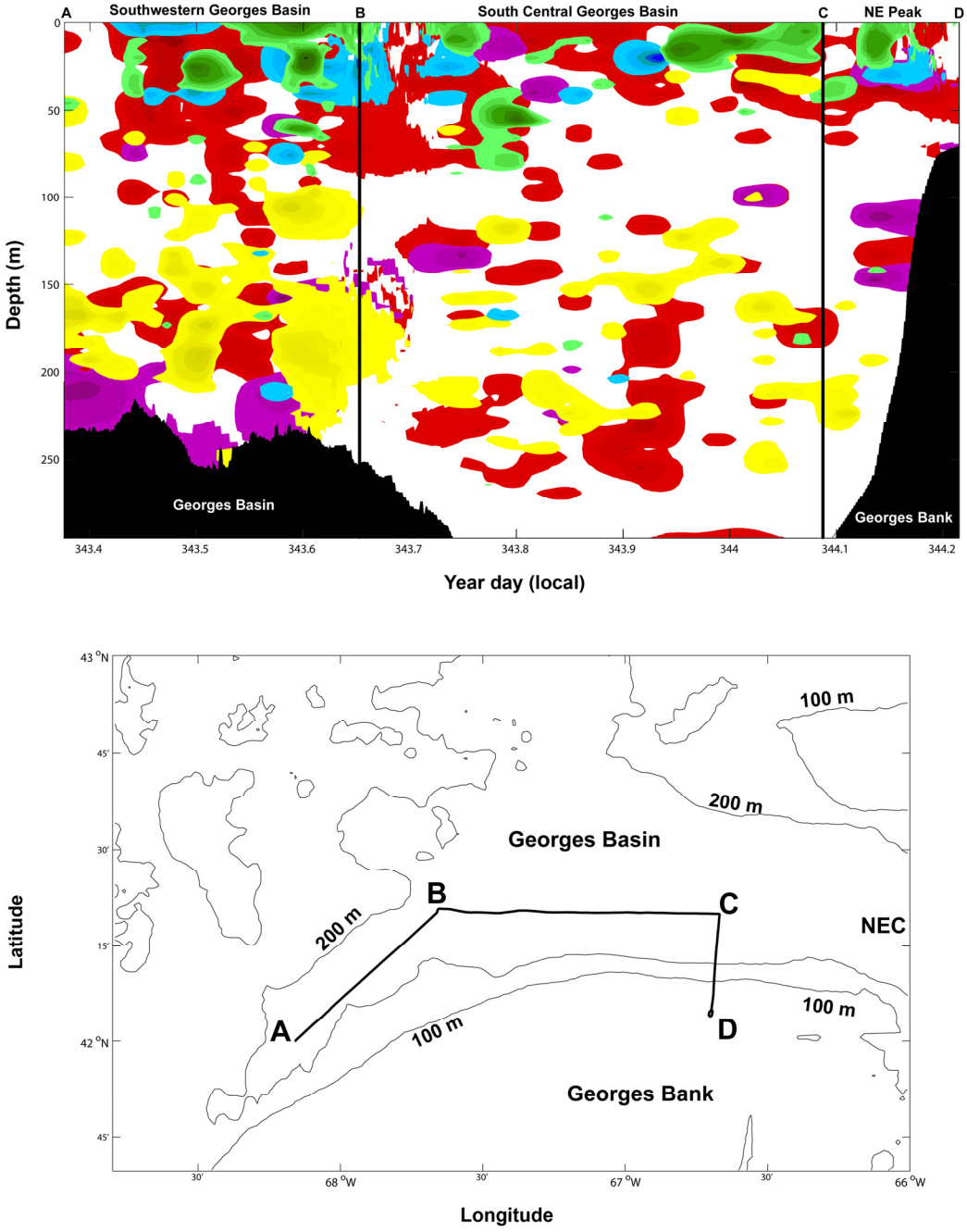


**Figure 6.5.** Top panel: Jordan Basin composite of higher abundance patches for *Calanus finmarchicus* (yellow, 50-200 n $m^{-3}$) and four potential invertebrate predators during December 1998: siphonophores (red, 3-55 n $m^{-3}$), ctenophores (green, 40-280 n $m^{-3}$), medusae (cyan, 20-120 n $m^{-3}$), and euphausiids (magenta, 10-60 n $m^{-3}$). Reference sections on top panel correspond to the sections shown in the map in the bottom panel.

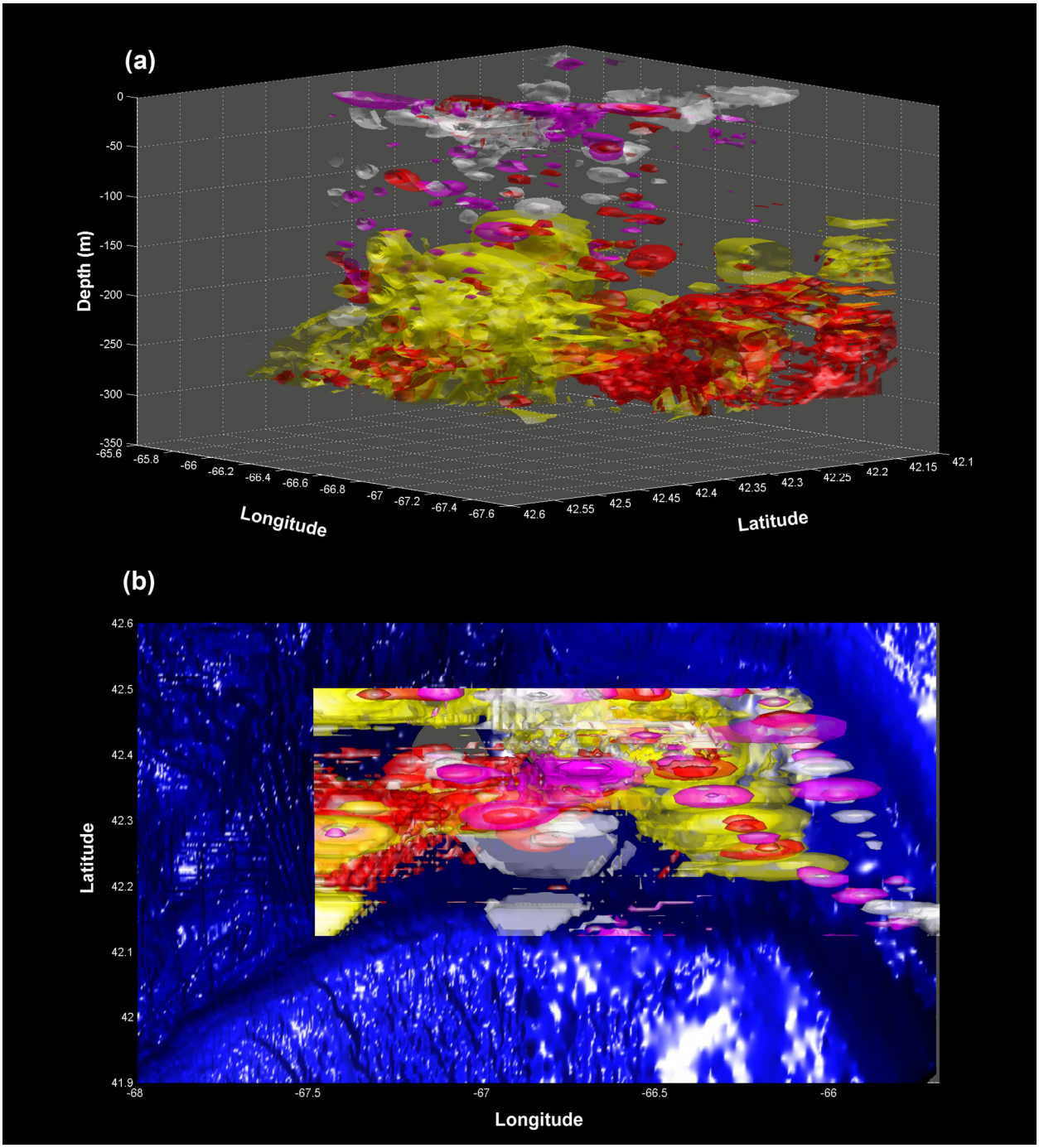


**Figure 6.6.** A) Georges Basin/Northeast Channel: A three-dimensional composite view from the northwestern of higher abundance patches for *Calanus finmarchicus* (yellow, 100-760 n $m^{-3}$) and four potential invertebrate predators during December 1999: siphonophores (red, 3-19 n $m^{-3}$), chaetognaths (white, 25-89 n $m^{-3}$), *Euchaeta norvegica* (orange,50-100 n $m^{-3}$), euphausiids (magenta, 30-122 n $m^{-3}$). B) Aerial view of the composite map, color-coded as in (A). The bathymetry of Jordan Basin was included in the plot for reference.

During December 1999, there was no inverse horizontal spatial relationship between *C. finmarchicus* and its predators, with the exception of the eastern boundary of the Northeast Channel, where chaetognaths and euphausiids were present but *C. finmarchicus* was not (Fig. 6.6a). Vertically, *C. finmarchicus* was inversely distributed with respect to chaetognaths and euphausiids (Fig. 6.6b). Chaetognaths and euphausiids were found above the dense patches of *C. finmarchicus* during December 1999. The only *Euchaeta norvegica* patch resolved by kriging was located inside the region dominated by *C. finmarchicus* at the bottom of Georges Basin. Siphonophores in the western side of Georges Basin were located inside the region dominated by *C. finmarchicus*. Although some high abundance patches also occurred inside the *C. finmarchicus*-dominated area, siphonophores in this part of Georges Basin were in low abundances. Other scattered patches of siphonophores were also located inside this area.

**6.4 Discussion**

Overwintering at deeper waters is thought to reduce the risk of predation (Kaartvedt, 1996) and to increase the retention of overwintering *C. finmarchicus* populations in the deep waters of the GOM (Johnson et al., 2006). Generally, in the three deep basins of the GOM, *C. finmarchicus* were scattered in the water column during December 1998, with the densest patches residing in waters deeper than 150 m. During the same period, high abundances of six predators were observed in the three deep basins at all depths. The opposite pattern was observed during December 1999, where *C. finmarchicus* was mainly found clustered in large dense patches in waters deeper than 150 m. Coincidently, during December 1999 lower abundances of gelatinous predators were observed. This inverse pattern could help explain the differences in *C. finmarchicus* abundances observed between December 1998 and December 1999.

*Calanus finmarchicus* above the sill depth (~190 m) during December 1998 would likely have been subjected to advection losses (wash over) induced by the mean current circulation of the Gulf of Maine (Johnson et al., 2006), while at the same time being subjected to high

predation pressure due to the predators' high abundance in the water column. During December 1999, low abundances were found in waters deeper than 150 m. Also, during December 1999, low abundances of predators were observed in all three deep basins compared to the same period in the previous year. This suggests lower predation pressure on *C. finmarchicus* and hence their higher abundances during December 1999 than during December 1998.

During both periods, Georges Basin had the lowest abundance of *C. finmarchicus*. Coincidently, this basin showed the greater abundances of siphonophores. The other five potential predators' abundances were either slightly higher or equal than the observed in Wilkinson and Jordan basins. The lowest abundance of *C. finmarchicus* in Georges Basin during both periods could be due to high mortality rates due to predation, suggested by the relatively higher abundance of predators with respect to the other two basins. Johnson et al. (2006) identified Georges Basin as having the lowest retention rates of *C. finmarchicus* in the Gulf of Maine. Another cause for observing lower *C. finmarchicus* abundances compared to Wilkinson Basin and Jordan Basin could be due to losses caused by advection processes (Chapter IV and below).

In their physical-biological model, Lynch et al. (1998) showed that after seeding the central basins with *C. finmarchicus*, and after three simulated months, the concentrations of *C. finmarchicus* were localized in the southern areas of the basin and extended towards the jet that seeds Georges Bank. Although their simulation model started in January and lasted until April, similar high *C. finmarchicus* abundance patches were found in the southern and southwestern areas of Jordan, Wilkinson and Georges basins during December 1998. Although some variability in the water currents would be expected, my results showed that at least during December 1998, the fate of *C. finmarchicus* diapausing populations was to be advected into these areas by the general mean circulation patterns of the Gulf of Maine, and by the local circulation patterns of each basin (both counterclockwise).

In some areas of the NE Atlantic, siphonophores have been responsible for reducing the copepod population to near zero (Greve, 1994). The inverse spatial distribution of *C. finmarchicus* and some predators during December 1998 could be interpreted as indicating the results of high predation pressure. At the same time, the vertical collocation of *C. finmarchicus* and siphonophores and medusae would have made *C. finmarchicus* prone to encountering high predation by gelatinous plankton. At least some indication of vertical migration was observed for siphonophores, but it was less clear for medusae during December 1998. At depths where high dense patches of gelatinous plankton occurred, the abundance of *C. finmarchicus* would likely have been reduced to non-detectable levels by the VPR.

Siphonophores and *C. finmarchicus* were located in to the same water masses in all three basins of the GOM (Chapters IV and V). However, siphonophores didn't coincide spatially with *C. finmarchicus* during December 1998. Despite their inverse vertical distribution during December 1998 in all three basins, siphonophores could have reduced the abundance of diapausing *C. finmarchicus* as siphonophores were present in almost the entire water column and occurred in low numbers overlapping low-abundance *C. finmarchicus* patches.

As discussed elsewhere, subsurface water currents decrease their speed towards the bottom of the basins (Hanna et al., 1998; Lynch et al., 1998). Local circulation patterns in the basins could have exacerbated the possible interaction between siphonophores and *C. finmarchicus* in waters shallower than 150 m. With vertically migrating siphonophores, they would have experienced higher dispersion rates towards the surface than at depth or near the bottom of the deep basins. The same would apply for *C. finmarchicus* during December 1998 when they were found in relatively high abundances from 50 and below. This could explain siphonophores dispersed patterns in waters shallower than 150 m in Wilkinson and Jordan Basin and the more clustered pattern in waters deeper than 200 m in Jordan Basin. More scattered siphonophores would constitute a mine field for patches of *C. finmarchicus* in the surface waters, with potentially higher encounter rates exacerbated by faster currents. This also

could mean that in the areas where siphonophores were found clustered they may have depleted *C. finmarchicus* at those depths, leaving only the clustered patches of diapausing *C. finmarchicus* observed in areas with low siphonophores abundances in all three deep basins during December 1998.

Euphausiids in Georges Basin during December 1998 could have imposed predation pressure upon *C. finmarchicus* overwintering at depths, especially since there was evidence of diel vertical activity in euphausiids during this period (Chapter V) and the fact that they were spatially collocated. Further, *Nanomia cara*, the main species of siphonophores identified in this work, is known to feed on both, *C. finmarchicus* and *Meganyctiphanes norvegica* in the Gulf of Maine (Rossi et al., 2008). In fact, in the presence of siphonophores, Rossi et al. (2008) found that euphausiids did not feed on *C. finmarchicus*, probably suggesting predation pressure over *M. norvegica* by *N. cara*. During both periods, siphonophores and euphausiids seemed to be related to the same waters masses, suggesting possible interactions between these taxa. This would suggest also that predation pressure on *C. finmarchicus* from the euphausiid *M. norvegica* would be mediated by the presence or absence of a common predator of these crustaceans.

Since no vertical diel activity was detected in western Georges Basin for medusae and ctenophores during December 1998, they probably imposed less predation pressure than euphausiids and siphonophores did in waters deeper than 100m. However, as in the case of Wilkinson and Jordan basins, *C. finmarchicus* in Georges Basin was found scattered from 0 to 100 m. This stratum also contained abundant siphonophores, medusae and ctenophores. The potential early awakening of diapausing *C. finmarchicus* during December 1998 (Chapter IV) may have put them in great danger of predation as they ascended given the high concentration of gelatinous plankton in the first 100 m surface waters.

During December 1999, chaetognaths were found in high abundances in all three deep basins. Seasonal declines in *C. finmarchicus* abundances in the Georges Bank area have been

related to the presence of the chaetognath *Sagitta* spp. (Davis, 1984; Meise and O'Reilly, 1996). However during December 1999 this did not seem to be the case for Wilkinson and Jordan basins, as *C. finmarchicus* was not collocated with chaetognaths. In fact, most chaetognath patches were found in waters shallower than 100 m, and diapausing *C. finmarchicus* was found mainly below 150 m. In addition, no vertical migration was detected for chaetognaths in Wilkinson and Jordan basins. In the south central Georges Basin, however, a large patch of chaetognaths was found along with patches of *Euchaeta norvegica*. Although some interaction between these two carnivorous animals could be present, it was interesting to observe that no *C. finmarchicus* was found in this central region in the south of Georges Basin. This could be an indication of possible predation of *C. finmarchicus*, whose population could have been reduced to undetectable levels in this region. Further, this region is also closer to the area where water masses from the Gulf of Maine are advected to the NE Peak, Georges Basin and to the NW Atlantic. The apparent absence of *C. finmarchicus* in this region could also indicate advection losses. Because of the large abundance of predators in this region, the predation pressure hypothesis seems more likely to explain the loss than an advective one. However, a coupled effect cannot be ruled out as an explanation of low abundances of *C. finmarchicus* in this region.

**6.5 References**


Conversi, A., S. Piontkovski, and S. Hameed. 2001. Seasonal and interannual dynamics of *Calanus finmarchicus* in the Gulf of Maine (Northeastern US shelf) with reference to the North Atlantic Oscillation. Deep Sea Research Part II: Topical Studies in Oceanography **48**: 519-530.

Davis, C. S. 1984. Predatory control of copepod seasonal cycles on Georges Bank. Marine Biology **82**: 31-40.

Fish, C. J. 1936. The biology of *Calanus finmarchicus* in the Gulf of Maine and Bay of Fundy. Biological Bulletin **70**: 118-141.

Johnson, C., J. Pringle, and C. Chen. 2006. Transport and retention of dormant copepods in the Gulf of Maine. Deep Sea Research Part II: Topical Studies in Oceanography **53**: 2520-2536.

Greene, C. H. and A. J. Pershing. 2000. The response of *Calanus finmarchicus* populations to climate variability in the Northeast Atlantic: basin-scale forcing associated with the North Atlantic Oscillation. ICES Journal of Marine Science **57**: 1536-1544.

Greene, C. H., A. J. Pershing, A. Conversi, B. Planque, C. Hannah, D. Sameoto, E. Head, P. C. Smith, P.C. Reid, J. Jossi, D. Mountain, M. C. Benfield, P. H. Wiebe, and E. Durbin. 2003. Trans-Atlantic responses of *Calanus finmarchicus* populations to basin-scale forcing associated with the North Atlantic Oscillation Progress in Oceanography **58**: 301-312.

Hannah, C. G., C. E. Naimie, J. W. Loder, and F. E. Werner. 1998. Upper-ocean transport mechanisms from the Gulf of Maine to Georges Bank, with implications for *Calanus* supply. Continental Shelf Research **17**: 1887-1911.

Johnson, C. L., A. W. Leising, J. A. Runge, E. J. H. Head, P. Pepin, S. Plourde, and E. G. Durbin. 2008. Characteristics of *Calanus finmarchicus* dormancy patterns in the Northwest Atlantic. ICES Journal of Marine Science **65**: 339-350.

Johnson, C., J. Pringle, and C. Chen. 2006. Transport and retention of dormant copepods in the Gulf of Maine. Deep Sea Research Part II: Topical Studies in Oceanography **53**: 2520-2536.

Kaartvedt, S. 1996. Habitat preference during overwintering and timing of seasonal vertical migration of *Calanus finmarchicus*. Ophelia **44**: 145-156.

Lynch, D. R., W. C. Gentleman, D. J. McGillicuddy Jr., and C. S. Davis. 1998. Biological/physical simulations of *Calanus finmarchicus* population dynamics in the Gulf of Maine. Marine Ecology Progress Series **169**: 189-210.

Meise, C. J. and J. E. O'Reilly. 1996. Spatial and seasonal patterns in abundance and age-composition of *Calanus finmarchicus* in the Gulf of Maine and on Georges Bank. Deep-Sea Research II: Topical Studies in Oceanography **43**: 1473-1501.

MERCINA. 2001. Oceanographic responses to climate in the Northwest Atlantic. Oceanography **14**: 76-82.

Rossi, S., M. J. Youngbluth, C. A. Jacoby, F. Pagès, and X. Garrofè. 2008. Fatty acid trophic markers and trophic links among seston, crustacean zooplankton and the siphonophores *Nanomia cara* in Georges Basin and Oceanographer Canyon (NW Atlantic). Scientia Marina **72**: 403-416.

## BIBLIOGRAPHY


Avent, S. R., S. M. Bollens, M. Butler, E. Horgan, and R. Rountree. 2001. Planktonic hydroids on Georges Bank: ingestion and selection by predatory fishes. Deep Sea Research Part II: Topical Studies in Oceanography **48**: 673-684.

Beardsley, R. C., A. W. Epstein, C. Chen, K. F. Wishner, M. C. Macaulay, and R. D. Kenney. 1996. Spatial variability in zooplankton abundance near feeding right whales in the Great South Channel. Deep Sea Research Part II: Topical Studies in Oceanography **43**: 1601-1625.

Benfield, M. C., C. S. Davis, P. H. Wiebe, S. M. Gallager, C. H. Greene, F. Werner, D. McGuillicuddy, and T. K. Stanton. 1999. Real time image analysis: instrument to model. ICES C.M.: 1999/M:06.

Benfield, M. C., C. S. Davis, P. H. Wiebe, S. M. Gallager, R. G. Lough, and N. J. Copley. 1996. Video Plankton Recorder estimates of copepod, pteropod and larvacean distributions from a stratified region of Georges Bank with comparative measurements from a MOCNESS sampler. Deep-Sea Research Part II: Topical Studies in Oceanography **43**: 1925-1945.

Benfield, M. C., P. Grosjean, P. F. Culverhouse, X. Irigoien, M. E. Sieracki, A. Lopez-Urrutia, H. G. Dam, Q. Hu, C. S. Davis, A. Hansen, C. H. Pilskaln, E. M. Riseman, H. Schultz, P. E. Utgoff, and G. Gorsky. 2007. RAPID: Research on Automated Plankton Identification. Oceanography **20**: 172-187.

Bigelow, H. B. 1924. Plankton of the offshore waters of the Gulf of Maine. Bulletin of the Bureau of Fisheries **40**: 1-509.

Brodeur, R. D., C. E. Mills, J. E. Overland, G. E. Walters, and J. D. Schumacher. 1999. Evidence for a substantial increase in gelatinous zooplankton in the Bering Sea, with possible links to climate change. Fisheries Oceanography **8:** 296-306.

Brooks, D. A. 1985. Vernal Circulation in the Gulf of Maine. Journal of Geophysical Research **90**: 4687-4705.

Broughton, E. A. and R. G. Lough. 2006. A direct comparison of MOCNESS and Video Plankton Recorder zooplankton abundance estimates: Possible applications for augmenting net sampling with video systems. Deep Sea Research Part II: Topical Studies in Oceanography **53**: 2789-2807.

Brown, W. S. and J. D. Irish. 1993. The annual variation of water mass structure in the Gulf of Maine: 1986-1987. Journal of Marine Research **51**:53-107.

Buckley, L. J. and E. G. Durbin. 2006. Seasonal and inter-annual trends in the zooplankton prey and growth rate of Atlantic cod (*Gadus morhua*) and haddock (*Melanogrammus aeglefinus*) larvae on Georges Bank. Deep Sea Research Part II: Topical Studies in Oceanography **53**(23-24): 2758-2770.

Bucklin, A. and T. D. Kocher. 1996. Source regions for recruitment of *Calanus finmarchicus* to Georges Bank: evidence from molecular population genetic analysis of mtDNA. Deep Sea Research Part II: Topical Studies in Oceanography **43**(7-8): 1665-1681.

Bumpus, D. F. 1973. A description on the circulation on the continental shelf of the east coast of the United States. Progress in Oceanography **6**: 111-157.

Campbell, R. W. and J. F. Dower. 2008. Depth distribution during the life history of *Neocalanus plumchrus* in the Strait of Georgia. Journal of Plankton Research **30**(1): 7-20.

Christensen, J. P., D. W. Townsend, and J. P. Montoya. 1996. Water column nutrients and sedimentary denitrification in the Gulf of Maine. Continental Shelf Research **16**: 489-515.

Chu, D. 2004. EasyKrig 3.0. http://globec.whoi.edu/software/kriging/easy_krig/easy_krig.html.

Clarke, G. L. 1940. Comparative richness of zooplankton in coastal and offshore areas of the atlantic. Biological Bulletin **78**: 226-255.

Climate Prediction Center, National Weather Service, National Oceanographic and Atmospheric Administration.ttp://www.cpc.ncep.noaa.gov/products/precip/CWlink/pna/nao.shtml.

Conover, R. J. 1988. Comparative life histories in the genera *Calanus* and *Neocalanus* in high latitudes of the northern hemisphere. Hydrobiologia **167/168**: 127-142.

Conversi, A., S. Piontkovski, and S. Hameed. 2001. Seasonal and interannual dynamics of *Calanus finmarchicus* in the Gulf of Maine (Northeastern US shelf) with reference to the North Atlantic Oscillation. Deep Sea Research Part II: Topical Studies in Oceanography **48**: 519-530.

Dale, T., S. Kaartvedt, B. Ellertsen, and R. Amundsen. 2001. Large-scale oceanic distribution and population structure of Calanus finmarchicus, in relation to physical environment, food and predators. Marine Biology **139**: 561.

Dalsgaard, J., M. St. John, G. Kattner, D. Müller–Navarra and W. Hagen. 2003. Fatty acid trophic markers in the pelagic marine environment: a review. Advances in Marine Biology **46**: 225-340.

Davis, C. S. 1984. Predatory control of copepod seasonal cycles on Georges Bank. Marine Biology **82**: 31-40.

Davis, C. S. 1987. Zooplankton life cycles. *In* Backus R. H. and D. W. Bourne (eds). 1987. Georges Bank. Cambridge, Ma, MIT Press**:** 256-267.

Davis, C. S., S. M. Gallager, M. Marra, S. W. Kenneth. 1996. Rapid visualization of plankton abundance and taxonomic composition using the Video Plankton Recorder. Deep Sea Research Part II: Topical Studies in Oceanography **43**: 1947-1970.

Davis, C. S., S. M. Gallager, M. S. Berman, L. R. Haury, and J. R. Strickler. 1992. The video plankton recorder (VPR): Design and initial results. Archiv für Hydrobiologie Beiheft Ergebnisse der Limnologie **36**: 67-81.

Durbin, E. G. and M. C. Casas. 2006. Abundance and spatial distribution of copepods on Georges Bank during the winter/spring period. Deep Sea Research Part II: Topical Studies in Oceanography **53**: 2537-2569.

Durbin, E. G., J. A. Runge, R. G. Campbell, P. R. Garrahan, M. C. Casas, and S. Plourde. 1997. Late fall-early winter recruitment of *Calanus finmarchicus* on Georges Bank. Marine Ecology Progress Series **151**: 103-114.

Durbin, E. G., P. R. Garrahan, and M. C. Casas. 2000. Abundance and distribution of *Calanus finmarchicus* on the Georges Bank during 1995 and 1996. ICES Journal of Marine Science **57**: 1664-1685.

Durbin, E. G., S. L. Gilman, R. G. Campbell, and Ann G. Durbin. 1995. Abundance, biomass, vertical migration and estimated development rate of the copepod *Calanus finmarchicus* in the southern Gulf of Maine during late spring. Continental Shelf Research **15**: 571-591.

Fish, C. J. 1936. The biology of *Calanus finmarchicus* in the Gulf of Maine and Bay of Fundy. Biological Bulletin **70**: 118-141.

Gallager, S. M., C. S. Davis, A. W. Epstein, A. Solow, and R. C. Beardsle. 1996. High-resolution observations of plankton spatial distributions correlated with hydrography in the Great South Channel, Georges Bank. Deep Sea Research Part II: Topical Studies in Oceanography **43**: 1627-1663.

Gislason, A., K. Eiane, and P. Reynisson. 2007. Vertical distribution and mortality of *Calanus finmarchicus* during overwintering in oceanic waters southwest of Iceland. Marine Biology **150**: 1253-1263.

Graham, W. M. 2001. Numerical increases and distributional shifts of *Chrysaora quinquecirrha* (Desor) and *Aurelia aurita* (Linné) (Cnidaria: Scyphozoa) in the northern Gulf of Mexico. Hydrobiologia **451**: 97-111.

Greene, C. H. and A. J. Pershing 2000. The response of *Calanus finmarchicus* populations to climate variability in the Northeast Atlantic: basin-scale forcing associated with the North Atlantic Oscillation. ICES Journal of Marine Science **57**: 1536-1544.

Greene, C. H. and A. J. Pershing. 2004. Climate and the conservation biology of North Atlantic right whales: the right whale at the wrong time? Frontiers in Ecology and the Environment **2**: 29-34.

Greene, C. H., A. J. Pershing, A. Conversi, B. Planque, C. Hannah, D. Sameoto, E. Head, P. C. Smith, P. C. Reid, J. Jossi, D. Mountain, M. C. Benfield, P. H. Wiebe, E. Durbin. 2003. Trans-Atlantic responses of *Calanus finmarchicus* populations to basin-scale forcing associated with the North Atlantic Oscillation. Progress in Oceanography **58**: 301-312.

Greene, C., M. C. Benfield, H. Sosik, P. Wiebe, A. Bucklin, L. McGarry, and K. Fisher. 1998b. R/V Oceanus Cruise 334 cruise report. U. S. GLOBEC, NW Atlantic/Georges Bank Study. 58 p. http://globec.whoi.edu/globec-dir/reports/oc334/cruise-report.html

Greene, C., M. C. Benfield, H. Sosik, P. Wiebe, L. McGarry, and K. Fisher. 1998a. R/V Oceanus Cruise 332 cruise report. U. S. GLOBEC, NW Atlantic/Georges Bank Study. 63 p. http://globec.whoi.edu/globec-dir/reports/oc332/oc332rpt.html

Greene, C., M. C. Benfield, P. Wiebe, and H. Sosik 1999a. R/V Endeavor Cruise 330 cruise report. U. S. GLOBEC, NW Atlantic/Georges Bank Study. 72 p. http://globec.whoi.edu/globec-dir/reports/en330/en330new.htm

Greene, C., M. C. Benfield, P. Wiebe, and H. Sosik. 1999b. R/V Endeavor Cruise 331 cruise report. U. S. GLOBEC, NW Atlantic/Georges Bank Study. 62 p. http://globec.whoi.edu/globec-dir/reports/en331/en331rpt.6sept2000.html

Greene, C., P. Wiebe, H. Sosik, M. C. Benfield, and A. Bucklin. 1997. R/V Endeavor Cruise 307 cruise report. U. S. GLOBEC, NW Atlantic/Georges Bank Study. 47 p. http://globec.whoi.edu/globec-dir/reports/en307/greenrpt.html

Greve, W. 1994. The 1989 German Bight invasion of *Muggiaea atlantica*. ICES Journal of Marine Sciences **51**: 355-358.

Hannah, C. G., C. E. Naimie, J. W. Loder, and F. E. Werner. 1998. Upper-ocean transport mechanisms from the Gulf of Maine to Georges Bank, with implications for *Calanus* supply. Continental Shelf Research **17**: 1887-1911.

Haury, L. R., J. A. McGowan, and P. H. Wiebe. 1978. Patterns and processes in the time-space scales of plankton distributions. Spatial pattern in plankton communities. J. H. Steele (*ed*). New York, Plenum Press. **3:** 277-327.

Heath, M. R. and R. G. Lough. 2007. A synthesis of large-scale patterns in the planktonic prey of larval and juvenile cod (*Gadus morhua*). Fisheries Oceanography **16**: 169-185.

Hirche, H. J. 1996. Diapause in the marine copepod, *Calanus finmarchicus* -a review. Ophelia **44**: 129-143.

Hopkins, T. S. and N. Garfield. 1979. Gulf of Maine intermediate water. Journal of Marine Research **37**: 103-139.

Irigoien, X. 2004. Some ideas about the role of lipids in the life cycle of *Calanus finmarchicus*. Journal of Plankton Research **26**: 259-263.

Johnson, C. L., A. W. Leising, J. A. Runge, E. J. H. Head, P. Pepin, S. Plourde, and E. G. Durbin. 2008. Characteristics of *Calanus finmarchicus* dormancy patterns in the Northwest Atlantic. ICES Journal of Marine Science **65**: 339-350.

Johnson, C., J. Pringle, and C. Chen. 2006. Transport and retention of dormant copepods in the Gulf of Maine. Deep Sea Research Part II: Topical Studies in Oceanography **53**: 2520-2536.

Kaartvedt, S. 1996. Habitat preference during overwintering and timing of seasonal vertical migration of *Calanus finmarchicus*. Ophelia **44**: 145-156.

Kane, J. 1984. The feeding habits of co-occurring cod and haddock larvae from Georges Bank. Marine Ecology Progress Series **16**: 9-20.

Kenney, R. D., H. E. Winn, and M. C. Macaulay. 1995. Cetaceans in the Great South Channel, 1979-1989: right whale (*Eubalaena glacialis*). Continental Shelf Research **15**: 385-414.

Kim, K., K. R. Kim, T. S. Rhee, and H. K. Rho. 1991. Identification of water masses in the YS and East China Sea by cluster analysis. Oceanography of Asian Marginal Seas. K. Takano. Amsterdam, Elsevier**. pp.** 253-267.

Li, X., J. D. J. McGillicuddy, E. G. Durbin, and P. H. Wiebe. 2006. Biological control of the vernal population increase of *Calanus finmarchicus* on Georges Bank. Deep Sea Research Part II: Topical Studies in Oceanography **53**: 2632-2655.

Lough, R. G. and D. G. Mountain. 1996. Effect of small-scale turbulence on feeding rates of larval cod and haddock in stratified water on Georges Bank. Deep Sea Research Part II: Topical Studies in Oceanography **43**: 1745-1772.

Lynch, D. R., C. V. W. Lewis, and F. E. Werner. 2001. Can Georges Bank larval cod survive on a calanoid diet? Deep Sea Research Part II: Topical Studies in Oceanography **48**: 609-630.

Lynch, D. R., M. J. Holboke, and C. E. Naimie. 1997. The Maine coastal current: spring climatological circulation. Continental Shelf Research **17**: 605-634.

Lynch, D. R., W. C. Gentleman, D. J. McGillicuddy Jr., and C. S. Davis. 1998. Biological/physical simulations of *Calanus finmarchicus* population dynamics in the Gulf of Maine. Marine Ecology Progress Series **169**: 189-210.

Meise, C. J. and J. E. O'Reilly. 1996. Spatial and seasonal patterns in abundance and age-composition of *Calanus finmarchicus* in the Gulf of Maine and on Georges Bank. Deep-Sea Research Part II: Topical Studies in Oceanography **43**: 1473-1501.

MERCINA. 2001. Oceanographic responses to climate in the Northwest Atlantic. Oceanography **14**: 76-82.

Miller, C. B. 2004. Biological Oceanography. Malden, MA, Blackwell Publishing. 402 p.

Miller, C. B., D. R. Lynch, F. Carlotti, W. Gentleman, and C. V. W. Lewis. 1998. Coupling of an individual-based population dynamic model of *Calanus finmarchicus* to a circulation model for the Georges Bank region. Fisheries Oceanography **7**: 219-234.

Mills, C. E. 1995. Medusae, siphonophores, and ctenophores as planktivorous predators in changing global ecosystems. ICES Journal of Marine Sciences **52**: 575-581.

Mills, C. E. 2001. Jellyfish blooms: are populations increasing globally in response to changing ocean conditions? Hydrobiologia **451**: 55-68.

Ohman, M. D., K. Eiane, E. G. Durbin, J. A. Runge, and H. J. Hirche. 2004. A comparative study of *Calanus finmarchicus* mortality patterns at five localities in the North Atlantic. ICES Journal of Marine Sciences **61**: 687-697.

Pershing, A. J., C. H. Greene, J. W. Jossi, L. O'Brien, J. K. T. Brodziak, and B. A. Bailey. 2005. Interdecadal variability in the Gulf of Maine zooplankton community, with potential impacts on fish recruitment. ICES Journal of Marine Science. **62**: 1511-1523.

Piontkovski, S. A., T. D. O'Brien, S. F. Umani, E. G. Krupa, T. S. Stuge, K. S. Balymbetov, O. V. Grishaeva, and A. G. Kasymov. 2006. Zooplankton and the North Atlantic Oscillation: a basin-scale analysis. Journal of Plankton Research **28**: 1039-1046.

Ramp, S. R., R. J. Schlitz, and W. R. Wright. 1985. The deep flow through the Northeast Channel, Gulf of Maine. Journal of Physical Oceanography **15**: 1790-1808.

Pringle, J. M. 2006. Sources of variability in Gulf of Maine circulation, and the observations needed to model it." Deep Sea Research Part II: Topical Studies in Oceanography **53**: 2457-2476.

Rogers, C. A., D.C. Biggs, and R.A. Cooper. 1978. Aggregation of the siphonophores *Nanomia cara* in the Gulf of Maine: observations from a submersible. Fisheries Bulletin **76**: 281-284.

Rossi, S., M. J. Youngbluth, C. A. Jacoby, F. Pagès, and X. Garrofè. 2008. Fatty acid trophic markers and trophic links among seston, crustacean zooplankton and the siphonophores *Nanomia cara* in Georges Basin and Oceanographer Canyon (NW Atlantic). Scientia Marina **72**: 403-416.

Saumweber, W. J. and E. G. Durbin. 2006. Estimating potential diapause duration in *Calanus finmarchicus*. Deep Sea Research Part II: Topical Studies in Oceanography **53**: 2597-2617.

Sherman, K., W. G. Smith, J. R. Green, E. B. Cohen, M. S. Berman, K. A. Marti, and J. R. Goulet. 1987. Zooplankton Production and the Fisheries of the Northeastern Shelf. *In* Backus R. H. and D. W. Bourne (eds). Georges Bank. Cambridge, Ma, MIT Press**:** 269-282.

Sullivan, B. K. and C. J. Meise. 1996. Invertebrate predators of zooplankton on Georges Bank, 1977-1987. Deep Sea Research Part II: Topical Studies in Oceanography **43**: 1503-1519.

Townsend, D. W. 1998. Sources and cycling of nitrogen in the Gulf of Maine. Journal of Marine Systems **16**: 283-295.

Warn-Varnas, A., A. Gangopadhyay, J. A. Hawkins, and A. R. Robinson. 2005. Wilkinson Basin area water masses: a revisit with EOFs. Continental Shelf Research **25**: 277-296.

Wiebe, P. H. and M. C. Benfield. 2003. From the Hensen net toward four-dimensional biological oceanography. Progress in Oceanography **56**: 7-136.

Wiebe, P. H., R. C. Beardsley, D. G. Mountain, and L. R. Gregory. 2006. Dynamics of plankton and larval fish populations on Georges Bank, the North Atlantic US GLOBEC study site. Deep Sea Research Part II: Topical Studies in Oceanography **53**: 2455-2456.

Wiebe, P. H., T. K. Stanton, C. H. Greene, M. C. Benfield, H. M. Sosik, T. C. Austin, J. D. Warren, and T. Hammar. 2002. BIOMAPPER-II: An integrated instrument platform for coupled biological and physical measurements in coastal and oceanic regimes. IEEE Journal of Oceanic Engineering **27**: 700-716.

Winemiller, K. O. and K. A. Rose. 1993. Why do most fish produce so many tiny offspring? The American Naturalist **142**: 585-603.

Wishner, K. F., J. R. Schoenherr, R. Beardsley, and C. Chen. 1995. Abundance, distribution and population structure of the copepod *Calanus finmarchicus* in a springtime right whale feeding area in the southwestern Gulf of Maine. Continental Shelf Research **15**: 475-507.

Xue, H., F. Chai, and N. R. Pettigrew. 2000. A model study of the seasonal circulation in the Gulf of Maine. Journal of Physical Oceanography **30**: 1111-1135

Youngbluth, M., T. Sørnes, A. Hosia, and L. Stemmann. 2008. Vertical distribution and relative abundance of gelatinous zooplankton, in situ observations near the Mid-Atlantic Ridge. Deep Sea Research Part II: Topical Studies in Oceanography **55**: 119-125.

## APPENDIX A: MATLAB ROUTINES EXAMPLES USED DURING DATA PROCESSING

### A.1 EXAMPLE CODE TO ESTIMATE ROIs DEPTHS USING ESS DATA SETS

Routine to obtain ROIs' depths using the ESS Data sets corresponding to each basin for each cruise. The following routine was repeated (looped) as many times as tapes were recorded and processed for each basin and cruise. Complete m-files were not printed for practical reasons. They are saved in the Laboratory of Zooplankton at the Department of Oceanography and Coastal Sciences, Louisiana State University.

---

```
load ‘filepath\ESS_Data_cruiseid\basin\cruiseid_basinid_ess.mat'
%cruiseid= oc334, en331; basin=wilkinson; jordan; georges; basinid=wb; jb; gb
cd 'filepath\cruiseid\tapenumber\taxon'
%tapenumber=three-digit format (001, 002…010 etc.)
%taxon=calanus; chaetognaths; ctenophores; euchaeta; euphausiids; medusae;
%siphonophores.
aa=dir;
        if length(aa)==2,
           d=2;
        else
           d=3;
        end;
        tmp=getfield(aa(d),'name');
        g=strmatch(tmp,'Thumbs.db');
        if g==1,
          c=4;
        else
          c=3;
        end;
 b=1;
        for a=c:length(aa),
          filenames(b,:)=getfield(aa(a),'name');
          b=b+1;
        end;

roi_times=str2num(filenames(:,5:12));
roi_times=roi_times./86400000;
yyyy=1998;
mm=12;
dd=4;
yd=datenum(yyyy,mm,dd)-datenum(yyyy-1,12,31);
roi_times=yd+roi_times -5/24;

for a=1:length(roi_times),
  k=find(ess(:,1)>=roi_times(a,1));
  ess_section=ess(k(1)-5:k(1)+5,:);
  newtime=[ess_section(1,1):0.1/(24*60*60):ess_section(end,1)]';
```

```
   ess_temp=interp1(ess_section(:,1),ess_section(:,2:end),newtime);
   ess_temp=[newtime ess_temp];
   k=find(ess_temp(:,1)>=roi_times(a,1));
   roi_time(a,1)=ess_temp(k(1),1);
   roi_depth(a,1)=ess_temp(k(1),2);
   roi_temperature(a,1)=ess_temp(k(1),3);
   roi_salinity(a,1)=ess_temp(k(1),4);
   roi_density(a,1)=ess_temp(k(1),5);
   roi_fluor(a,1)=ess_temp(k(1),6);
   roi_trans(a,1)=ess_temp(k(1),7);
   roi_lat(a,1)=ess_temp(k(1),8);
   roi_lon(a,1)=ess_temp(k(1),9);
   clear newtime ess_temp;
end;
 taxon_tapenumber=[roi_time, roi_depth, roi_temperature, roi_salinity, roi_density, roi_fluor, roi_trans, roi_lat, roi_lon];
 clear a aa ans b c ess_section filenames g k roi_density roi_depth roi_fluor roi_lat roi_lon roi_salinity roi_temperature roi_time roi_times roi_trans tmp yd
```

**%…. [loop until last tape is read]**

basin_cruiseid_taxon=[taxon_tapenumber (i.e. 001);...taxon_tapenumber (i.e. 017];

**%The number of tapes varied for each cruise, for each basin and for each category. %Some taxa were not recorded in some tapes. When that was the case, such tapes were %not included in the routine.**

save 'filepath\basin_cruiseid\depth_location\basin_cruiseid_taxon'  basin_cruiseid_taxon;

**%Naming convention was mine. I name each output in such a way that it was unique and %easy to recognize. As a result file names were often long, but were useful to prevent %mistakes in future data processing.**

**%As a quality data control after running the routine I plotted the newly obtained dataset %so I could spot any potential problem.**

```
figure(1)
plot(ess(:,1),ess(:,2))
hold on
plot(basin_cruiseid_taxon(:,1),basin_cruiseid_taxon(:,2),'ro')
set(gca,'ydir','reverse')

figure(2)
plot(ess(:,9),ess(:,8),'.-')
hold on
plot(basin_cruiseid_taxon (:,9), basin_cruiseid_taxon (:,8),'r.-')
```

## A.2 EXAMPLE CODE TO ESTIMATE ABUNDANCES USING ROI DEPTHS AND ESS INFORMATION

Routine used to estimate abundances for *Calanus finmarchicus*, *Euchaeta norvegica*, ctenophores, and chaetognaths. Similar routine was used to calculate siphonophores abundance; however, 'bugs_per_liter' (see the code below) was multiplied by a correction factor. Correction factors are reported in Table 2.2 (Chapter II, GENERAL METHODS).

---

```
load 'filepath\basin_cruiseid\depth_location\basin_cruiseid_taxon.mat'
%basin = wilkinson; jordan; georges
%cruise = oc334; en331
%taxon = calanus; euchaeta; ctenophores; chaetognaths

load 'filepath\ESS_Data_cruiseid\basin\cruiseid_basinid_ess.mat'
%basinid = wb (Wilkinson Basin); jb (Jordan Basin); gb (Georges Basin)

    cruiseid_ess.time=ess(:,1);
    cruiseid _ess.smpressure=ess(:,2);
    cruiseid _ess.latitude=ess(:,8);
    cruiseid _ess.longitude=ess(:,9);
    cruiseid _ess.temperature=ess(:,3);
    cruiseid _ess.salinity=ess(:,4);
    cruiseid _ess.density=ess(:,5);
    cruiseid _ess.fluorescence=ess(:,6);
    cruiseid_ess.transmisometry=ess(:,7);

%Calculate the time interval you wish to estimate abundances at (One (1) minute was used in all cases).

interval=input('Enter the time interval (min) you want for abundance calculations: ');
time_array=[ess(1,1):interval/(24*60):339+10/24+21/(24*60)]';

%'time_array' ending time varied among cruises and changed depending on the basin and cruise being processed.

%Bin the data into the time intervals
[nbugs]=histc(basin_cruiseid_taxon(:,1),time_array);
nbugs=nbugs(1:end-1);
vol_per_interval=interval*60*60*3.9/1000;
bugs_per_liter=nbugs/vol_per_interval;
bug_times=time_array-((interval/2)/(24*60));

%Calculate the mean_depth for each time interval
bug_depths=interp1(cruiseid_ess.time,cruiseid_ess.smpressure,bug_times);
bug_lat=interp1(cruiseid_ess.time,cruiseid_ess.latitude,bug_times);
bug_lon=interp1(cruiseid_ess.time,cruiseid_ess.longitude,bug_times);
```

```
bug_temp=interp1(cruiseid_ess.time,cruiseid_ess.temperature,bug_times);
bug_sal=interp1(cruiseid_ess.time,cruiseid_ess.salinity,bug_times);
bug_density=interp1(cruiseid_ess.time,cruiseid_ess.density,bug_times);
bug_fluor=interp1(cruiseid_ess.time,cruiseid_ess.fluorescence,bug_times);
bug_trans=interp1(cruiseid_ess.time,cruiseid_ess.transmisometry,bug_times);
```

**%Plot data to verify that time calculations are not off face.**

```
a1=plot(cruiseid_ess.time,cruiseid_ess.smpressure,'k-');
hold on;
a2=scatter(bug_times(1:end-1),bug_depths(1:end-1) ,25,bugs_per_liter,'o','filled');
set(gca,'ydir','reverse')
```

**%The complete environmental and physical parameters from BIOMAPER-II are saved as %ascii files as follows:**

```
taxon_ess=[bug_times(1:end-1), bug_depths(1:end-1), bug_temp(1:end-1), bug_sal(1:end-1),
bug_density(1:end-1),…
bug_fluor(1:end-1), bug_trans(1:end-1), bug_lat(1:end-1), bug_lon(1:end-1), bugs_per_liter];

save ‘filepath\basin_cruiseid\density_outputs\taxon_density_ess_cruiseid', 'taxon_ess', '-ascii'
```

**%To Krig the data in 2D and plot it in a 3D graph, save ascii data as follows:**

```
taxon_2D=[bug_times(1:end-1), bug_depths(1:end-1), bugs_per_liter];

save (‘filepath\basin_cruiseid\density_outputs\taxon_density_cruiseid_2D', 'taxon_2D', '-ascii')
```

**% To Krig the data in a 3D fashion, save ascii data as follows:**

```
taxon_3D=[bug_lon(1:end-1), bug_lat(1:end-1), bug_depths(1:end-1), bugs_per_liter];

save 'filepath\basin_cruiseid\density_outputs\taxon_density_cruiseid_3D' ‘taxon_3D’ -ascii
```

## A.3 EXAMPLE CODE TO ESTIMATE EUPHASUIID FRACTIONS USED TO ESTIMATE THEIR ABUNDANCES (SEE APPENDIX A.4)

The following is an example of fraction estimation of euphausiids for Georges Basin, OC334 (December 1998). A modified version of this code was used for the other basins and cruises.

Basically, when the code is run, a window opens and display a tiff image of the euphausiid, the observer will estimate the 'visible fraction' of the organism, close the window, enter a fraction value (a maximum of 1 when the entire animal was imaged) in the command window, hit enter, and repeat the loop until the last euphausiids image is shown.

The output is automatically saved as a .mat file containing two columns (Column one: Year day (time); and column two: the value of the fraction visible of the animal. This output is utilized to calculate the euphausiid abundances (see Appendix A.5).

Similar method was utilized to estimate medusae visible fractions (Chapter II: GENERAL METHODS).

---

```
%%GEORGES BASIN, OC334
%Georges Basin tapes: 37-46

taxa='euphausiids';
dir_prefix=filepath\tape0';
dir_suffix=sprintf('\\%s',char(taxa(:,:)));

for i=37:41;
   cd_text=sprintf('%s%d%s',dir_prefix,i,dir_suffix);
   cd(cd_text);
   pwd;

   aa=dir;
   if length(aa)==2,
      d=2;
   else
      d=3;
   end;
   tmp=getfield(aa(d),'name');
   g=strmatch(tmp,'Thumbs.db');
   if g==1,
      c=4;
```

```
    else
       c=3;
    end;

    b=1;
    for a=c:length(aa),
      eval(['filenames' num2str(i) '(b,:)' '=getfield(aa(a), ''name'');']);
      b=b+1;
    end;

    milliseconds=str2num(eval(['filenames' num2str(i) '(:,5:12)']));
    eval(['visible' num2str(i) '=zeros(length(milliseconds),2);']);
    eval(['visible' num2str(i) '(:,1)' '=milliseconds;']);


    for a=1:length(milliseconds),
       winopen(eval(['filenames' num2str(i) '(a,:)']))
       %WARNING: convert pct into tif files or select 'PictureViewer
       %Apple Inc. under the 'open with' button on the properties window
       %so Matlab knows what program to use to open the file. Otherwise,
       %Matlab won't open the pct file.
       eval(['visible' num2str(i) '(a,2)' '=input(''Enter the fraction visible of the euphausiid: '');']);
    end;
    clear milliseconds

    %Convert timestamp to local time on visible variables
    %tapes 37-41 were recorded on December 9, 1998. GMT time.
    %(no euphausiids videotaped after midnight on tape 041)

    roi_times=(eval(['visible' num2str(i) '(:,1)'])./86400000;
    yyyy=1998;
    mm=12;
    dd=9;
    yd=datenum(yyyy,mm,dd)-datenum(yyyy-1,12,31);
    eval(['visible' num2str(i) '(:,1)' '=yd+roi_times -5/24;']);
    clear roi_times
end;

for i=42:44;
    cd_text=sprintf('%s%d%s',dir_prefix,i,dir_suffix);
    cd(cd_text);
    pwd;

    aa=dir;
    if length(aa)==2,
       d=2;
    else
       d=3;
    end;
    tmp=getfield(aa(d),'name');
    g=strmatch(tmp,'Thumbs.db');
    if g==1,
```

```
      c=4;
   else
      c=3;
   end;

   b=1;
   for a=c:length(aa),
     eval(['filenames' num2str(i) '(b,:)' '=getfield(aa(a), ''name'');']);
     b=b+1;
   end;

   milliseconds=str2num(eval(['filenames' num2str(i) '(:,5:12)'])); %#ok<ST2NM>
   eval(['visible' num2str(i) '=zeros(length(milliseconds),2);']);
   eval(['visible' num2str(i) '(:,1)' '=milliseconds;']);


   for a=1:length(milliseconds),
      winopen(eval(['filenames' num2str(i) '(a,:)']))
      %WARNING: convert pct into tif files or select 'PictureViewer
      %Apple Inc. under the 'open with' button on the properties window
      %so Matlab knows what program to use to open the file. Otherwise,
      %Matlab won't open the pct file.
      eval(['visible' num2str(i) '(a,2)' '=input(''Enter the fraction visible of the euphausiid: '');']);
   end;
   clear milliseconds

   %Convert timestamp to local time on visible variables
   %tapes 42-44 were recorded on December 10, 1998. GMT time.
   %(45 did not contained euphausiid ROIs)

   roi_times=(eval(['visible' num2str(i) '(:,1)'])./86400000;
   yyyy=1998;
   mm=12;
   dd=10;
   yd=datenum(yyyy,mm,dd)-datenum(yyyy-1,12,31);
   eval(['visible' num2str(i) '(:,1)' '=yd+roi_times -5/24;']);
   clear roi_times
end;

for i=46;
   cd_text=sprintf('%s%d%s',dir_prefix,i,dir_suffix);
   cd(cd_text);
   pwd;

   aa=dir;
   if length(aa)==2,
      d=2;
   else
      d=3;
   end;
   tmp=getfield(aa(d),'name');
   g=strmatch(tmp,'Thumbs.db');
```

```
    if g==1,
       c=4;
    else
       c=3;
    end;

    b=1;
    for a=c:length(aa),
      eval(['filenames' num2str(i) '(b,:)' '=getfield(aa(a), "name");']);
      b=b+1;
    end;

    milliseconds=str2num(eval(['filenames' num2str(i) '(:,5:12)'])); %#ok<ST2NM>
    eval(['visible' num2str(i) '=zeros(length(milliseconds),2);']);
    eval(['visible' num2str(i) '(:,1)' '=milliseconds;']);

    for a=1:length(milliseconds),
       winopen(eval(['filenames' num2str(i) '(a,:)']))
       %WARNING: convert pct into tif files or select 'PictureViewer
       %Apple Inc. under the 'open with' button on the properties window
       %so Matlab knows what program to use to open the file. Otherwise,
       %Matlab won't open the pct file.
       eval(['visible' num2str(i) '(a,2)' '=input("Enter the fraction visible of the euphausiid: ");']);
    end;
    clear milliseconds

    %Convert timestamp to local time on visible variables
    %tapes 46 was recorded on December 10, 1998. GMT time.
    %(45 did not contained euphausiid ROIs)

    roi_times=(eval(['visible' num2str(i) '(:,1)'])./86400000;
    yyyy=1998;
    mm=12;
    dd=10;
    yd=datenum(yyyy,mm,dd)-datenum(yyyy-1,12,31);
    eval(['visible' num2str(i) '(:,1)' '=yd+roi_times -5/24;']);
    clear roi_times
end;

euphausiids_fraction=[visible37; visible38; visible39; visible40;...
     visible41; visible42; visible43; visible44; visible46];

save 'filepath\georges_oc334\density_outputs\georges_oc334_euphausiids_fraction.mat'…
          'euphausiids_fraction'
```

## A.4 EXAMPLE CODE TO ESTIMATE EUPHAUSIIDS ABUNDANCES USING 'EUPHAUSIIDS_FRACTIONS' (SEE BELOW) AND ESS INFORMATION

Routine utilized to estimate euphausiids abundances utilizing the euphausiids visible fraction output from Appendix A.4 (georges_oc334_euphausiids_fraction.mat). This particular example illustrates the case for Georges Basin, OC334 (December 1998).

Similar routine was utilized to calculate medusae abundances utilizing the output from the estimation of visible fractions.

---

**%% GEORGES BASIN, OC334**

```
load 'filepath\georges_oc334\depth_location\georges_oc334_euphausiids.mat'

load 'filepath\ESS_Data_OC334\Georges\oc334_gb_ess.mat'
   ess=oc334_gb_ess;    clear oc334_gb_ess
   ess(any(isnan(ess),2),:) = []; %This takes care of missing values
load 'filepath\georges_oc334\density_outputs\georges_oc334_euphausiids_fraction.mat'

        oc334_ess.time=ess(:,1);
        oc334_ess.smpressure=ess(:,2);
        oc334_ess.latitude=ess(:,8);
        oc334_ess.longitude=ess(:,9);
        oc334_ess.temperature=ess(:,3);
        oc334_ess.salinity=ess(:,4);
        oc334_ess.density=ess(:,5);
        oc334_ess.fluorescence=ess(:,6);
        oc334_ess.transmisometry=ess(:,7);
```

**% Calculate the time interval you wish to estimate abundances at (One minute was %utilized for all basins for all cruises).**

```
interval=input('Enter the time interval (min) you want for abundance calculations: ');
time_array=[ess(1,1):interval/(24*60):344+5/24+12/(24*60)]';
```

**%end time of last tape recorded (tape 46) on GB, that is 344.2167 (05:12:08 local time). %Corroborated.**
**% Calanus finmarchicus had the max. time (344.2098) on taxa arrays**

**% Bin the data into the time intervals**

```
nbugs=zeros(length(time_array)-1,1);
for a=1:length(time_array)-1,
   k=find(euphausiids_fraction(:,1)>=time_array(a)                                    &
euphausiids_fraction(:,1)<time_array(a+1));
nbugs(a,1)=sum(euphausiids_fraction(k,2));
end;
vol_per_interval=interval*60*60*3.9/1000;
bugs_per_liter=nbugs/vol_per_interval;
```

```
bug_times=time_array-((interval/2)/(24*60));

% Calculate the mean_depth for each time interval
bug_depths=interp1(oc334_ess.time,oc334_ess.smpressure,bug_times);
bug_lat=interp1(oc334_ess.time,oc334_ess.latitude,bug_times);
bug_lon=interp1(oc334_ess.time,oc334_ess.longitude,bug_times);
bug_temp=interp1(oc334_ess.time,oc334_ess.temperature,bug_times);
bug_sal=interp1(oc334_ess.time,oc334_ess.salinity,bug_times);
bug_density=interp1(oc334_ess.time,oc334_ess.density,bug_times);
bug_fluor=interp1(oc334_ess.time,oc334_ess.fluorescence,bug_times);
bug_trans=interp1(oc334_ess.time,oc334_ess.transmisometry,bug_times);

%plot this to verify that time calculations are not off face.

a1=plot(oc334_ess.time,oc334_ess.smpressure,'k-');
hold on;
a2=scatter(bug_times(1:end-1),bug_depths(1:end-1),25,bugs_per_liter,'o','filled');
set(gca,'ydir','reverse')

%The complete environmental and physical parameters from biomaper are saved as ascii
%files as follows:

euphausiids_ess=[bug_times(1:end-1), bug_depths(1:end-1), bug_temp(1:end-1),
bug_sal(1:end-1), bug_density(1:end-1),...
bug_fluor(1:end-1), bug_trans(1:end-1), bug_lat(1:end-1), bug_lon(1:end-1), bugs_per_liter];

save ‘filepath\georges_oc334\density_outputs\euphausiids_density_ess_gb_oc334',…
 'euphausiids_ess', '-ascii'

%To Krig the data in 2D and plot it in a 3D graph, save ascii data as follows:
euphausiids_2D=[bug_times(1:end-1), bug_depths(1:end-1), bugs_per_liter];

save ‘filepath\georges_oc334\density_outputs\euphausiids_density_gb_oc334_2D',…
 'euphausiids_2D', '-ascii')

%No 3D array was created. Data set not suitable for 3D kriging. For all the other cases, a
3D array was saved to be able to krig the abundances and visualize them in a 3D fashion.
```

## APPENDIX B: VARIOGRAM/CORRELOGRAM PARAMETERS USED FOR KRIGING PLANKTON ABUNDANCES AND ENVIRONMENTAL PARAMETERS

EasyKrig 3.0 was utilized to krig data and the software can be downloaded from:

http://globec.whoi.edu/software/kriging/easy_krig/easy_krig.html.

**Table B.1.** Optimum Variogram/Correlogram parameters used to krig (3D) abundances for taxa/categories collected in Wilkinson Basin during December 1998 (OC334). The general exponential-Bessel model was used in all cases.

| taxon or category | Variogram/Correlogram Model Parameters | | | | | |
|---|---|---|---|---|---|---|
| | nugget | sill | length | power | hole scl | range |
| *Calanus finmarchicus*** | 0.037 | 0.732 | 0.169 | 1.608 | 0 | 0.611 |
| chaetognaths* | 0 | 0.95202 | 0.085817 | 1.5816 | 0 | 0.95 |
| ctenophores**† | 0.31529 | 1.5294 | 0.028284 | 2.3 | 0 | 0.74242 |
| *Euchaeta norvegica** | 0.0 | 0.9 | 0.092398 | 1.7359 | 0 | 0.6 |
| Euphausiids | 0 | 1.0 | 0.05 | 1.6 | 0 | 0.6 |
| medusae* | 0.05 | 0.9 | 0.05 | 1.4 | 0 | 0.5 |
| siphonophores* | 0.01 | 1.053 | 0.085 | 1.8 | 0 | 0.7 |

* Search radius and the Maximum Kriging Points used for kriging were 0.3 and 30, respectively.
** Search radius and Maximum Kriging Points used for kriging were 0.5 and 40, respectively.
† A value greater than the usual 2.5 relative variance was used.

**Table B.2.** Optimum Variogram/Correlogram Parameters used to krig (3D) abundances for taxa/categories collected in Wilkinson Basin during December 1999 (EN331). The general exponential-Bessel model was used in all cases.

| taxon or category | Variogram/Correlogram Model Parameters | | | | | |
|---|---|---|---|---|---|---|
| | nugget | sill | length | power | hole scl | range |
| *Calanus finmarchicus** | 0.037 | 0.732 | 0.169 | 1.608 | 0 | 0.611 |
| chaetognaths | 0 | 1.2 | 0.1 | 1.2 | 0 | 0.6 |
| Ctenophores | 0 | 1.1 | 0.17 | 1.1 | 0 | 0.6 |
| *Euchaeta norvegica* | 0 | 1.07 | 0.05 | 1.1 | 0 | 0.7 |
| euphausiids** | 0 | 1.3 | 0.1 | 1.2 | 0 | 0.7 |
| Medusae | 0 | 0.85 | 0.06 | 1.45 | 0 | 0.5 |
| siphonophores | 0 | 1.0 | 0.06 | 1.1 | 0 | 0.5 |

* Search radius and the Maximum Kriging Points used for kriging were 0.3 and 30, respectively.
** Search radius and Maximum Kriging Points used for kriging were 0.5 and 40, respectively.

**Table B.3.** Optimum Variogram/Correogram Parameters used to krig (3D) abundances for taxa/categories collected in Jordan Basin during December 1998 (OC334). The general exponential-Bessel model was used in all cases.

| | Variogram/Correlogram Model Parameters | | | | | |
|---|---|---|---|---|---|---|
| taxon or category | nugget | sill | length | power | hole scl | range |
| *Calanus finmarchicus* | 0.0 | 0.85 | 0.16 | 1.2 | 0.0 | 0.6 |
| chaetognaths | ----- | ----- | ----- | ----- | ----- | ----- |
| ctenophores | 0.0 | 0.65 | 0.06 | 1.0 | 0.0 | 0.5 |
| *Euchaeta norvegica* | 0.0 | 0.85 | 0.09 | 1.1 | 0.0 | 0.65 |
| Euphausiids | 0.0 | 1.1 | 0.21 | 0.96 | 0.0 | 0.6 |
| Medusae | 0.0 | 1.5 | 0.098 | 1.5 | 0.0 | 0.6 |
| siphonophores | 0.0 | 0.9 | 0.07 | 1.0 | 0.0 | 0.7 |

**Table B.4.** Optimum Variogram/Correogram Parameters used to krig (3D) abundances for taxa/categories collected in Jordan Basin during December 1999 (EN331). The general exponential-Bessel model was used in all cases.

| | Variogram/Correlogram Model Parameters | | | | | |
|---|---|---|---|---|---|---|
| taxon or category | nugget | sill | length | power | hole scl | range |
| *Calanus finmarchicus* | 0.0 | 0.9 | 0.1 | 1.5 | 0.0 | 0.5 |
| chaetognaths | 0.0 | 1.12 | 0.1 | 1.2 | 0.0 | 0.7 |
| ctenophores | ----- | ----- | ----- | ----- | ----- | ----- |
| *Euchaeta norvegica* | 0.0 | 0.83 | 0.12 | 1.2 | 0.0 | 0.5 |
| Euphausiids | 0.0 | 1.15 | 0.1 | 1.3 | 0.0 | 0.5 |
| Medusae | ----- | ----- | ----- | ----- | ----- | ----- |
| siphonophores | 0.0 | 1.1 | 0.09 | 1.1 | 0.0 | 0.5 |

**Table B.5.** Optimum Variogram/Correogram Parameters used to krig (2D) abundances for taxa/categories collected in Georges Basin during December 1998 (OC334). The general exponential-Bessel model was used in all cases.

| | Variogram/Correlogram Model Parameters | | | | | |
|---|---|---|---|---|---|---|
| taxon or category | nugget | sill | length | power | hole scl | range |
| *Calanus finmarchicus* | 0.0 | 0.95 | 0.067 | 1.2 | 0.0 | 0.5 |
| chaetognaths | ----- | ----- | ----- | ----- | ----- | ----- |
| ctenophores | 0.0 | 1.3 | 0.045 | 1.28 | 0.0 | 0.3 |
| *Euchaeta norvegica* | ----- | ----- | ----- | ----- | ----- | ----- |
| Euphausiids | 0.0 | 0.98 | 0.063 | 1.16 | 0.0 | 0.4 |
| Medusae | 0.0 | 1.26 | 0.06 | 1.1 | 0.0 | 0.4 |
| siphonophores | 0.0 | 1.17 | 0.083 | 1.25 | 0.0 | 0.6 |

**Table B.6.** Optimum Variogram/Correogram Parameters used to krig (3D) abundances for taxa/categories collected in Georges Basin/NE Channel during December 1999 (EN331). The general exponential-Bessel model was used in all cases.

| | Variogram/Correlogram Model Parameters | | | | | |
|---|---|---|---|---|---|---|
| taxon or category | nugget | sill | length | power | hole scl | range |
| *Calanus finmarchicus* | 0.0 | 1.1 | 0.088 | 1.24 | 0.0 | 0.5 |
| chaetognaths | 0.0 | 1.5 | 0.25 | 0.72 | 0.0 | 0.5 |
| ctenophores | ----- | ----- | ----- | ----- | ----- | ----- |
| *Euchaeta norvegica* | 0.0 | 1.0 | 0.077 | 0.99 | 0.0 | 0.7 |
| Euphausiids | 0.0 | 1.215 | 0.092 | 1.18 | 0.0 | 0.6 |
| Medusae | ----- | ----- | ----- | ----- | ----- | ----- |
| siphonophores | 0.0 | 0.907 | 0.063 | 1.2 | 0.0 | 0.46 |

**Table B.7.** Optimum Variogram/Correeologram Parameters used to krig (3D) temperature data collected on cruises OC334 (December 1998) and EN331 (December 1999). The general exponential-Bessel model was used in all cases. During data preparation, a 10 point Reduction Factor and a 10 point support were set using Mean Filter.

| | Variogram/Correlogram Model Parameters | | | | | |
|---|---|---|---|---|---|---|
| Basin/Cruise | nugget | sill | length | power | hole scl | range |
| WB/OC334 | 0.0 | 2.46 | 0.79 | 1.74 | 0.0 | 0.95 |
| JB/OC334 | 0.0 | 1.108 | 0.32 | 1.8 | 0.0 | 0.95 |
| GB/OC334* | 0.0 | 1.44 | 0.36 | 2.0252 | 0.0 | 0.95 |
| WB/EN331 | 0.0 | 1.37 | 0.45 | 1.53 | 0.0 | 0.95 |
| JB/EN331 | 0.0 | 1.26 | 0.31 | 1.1 | 0.0 | 0.95 |
| GB/EN331 | 0.0 | 1.1935 | 0.29633 | 0.74351 | 0.0 | 0.95 |

*2D kriging was performed for this dataset.

**Table B.8.** Optimum Variogram/Correeologram Parameters used to krig (3D) salinity data collected on cruises OC334 (December 1998) and EN331 (December 1999). The general exponential-Bessel model was used in all cases. During data preparation, a 10 point Reduction Factor and a 10 point support were set using Mean Filter.

| | Variogram/Correlogram Model Parameters | | | | | |
|---|---|---|---|---|---|---|
| Basin/Cruise | nugget | sill | length | power | hole scl | Range |
| WB/OC334 | 0.0 | 2.3838 | 0.7367 | 2.5445 | 0.0 | 0.95 |
| JB/OC334 | 0.05 | 1.57 | 0.62 | 4.02 | 0.0 | 0.95 |
| GB/OC334* | 0.0 | 2.29 | 0.68 | 2.52 | 0.0 | 0.95 |
| WB/EN331 | 0.0 | 2.62 | 0.967 | 1.98 | 0.0 | 0.95 |
| JB/EN331 | 0.0 | 2.47 | 0.89 | 2.134 | 0.0 | 0.95 |
| GB/NEC/EN331 | 0.0 | 1.6067 | 0.62961 | 2.8886 | 0.0 | 0.95 |

*2D kriging was performed for this dataset.

## VITA

Christian Briseño-Avena was born in January, 1982 in Tepatitlan de Morelos, in the Mexican state of Jalisco. He graduated from the Regional High School of Puerto Vallarta in 1999. He earned a Bachelor of Science Degree in biology in the Universidad de Guadalajara, Mexico, in December 2004. Shortly after graduation he worked as a research assistant at the *Instituto de Botánica de la Universidad de Guadalajara* (IBUG). There, he worked for two years under supervision of botanist Dr. Aarón Rodriguez before joining the Master of Science program in the Department of Oceanography and Coastal Sciences at Louisiana State University in January 2006. Christian will receive his Master of Science Degree in August 2009.